Daylighting Performance of Tubular Solar Light Pipes: Measurement, Modelling and Validation

By

Xiaodong Zhang

A thesis submitted to Napier University for the degree of Doctor of Philosophy

November 2002

Daylighting Performance of Tubular Solar Light Pipes:
Measurement, Modelling and Validation

献给我的家人和我的祖国中国

To my family and my motherland China

ABSTRACT

The innovation of natural daylighting light pipe took place more than twenty years ago. Since then its daylighting performance has been reported in a number of studies. To date, however, no mathematical method that includes the effect of straight-run and bends within light pipes has been made available. Therefore, a general mathematical model for light pipes is desirable to assess and predict its daylighting performance. Furthermore, such a general model can enable the assessment of light pipe system's efficiency and potential in energy saving.

A modified form of daylight factor, Daylight Penetration Factor (DPF), has been introduced to build a sophisticated model that takes account of the effect of both internal and external environmental factors, and light pipe configuration. Measurements and mathematical modelling activities aimed at predicting the daylighting performance of light pipes with various configurations under all weather conditions in the UK were undertaken. A general daylighting performance model, namely DPF model, for light pipes was developed and validated. The model enables estimation of daylight provision of the light pipes with a high degree of accuracy, i.e. R^2 values of 0.95 and 0.97 for regression between predicted and measured illuminance were respectively obtained for the above model.

The DPF model uses the most routinely measured radiation data, i.e. the global illuminance as input. Considering that in real applications, light pipes installed in a particular building may not receive the full amount of global illuminance as measured by local meteorological office. This may be due to partial shading of the light pipe top collector dome. Therefore, to enable the application of the DPF model in practical exercises fundamental work on sky diffuse illuminance measurements have been undertaken.

An exhaustive validation has been carried out to examine the DPF model in terms of the structure of the model and its performance. The DPF model was compared against studies by other independent researchers in the field. Independent data sets gathered from a separate site were used to validate the performance of the DPF model. Comprehensive statistical methods have been applied during the course of validation. Relevant, brief economic and environmental impact of the technology under discussion has also been undertaken.

One of the main achievements of this work is the mathematical method developed to evaluate the daylighting performance of light pipes. The other main achievement of this work is the development and validation of the DPF models for predicting light pipes' daylighting performance.

DECLARATION

I hereby declare that the work presented in this thesis was solely carried out by myself at Napier University, Edinburgh, except where due acknowledgement is made and that it has not been submitted for any other degree.

XIAODONG ZHANG (CANDIDATE)

1st Dec 2002

DATE

ACKNOWLEDGEMENTS

I must thank my supervisors, Professors Tariq Muneer, Jorge Kubie and Mr Terry Payne for their constant encouragement, support and guidance throughout the period of my research.

This work would not have been possible without the financial support from Napier University, and I offer my gratitude to all involved in funding this project.

To my friends and colleagues at Napier University, I warmly acknowledge your friendship and support: Abdulaziz Imtithal, Dr Ana Booth, Dr Baolei Han, Dr Neil Hey, Dr Tom Grassie, Bill Campbell, Bill Young, Fatema Fairooz, George Pringle, Ian Campbell, Kevin McCann, Muhammad Asif, Randall Claywell and Stewart Scotland Hill. I thank Professor A Kudish (Israel) and Associate Professor J Lam (Hong Kong) for providing data for mathematical modelling. I thank Dr Gabriel Lopez for his friendship and advice in the evening before my viva. I must give credit to Miss Amina Muneer for lending me her room, from time to time, as a laboratory for light pipe performance measurements.

Credit is due to David Jenkins (Monodraught TCS) for developing Lux plot based on DPF model.

I'd like to thank my parents, Shuying Gong and Xinhua Zhang, for supporting me the past twenty-eight years. Without your love and education, I could not achieve anything.

CONTENTS

LIST OF FIGURES

LIST OF TABLES

NOMENCLATURE

a_0 - a_{10}	Coefficients used in Eqs. 6.9 - 6.13
A_p	Light pipe aspect ratio for straight light pipes (=light pipe length / diameter)
A_{pe}	Light pipe aspect ratio for elbowed light pipes
b	Radiance distribution index
B_n	Normal beam irradiance (W/m^2)
d #	The distance between the projection of the diffuser centre on the working plane and the point of interest (m)
D	Distance from light pipe diffuser to a given position P(x, y, z) (m)
DF	Daylight factor
$DPF_{(x, y, z)}$	The light pipe daylight penetration factor for position P (x, y, z)
E_{ed}	Horizontal diffuse irradiance (W/m^2)
E_{eg}	Horizontal global irradiance (W/m^2)
E_{vd}	Horizontal diffuse illuminance (lux)
E_{vg}	Horizontal global illuminance (lux)
$E_{estimated}$	Estimated internal illuminance (lux)
$E_{internal}$	Internal illuminance at a given point (lux)
$E_{internal\ (x,y,z)}$	Internal illuminance at the point $P_{(x,y,z)}$ (lux)
$E_{measured}$	Measured internal illuminance (lux)
f	Diffuse irradiance that is obscured by shadow band: Drummond's method (W/m^2)
f_D	The diffuser factor
f_{len}	The equivalent-length factor
f_{loss}	The energy-loss factor
F_e	External environmental factors
F_g	Light pipe configuration factors
F_i	Internal environmental factors
F_D	Drummond diffuse irradiance correction factor based on isotropic radiance distribution
F_P	Proposed diffuse irradiance correction factor based on anisotropic radiance distribution
$F_{v(x,y,z)}$	The view factor between light pipe diffuser and a plane element at P(x,y,z)
G	Horizontal global irradiance (W/m^2)
H	Height of the diffuser over the working plane
i	Angle at which light incident on the reflecting surface of light pipe tube (degree)
I_n	The intensity of radiation in normal direction
I_θ	Intensity of radiation along a direction that has angle θ with the normal to a radiation-emitter
IL	horizontal diffuse illuminance (lux)
k_t	Sky clearness index
L	Length of the straight light pipe (m)
L_b	Length of the light pipe bend (m)
L_z	Zenith radiance ($W\ m^{-2}\ sr^{-1}$)
L_{vz}	Zenith luminance (Cd/m^2)
$L_{v\theta}$	Zenith luminance of a sky patch of a altitude of θ (Cd/m^2)
m	Coefficient used in Eqs. 6.9 - 6.13

N	Number of bends
P	The proportion of the sky area obscured by the shadow band
$P_{(x, y, z)}$	A given location at which illuminance is to be estimated
R	Radius of light pipe tube (m)
t	Hour angle (radian)
t_0	Sunset hour angle (radian)
T	Transmission of daylight within light pipe tube
W	View angle of the shadow band subtended at the diffuse irradiance sensor
x	The distance between a bunch of incident light and the axis of light pipe tube (m)
α	Solar altitude (radian) = α_s
β	Slope of any given tilted surface (radian)
δ	Sun's declination (radian)
ϕ	Light pipe diameter (mm)
γ	Angle between the considered point and the position of the sun (radian)
φ	Latitude of the measurement site (degree)
θ	The altitude of a given sky patch (radian)
ρ	Surface reflectance of mirrored light pipe
ξ	Zenith angle in Perez model, (radian)
ψ	Azimuth of a sky patch (radian)

1. INTRODUCTION

Energy is an essential component for all activity and is required for the production of all goods and the provision of all services. For thousands of years human society has been using fossil fuel as a major form of energy resource. However, because human activity accelerates, fossil fuels are being depleted at a faster rate than ever before. All forms of fossil fuels have their respective cycle of domination and depletion phase (Fig. 1.1). According to the energy statistics published by BP [1], the world's resource to production ratio is projected to be 62 years, as shown in Table 1.1. Therefore, the current scenario of fossil fuels depletion is causing concerns across the world, especially in the developed nations. The solution to above challenge consists of two aspects, namely, to save energy and to exploit renewable energy.

A topic closely related to energy conservation is the issue of environment protection. Throughout the world, the concern on the negative impacts of excessive energy consumption on natural environment is arising. In this respect, one major argument has been on the associated problem of thermal pollution from conventional power plants [2]. The International Panel for Climate Change has argued that the world is definitely getting warmer. In England, the 1990s experienced four out of the five warmest years in a 340-year record, with 1999 being the warmest year ever recorded. Global warming and its affiliated changes in the world's climate would have enormous consequences for people, economies and the environment. Many projections of the world's future climate show more intense rainfalls or snowstorms, which are likely to lead to large-scale flooding of many locations. Between the 1960s and the 1990s, the number of significant natural catastrophes such as floods and storms rose three-fold, and the associated economic losses rose by a factor of nine. Therefore, the global warming and its associated disastrous climatic impacts on the environment and economics have made it necessary for the whole human society to explore more efficient and environmentally friendly energy resources. Present research on the innovative daylighting device light pipe that utilizes solar energy is a new effort towards this end.

1.1 THE UTILIZATION OF ELECTRICITY

Nowadays, energy that takes the form of electricity and fuel has become the backbone of our society. However, during the cause of converting primary fuels into final use energy, a substantial part of energy is lost. Figure 1.2 shows the energy flows in the UK for the year of 1998 [3]. It is shown that in the year of 1998, the UK final users consumed 169.4 million tonnes of oil equivalent energy, out of which electricity accounts for 31.7 million tonnes. Within the 31.7 million tonnes of electricity, 25.2 million tonnes were generated by nuclear power station, and the other 6.5 million tonnes were produced by thermal-electricity plant. The conversion efficiency of a typical nuclear station in the UK is about 37 per cent [4]; while for conventional steam stations, the ratio of fuel used for electricity generation to electricity generated is about 12 per cent. Therefore, the overall energy efficiency for electricity generation is poor with the utility ratio lower than 25 per cent.

The use of electricity is not only inefficient but also environmentally detrimental. The combustion of fossil fuels is responsible for the majority of emissions of carbon dioxide CO_2, sulphur dioxide SO_2 and nitrogen oxides NO_2 [4]. Carbon Dioxide is the main greenhouse gas, which may contribute to global warming and climate change. Sulphur dioxide and oxides of nitrogen are the main cause of acid rain. According to the UK Energy Sector Indicators, in the UK emission of CO_2 from power station is the largest single source, which accounts for 26.7% of the total emissions. As to SO_2 and NO_2, corresponding figures are 57.1% and 21.2% respectively. Nuclear power station is also environmentally harmful because the potential hazard posed by nuclear waste to the natural environment. Therefore, the reduction of electricity production and consumption not only saves energy resources, but also protects the natural environment that our human society relies on.

1.2 DAYLIGHTING AND ENERGY CONSERVATION

In the United Kingdom, electrical lighting accounts for an estimated 5% of the total primary energy consumed per annum. Office buildings in the UK may consume up to 60% of their total energy in the form of electric lighting [5]. The total amount of electricity consumed by domestic household appliances increased by 85% between 1970 and 1998 [4]. According to the UK Energy Sector

Indicators, for a typical domestic household, lighting accounts for more than 23% of total electricity consumption. Exploitation of daylight can thus produce significant savings. Research has shown that savings of 20% to 40% are attainable for office buildings that utilise daylight effectively. Benefits and savings associated with daylight design are manifold. Reductions in lighting energy have the knock-on effect of lowering cooling and heating energy consumption in a building [6]. Another significant benefit of using daylight is it is totally free and clean, which makes it one of the most cost-effective means of reducing electricity consumption. Therefore, applying more efficient daylighting designs in buildings will contribute to energy conservation and environmental improvement.

1.3 DAYLIGHTING AND LIFE

Nowadays, people spend most of their lives in buildings, e.g. offices, houses factories, supper markets, stadiums and so on. These buildings are shelters for humans to provide them safety and comforts. However, in seeking shelter, people also need to be in touch with the external environment. Daylight enables a visual contact to the outside world. Daylight is also required to enhance the appearance of an interior and its contents by admitting areas of light and shade that give shape and detail for objects. The inclusion of daylight in the workspace provides workers with social and physiological benefits.

Sunlight variation affects many activities of being on the earth. Humans are also affected to seasonal and daily variation of sunlight. Daylight that is brought into interior space tells people the change of external environmental and therefore releases the feeling of isolation and monotony. Research has shown that daylight has an important bearing on the human brain's chemistry. Light entering via eyes stimulated the nerve centres within the brain, which controls daily rhythms and moods. Further research has also established a link between human exposure to light and Serotonin, a substance identified as a neurotransmitter. Lack of Serotonin is known to be a cause of depression. By receiving enough amount of daylight, people can positively adjust the production of Serotonin so as to tune their physical and spiritual condition better. Therefore, daylight affects multi-aspects of human life and has an important bearing on the whole society.

1.4 DAYLIGHTING IN BUILDINGS

The source of daylighting is the sun. The sun is a huge nuclear reactor that has been continuously emitting solar radiation for around 4.5 billion years. It should remain more or less as it is for another 5.5 billion years [7]. The term solar radiation refers to the energy emanating from the sun. Daylight is the part of energy contained within the visible part of the solar radiation spectrum. Human eye is the organ by which human being perceive daylight. It receives light that is omitted or reflected by objects, and converts the light rays into signals that can be recognized by the brain, which produces the perception of vision. Daylight itself has a continuous spectrum with apparent difference in brightness. Human eye's sensitivity to spectral colour varies from violet to red, which is corresponding to the solar radiation spectrum of 0.39 to 0.78 μm. Although daylight covers only a narrow band of the whole solar radiation spectrum, it has a fundamental and significant bearing on human being's life on the earth.

On the earth, daylight has two components, one is the direct beam (sunlight) from the sun, and the other is the sky-light. The latter one is a result of the scattering of sunlight within the ambient atmosphere of the earth. For a building, the more light it admitted, the better its habitants can see. However, the daylight quantity should be controlled to be in a range. Too much daylight can be troublesome in some situations. For example, residents may feel discomfort by direct sunray in their field of view. Solar heat gain is another killer of building design. The use of large glazed area in an attempt to admit more daylight can cause solar overheating. However, compared to sunlight, sky-light is cooler, gentler, diffuse and more visible with a significantly smaller infrared component. Thus, in situations where daylight is desired with minimal solar heat gain, sky-light can provide the best quality of daylight.

Compared to artificial light, daylight is of better quality. The good colour rendering qualities of natural light helps to reduce eyestrain. Another benefit of using daylight is it improves the health of human body. Lack of daylight exposure for a long time has been found to be the cause of mood swings and depression. People also react to changing seasons with altered moods and behaviour. This phenomenon exacerbates in some high-latitude location where people suffer lack of daylight seasonally. For example, the common disorder among people who live in Northern Europe has been diagnosed as seasonal affective disorder (SAD). Therefore, to allow sufficient daylight in building design has a

significant bearing on maintaining and improving occupants' health condition. To admit as much as possible daylight into buildings and meanwhile to minimize the glare and solar gain level is an important balance that building designers need to achieve.

1.5 WINDOWS AS TRADITIONAL DAYLIGHTING DEVICES

Window is the mostly widely used daylighting device in buildings. The main function of a window has been described as, "to provide an outside view and to permit light to penetrate the interior of a building in such quantity and with such distribution that it provides satisfactory interior lighting results" [8]. Therefore, the application of windows in buildings design is more than illuminating engineering; it is also a science on living and working environmental healthy. It is often stated, that people prefer to work where there are windows and that the exclusion of daylight leads to a sense of deprivation and a lack of well being. However, in practise the design and application of window is limited by various reasons apart from lighting.

One handicap of using window in buildings is that the window's performance is greatly constrained by the external natural and man-made obstructions. As a solution, larger sized windows are used to compromise the lack of incident daylight due to external obstruction. However, this can produce some thermal, visual and acoustic discomfort related problems. Large windows may be a main reason for extra solar gain or heat loss, discomfort and disability glare, strong noise, and concerns for safety as well. During the last decade, window technology has seen dramatic changes. The appearance of multi-glazed window with low-emissivity coatings, gas cavity fillings and insulating frame has greatly improved window's thermal, visual and acoustic performances. Nevertheless, the application of these new techniques is presently costly.

There are also circumstances where windows cannot be used as daylighting devices. For examples, for interior room within large buildings or corridors between rooms where daylight cannot reach, windows are not applicable. However, in some of these cases, skylight has been used extensively and satisfactorily as daylight provider. A skylight can be considered as a horizontal or sloped window on the roof of a building. Skylight works effectively in daylighting a perimeter zone of a building. However, the design of skylight can be a difficult task. When skylight admits sky diffuse light into

buildings, it also allows sunlight penetrate into interior spaces. Sunlight transferred through skylight can cause heat and visual discomfort. Therefore, decisions have to be made on the size and orientation of skylight with regard to the balance between the admission of sufficient daylight and exclusion of excessive sunlight.

Both windows and skylights can be classified as conventional passive daylighting devices. A main feature of passive solar devices is they use the form and fabric of buildings to admit, store and distribute solar energy for heating and lighting without additional energy input and consumption. A good "one-off" design of passive solar device can provide both environmental and economical benefits. However, a major difficulty in designing windows and skylights is the design of control system or mechanism that can ensure the maximum use of desirable daylight, and minimize the induction of solar and vision discomforts. People realise conventional windows have two major drawbacks. First, the most concentrated form of natural light, namely sunlight, is effectively useless as a working illuminant, and secondly in a deep building without rooflights daylighting is restricted to areas near the window [9]. Therefore, in the last twenty years, effort has been made to develop innovative daylighting systems that can improve the distribution of daylight in a space, and to control direct sunlight so that it can be used as an effective working illuminant.

1.6 INNOVATIVE DAYLIGHTING DEVICES AND LIGHT PIPES

Generally there are five types of innovative daylighting devices including mirrors, prismatic glazing, light shelves, atrium and light pipes. There are also various occasions where unique daylighting designs are applied to serve both lighting and other purpose. For instance, Figure 1.3 shows the solar chandeliers used in Manchester Airport departure lounge.

1.6.1 Mirror, prismatic glazing, light shelf and atria

In daylighting design, mirrors are mainly used to collect, reflect and redirect direct sunlight. A simple mirrored louver system is shown in Fig. 1.4. This system intends to make use of direct sunlight in a controlled way so as to improve the daylight distribution within an interior area. There are also more complicated mirror systems that can lead sunlight into areas deep within buildings. Figure 1.5 shows a

heliostat system that is used in a university building in Minneapolis. The system beams the sunlight through a lens into an underground laboratory, saving electrical lighting and cooling costs [10].

Prismatic glazing can be used to alter the direction of incoming daylight. When beam traverses a prism, its path is turned through 90° or smaller angle. This refraction phenomenon enables prismatic glazing to be used as a substitute for mirrored louvres system shown in Fig. 1.4. There are also sunlight-excluding prism systems that reject sunlight throughout the year, but admit diffuse light from higher in the sky. The diffuse light is then directed to the ceiling so as to provide a controlled and comfortable daylit interior.

Light shelves work on the principle of reflection to redirect sunlight and sky light. The light shelves are horizontally or nearly horizontally placed reflective baffle mounted up a window, or between a view window and a clerestory window. Both interior light shelves and exterior light shelves can be used. Figure 1.6 shows an interior light shelve being placed between a view window and a clerestory window. Daylight from the clerestory window is reflected to the ceiling and then further diffused more evenly into the deep area of the room. When there is no direct sunlight, light shelves can help to improve the uniformity of light in the space.

Atrium, or called covered courtyard have been commonly used in North America and has been entering the UK as well [10]. Atrium is rather an innovative building design concept more than an daylighting technique. They create new dimension to large buildings that provides more useable and pleasant daylit space for occupants. Figure 1.7 shows generic forms of atrium buildings.

1.6.2 Light pipe

Light pipe is an innovative design to direct daylight into deep areas within buildings where daylight cannot reach. The system is crudely analogous to the fibre optic cable, the difference being that the latter device has much higher transmission efficiency. A schematic of light pipe system is shown in Fig. 1.8. Daylight is gathered via a polycarbonate dome at roof level and then transmitted downwards to interior spaces within buildings. The internal surface of the light pipe is coated with a highly reflective mirror finish material (typically with a reflectance in excess of 0.95) that helps in achieving a

reasonable illuminance indoors when daylight is introduced via a light diffuser. The light-reflecting tube is adaptable to incorporate any bends around building structural components.

Like other innovative daylighting devices, light pipe utilizes sunlight that accounts for two thirds of global illuminance in a clear day. Both sky daylight components are gathered by light pipe and then transmitted and diffused into interior where need to be day lit. Because of its main structure as a well-sealed tube, light pipe has added potential advantage in reducing excessive solar gain. Since piped daylight emits off only from light pipe diffuser, the output daylight is easier to control than other innovative daylighting systems. Light pipe's flexibility in its structure, allows designers put diffusers directly upon where need to be lit, so as to achieve a good internal daylight distribution.

The combined use of windows and light pipes can reduce glare and further improve the balance of daylighting within a room. In daylighting, there has always been a dilemma for designers. It is that on one hand large exposure of sky through window is not encouraged because it can cause vision discomfort, while on the other hand a high daylight factor is always preferable and important for building users. Furthermore, many architects object to unilateral daylighting, due to the excessive highlight and shadow it may cause. However, by applying light pipes above problems can be solved. By introducing redirected and diffused daylighting into deep area of a room, glare from windows is reduced and daylighting is of a better uniformity. For skylight designers, the attempt to admit more sky diffuse light by enlarging the façade area always involves danger of introducing undesirable sunlight into buildings. As a comparison, light pipes transmit sunlight and sky diffuse light by multi-reflect mechanism; therefore the output daylight is much more uniform and diffused than that by a skylight. Another potential advantage that light pipe possesses is that it can be used in multi-storey buildings, while the use of skylight is usually limited to the perimeter zone of a building.

As addressed before, the applications of light pipes in buildings can bring multi-fold benefit. Compare to other innovative daylighting devices, light pipe seems also have potential advantages in terms of visual and thermal performance and applicability. Moreover, the fact that light pipes have been commonly used in the USA and Australia implies its further development in the United Kingdom and Europe. However, for most UK and European daylighting designers, light pipe is still a relatively new

concept [11]. Research that focus on the evaluation of light pipe's daylighting performance is therefore in need to reveal its perspective and to push forward its development.

1.7 AIMS OF THE PRESENT RESEARCH

The difficulties in identifying all decisive factors that affect the performance, and in quantitatively weighing the contributions of these decisive factors are the main barriers to appraising light pipe's efficiency. The complexity in the mechanism by which light pipes transmit daylight makes it difficult to appraise the performance by means of physical modelling. On the other hand, prior to this research, the lack of light pipe performance data that include both sufficient environmental and geometrical data made it impossible neither to model the performance using mathematical methods.

The overall objective of this work is to provide a general mathematical model for the prediction of light pipe daylighting performance. Although the performance of light pipe has been investigated in a number of studies [12-14], up to the initiation of this research no mathematical method that includes the effect of both geometrical and environmental factors has been made available. End goals are to be achieved following a logical process from raw data collection to evaluation of mathematical models. The aims of the current research are presented below in turn.

(1) To conduct a literature review of works in the field in order to provide a basic grounding in the subject matter and familiarise ones self with methodologies against which the present work may be compared. By literature research, it is intended to summarise the to date development in light pipes daylighting performance measurement and simulation. The search focuses particularly on the prediction of performance of light pipe systems of various designs and under different weather conditions.

(2) To develop a logical method of building mathematical model for predicting the daylighting performance of light pipes. Although the complexity in the working mechanism of light pipe makes it difficult to appraise its performance, to the aid of mathematical software and the computing ability by PC, it is possible to develop a computer model so as to describe light pipe's daylight transmission characters in a mathematical manner. As an instant result of a project of limited resource, the proposed

mathematical model can have a limited applicability. However, more importantly the study aims to produce a valid research method, and a framework under which further development in daylighting performance modelling can be conducted in a consistent direction leading to the final solution. This aim, as a principle guides the implement of the present research from the day one to the end, and is therefore embodied through out this report. The work conducted and the conclusions drawn to satisfy this aim can be found in Chapter 4.

(3) To form a substantial foundation for mathematical modelling by monitoring daylighting performance of light pipes both in real application and in test rooms. Extensive and detailed geometrical and environmental data, namely the light pipe configuration information, internal illuminance and external weather conditions, sun's position and so on need to be gathered. Measurements on the performance of light pipes in separate test rooms are to be undertaken so as to enable the validation of the proposed model using independent data. This work is presented in Chapter 5.

(4) To analyse the working mechanism of light pipes. By analysing the measured data and physical reasoning, build the analytical framework relating the input and output of the proposed model, and identify the most decisive factors that affect light pipe's daylighting performance. To determine the "best" mathematical expression to describe the daylighting transmission pattern of light pipe, choose suitable solar radiation data as input and, choose the "best" internal daylight distribution model to describe the output of the proposed model. To validate the proposed model using independent data by means of statistical evaluation. The work is reported in Chapters 6 and 8.

(5) For solar energy applications design, global and diffuse horizontal irradiance and beam normal irradiance are the three most important quantities. Global horizontal illuminance (E_{vg}) can be easily measured using a pyranometer. As to the measurement of diffuse horizontal illuminance (E_{vd}), the most common approach is to use a shadow band aided pyranometer to intercept beam irradiance. The measurements on E_{vg} and E_{vd} are widely available around the world by local Met Offices. In real light pipe applications, trees and buildings that obscure part of sky diffuse light and sometimes sun beam reduce the input illuminance to the light pipe systems. Under such conditions, to apply the proposed

model, total available illuminance need to be estimated based on E_{vg} and E_{vd} data available from local Met Offices.

Napier University CIE first-class solar radiation station is currently using the shadow band device to provide the horizontal diffuse irradiance data. However, it is well known that the shadow band that is used to block the sunshine also shades some diffuse irradiance as well. Hence it is necessary to correct the measured diffuse irradiance obtained using the shadow band instrument. The most commonly used method to correct the shadow band diffuse data is the Drummond method. However, Drummond method is purely geometrical and therefore underestimates the true diffuse value. To obtain a more accurate estimation of the true diffuse irradiance, new correction method based on anisotropy model shall be developed. Work carried out for this aim and conclusion drawn are reported in Chapter 7.

(6) In recent years, solar light pipes have firmly set their foot within the UK market place [15]. However, till this research no design tool for light pipe practices, which is based on sophisticated mathematical model, has been made available. The understanding of light pipe's daylighting performance by designers in the UK is neither clear nor more valid than limited experience, if there is. Moreover, because the lack of model that can predict the performance of light pipes, the assessment of the potential contribution of daylighting using due product to energy saving is rather crude and empirical. Research on identifying the potential barriers to exploit daylight in Britain [10] concluded that, to increase the exploitation of daylight in the UK it appears necessary to overcome, by education and demonstration, countervailing tendencies hold by those designers who are lack of credence on daylighting. Therefore, work of producing a convenient design guideline for light pipe practices, which is based on the proposed mathematical model, is suggested. The proposed model also enables the estimation of electricity saving due to light pipe applications under the UK climate, which can provide useful information base for national policy decision-makers. This work is reported in Chapter 8.

(7) During the course of present research, the commercial development of light pipe in the UK has been quite rapid. One main progress in improving light pipe's daylighting performance is the application of translucent type of diffuser. Therefore it would be worth to investigate the effect of using new type of diffuser on light pipe's daylighting performance. These work are addressed in Chapter 6.

(8) Daylight factor has been accepted as an industry standard for window design. However, for innovative daylighting devices and some of the new designs, especially those that utilize not only sky-light but also sunlight, to date no general method is available to assess their daylighting performance. Based on the concept of light pipe daylight penetration factor, DPF, introduced in present study along with other well-established design methods such as daylight coefficient a reference method may be adopted for an agreed standard. In this respect, it will avail to propose an approach based on a Figure of Merit (FoM) to the purpose of introducing a general method for assessing all daylighting devices. Work on this is reported in Chapters 6 and 9.

REFERENCES

1. http://WWW.bp.com/worldenergy/

2. Muneer, T. (1991) Blow for N-plants on global warming *The Scotsman* 3 June

3.The Department of Trade and Industry (2000) *UK Energy Flows 1998*

4.The Department of Trade and Industry (1999) *UK Energy Sector Indicators*, 6

5. Muneer, T. (1997) *Solar radiation & daylight models for the energy efficient design of buildings*, Architectural Press, Oxford

6. Zhang, X and Muneer, T. (2000) A Mathematical Model for the Performance of Light pipes *Lighting Research and Technology*, 32 (3), 141-146

7. http://www.hao.ucar.edu/public/education/general/general.html

8. Hopkinson, R. G., Petherbridge, P., and Longmore J. (1963) *Daylighting*, Heinemann, London

9. Littlefair, P. J. (1989) Innovative daylighting systems, *Designing for Natural and Artificial Lighting*, Building Research Establishment

10. Crisp, V. H. S. and Littlefair, P. J., Cooper, I. and McKennan G. (1988) *Daylighting as a Passive Solar Energy Option: an assessment of its potential in non-domestic buildings*, Building Research Establishment Report, ISBN 0851252877

11. Muneer, T., Abodahab, N., Weir, G., Kubie, J. (2000) *Windows in Buildings – thermal, acoustic visual and solar performance.* Architectural Press, Oxford

12. Shao, L. (1988) Mirror lightpipes: Daylighting performance in real buildings *Lighting Research and Technology*, 30 (1), 37-44

13. Yohannes, I. (2001) *Evaluation of the Performance of Light pipes Used in Offices*, PhD Thesis, Nottingham, Nottingham University

14. Oakley, G., Riffat, S. B. and Shao, L. (1999) Daylight performance of lightpipes *Proceedings of the CIBSE National Conference*, Harrogate, London, Chartered Institution of Building Services Engineers, 159-174

15. Zhang, X. and Muneer, T. (2002) A Design Guide for Performance Assessment of Solar Light pipes *Lighting Research and Technology*, 34(2), 149-169

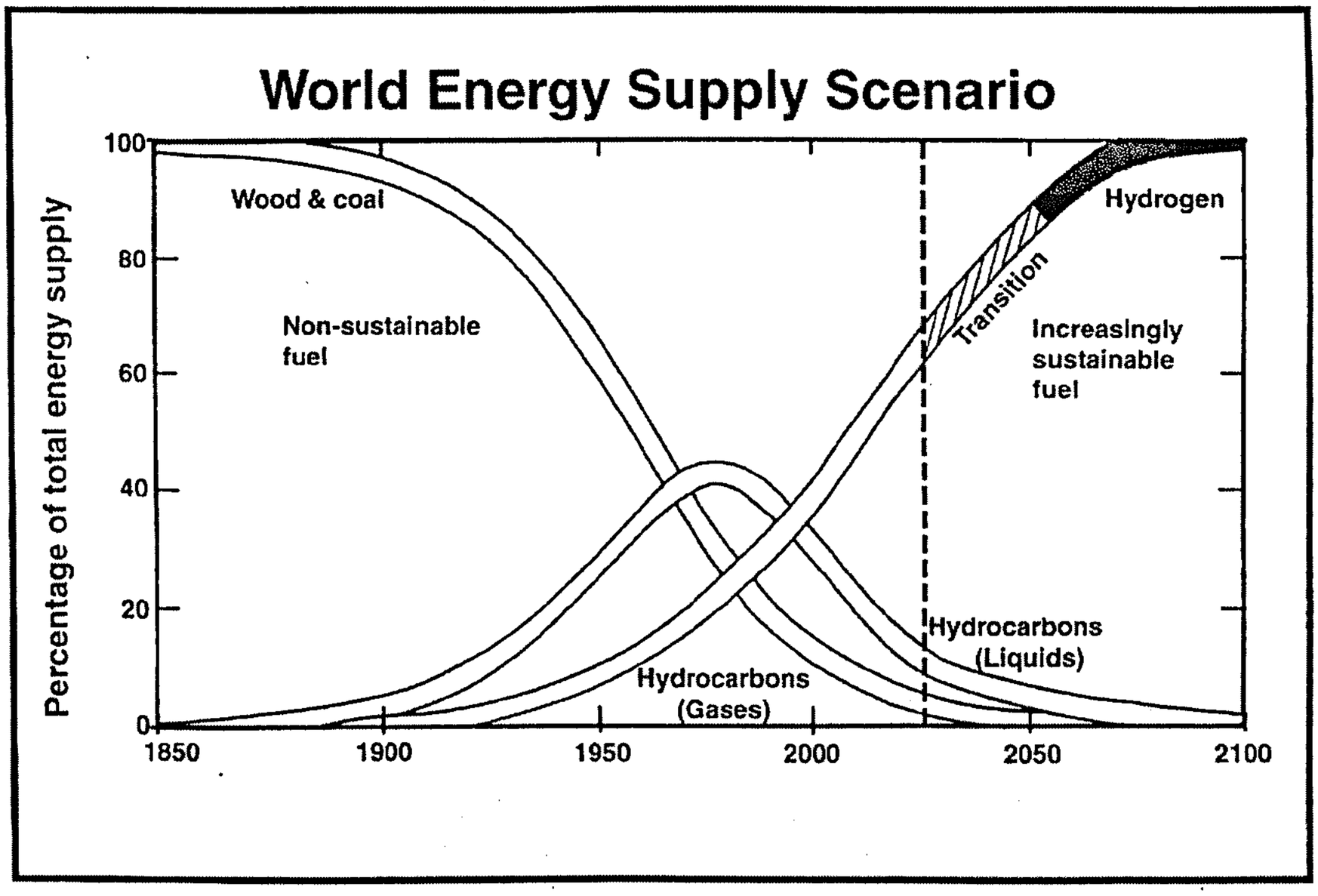

Figure 1.1 World energy supply scenario

dti
Department of Trade and Industry

UK ENERGY FLOWS 1998 (MILLION TONNES OF OIL EQUIVALENT)

A PUBLICATION OF THE GOVERNMENT STATISTICAL SERVICE

NATURAL GAS — IMPORTS
COAL — IMPORTS
ELECTRICITY — HYDRO, IMPORTS & SECONDARY ELECTRICITY
MANUFACTURED FUELS
PETROLEUM — CRUDE OIL AND NGL — IMPORTS
PETROLEUM — REFINED PRODUCTS — IMPORTS

PRIMARY SUPPLY[1] 243.9
PRIMARY DEMAND[1] 242.0

INDIGENOUS PRODUCTION AND IMPORTS [309.6]

NATURAL GAS 91.1
COAL 40.8
ELECTRICITY 25.2
PETROLEUM 209.7

Gas stocks
Coal stocks
Product stocks
Crude stocks
Primary supply 87.0
Primary demand 81.8
POWER STATIONS
OIL REFINERIES

EXPORTS AND MARINE BUNKERS 166.4

CONVERSION LOSSES 91.7
ENERGY INDUSTRY USE AND DISTRIBUTION LOSSES 25.6
NON-ENERGY USE 15.1

IRON & STEEL 4.4
OTHER INDUSTRY[1] 30.5
TRANSPORT 53.8
DOMESTIC[1] 46.0
OTHER FINAL CONSUMERS[1] 21.7

TOTAL FINAL CONSUMPTION [166.4]

FOOTNOTES

1. Includes renewables

2. This flow chart has been produced using the style of balance and figures in The 1999 UK Digest of Energy Statistics, Table 1.1.

Figure 1.2 UK Energy Flows 1998, dti, Department of Trade and Industry, 2000

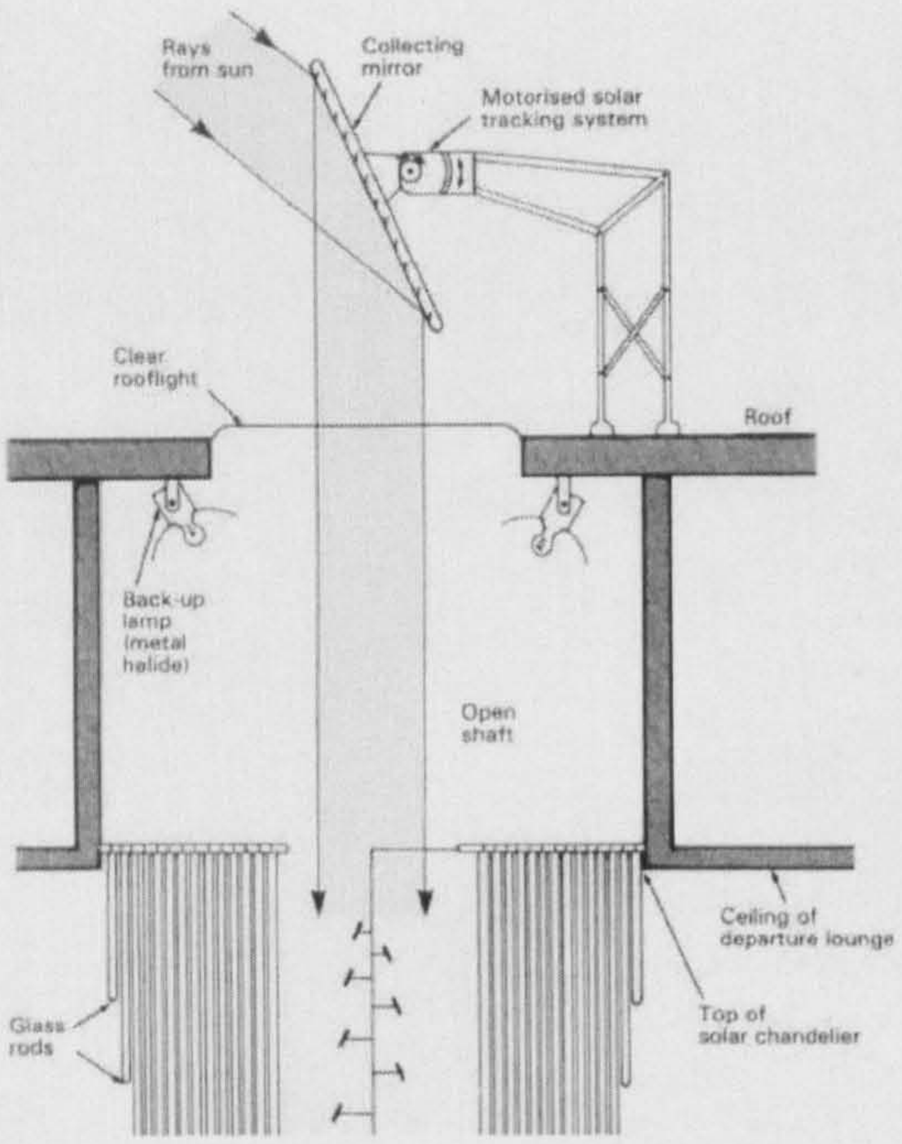

Figure 1.3 Manchester Airport departure lounge with solar chandeliers

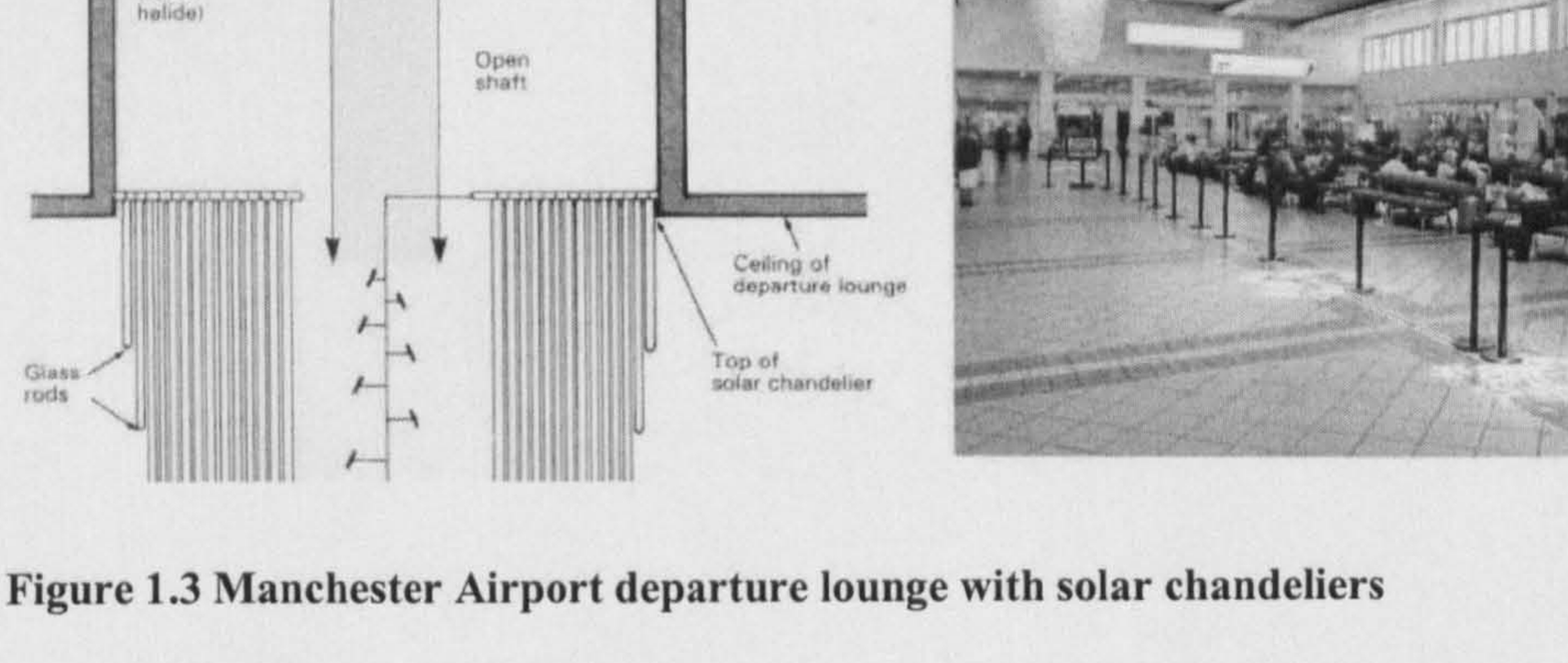

Figure 1.4 Beam sunlight in a side-lit room

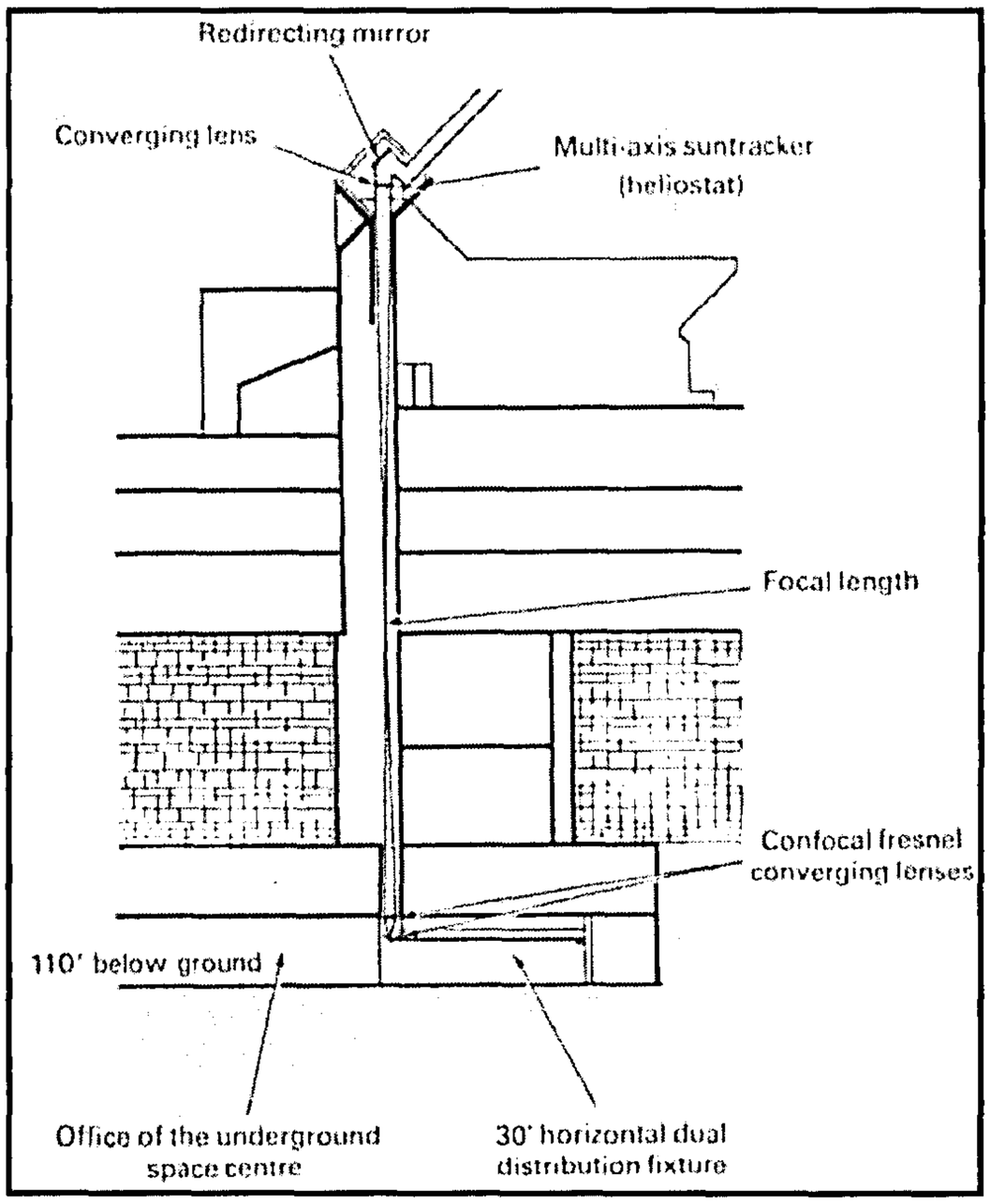

Figure 1.5 Underground daylighting at the Space Centre building, University of Minnesota, Minneapolis, USA

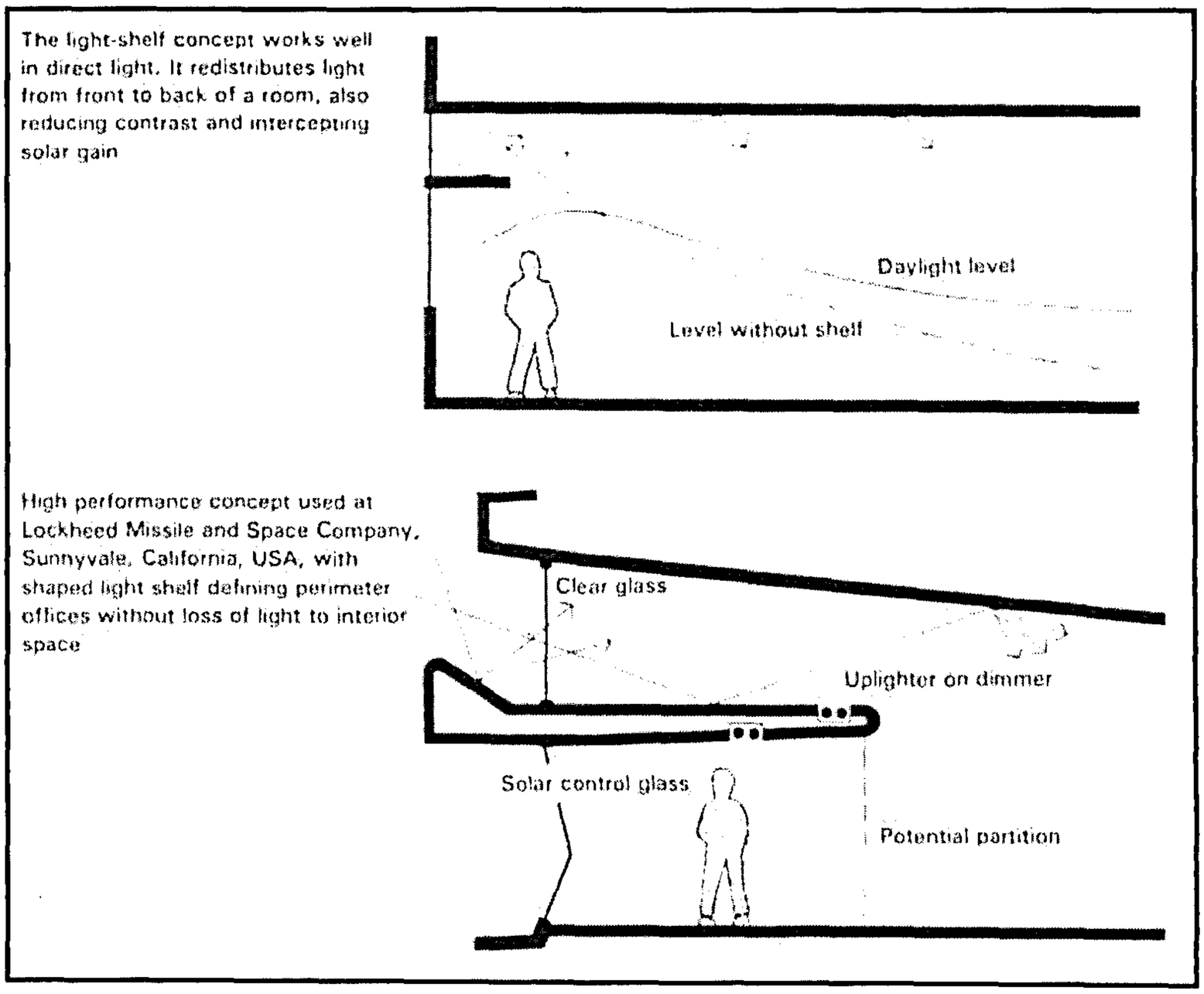

Figure 1.6 Concept of light shelves

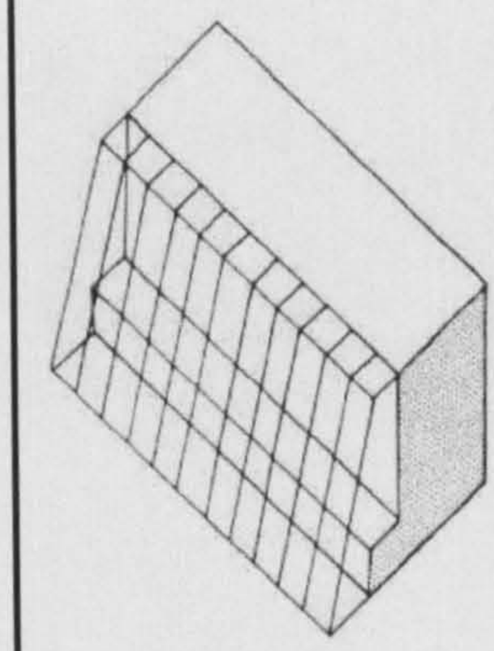

Single-sided or conservatory atrium

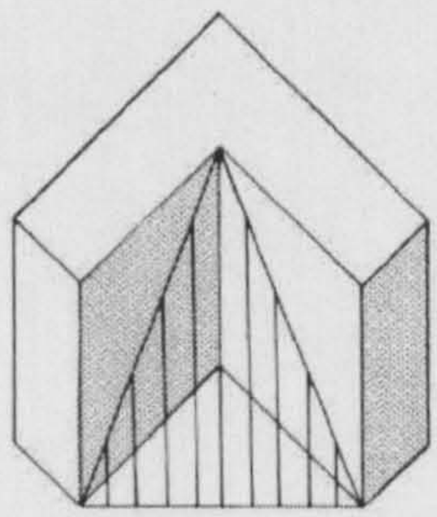

Two-sided atrium (two open sides)

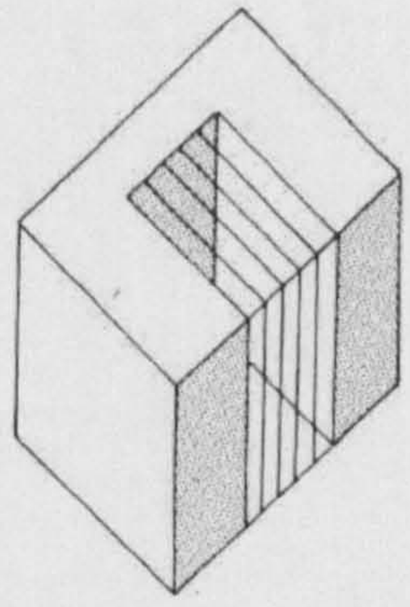

Three-sided atrium (one open side)

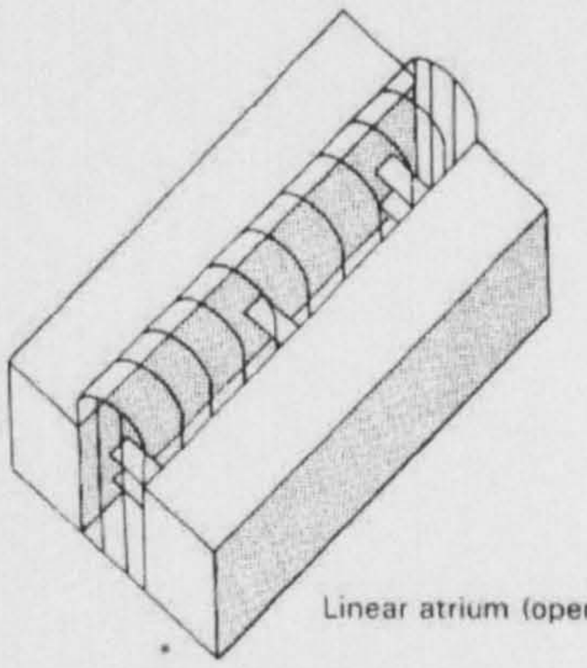

Linear atrium (open ends)

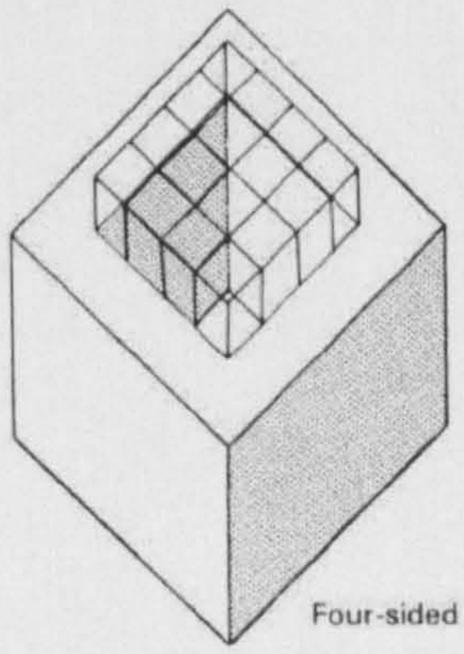

Four-sided atrium (no open sides)

Figure 1.7 Generic forms of atrium buildings

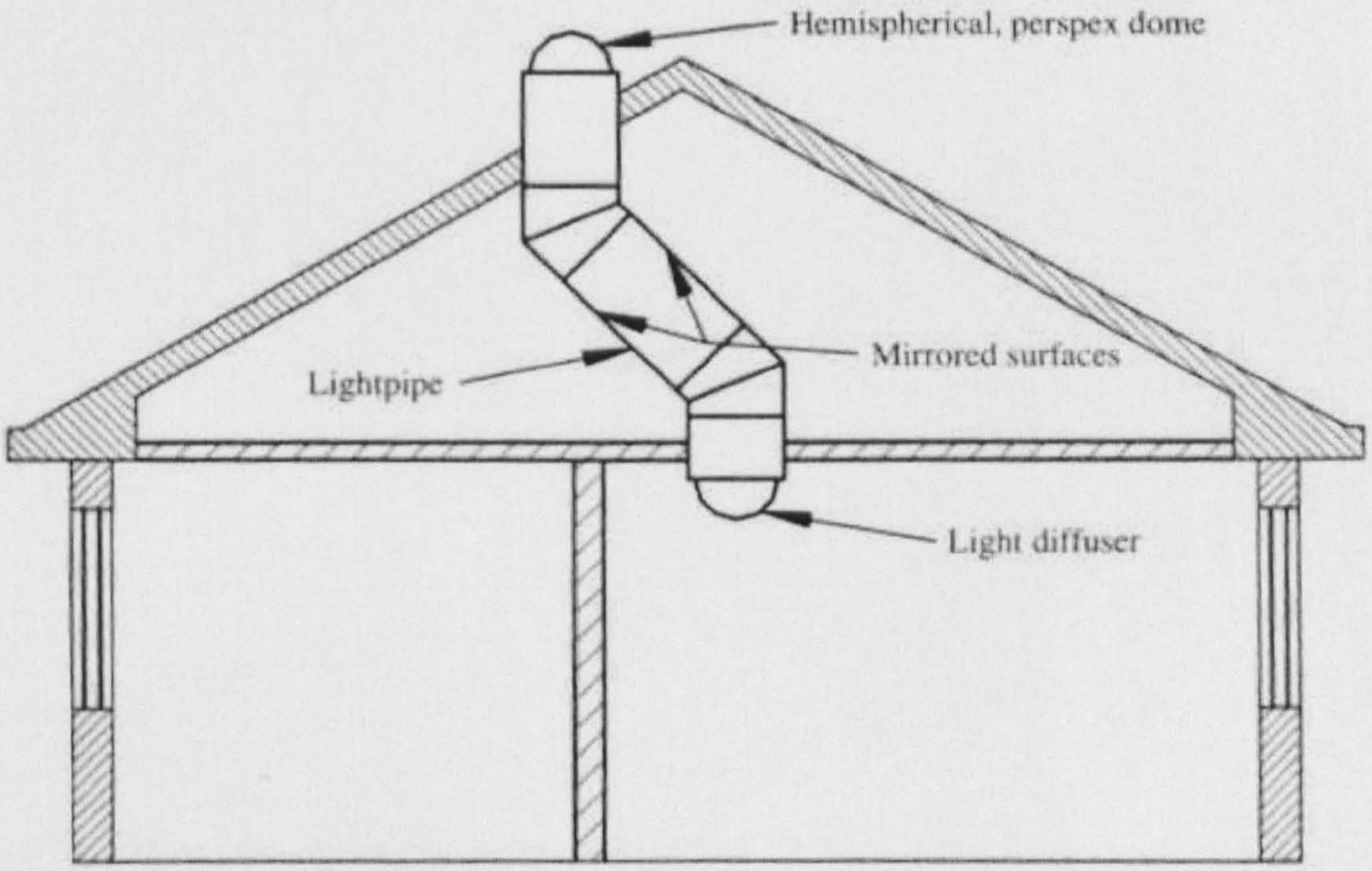

Figure 1.8 A schematic of light pipe system

Table 1.1 World fossil fuel reserves to production ratio, years (BP 1999 statistics)

North America	11
S & Central America	65
Europe	18
Africa	100
Asia Pacific	42
World	62

2. SOLAR LIGHT PIPE AS AN INNOVATIVE DAYLIGHTING DEVICE

The idea of piping light from a remote source to an interior space for illumination purpose appeared about 120 years ago. Originally designed to distribute central electronic light into buildings, light pipe is now being adopted and applied world-widely for both artificial and natural daylighting purposes. Commercially available light pipe systems that employ daylight as lighting source have been used in Australia, America, and Canada. Within Britain alone there are now a number of companies that are profitably trading daylighting light pipe, or called "solar light pipe" products and with an enviable growth rate. With the increasing use of solar light pipes, more attention is being paid to their development, especially to the daylighting performance evaluation of the device. Present study is the production of the prior development of light pipe, and at the same time aims at pushing a further development of this innovative device. It is therefore necessary and desirable to give a full context of the historical development of light pipe systems, so as to present the position and significance of present study.

2.1 THE DEVELOPMENT OF SOLAR LIGHT PIPE SYSTEM

The earliest formal record that can be found on light pipe innovation may be the patent that was registered in the United States by William Wheeler from the Massachusetts State in September 1881. This registered patent initially reified the idea of light pipe as an apparatus for lighting dwellings and other structures. This patented invention, relates to a system of lighting and to a special apparatus whereby any desired amount of the light-producing energy employed is converted into light-vibrations at a central or single place, from which the light generated is transmitted and distributed to and dispersed at any number of places which it is desired to illuminate by optical conduction, division, and dispersion of light [1]. It was indicated by the inventor that before this invention, there had been designs of transmitting beams, or said parallel rays, through enclosed passages and clear space to produce secondary lights from one luminary source for lighting purposes. Although the inventor outlined that light pipe is adaptable to any light sources, his design seemed not being able to utilize natural daylight as lighting source.

Nowadays, because the long distances over which light pipe can operate, it has been regarded as "perhaps the most technologically exciting innovative daylighting systems" [2]. Light pipe's advantage of being able to bring light into core areas within buildings has been noticed long time ago. Figure 2.1 shows an invention by Hanneborg from Norway in 1900 [3]. Sunlight is collected by a so-called "light-collector" placed on top of the roof and beamed through a vertical "light-conveyer" to the cellar, where a light distributor is placed for lighting the room. Another near example of the same sort is the light pipe system in the University of Minnesota, as shown in Fig. 1.5. Sunlight is collected by a heliostat on the roof and beamed through lenses to a working place 110 ft below the ground. Above two light pipe systems can be called as "Heliostats light pipe" systems. Heliostats light pipe system mainly relies on optical devices, namely mirrors and lenses to collect and transmit sunlight. The common feature of Heliostats light pipe systems is the use of device that can track the sun at times. Due to the costly expense and complex control required by the sun-track device, this sort of light pipe system has not been widely used.

Having realized the drawback of "Heliostats light pipe" system, during the last five or six decades, researchers made most efforts to develop more cost-effective light pipe system. Research has been focused on improving the transmittance of the "tube" part of light pipe systems, to avoid the dependence upon sun-tracking devices, mirrors and lenses. The most basic form of light pipe tube is simply an empty shaft with ordinary mirrors on the walls, along which a collimated beam of light can travel [4]. Reflective metal tubes was proposed but any off-axis light has to undergo multiple reflections, with the result that only closely collimated beams do not become attenuated after a few metres within the tube [2]. Fibre optic bundles can have very good transmission characteristics [5], but tend to be prohibitively expensive [6].

In 1980s, new development of highly reflective materials emerged. Whitehead et al [4,7,8] proposed a hollow acrylic prismatic light tube that has a transmittance of between 0.95 and 0.97. At the same time, different approaches have been taken to improve the light transmittance of light tube. One example is the application of metallic coating and finishing technique to the inner surface of light tube. Another notable progress in this respect is the use of PET (Polyethylene terephthalate) film. The appearance of above techniques has accelerated the development of light pipe systems.

In 1990s, innovations of light pipes by different inventors emerged in endlessly. Sutton patented a "tubular skylight" in 1994 in the USA [9], as shown in Fig. 2.2. According to Sutton, the system comprises a tubular body, a first transparent cover and a second transparent cover. The material of the tubular body is either metal, fibre or plastics, and has a finish which is a highly reflective polish or coating, as found on "1150 alloy aluminium", electroplating, anodising or metalized plastic film. As a device to enhance the performance of the said system, a reflector is located within light-permeable chamber and extending above the roof, to collect more sunlight incident into the system.

In 1996 however, Bixby pointed out that above Sutton's invention "requires the use of a reflector located within the light-permeable chamber and mounted above the roof line. Even when strategically positioned along the path of the sun, the use of an above roof reflector blocks a significant portion of the sunlight which would otherwise enter the system and illuminate the building if the reflector was not present". Bixby registered his invention of tubular skylight for natural light illumination of residential and commercial buildings in 1996 [10]. Figure 2.3 shows the Bixby tubular skylight system. Bixby's system comprises a highly reflective tubular body positioned in the space between a building's roof and ceiling with a first end with a semi-spherical transparent globe attached to a roof assembly, and a second end attached to a ceiling assembly. The ceiling assembly comprises a semi-spherical, light diffusing cap and a molded ceiling mount with a straight sleeve.

The development of solar light pipe has been an on-going process. The latest development on improving the collimation of internal daylight delivered by light pipes has been reported by O'Neil [11]. Compared to previous arts of light pipe system, O'Neil's tubular skylight uses light tube of cone shape instead of straight column shape. Figure 2.4 shows the comparison. The cone shaped reflective tube is constructed with a larger cross sectional area near the radiant energy-delivering aperture than near the radiant energy-collecting aperture. By this new design, the collected daylight can be collimated and delivered to the desired area of the room directly beneath the luminaire. According to O'Neil, "as proven by experimental results, the new passive collimating tubular skylight provides significant advantages over the prior art, including better solar energy collection, higher throughput optical efficiency, improved radiant energy collimation, enhanced interior illumination levels, and more

precise positional control of the interior illumination". However, O'Neil did not give sufficient and detailed information on the type and material of the luminaire being used in his design. As an integral part of light pipe system, the design and property of the energy-delivering aperture, or called luminaire, or diffuser by some literature, has been found having important effect on the daylighting performance of the system [12,13]. Therefore, in practical applications, the design of light pipe systems needs to take account of the design of luminaire.

An English company, Monodraught, have been manufacturing and trading light pipe systems successfully within Europe. By the year of 2000, more than 3000 Monodraught light pipe systems have been installed throughout the UK in comparison with the figure of about 50 for the year 1997. Monodraught light pipe systems adopt diffusers of various property and design according to different needs in real practices. A typical Monodraught light pipe system is shown in Fig. 2.5. Daylight is gathered via a polycarbonate dome at roof level and then transmitted downwards to interior spaces within buildings. The light-reflecting tube is adaptable to incorporate any bends around building structural components. The internal surface of the light tube is laminated with Reflectalite 600, a silverised PET film [14]. The reflective silver layer is sandwiched between the PET film and the aluminium base, which helps in achieving a reasonable illuminance indoors when daylight is introduced via a light diffuser.

There are various kinds of diffusers that can be employed in Monodraught light pipe system, including dome opal, dome clear, recessed opal and recessed clear diffusers. The recessed diffusers are more effective in keeping out dust and preventing heat loss. Opal diffusers are of better diffusive property, and hence enable an even spread of daylight within the interior, while clear diffusers possess a better transparency and therefore can maximum the penetration of daylight. In occasions where soft and uniform daylighting is required, the former kind of diffuser has been widely used. For application like open space in deep-plan buildings and corridors where the brightness becomes priority, the latter kind of diffuser is more suitable. The development of light pipe diffuser is an on-going process. News from Monodraught reports that a new type of diffuser of diamond shape is being developed and will be introduced into the market place soon.

As a conclusion, the development of solar light pipe system has been continuing ever since 100 years ago. Although historically there have been light pipe system of various designs, they generally have three main components, namely the daylight collecting device, daylight transmitting device and daylight emitting device. Accordingly, the development of light pipe art has been focusing on these three components. It has been realized that the improvements on each part of light pipe system will upgrade the total daylighting performance of the system. However, to date no general method has been made available to evaluate and compare the performance of various light pipe systems. One major aim of present study is to establish a generalized standard by which light pipe systems can be compared against each other, or even against other daylighting devices like windows. With the aid of such a proposed generalized standard, it is hoped that the development of light pipe family can be more systematic and clearer.

2.2 THE CONCEPT OF LIGHT PIPE

The term of light pipe has been long used to name the family of non-image devices that can transmit light from either artificial or natural light source to building interiors for lighting purpose. Because the development and application of light pipes to modern buildings have been new and fast, so far no international standardized categorizing and / or naming system has been made available to define and describe the content of the family. It is possible however, as a first step, to divide the huge light pipe family into three groups. The three groups are first, light pipes using artificial lighting as light source; second, light pipes using external daylight as light source and the third, light pipes using both artificial light and external daylight as light sources. The light pipe group that uses external daylight as light source is also widely called solar light pipe since the ultimate source of daylight is the sun. As addressed in Introduction, because the present study emphasizes the significance of utilizing and exploiting renewable energy, solar light pipe is the main concern of present research.

Within the group of solar light pipe, further classification can be defined. The CIE has set up a committee TC 3-38 to establish an international standard as a framework for guiding and regulating the development of solar light pipe systems. One major issue on the standardization identified by the TC 3-38 is what constitutes a solar light pipe system. The answer to this question has been given as, there are three major types defined by their collecting methods - active zenithal (e.g. Heliostat systems), passive

zenithal (e.g. commercially available Solatube, Sunscope, Sunpipe etc systems) and horizontal (e.g. anidolic ceilings). Among above three types, the passive zenithal tubular light pipe has become the most widely used solar light pipe system. The family map of light pipe system is now shown in Fig. 2.6. Present research focuses on the daylighting performance of passive solar zenithal tubular light pipe systems. In the following body of this thesis, if not specified, the name of "light pipe" refers to passive solar zenithal tubular light pipe.

A passive solar zenithal tubular light pipe system can be defined as a tubular vertical light guidance system that passively collects and transmits external natural daylight to building interiors for lighting purpose. A scheme of two typical passive solar zenithal tubular light pipe systems is shown in Fig. 2.7. Typical passive solar zenithal tubular light pipe system has three components, namely fixed daylight collection device, tubular light guide that employs internal reflection mechanism for daylight transmission, and light-demitting apparatus for dispersing daylight into designated areas.

2.3 THE STRUCTURE OF PASSIVE SOLAR ZENITHAL TUBULAR LIGHT PIPE

Passive solar zenithal tubular light pipe is the most commercially available light pipe system in the UK market place. Light pipes provided by different traders or manufacturers are to various extent slightly different from each other. For example, a light pipe company may have their own-patented technique in fixing the light tube on or within a roof structure, or in preventing leakage of rain. However, in terms of their basic structure, light pipes by different makers are generally the same.

The majority of commercially available light pipes consist of three main components associated with sealing components. The three main components are daylight collector, light pipe tube and diffuser. Daylight collector is fitted at the top end of the light tube, usually on the roof, which acts as a semi-lens to collect daylight and as a cap to prevent the ingress of water and dust. At the bottom end of the pipe fitted the diffuser, usually to the ceiling to allow the distribution of the daylight into the interior room space. Properties of main components of light pipe are described below.

2.3.1 The daylight collector

Daylight collector is a clear dome that is mounted on the outside of the roof. The dome is manufactured from clean polycarbonate that removes undesirable ultra violet (UV) light and seals the light pipe against ingress of dust and rain. The dome usually meet the requirements of fire resistance and due to its shape is self-cleaning.

2.3.2 The light pipe tube

The pipe is constructed from a metal tube, typically of alloy aluminium material. The inner surface of the tube is laminated by applying metalize PET (Polyethylene Terephthalate) film or TIR (Total Internal Reflective) prismatic optic film. Figure 2.8, for instance shows a Monodraught (UK) light tube that uses Reflectalite 600, a silverised PET film as its internal reflective coat. The reflective silver layer is sandwiched between the PET file and the aluminium base substrate. The presence of an UV inhibitor in the Reflectalite provides outstanding QUV durability with no delamination and with no decrease in total reflectance when subjected to the extreme conditions of UV light.

2.3.3 The diffuser

The diffuser takes the form of a white polycarbonate dome mounted on the ceiling inside the room to be illuminated. The material of diffuser vary in its property of transparency, so as to meet different needs for light distribution within the room. For example opal diffusers, which are made of semi-translucent polycarbonate material, are usually applied in places where uniform daylighting is required. While clear diffusers, which are made of transparent polycarbonate materials are preferred in applications such as corridors in deep-plan buildings where the quantity of light becomes priority.

The shape of a diffuser can be flat, convex, and concave. Monodraught (UK) has recently developed a new range of diffusers that are manufactured from clear polycarbonate with a crystal effect finish. The development of a new type of diffuser of diamond shape is also underway. Figure 2.9 shows the appearances of different types of diffuser, and Fig. 2.10 demonstrates the different daylighting effects achieved by a clear diffuser and an opal diffuser respectively.

2.3.4 Sealing components

The application of light pipe systems requires the installation of sealing components to the purpose of achieving high heat resistance and preventing solar gain. The seal of the light tube is also important to keep dust, noise, insects, rain and snow out of the building interiors. A brushed nylon gasket at the top of the pipe prevents condensation, dust and rain from entering the system but still allows the airs to expand and contract when subject to solar gain. The closed cell gasket at ceiling level seals the daylight collector and all the vertical joints are sealed with silicon and aluminium tape.

2.3.5 Complete light pipe system

An exploded view of a typical light pipe system, by Monodraught (UK) is shown in Fig. 2.11, all the main components and associated sealing components are shown.

2.4 WORKING MECHANISM OF LIGHT PIPE

Passive solar tubular light pipes are designed to collect light from both the sky and the sun. The two components of daylight illuminance are collected by the hemisphere shaped dome, followed by multiple reflection of sunlight and skylight through the reflecting tube. Daylight then reaches the inner surface of the light pipe diffuser wherein a refraction followed by a light-scattering takes place before it is introduced within buildings. Figure 2.12 shows the general process of daylight collection, transmission and distribution within buildings. The complexity of light pipe's working mechanism consists three aspects, namely the optical process, the external daylight environment and the design of light pipe. The three aspects are analysed as follows.

2.4.1 Optical process

The first aspect is the complicated optical process that takes place within light tubes and diffusers. Initially daylight collected by dome enters light pipe, then a mixed multi-reflection of sunlight and sky diffuse illuminances occurs when daylight is transmitted through and diffused within the light tube.

After that, a refraction phenomenon happens in light pipe diffuser when diffused sunlight and sky diffuse illuminances are further diffused and finally scattered into the interior space.

2.4.2 External daylight environment

The second aspect is the complexity of external daylight as the input to the light pipe system. Throughout the year, the quantity and proportion of sunlight and sky diffuse radiation are not constant. When sunlight is available, the change of sun's position causes the variation of the incident angle at which the sunray enters light tube. This implicates that the pattern sunlight travel through light tube is continuously changing when sunlight is available (Fig. 2.13). When the sky is overcast or when clouds block the sun, skylight becomes the major external daylight source. However, it is well known that the luminance distribution of the sky is not uniform. The sky vault can be divided into small patches as shown in Fig. 2.14. Each sky patch has its own position and brightness; so the transmission of the sky illuminance from each patches various. Furthermore, the sky illuminance distribution is affected by the position of sun, the clarity of the sky, the position of random clouds and so on. Therefore, the process of sky-light entering light tube and travelling within the tube is a highly dynamic process. Figure 2.14 shows the sky illuminance emitted from one sky patch enters and travels within the light tube.

2.4.3 The design of light pipe

The third aspect is the design of light pipes. Light pipes vary in their geometric configurations, including the length, the width and the number of bends incorporated in a light pipe system. Light tubes applying different internal coating have different internal reflectance. For a given external environment and at a given point of time, light pipes of different configurations and having different internal coating materials produce different daylighting performance. For any given weather condition and sun's position, the cross area of a light pipe, affects the light pipe's external illuminance admittance. Since the daylight illuminance is transmitted by means of internal reflection within the light tube, and the reflectance although usually high is less than 1, a light pipe's overall transmittance is affected by the number of reflections required for a ray of light to descend the light tube and the tube's reflectance. The higher the internal reflectance of the light tube, the higher is the system's daylight transmittance.

The less the number of reflection required to descent the entire light tube, the better would be the system's performance.

2.5 SUMMARY

The idea of piping light from a central artificial light source to building interiors for lighting purpose emerged more than one century ago. However, the development of guiding daylight into buildings for daylighting purpose is new. In the last two decades, the breakthrough in terms of new reflective materials and processing technique accelerated the development of light pipes. The most commercially available light pipe is the passive solar zenithal tubular light pipe. Present study focuses on the daylighting performance measurement, modelling and prediction of this kind of light pipe.

The working mechanism of passive solar tubular light pipe is complicated. The difficulties in identifying all decisive factors that affect the performance, and in quantitatively weighing the contributions of these decisive factors have been the main barrier to appraising light pipe's efficiency. Present study aims to conquer this barrier so as to push further the development of light pipe systems.

REFERENCES

1. Wheeler, W. (1881) U.S. Patent No. 247229, United States Patent and Trademark Offfice, http://www.uspto.gov

2. Littlefair, P. J. (1990) Innovative daylighting: Review of systems and evaluation methods *Lighting Research and Technology*, 22(1), 1-17

3.Hanneborg, O. B. H (1901) U.S. Patent No. 668404, United States Patent and Trademark Offfice, http://www.uspto.gov

4. Whitehead, L. A., Brown, D. N. and Nodwell, R A. (1984) A new device for distributing concentrated sunlight in building interiors *Energy and Buildings*, 6(2), 119-125

5. Fraas, L. M., Pyle, W. R. and Ryason, P. R. (1983) Concentrated and piped sunlight for indoor illumination, *Applied Optics*, 22(4), 578-582

6. Smart, M. and Ballinger, J. (1976) Tracking mirror beam sunlighting for interior spaces, *Solar Energy*, 12(5), 12-19

7. Whitehead, L. A., Nodwell, R. A. and Curzon, L. (1982) New efficient light guide for interior illumination, *Applied Optics* 21(15), 2755-2757

8. Whitehead, L. A., Scott, J. E., Lee, B. and York, B. (1986) Large-scale core daylighting by means of a light pipe, *Proceedings of the 2nd Internatinal Daylighting Conference*, Long Beach, Mclean, VA: Cable Associates, 416-419

9. Steven, M. and Sutton (1992) U.S Patent No. 5,099,622, United States Patent and Trademark Offfice, http://www.uspto.gov

10. Joseph, A. and Bixby (1996) U.S. Patent No. 5,546,712, United States Patent and Trademark Offfice, http://www.uspto.gov

11.O'Neil, M. (2002) U.S. Patent No. 6,363,667, United States Patent and Trademark Offfice, http://www.uspto.gov

12. Edmonds, I. R., Moore G. I., Smith G. B. and Swift P. D. (1995) Daylighting enhancement with light pipes coupled to laser-cut light-deflecting panels *Lighting Research and Technology*, 27(1), 27-35

13. Carter, D. J. (2002) The measured and predicted performance of passive solar light pipe systems *Lighting research and Technology*, 34(1), 39-52

14. http://www.solarsaver.co.uk/Monodraught/sunpipe/inf-com.htm

No. 668,404. Patented Feb. 19, 1901.

O. B. H. HANNEBORG.

APPARATUS FOR TRANSMITTING SUNLIGHT TO BASEMENTS OR OTHER STORIES.

(Application filed Feb. 26, 1900.)

(No Model.)

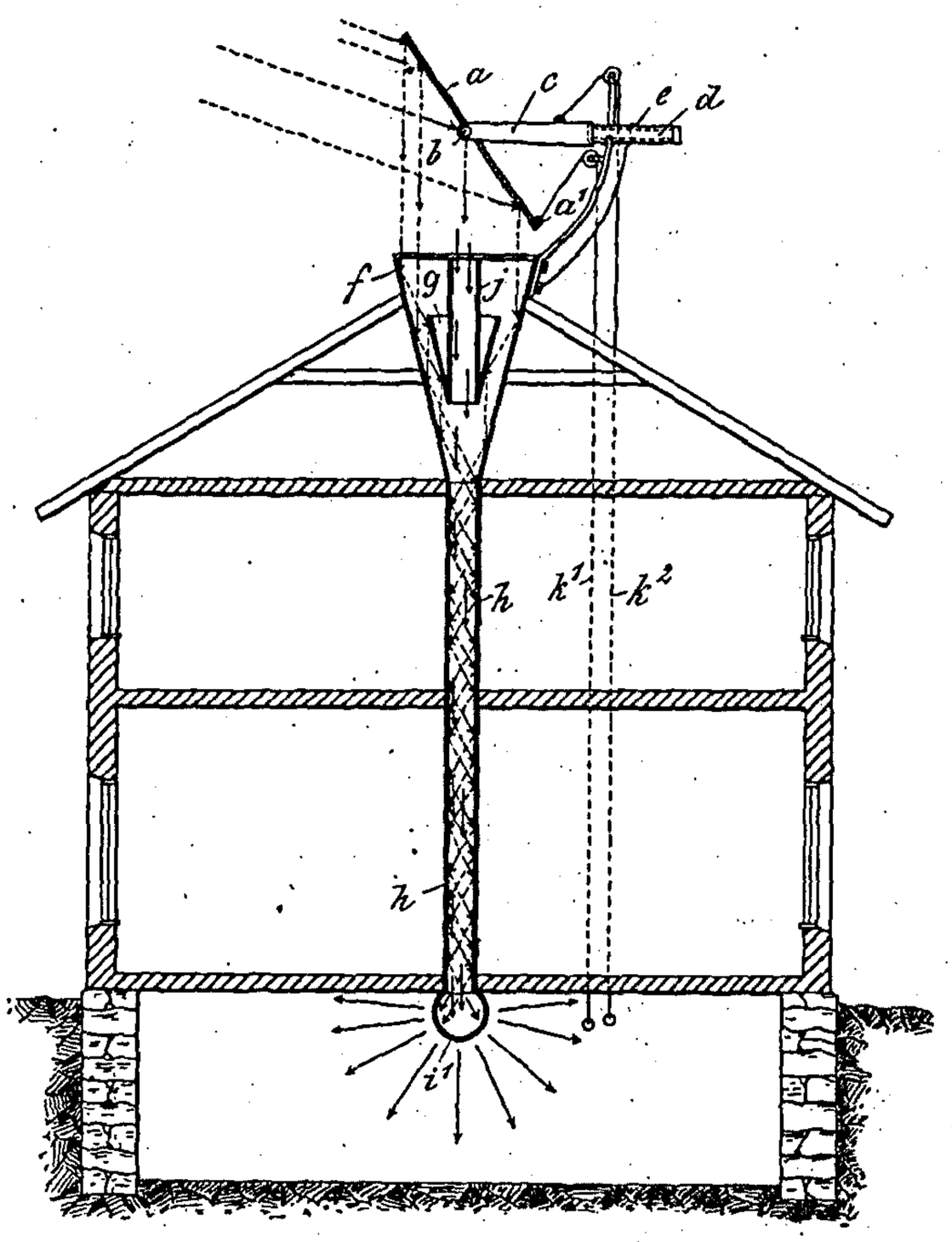

Witnesses:
Ella L. Giles
Attorney

Inventor:
O. B. H. Hanneborg.
per Richards
Attorneys

THE NORRIS PETERS CO., PHOTO-LITHO., WASHINGTON, D. C.

Figure 2.1 Invention by Hanneborg from Norway in 1900: apparatus for transmitting sunlight into basements or other stores (Ref.3)

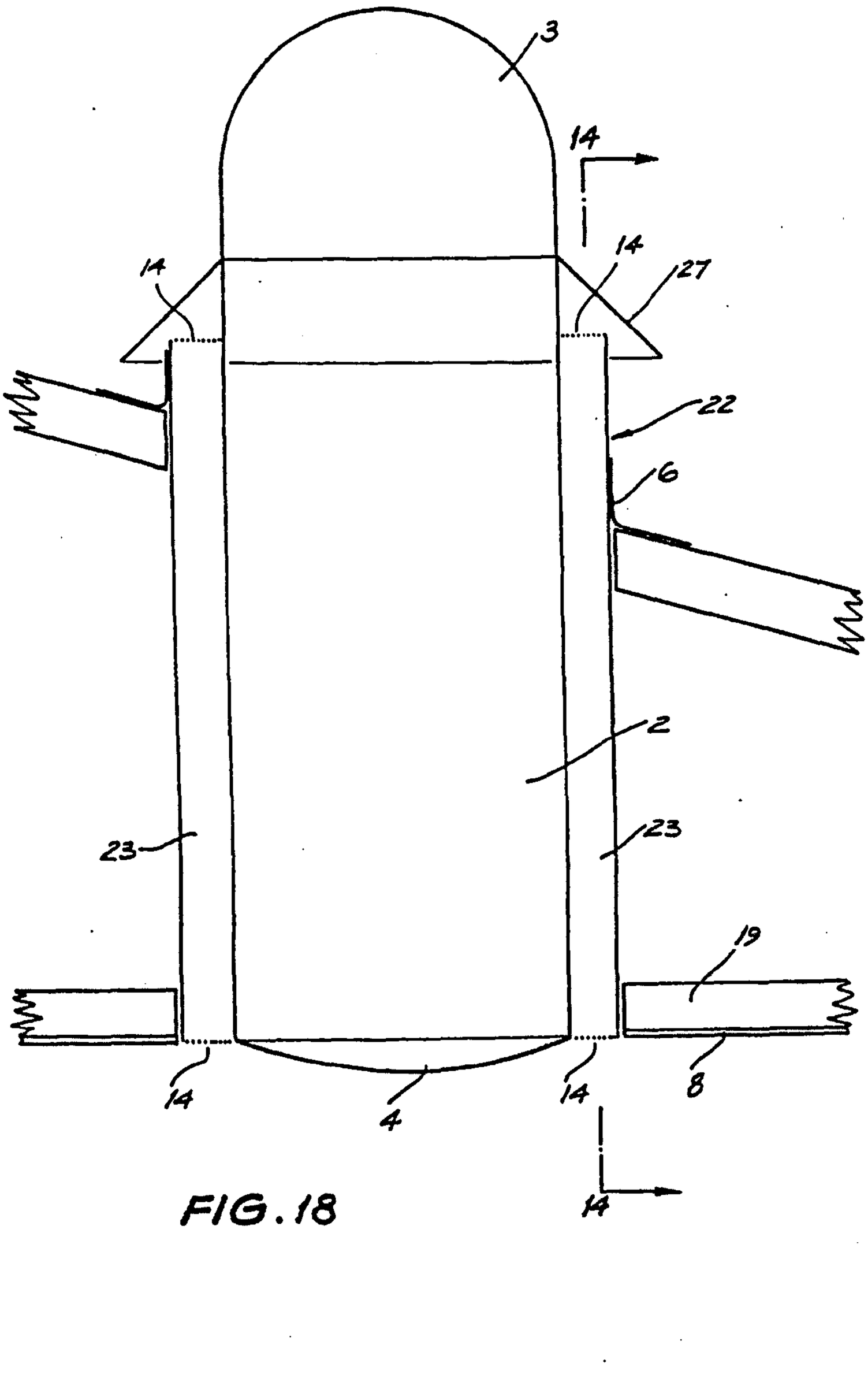

FIG. 18

Figure 2.2 Sutton patented tubular skylight in 1994 in the USA

FIG. 1

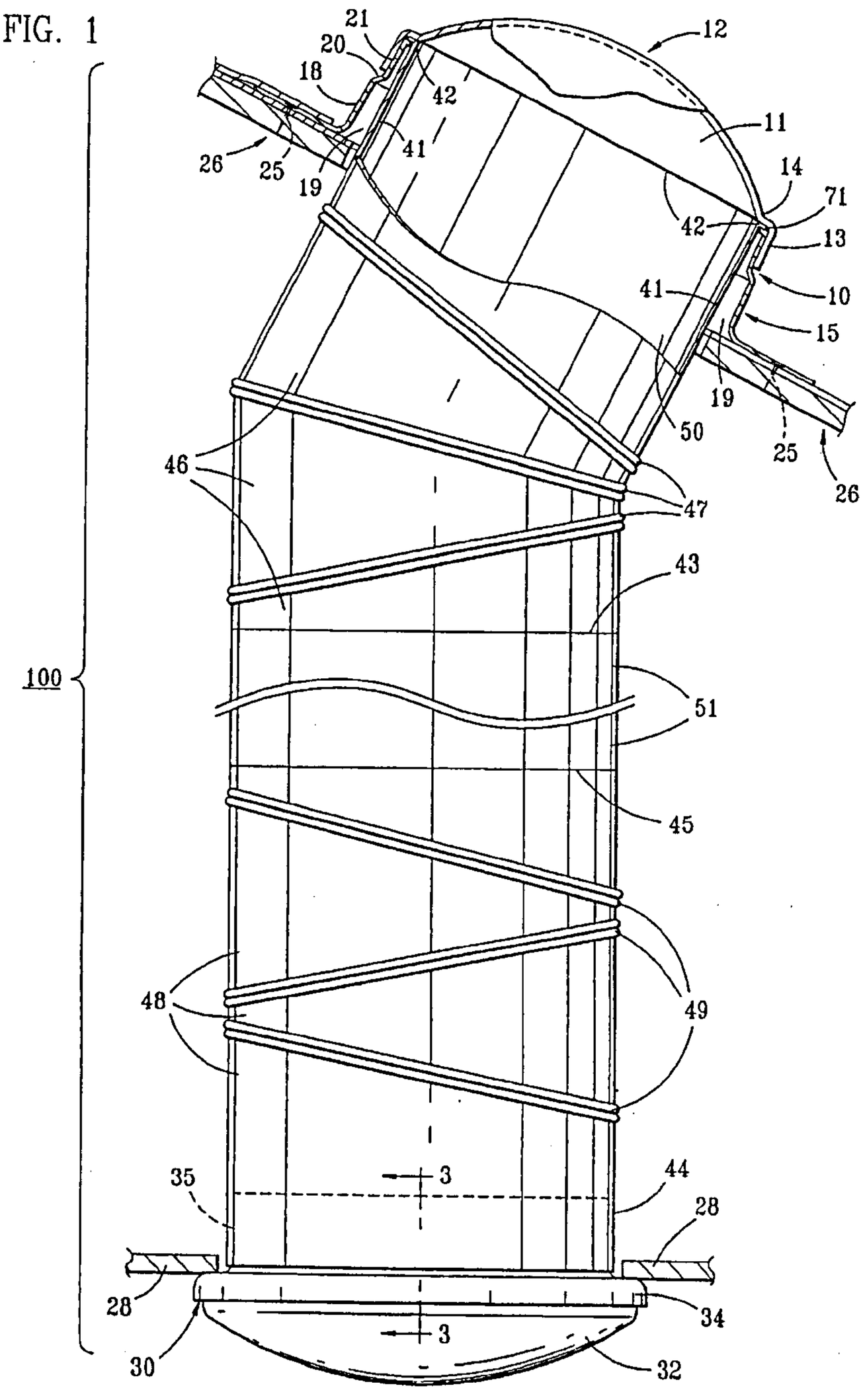

Figure 2.3 Bixby tubular skylight systems

Fig. 2 A

Prior Art

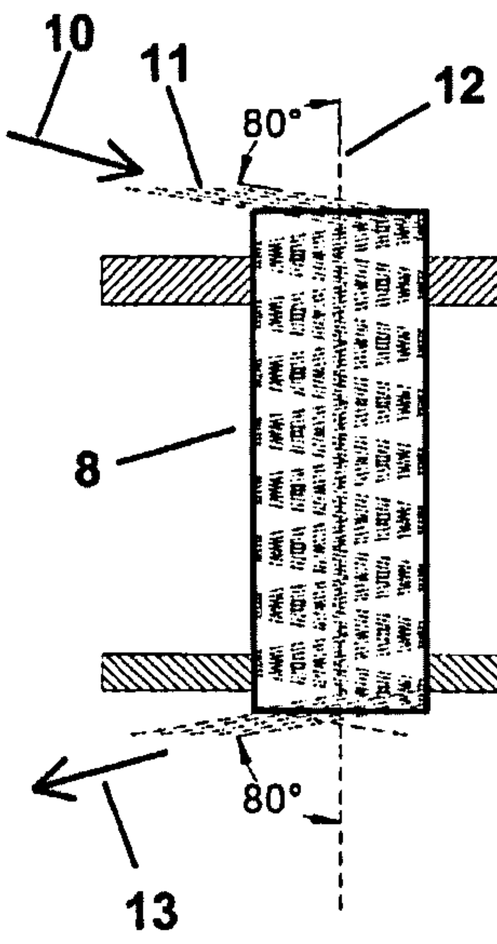

Fig. 2 B

Improved

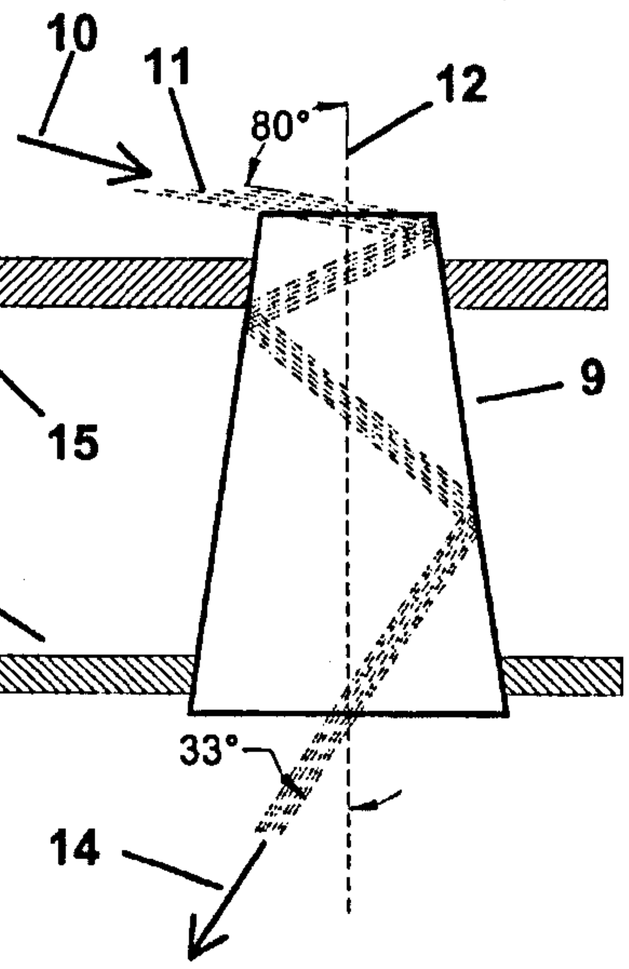

Figure 2.4 Comparison of O'Neil's cone shaped light tube against conventional column light tube

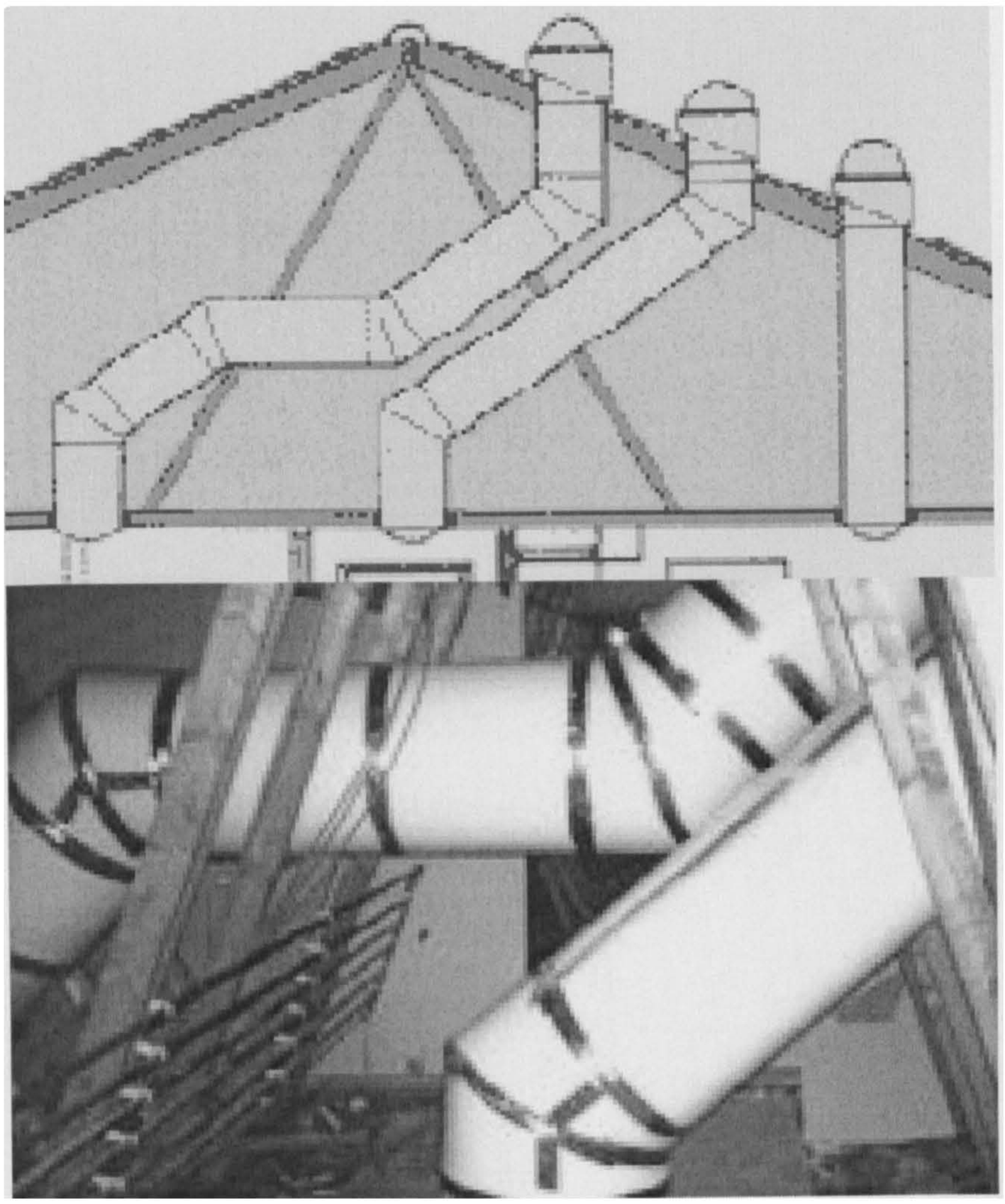

Figure 2.5 Typical Monodraught light pipes

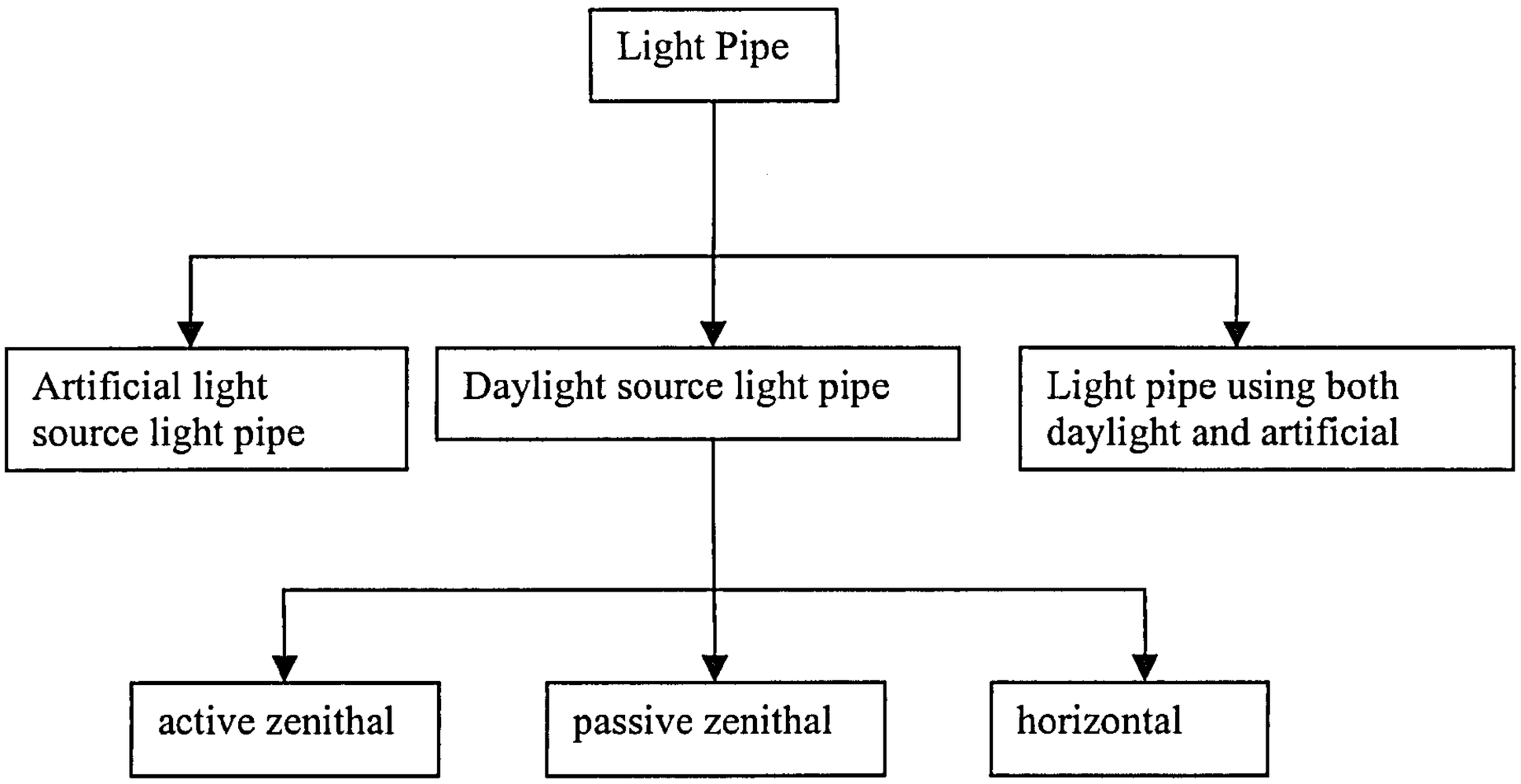

Figure 2.6 The family map of light pipe

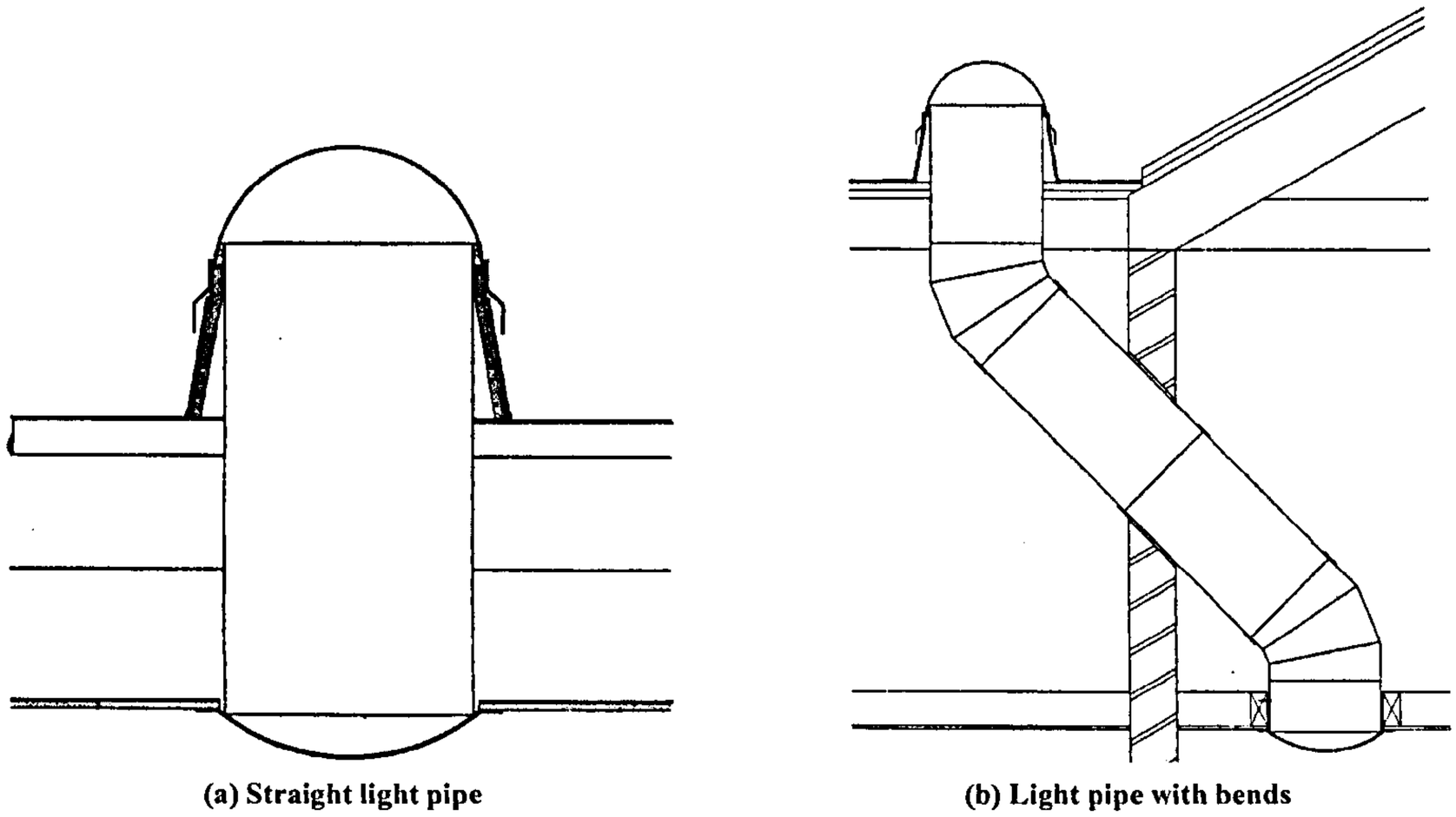

(a) Straight light pipe **(b) Light pipe with bends**

Figure 2.7 Schematic diagram of passive solar zenithal tubular light pipe

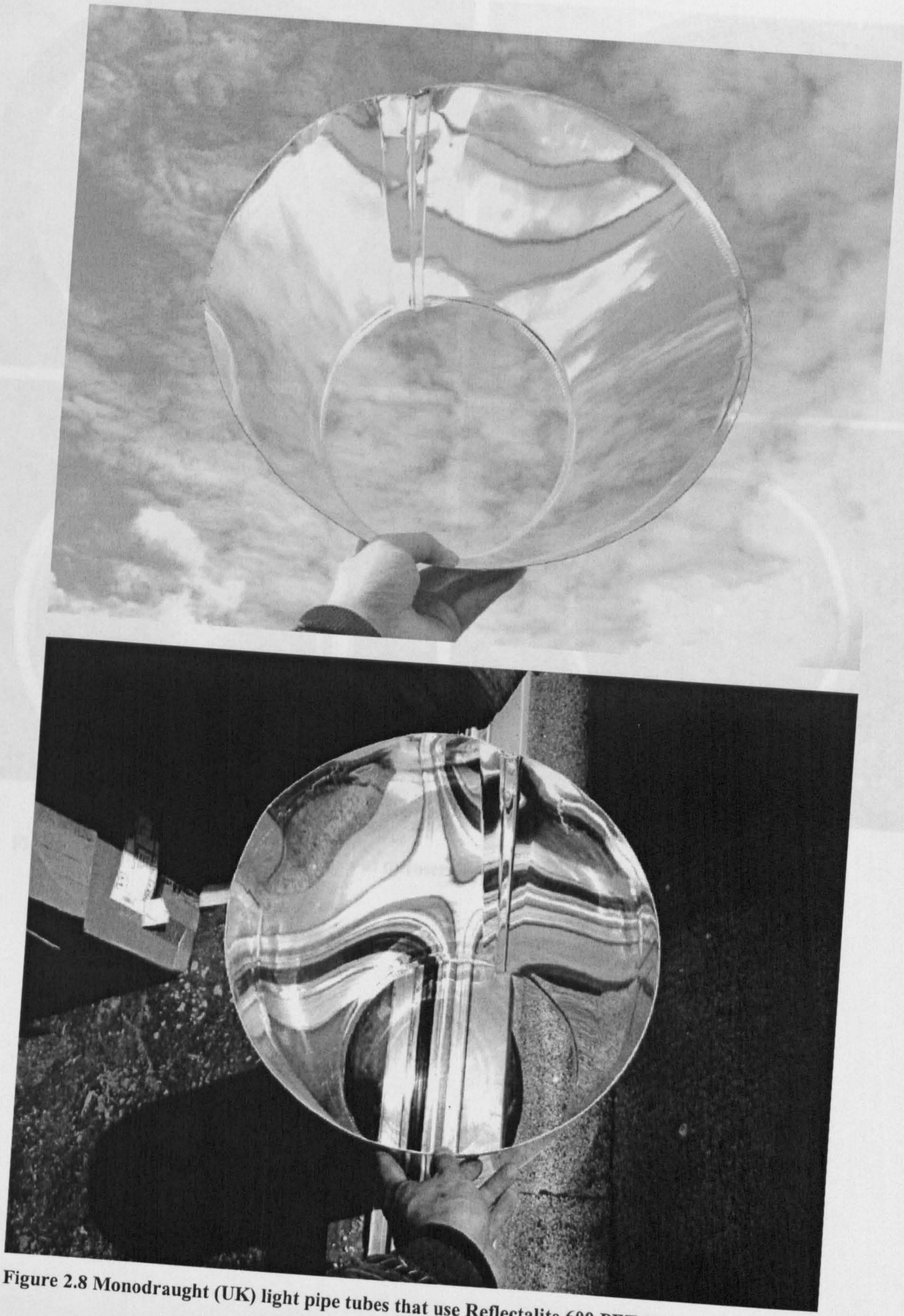

Figure 2.8 Monodraught (UK) light pipe tubes that use Reflectalite 600 PET film

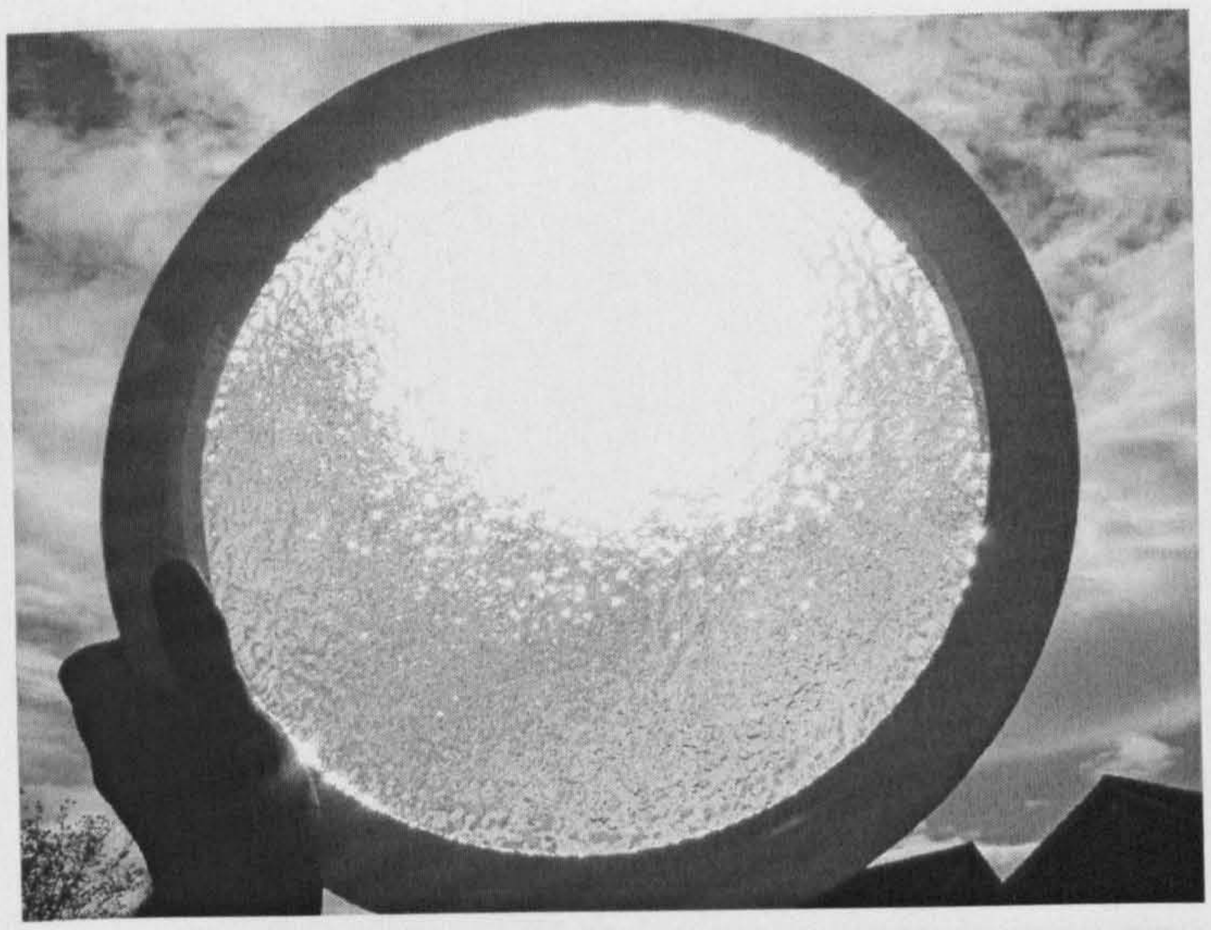

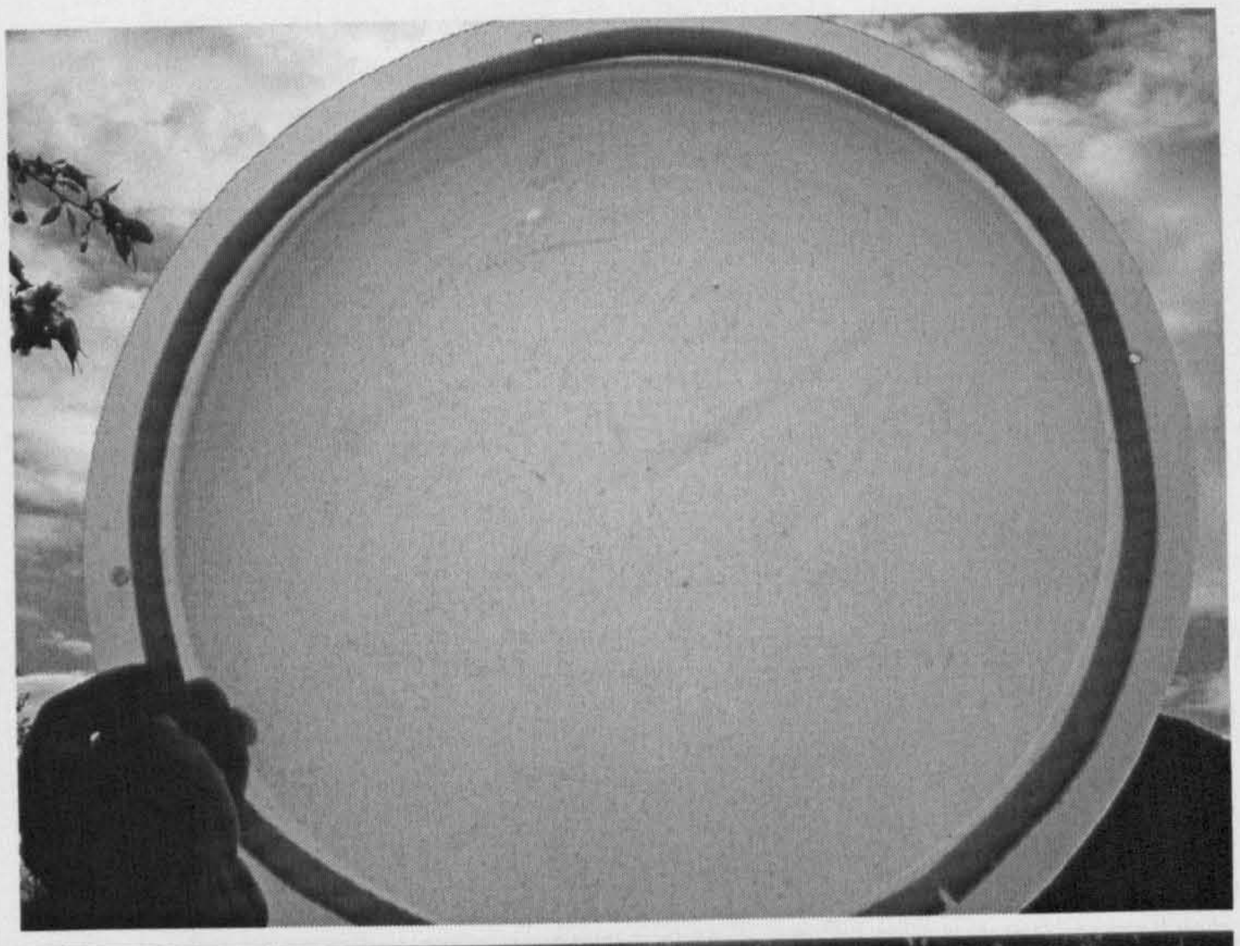

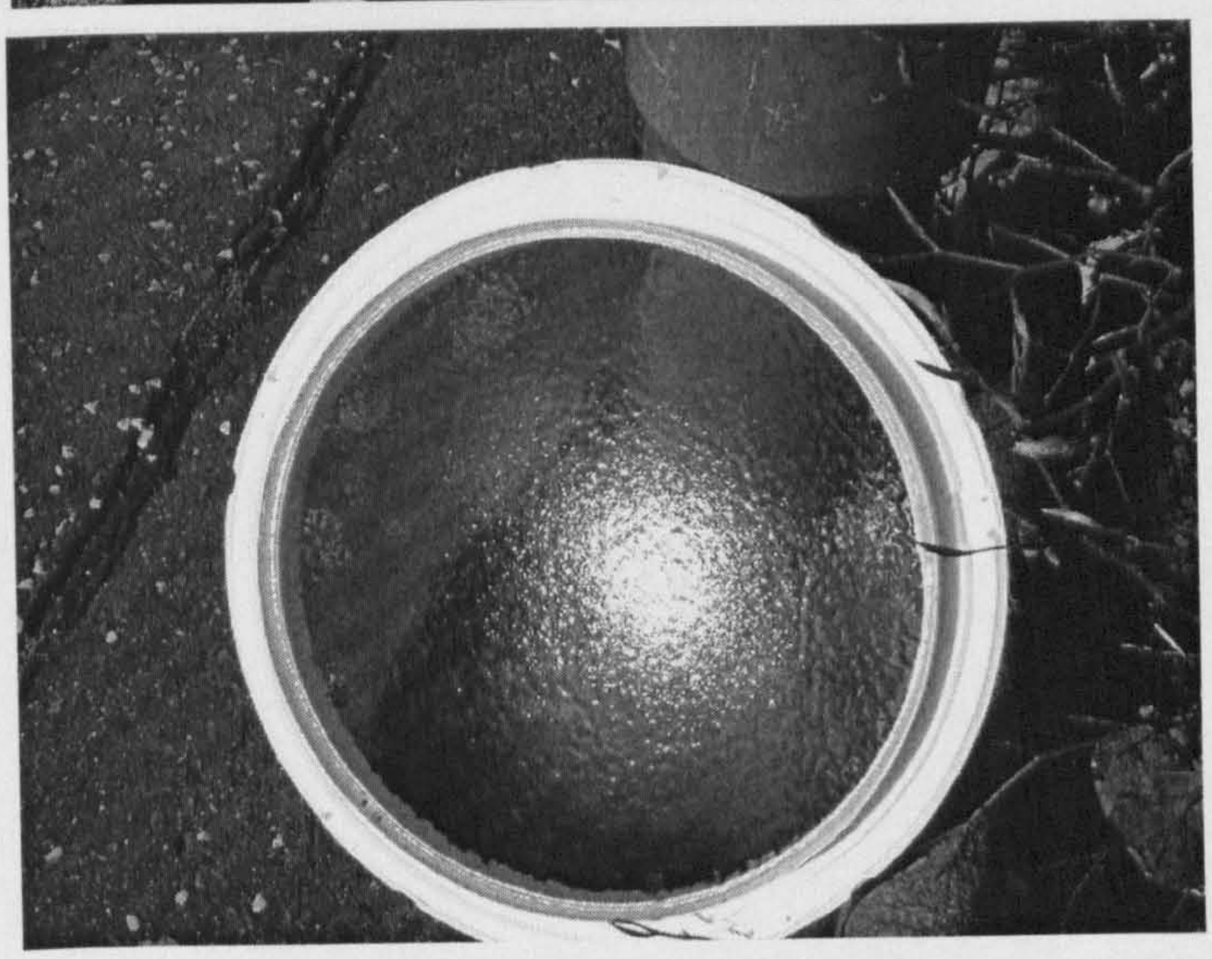

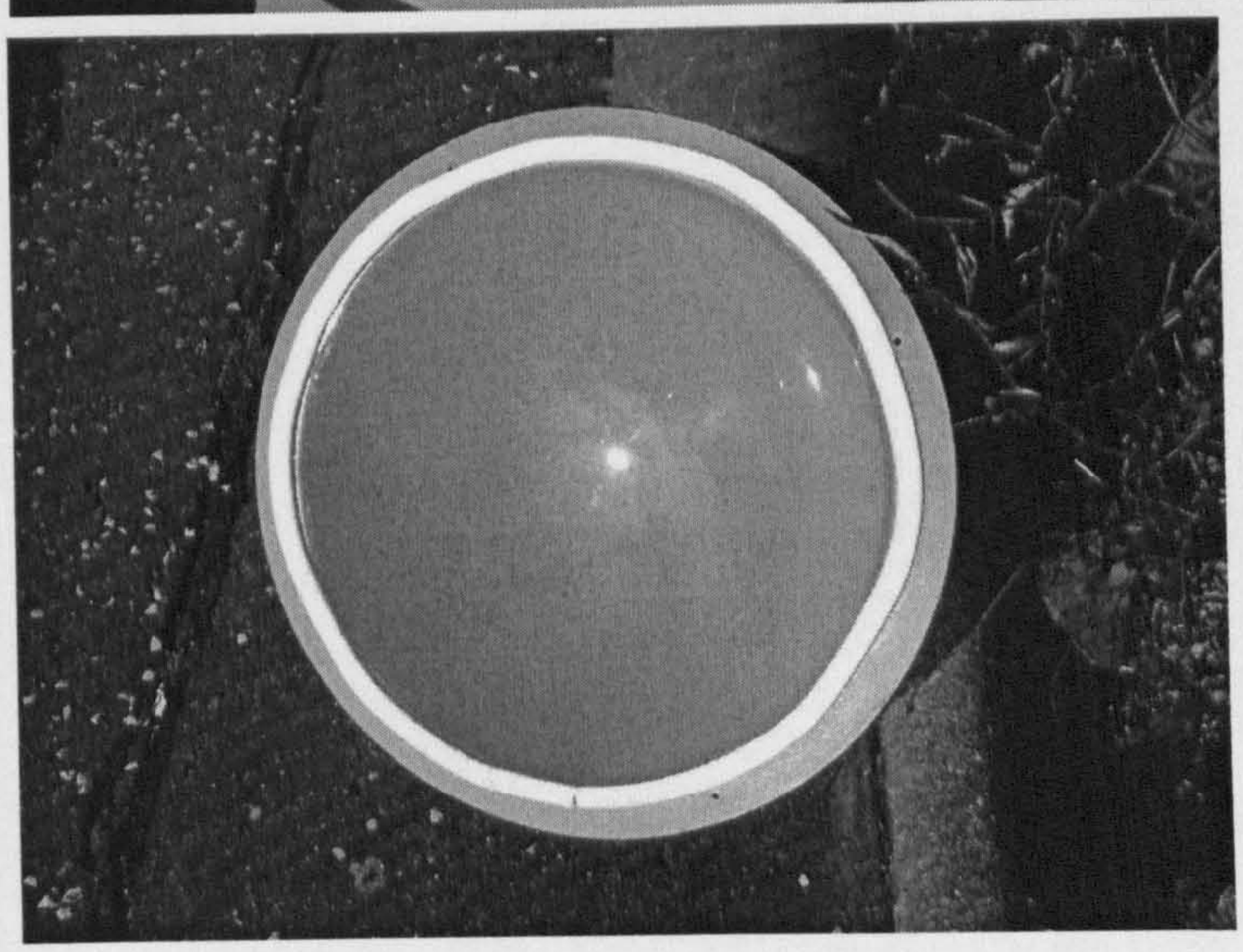

Figure 2.9 Appearances of different types of diffuser

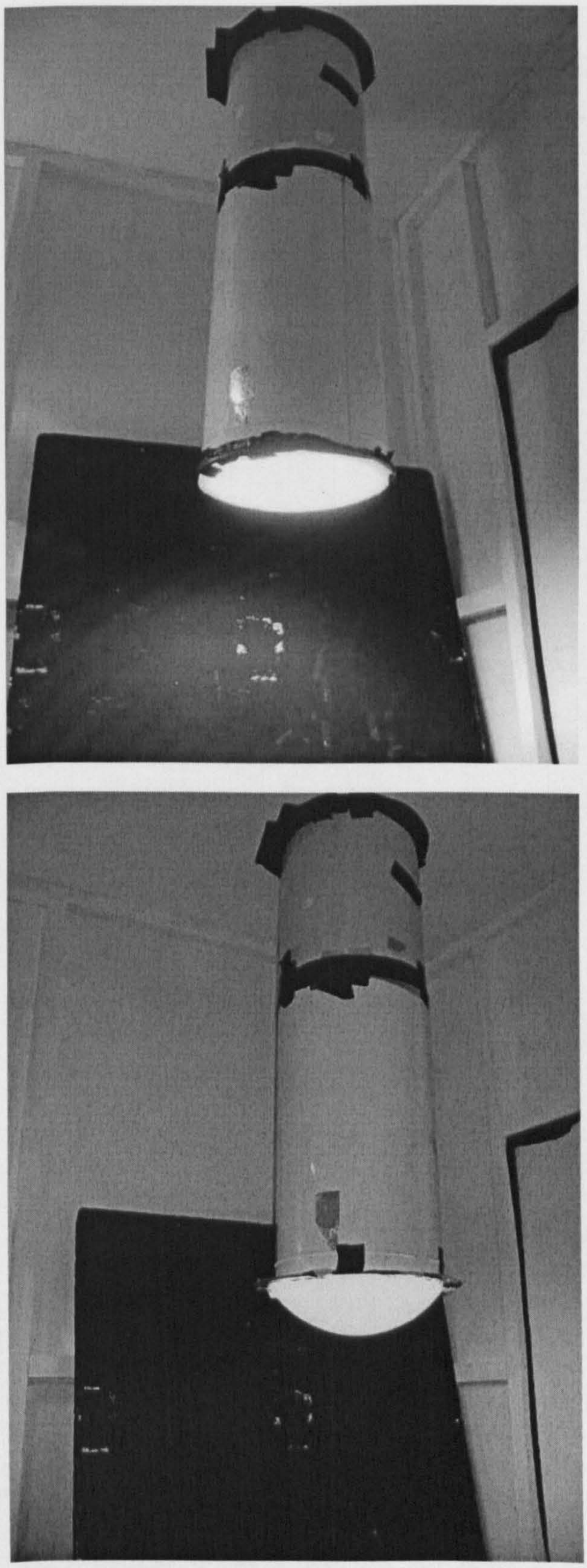

Figure 2.10 Demonstration of the different daylighting effects by a clear diffuser and an opal diffuser

Components For Flat Roof Application

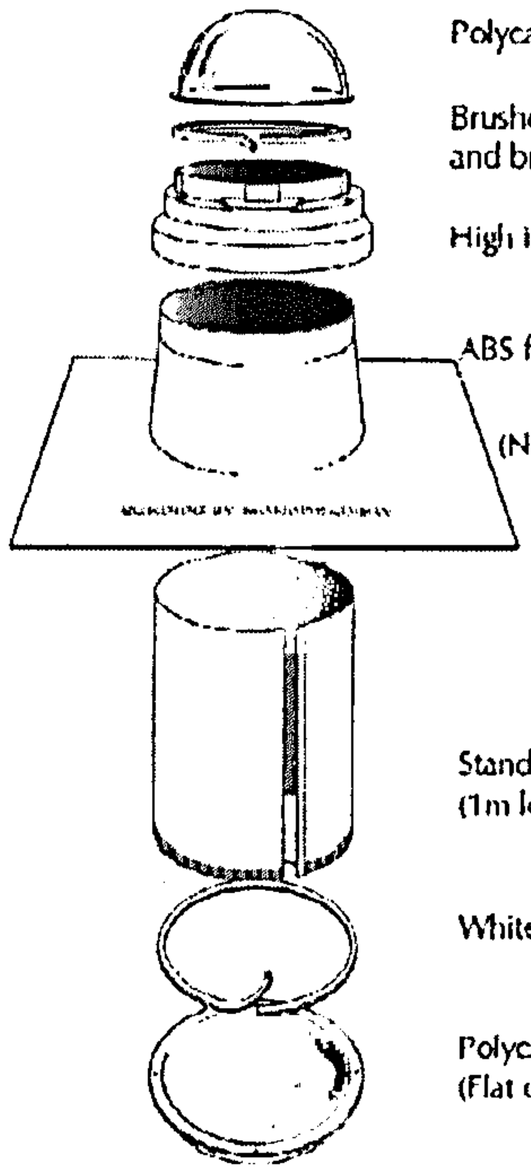

Polycarbonate, UV treated top dome.

Brushed nylon condensation trap
and breathable gasket.

High impact ABS collar with fixing lugs.

ABS flat roof flashing plate for flat roof application.

(Note: Alternative galvanised flashing will be
required for asphalt roof installation.

Standard 610mm sections of Reflectalite 600
(1m lengths also available)

White compressible ceiling seal.

Polycarbonate ceiling dome.
(Flat diffusers also available)

(All screws and fixings provided).

Components for Pitched Roof Applications

- slate roof -

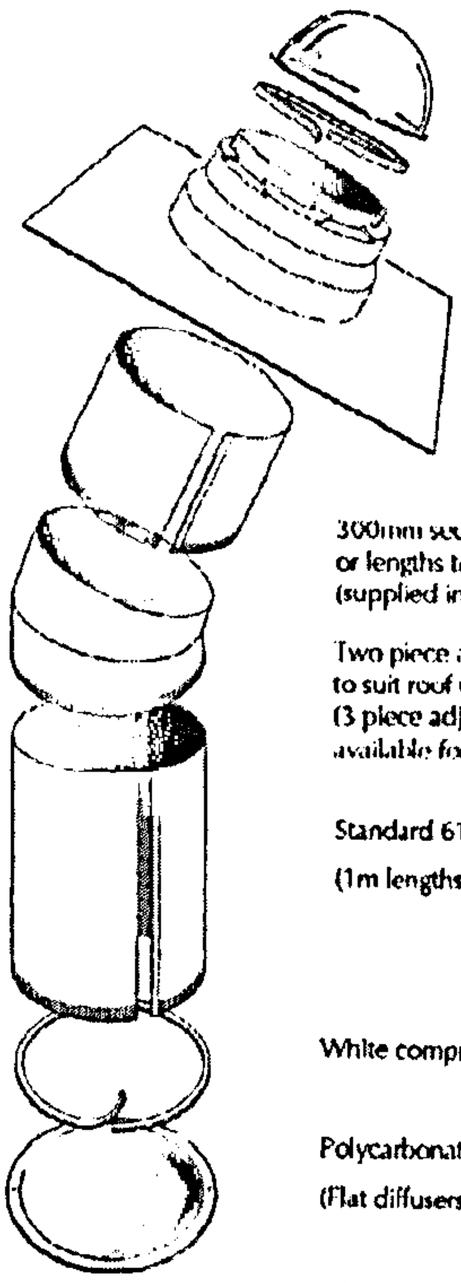

Polycarbonate, UV treated dome.

Brushed nylon condensation trap
and breathable gasket.

One piece ABS flashing plate.
(for tiled roofs 5mm upstands are
incorporated into the flashing plate
to the top and sides and Alfas 'C' Seal
is provided for weatherproofing).
A Code 4 lead skirt is provided for
flashing to tiles.

300mm section of SunPipe
or lengths to suit roof construction
(supplied in 2ft (610mm) long sections.)

Two piece adjustable elbow
to suit roof up to 30° pitch.
(3 piece adjustable elbow
available for roofs up to 45° pitch)

Standard 610mm sections of Reflectalite 600
(1m lengths also available)

White compressible ceiling seal.

Polycarbonate ceiling dome.
(Flat diffusers also available)

All screws and fixings provided.

Figure 2.11 An exploded view of a typical light pipe system by Monodraught (UK)

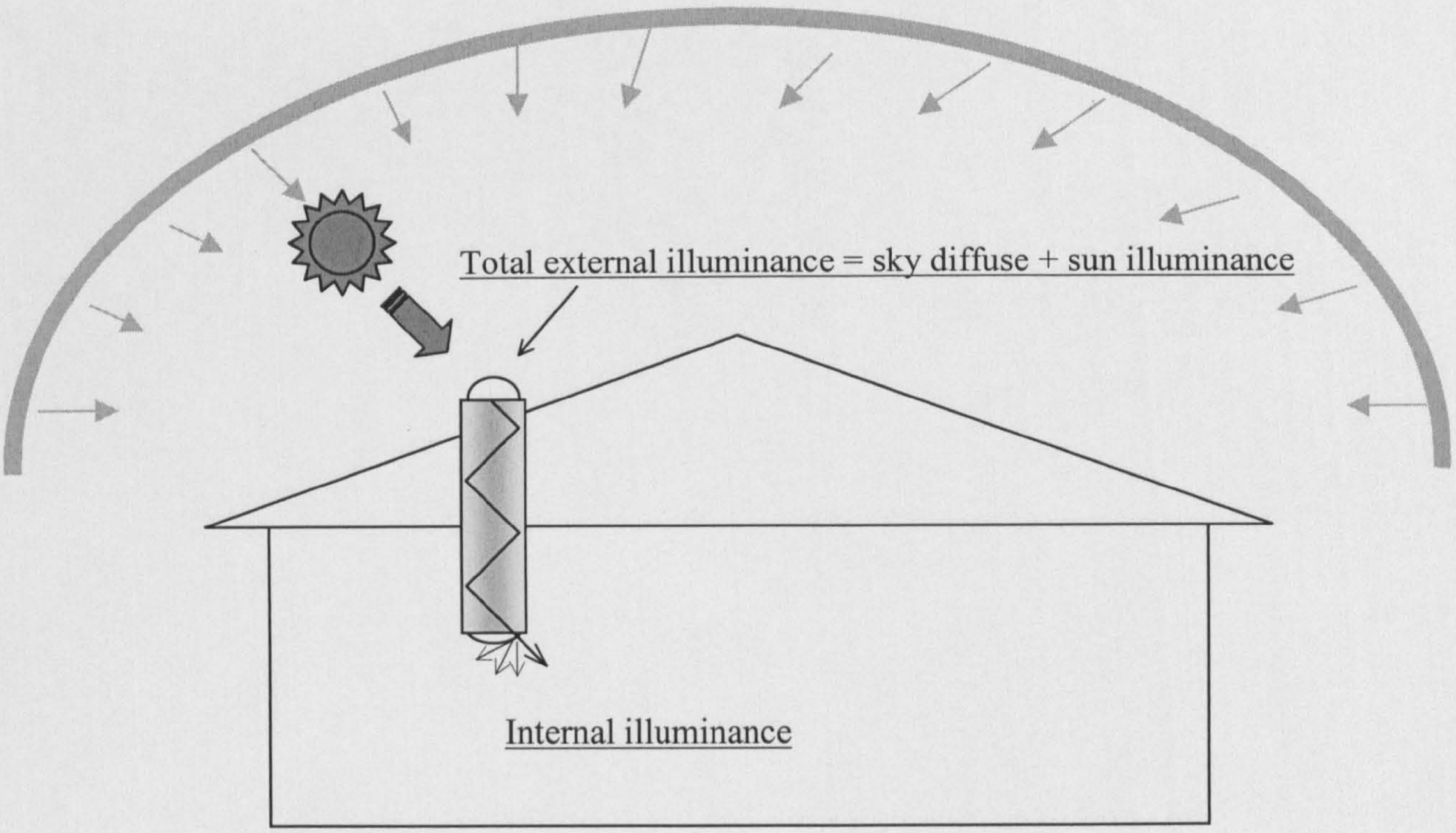

Figure 2.12 A general process of daylight collection, transmission and distribution through light pipes

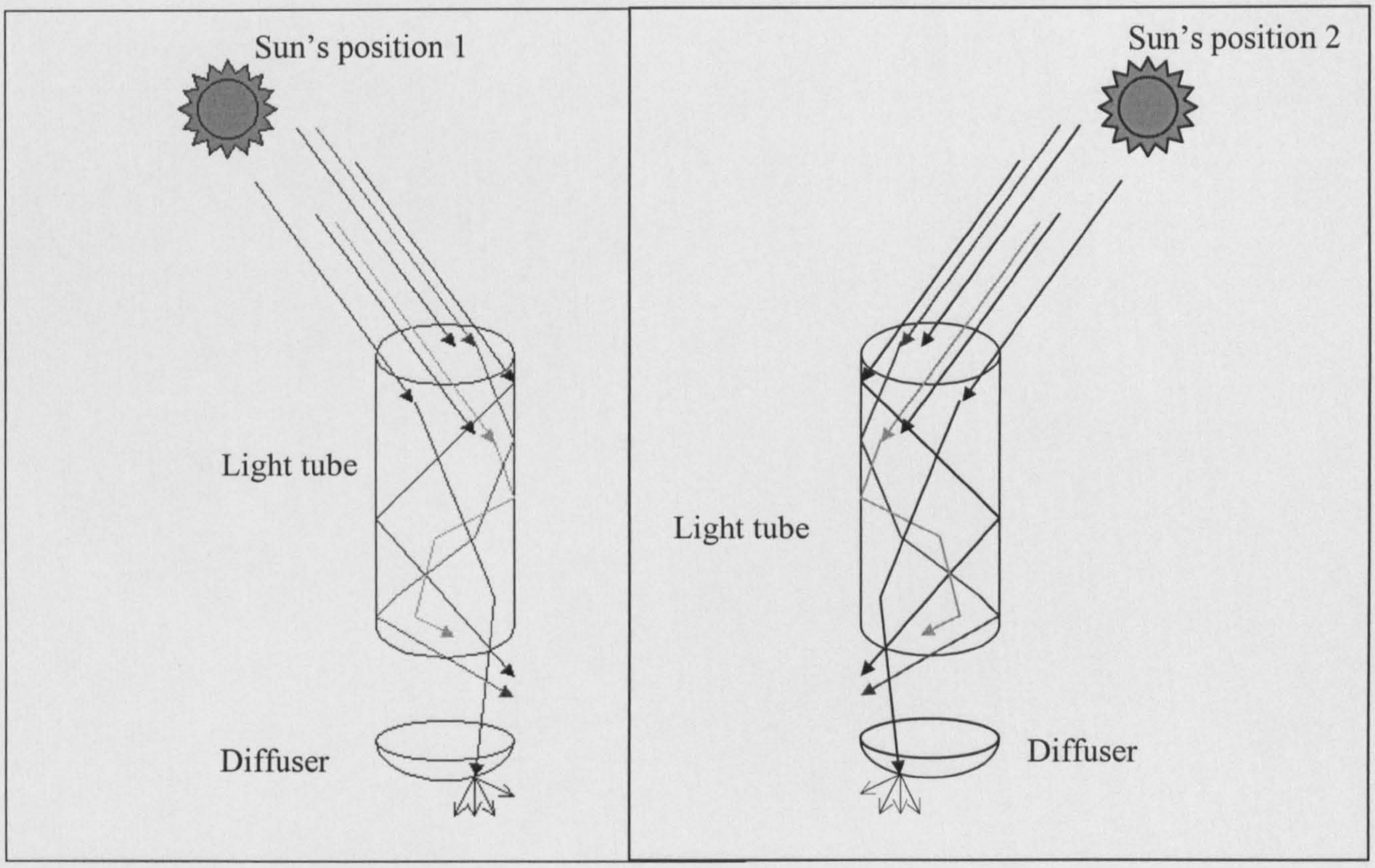

Figure 2.13 The pattern sunlight travel through light tube

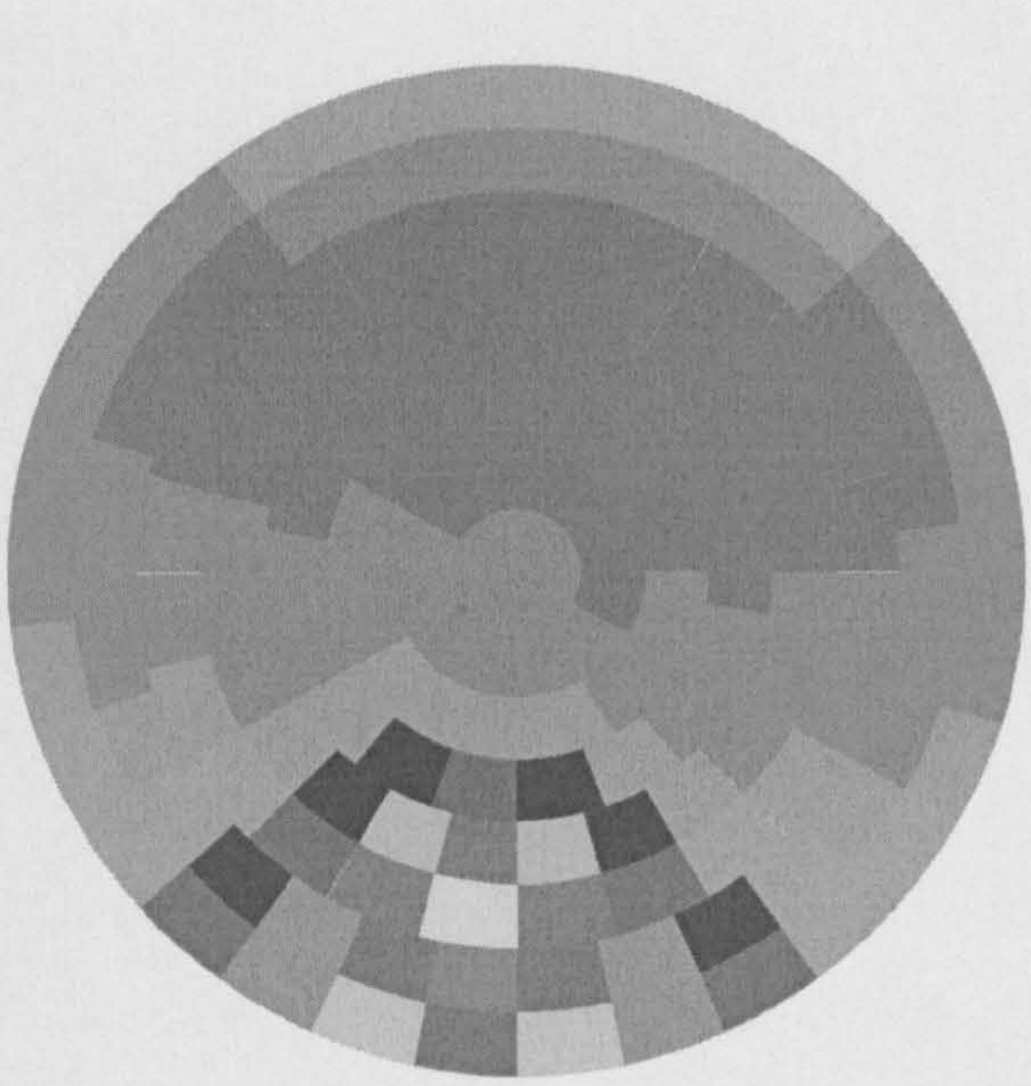

(a)

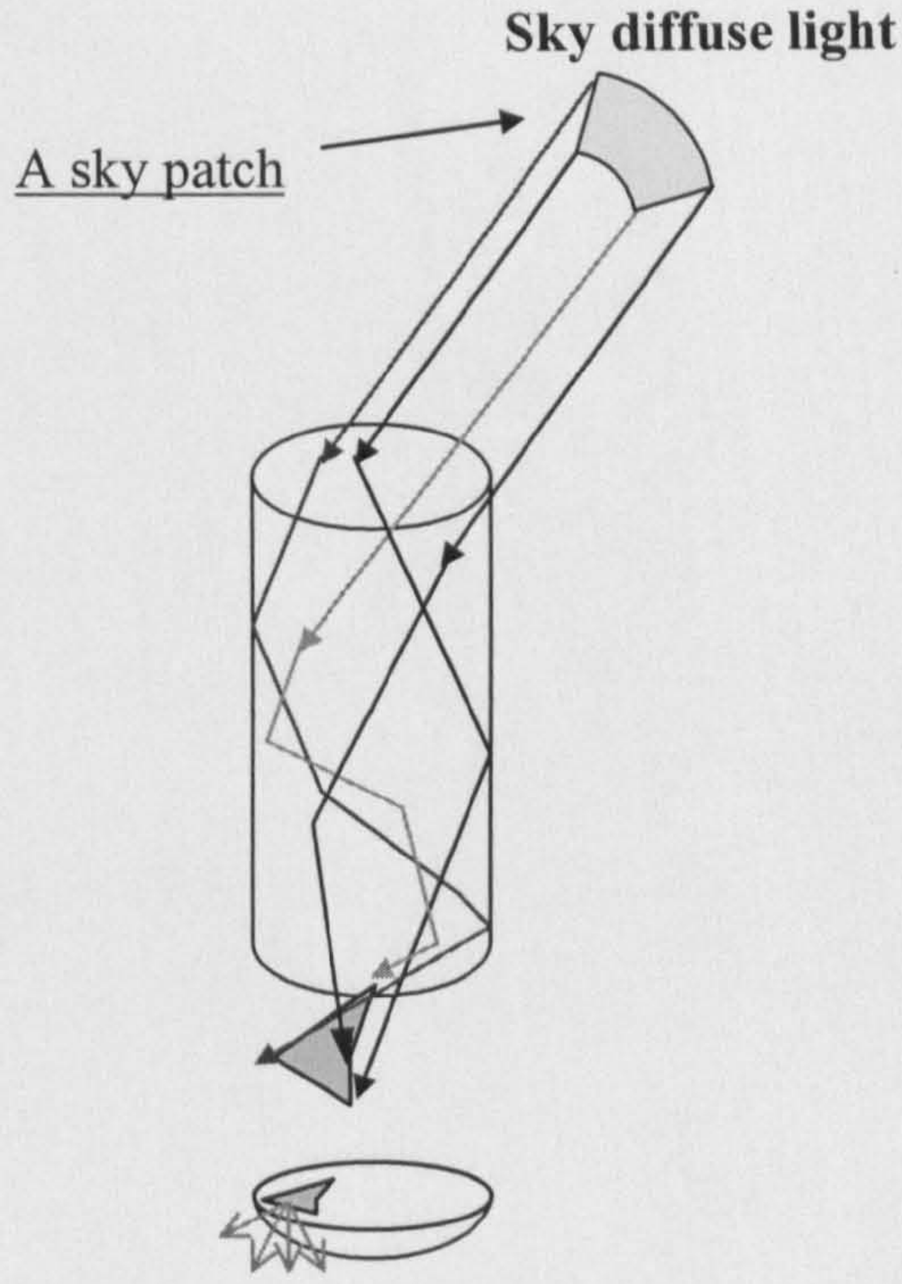

(b)

Figure 2.14 Sky vault divided into small patches with respective luminance

3. PREVIOUS WORK

The literature review focused on the following topics and region of work that directly relevant to the present study:

- Light pipe applications
- Working mechanism of light pipes
- Research methods for evaluating the efficiency of light pipe
- Design methods for light pipes

The daylighting performance of passive solar tubular light pipes as natural daylighting device has been reported in a number of studies. These studies are mainly on the following four aspects: daylighting performance of light pipe applications, working mechanism of light pipes, characterizing the transmittance of light pipe's main components including solar collector, tube and diffuser and developing design tool for light pipes under "design sky" conditions.

Experimental studies carried out by Shao [1] and Yohannes [2], reported the performance of light pipes of various designs under changing weather conditions: sunny, overcast, heavily overcast, and overcast with rain. Abundant illuminance of up to 450lux was reported in test rooms, and internal/external illuminance ratio variance from 0.1% to 1% was reported. Oakley's study [3] on 330-mm diameter light pipes of differing lengths showed that the illuminance could be as high as 1538lux. An average illuminance of 366lux and a mean internal-to-external ratio of 0.48% were obtainable.

Mathematical equations had been developed to describe the performance of mirror light tubes. These work have focused on the estimation of the light pipe tube's transmittance under laboratory conditions. Zastrow et al did theoretical work on the transmission of mirrored light pipe tube [4]. Swift et al [5] gave an integral equation involving light pipe tube's parameters, reflectivity, aspect ratio and the angle of incidence of the incident radiation. Edmonds et al [6] expressed the transmission of light pipe tube as a function of light pipe tube parameters, reflectivity and aspect ratio and solar altitude.

Studies undertaken at the University of Technology, Sydney [6] investigated the enhanced daylighting performance of light pipes coupled to laser-cut light-deflecting panels. It was reported that the illumination that can be achieved with a vertical light pipe decreases rapidly as the elevation of the incident light decreases. The outputs of light pipes depend strongly on sun's position and diffuser design. It was concluded that the daylighting of small rooms via light pipe may be enhanced by deflecting low-elevation light more directly through the light pipe using laser-cut light deflecting panels.

Work undertaken by Carter [7] put forward a design method intended for use either freestanding or in conjunction with existing daylight analysis methods. Considering that the magnitude of luminous flux entering the system is a function of unknown sky conditions, Carter's based his work [7] on the assumption of a "design sky", which restricted the applicability of this method in real practises.

Detailed description, analysis and appraisal of above previous work are presented separately below.

3.1 APPLICATIONS OF LIGHT PIPES

The daylighting performance of passive solar tubular light pipes has been monitored in both real and laboratorial environments. In the UK, literatures on the research in this respect have mainly been reported by the research team based Nottingham University and Liverpool University. Research carried out by L Shao et al [1] in Nottingham University demonstrated the daylighting performance of light pipes in real applications. Field measurements carried out at four sites have been reported. The four sites are the Pearl Centre in Peterborough, the Gurney Surgery in Norwich, the Rivermead Court in Marlow and the Guildford College in London. G. Oakley et al [3] reported the performance of six light pipes in three different applications, namely a workshop, a residential landing and a small office. The locations of the applications are the Beacon Energy Ltd, the West Beacon Farm and the Beacon Energy Centre, which are all located southwest of Shepshed in Leicestershire.

3.1.1 Applications of light pipes in residential and office buildings

Measurements on light pipe's daylighting performance in real buildings by Shao [1], Yohannes [2] and Oakley's study [3] have presented general and broad pictures of applications of the device. Positive and qualitative conclusions have been drawn on the overall efficiency of the device and the benefits of employing it in real applications. Importantly it has been made clear that the design technique of light pipes plays an important role in the application of the device. Shao et al concluded that light pipes "can be effective devices for introducing natural daylight into buildings, provided they are designed with care". Oakley et al concluded that light pipes "are proficient devices for introducing daylight into buildings", and "the most effective light pipes are straight, short ones with low aspect ratios and consequently larger diameter light pipes would probably be more effective". These implicated that the light pipe itself was a complex system and required extensive research to provide detailed and quantitative evaluations of it.

It was found that the performance of light pipe system was not only dependent on the geometrical configurations of the system. External meteorological and geographical conditions have been found to have effect on the performance of light pipes. Shao et al and Oakley et al measured the daylighting performances of light pipes under different weather conditions and used the ratio of internal total illuminance to external total illuminance as an indicator of the performance. It was found that the ratio seemed to vary with different weather conditions and solar altitudes. Shao et al found that when the sky was overcast, the ratio of internal to external illuminance increased. This interesting phenomenon was explained as "probably due to most of light from an overcast sky originating from around the zenith and undergoing fewer reflections/absorptions as it travels down the light pipe". However, both weather condition and solar altitude are not independent. Therefore no certain conclusions on the effect of weather condition, and the effect of solar altitude on the daylighting performance can be given based on the measurements. It was therefore realized that to reveal the relationship between weather conditions and solar altitude, and the performance of light pipes, vast database that can provide necessary information on both light pipe itself and its ambient external environment is needed.

Furthermore, by examining the study by Shao et al and Oakley et al, it was found that the internal illuminance distribution plays an indispensable role in the evaluation of the performance of the device. Shao found "the concept of daylight factor is not appropriate here as the sky was clear and dose not meet the overcast condition upon which the daylight factor is based". Therefore, instead of conventional daylight factor, the ratio between internal illuminance and external illuminance was used to indicate the performance of light pipes. However, it must be pointed out the ratio is dependant on the points of interest. For a given light pipe system under a given external and internal environmental conditions, the ratio for different points within the room, which have various vertical and horizontal distances from the centre of light pipe diffusers have different values for the ratio. Therefore, as an indicator of light pipe daylighting performance, the ratio shall be defined as a dimensional variety that can describe the internal illuminance distribution due to the light pipes.

Useful information on light pipe design has been given by Shao et al and Oakley et al. Qualitative relationships between the aspect ratio and the performance, the use of bends and the performance, the weather condition and the performance have been presented. Basic instructional principals such as to "avoid excessive aspect ratios and numbers of bends" have been suggested. However, the attempt to design light pipe systems in real applications using only basic principals and qualitative relationships might not be successful. Designers need to know the output of a certain light pipe under certain external and internal conditions with certain confidence. Most of the measurements on light pipes in real buildings carried out by Shao et al and Oakley et al monitored the total output of a group of light pipes, where each individual light pipe had its own configuration and was positioned in different places. It shall also be born in mind that the output of light pipes measured in real applications could be affected by the shading of interior layout, for examples the shade of furniture and reflection from walls. These facts increase the difficulty in producing exact evaluation and comparison of the daylighting performance of light pipes. In consideration of the present work, it was thought that the mathematical modelling should be based on measurements undertaken in laboratories.

3.1.2 Large-scale core daylighting by light pipe

In 1987, Whitehead [8] reported an application of large-scale core daylighting by means of light pipe system. The light pipe system was applied to a five-story conventional office building in Toronto, Canada. The illuminated area consisted of an 186m^2 core region of the top floor of the building. The system included five main components, namely, sun tracking device, focusing mirrors, roof apertures and prism light guide input elbows, prism light guides and electrical lights. According to the scheme of the application given by the authors, there were eight identical sun-tracking and light distribution systems, installed every 1.22 meters in a row. It was reported that each light guide of approximately 1.22 meters in diameter could illuminate 23m^2 of office space well in excess of 1280lux. It was also concluded by Whitehead that a core daylighting system such as this would be cost effective.

In 1990, McCluney studied the application of using water-filled light pipes to transport concentrated beam solar radiation from a solar collection system to a utilization system. According to McCluney, a system of such can be for the daylighting of the core interior spaces of buildings, spaces that are far removed from outside walls or the roof and are therefore not amenable to conventional daylighting with sidelight or toplights. McCluney studied the effect of absorption by water on the color of light and the colorimetry of water-filtered light. McCluney reported that the distance which daylight can be transmitted before its color becomes objectionable in comparison with warm white fluorescent light appeared to be 6-8m. The distance for a significant drop in the color-rendering index of the daylight transmitted by the system was reported as about 10m. It was found that the visible transmittance of 5 and 10m long pipes was about 28% and 19%. It was concluded that water-filled light pipes could be used to bring cool, filtered sunlight indoors in a controlled manner [9].

3.1.3 Light pipe coupled to laser-cut light-deflecting panels

Edmonds [6] studied the enhanced performance of light pipes coupled to laser-cut light-deflecting panels (LCP). Edmonds pointed out "although light pipes are effective sources or natural illumination for deep areas within buildings, the daylighting performance of the device decreases rapidly as the elevation of the incident light decreases". It was found that the combination of laser-cut light deflecting

panels with light pipes enhanced the illumination performance for all angles of elevation below about 60°. Laser-cut light-deflecting panels are of a material that combines light deflecting properties with good viewing transparency. The material is of similar thickness to conventional glass glazing, and is produced by laminating laser cut acrylic sheet between sheets of glass [10]. It was found that the large enhancement was obtained in winter months, when sunlight is incident at low elevation all day. For a light pipe 0.3m in diameter and 7.2m in length but without LCP, the transmittance of it falls below 0.1 for sun elevation below about 45°. While as a comparison, when such a light pipe is coupled with a LCP device, the transmittance above 0.1 extends to sun elevation as low as 10°. It was therefore concluded that the enhancement at low elevations extends the time during which light pipes were useful [6].

Edmonds et al [11] also gave the theory of using extractors and emitters in light pipe system within large commercial buildings. The author discussed the application of hollow light pipe for the distribution of sunlight from the roof or façade into the deep interior of a building. It was found this application was suited to climates with a high direct sun component. However, to use sunlight in buildings more effectively, a device at the façade to direct sunlight into a light pipe and devices to extract light from the light pipe and distribute the light into interior shall be included in the system. Devices for the extraction of light are given the name of "extractors" and devices for light distribution as "emitters". Edmonds et al studied the application of using laser-cut light-deflect panel as extractors and emitters for light distribution from hollow light pipes. It was concluded that it was feasible to produce extraction and emission devices for light pipes from simple assemblies of laser-cut panels. The extractors and emitters may be used with rectangular light pipes to provide light distributions similar in most respects to those obtained from conventional luminaries. According to the author, this technology is also applicable to remote-source lighting systems where the sources may be either sunlight or artificial light.

3.1.4 Light pipe system using both natural and artificial light

Aizenberg et al [12] reported the application of slit light pipes in the Chkalovskaya Moscow subway station. The central hall of the station was illuminated by a rectilinear (60m long) structure suspended under the oval dome of the main hall. The structure consisted of cylindrical multi-slot light pipes

alternating with 12 cubes. According to the above-mentioned author, the use of hollow light pipes to illuminate the subway station not only permitted new architectural solutions, but also yielded good economic indices of the system. The number of lighting points in the all was reduced by a factor of 30 and the extent of the electrical grid was reduced by a factor of three. Aizenberg et al stated that an important advantage of lighting systems based on light pipe "might be further reduction in maintenance costs as the light sources may be easily accessed to maintenance personnel without the need for tall ladders or cherry pickers". The operational experience of over 12 years confirmed the high reliability of the system. The authors concluded that the afore mentioned station, namely Moscow subway station was the first station where the problem of light-system operation had been completely solved, since "access to the input units for lamp replacement and modification of the electrical system presents not difficulties, requires no special equipment, and may be accomplished by a single electrician at any time". According to Aizenberg et al [12] the application of similar artificial lighting system that used light guide was also found in Moscow ring high way. This shows the wide applicability of artificial light source light guide system.

Aizenberg et al [13] proposed and studied a solar and artificial light pipe system called "Heliobus" used in a school building in SanktGallen, Switzerland. It is a four-story building, within which there are recreation halls at the centre of each floor. The Heliobus system was built to light these recreation areas. The system comprised the following basic elements: a solar light collector, an intermediate element, a unit containing electric light sources, a vertical hollow light pipe and a diffuser. According to the above-mentioned authors, the working mechanism of the system is: solar light rays captured by the light collector are directed through the intermediate device (by its reflecting surfaces) into the light pipe and then diffused into areas to be lit. In case of lack of daylight, a luminous flux of electric light source is directed by an optical system located in the intermediate device. Aizenberg et al stated that the performance of the system was highly appreciated by teachers, administrators and school pupils. Tests conduced by Aizenberg showed that the system provided good daylighting even under a cloudy sky when the sun was absent. It was concluded by afore mentioned authors that the system totally met the requirements for lighting under all weather conditions, with energy consumption reduced significantly due to shortening of electric lighting operation.

3.1.5 Integration of light pipe daylighting and natural ventilation systems

Shao and Riffat [14] investigated the technique of integrating light pipe natural daylighting and natural ventilation using passive stack system. The system has a bi-layer structure. In the middle of the structure is the light pipe, lined with a highly reflective material. The light pipe is surrounded by an annular space that acts as a stack for the exhaust air. The system can be further combined with a heat pipe based solar heating system that can enhance the natural ventilation. By experimental methods, the authors studied the daylighting and ventilation performance of the integrated system. The daylighting performance enhancement of light pipe due to LCP (Laser-cut Panel) was also examined. It was found light transmitted through the light pipe was higher on clear/sunny days than on overcast days, but the uniformity of the illuminance in the test chamber was greater on overcast/cloudy days. Solar infrared transmission was found to be 1.5% on a cloudy day compared with 1.4% on a sunny day. Light pipe transmitted marginally less infrared radiation than visible light. It was shown that by fitting a LCP to a light pipe, higher level of daylight transmittance could be achieved for certain periods of the day, depending on the orientation of the LCP. It was found that an eight air changes per hour were achieved with the natural stack effect. The authors concluded that the most suitable building types for the application of the integrated system were educational, office and retail buildings.

Oakely [15] also studied the integrated system of light pipe and ventilation stack. The system has two channels. The central channel is a light pipe that guides daylight into occupied space; while the outer channel, also called ventilation stack, enables passive stack ventilation. The study monitored the performance of two light pipes with diameter of 2.15m and 2.20m in length in outdoor environmental chambers. Using tracer-gas method, above-mentioned researches measured the low velocity airflow rates and natural stack ventilation. Results given by the author suggested a good correlation between solar altitude, internal illuminance values and the external illuminance values. It was shown that by fitting a LCP panel to a light pipe, much higher levels of daylight could be achieved. It was found that the typical air change rate through the passive stack was about eight air changes per hour in winter, and the temperature inside the test chamber was controlled stable at approximately 20°C. The authors concluded that light pipes were proficient devices for introducing daylight into buildings and reducing costs.

Smith et al [16] reported the evaluation of dichroic material for enhancing light pipe daylighting and natural ventilation in an integrated system. It was stated by the authors that, "the integration of natural daylighting and ventilation system reduces system costs and payback period as well as make both technique more attractive to users". It was found that by constructing light pipe using dichroic materials, the infrared part of the solar radiation was allowed to be transmitted to the ventilation stack, while the visible light was guided by the light pipe into interior space. The heat gain to the interior can therefore be reduced and the thermal stack effect strengthened. The transmittance of a dichroic light pipe was found to be similar to that of a light pipe with a 95% specular reflectance. The infrared radiation transmitted through the dichroic material into a passive stack was found to enhance the natural ventilation flow by up to 14%. It was concluded by the authors that the dichroic material removed approximately half of the solar heat in daylight, and thus provided natural daylight without overheating.

3.1.6 The use of light pipe systems in deep plan buildings

Daylighting possesses good potential for applications in area such as tropics where the sky is luminous. However, because the depth of penetration of daylight through windows into deep plan buildings is limited, the full utilization of daylight is restricted. It was realized that the limitation of windows could be complemented by purpose designed light pipe systems. Surapong et al [17] developed a technique for the use of sunlight through light pipe system in multi-storey buildings. Measurements on the internal illuminance and temperature were undertaken and the results were compared against calculated values. Surapong et al used elementary ray-tracing method in modelling internal daylight illuminance and employed analogous model for calculating heat transfer. According to the computed and measured internal illuminance data given by the authors, Mean Bias Error (MBE), Root Mean Square Error (RMSE) and Percentage Averaged Deviation (PAD) were derived. It was noted that the averaged measured internal illuminance value was as high as 1400lux. The MBE was found to be 308lux, which was about 22% of the averaged measured internal illuminance. Corresponding figures for RMSE were found as 808lux and 57%. The PAD was found to be 35%. Based on the comparison between measured and computed data, the afore-mentioned authors also pointed out that there might be a higher level of uniform reflection than assumed. The authors concluded that the analysis method developed by them was suitable and sufficiently accurate.

A case study on the use of light pipes for deep plan office buildings was carried out in Malaysia by Hansen et al [18]. The case study examined development work on the application of light pipe system for a high rise building in Kuala Lumpur, Malaysia. Light pipes were used in the high-rise building. For each floor, four light pipes coupled with LCP (Laser-cut Panel) were used to improve the daylighting performance. The method of scale modelling was used to simulate the daylighting performance of light pipe. In predicting the daylighting performance of light pipe, elementary theory was used. The calculated results were compared with measured values for various solar elevations. It was found that light pipes coupled with LCP had a good performance for deep plan buildings. The authors concluded that the use of light pipes "will increase the passive zone in the building and hence reduce energy consumption by the use of daylight". It was suggested, however, that further study needed to be done in order to obtain a better distribution of the out coming light from the light pipe system.

3.1.7 A solid light guide system: air-clad optical rod

Researchers in Nottingham University [19] proposed a novel "light rods" system that can be used to transport light from the exterior of a building into its interior spaces. These rods were designed sufficiently small so that it can be fitted into most existing buildings without structural modification. The light rod system combines high transmittance efficiency with small cross-sectional area. The system relies on the principal of total internal reflection and makes use of the transmittance properties of industrial grade extruded Polymethyl methacrylate. Comparison was made between light rod and light pipe in terms of daylight transmittance. It was found that when external illuminance was greater than 35000lux light pipe (aspect ratio = 4) performed better than light rod (aspect ratio = 24), while when external illuminance was lower than 35000lux, the latter device performed better than the former one. It was concluded that light rod "transmit at a similar efficiency to a standard light pipe that has an aspect ratio 6 times smaller", and "the small diameter of the device gives it the potential to provide daylighting where light pipes cannot be installed" [19].

3.2 WORKING MECHANISM OF LIGHT PIPES

The working mechanism of passive solar light pipes is most widely described and understood as "daylight is gather by the light pipe dome, and then transmitted through the reflective light pipe tube by

multi-reflection, followed by being distributed by light pipe diffuser into internal space within buildings". Above description although rough and simple, is correct, giving a general picture of how daylight is transmitted through light pipes. However, since daylight has two important components, namely the sunlight and sky-light which are of great difference in their property, with the quantity and proportion of each components changing dynamically, the performance of light pipe systems changes from time to time.

3.2.1 Understanding of the daylight transmission within light pipes

The understanding of the complex process that sunlight and sky-light travels through light pipes forms the basis on which a sophisticated performance model can be constructed. Previous works on this subject have been seen. However, emphasis was only put on the explanation of the transmission of parallel light (or sunlight) within light pipe tubes [1, 4, 5, 6]. Sky diffuse light is the second most important component of daylight, but the contribution of this component to the daylighting performance of light pipes has rarely been studied.

The quantity and proportion of the two components of daylight vary with the changing of sky conditions. When the sky is clear, horizontal diffuse illuminance can be as high as 1/3 or more of horizontal global illuminance; while when the sky is overcast horizontal diffuse illuminance can be equal to the global illumiance; and when the sky is part-overcast, the proportion of diffuse illumiannce to global illuminance varies dymatically but can reach as high as 50%. The transmission of sky diffuse illuminance can have important influence on the overall efficiency of light pipe systems.

Study on the transmission of sky diffuse light within light pipes was carried out by BBRI (Belgian Building Research Institute) [20]. Measurement on the diffuse illuminance decrease in a 330 mm light pipe tube along the length of it was undertaken under overcast sky conditions. It was reported that diffuse illuminance transmitted by a light pipe had two components, namely the direct view part and the reflected part. It was shown that the direct view of sky decreased very quickly from 100% to 1% after 1 meter, while the reflected part decreased 29% per meter. These implied that the physical processes of the transmissions of the two daylight components within light pipes were different.

3.2.2 Critical appraisal

On light pipe system's transmittance of daylight, most efforts have been put on the theoretical calculation of light pipe tube's transmittance of parallel artificial or sunlight [1, 4, 5, 6]. Zastrow et al [4] related the transmittance of a mirror light pipe to its surface reflectance, the angle between the incident light and the light pipe's axis, the length of the light pipe tube, and the diameter of the light pipe tube. Swift et al [5] and Edmonds et al [6] established more complicated relationship between the transmittance of light pipe tube, and the configurations and the incident angle of parallel light. However, the application of above methods to the design of light pipes in real practise may not be successful. This is because these methods cannot describe the transmittance of sky diffuse illuminance within light pipe systems. As an example, when the sky is complete overcast, the calculations based on above methods are not applicable, since the input into the light pipe is only diffuse illuminance and there is no sunlight component.

BBRI's work [20] on the evaluation of the loss of diffuse illuminance along light pipe tube revealed that the transmission of this daylight component is complex and different from that of the sunlight component. However, BBRI' work is only conducted under overcast sky conditions. Therefore the conclusion drew by BBRI is not necessarily applicable to other weather conditions. The reason for this is that the sky illuminance distribution is not uniform. Figure 3.1 graphically presents the radiance or luminance distributions that have been widely reported in literatures [21]. Figure 3.2 shows the different sky illuminance distribution under different weather conditions. Thus, the transmittance of sky diffuse illuminance may vary under different weather conditions, which implies that the 29% per efficiency drop can only be applied to real light pipe design with limited confidence. It is therefore realized that, to produce a mathematical model that can describe the transmission of sky diffuse illuminance within light pipes, measurements on light pipes of various configurations under all weather conditions need to be undertaken.

3.3 RESEARCH METHODS FOR EVALUATING THE EFFICIENCY OF LIGHT PIPES

Pervious work on the efficiency of light pipes focused on the evaluation of transmittance of the three main components of light pipes namely the solar collector (or called dome), the light pipe tube and the

diffuser. Different researchers have taken different approaches towards the purpose of assessing the efficiency of the components. The procedures that were taken and the results that were given by these previous studies are presented below followed by critical appraisal.

3.3.1 The efficiencies of light pipe solar collectors and diffusers

Light pipe solar collector is the first part of the light pipe system that daylight passes through. The efficiency of solar collector influences the performance of the whole light pipe system. The most widely used and commercially available light pipe solar collectors are the clear acrylic dome and the clear polycarbonate dome. The evaluations of solar collectors have been focusing on this particular type of dome. Pervious works done on this subject have been reported by BBRI (Belgian Building Research Institute) [20] and Carter [7].

BBRI carried out measurements to test the solar energetic properties of solar collectors (by Monodraught (UK) Ltd) of various materials. The theoretical values for normal light transmittance of clear acrylic and polycarbonate domes were reported as 84.3% and 81.3% respectively. Experiment aimed to determinate the hemispherical transmittance of solar collectors (by Monodraught Ltd) was also undertaken. Two luxmeters, one put under a solar collector, and the other outside of it serving as a reference meter were employed. Readings from the former luxmeter was compared to the latter one to obtain the efficiency ratio. The value of the ratio amounted to 80% for solar collectors. It was therefore found that, "the use of the normal values instead of the hemisphere values does not lead to a different result".

The theoretical values for normal light transmittance of light pipe diffusers of various diameters were also measured by BBRI. The tested diffusers were Monodraught opal dome diffusers of diameters 330 mm, 450 mm and 530 mm, and the transmittances for the diffusers were reported as 53%, 50% and 54% respectively. Although Monodraught opal dome diffusers were of convex shape, no experiments were undertaken by BBRI to determine the hemispherical transmittance of the diffusers.

Above values obtained by BBRI were then compared against the values given by manufacturers of light pipes. It was remarked in BBRI's report that "these manufacturer specified values seem to be quite idealistic and lead to a performance that is almost twice as good as the real performance".

Carter [7] studied the relationship between the aspect ratio of light pipe (with solar collector and diffuser) and the transmittance of light pipe. In his work, Carter used data provided by Love et al [22] on above-mentioned relationship. Love et al produced the relationship between pipe efficiency and aspect ratio for light pipes without solar collector or diffuser under overcast sky conditions. To employ the data by Love et al, Carter used the values of 88% as the hemispherical transmittance of solar collector, and 60% for diffusers to correct the values given by Love et al.

3.3.2 The efficiency of light pipe tube

The earliest work on the transmission of mirrored light pipe tube seems to be the theoretical calculation given by Zastrow et al [4]. Zastrow et al gave a simple formulation to relate the transmittance of a mirror light pipe tube to its surface reflectance (ρ), the angle between the incident light and the tube's axis (θ), the length of the tube (L), and the effective diameter of the tube (d_{eff}). It is

$$T = \rho^{L * \tan\theta / deff} \quad (3.1)$$

where T is the transmittance, i.e. the ratio of the amount of light transmitted by light pipe tube to the incident light.

Swift et al [5] gave an equation to describe the transmission of collimating light within mirrored light pipe tube. The equation is

$$T = (4/\pi)\int_{s=0}^{d} [s^2/(1-s^2)^{1/2}] R^{\mathrm{int}(p\tan\theta/s)} \times \{1-(1-R)[p\tan\theta/s - \mathrm{int}(p\tan\theta/s)]\} ds \quad (3.2)$$

where T is the transmittance of the light pipe tube, i.e. the ratio of the amount of transmitted light to that of incident light, R is the reflectance of the interior surface of the light pipe tube, p is the aspect

ratio of the light pipe tube, θ is the angle between the incident light and the light pipe tube axis, int is the integer function, that is int(a) is the integer less than or equal to a.

Swift et al compared the theoretical transmission given by Eq. 3.2 against the measured data. The transmissions of 25 mm diameter plastic tubes (internal surface filmed by 3M Silverlux ™) with a range of aspect ratio were measured. The light source was a HeNe laser whose beam was expanded to be collimated with a diameter of 50 mm. The transmission of light pipe tubes of the aspect ratio of 2, 4, 6, 8 and 10 was measured as a function of the angle of incidence of the collimated beam. The angles of incidence were 0 to 85 degrees in step of 5 degrees. The experimental results were found in a good agreement with the calculated values.

The light transmission performance of light pipe tube was also given by Edmonds et al [6],

$$P = 4I_0T_{atm}\sin\theta\int_{x=0}^{R}[(R^2-x^2)^{1/2}/R]\rho^{L/2R\cos i\tan\theta}dx \qquad (3.3)$$

where P is the power transmission of light through light pipe tube, I_0 is the extraterrestrial intensity (1353 W/m^2), T_{atm} is the transmission of the atmosphere, θ is the elevation of sunlight, R is the radius of light pipe tube, ρ is the reflectance of the tube, L is the length of the tube, and *i* is the angle on which a bunch of sunlight reflects on the internal surface of light pipe tube.

3.3.3 The efficiency of light pipe bends

The efficiency of light pipe bends was studied mainly by means of experiments. Oakley et al [3] compared the ratio of internal to external illuminance, which were due to two light pipes, one straight and the other elbowed with three bends. It was reported that, the internal to external ratio for the elbowed light pipe ("light pipe A") averaged at approximately 0.3%, and 0.5% for the straight light pipe ("light pipe E"). Oakley et al hence concluded that because the average ratio of position E to A was found as 1.78, light pipe E was on average 43% better than light pipe A and therefore A losed 14% light output per bend. It was pointed out that the figure of 14% contradicted Monodraught's figure of 8% loss per bend.

The effect of light pipe tube bends on the efficiency of light pipes was also tested by Love et al [22]. Bends of test angles of 30, 60 and 90 degrees were tested. Internal illuminances were measured with and without light pipe systems (SunScope) that used different numbers of bends. Measurements were collected for each of the tests, and the data were used to calculate average transmittance of the elbow joint at each of the test angles. It was reported that the transmittance values for 30 degrees light pipe bends ranged from 70% to 90% with majority of measurements concentrated about 80%.

3.3.4 Critical appraisal

Efficiencies of light pipe solar collectors and diffusers

BBRI [20] carried out extensive measurements on the efficiency of light pipe solar collectors of various materials and shapes. Measurements were also undertaken by BBRI to compare the transmittances of solar collectors under hemisphere ambient illuminance and normal incidence illuminance conditions. Carter [7] referred and used the transmission values for light pipe solar collector and diffusers given by Love et al [22]. However, these values were not found in Love et al's work. Therefore, it is more likely that the findings of BBRI [20] are more accurate and can be used with higher confidence than the latter one.

It was not explained in BBRI's report [20] why no comparison between the transmittances of diffusers under real and laboratorial testing conditions was undertaken. This may be due to the highly dynamic and complicated output of illuminance transmitted by light pipe tube, which makes the comparison difficult to implement. It has been addressed in Section 2.4 that the working mechanism of light pipe diffusers is complex. The attempt to evaluate its performance separately from other components of light pipe system does not necessarily lead to an applicable result. Light pipe diffuser is an integral part of light pipe system; therefore it may be more practical to assess its performance with other components as an entirety.

Efficiencies of light pipe tube

Zastrow et al [4] gave a simply equation to describe the transmittance of light pipe tube. However, as pointed out by Swift et al [5], "the reliance of the transmission on the three parameters p (aspect ratio), R (reflectance) and θ (the incidence anlge) does not allow a straightforward statement about the conditions under which the theory of Zastrow et al is a good approximation". It was further commented by Swift that in the main however Zastrow et al's model "is valid under the conditions of low p, high R and low θ", and "for calculations of the transmitted spectrum and colour coordinates it is anticipated that the theory of Zastrow and Wittwer will give incorrect values".

Calculated results due to Eq. 3.2 given by Swift et al were compared against measured data. It was noticed that, as reported by Swift et al "the value of reflectivity used in these results is 0.967 and was determined by fitting the experimental results to the corresponding theoretical calculation. The theoretical calculation are sensitive to the choice of reflectivity, with changes in R of 0.001 resulting in noticeable difference in the calculated curve." It was noticed that the reflectivity of the reflective sheet 3M Silverlux was found to be 0.972, which is about 0.005 higher than the fitted value. Although Swift et al pointed out that due to dust and aging, the reflectance of the sheet used in light pipe tubes might be expected to be slightly lower; this apposes the question on the accuracy of Eq. 3.2. Equation 3.2 is not integrable, and the transmittance of light pipe tubes must be obtained using numerical techniques.

Equation 3.3 given by Edmonds enabled the relative comparison of the transmitted power by light pipe tubes under different sun elevation angle, aspect ratio and reflectance conditions. However, Eq. 3.3 is based on a key weighting-factor $(R^2-x^2)^{1/2}/R$, which was used when averaging over rays equally spaced across the tube. A main weakness of Edmonds et al's Eq. 3.3 is it is not validated by comparison between theoretical values and measured data. According to Eq. 3.3, Edmonds et al gave theoretical plot showing the relative transmitted power as a function of sun elevation, surface reflectance and aspect ratio. However, it was reported that the plots were made by normalising to the power transmitted when the sun elevation equals 90 degrees. This implies that although the plot shows the effects of sun

elevation, surface reflectance and aspect ratio, it cannot be used directly in real light pipe design, because these figures cannot give absolute values.

The efficiency of light pipe bends

Oakley et al compared the illuminances due to two light pipes one with and the other without bends, and based on a rough calculation, gave 86% as the transmittance of one light pipe tube bend. However, the illuminances were not measured separately for the two light pipes, and considering the changing of external environment and the non-uniform interior layout, it is difficult to quantify the reliability of the results. This restricts the application of this result to real designs.

Love et al's study is more sophisticated and provided the evaluation of the efficiency of bends in more details. It was realized by Love et al however, that the geometry of light pipe (SunScope) system with elbow joints was too complicated to allow for any specific conclusions. Nevertheless, Love et al pointed out that the transmittance of a single elbow joints is about 10 percent lower than the transmittance of a single straight section of 330 mm light pipe (SunScope). It is noticeable that the figure of 10 percent (indicating a transmittance of 90%) however contradicts to the averaged transmittance of 80% given by the author. It was also concluded that the transmittance of a light bend was found to be affected by sky conditions, solar altitude and the geometrical configuration of the bend. This implies that the light transmission within light pipe bends can be complex, and it may be more practical to assess bends' performance as one integral part of the whole light pipe system.

3.4 THE DESIGN OF LIGHT PIPES

The design of light pipes should base on methods that can predict the performance of the whole light pipe system under all weather conditions. Designers need to know the values of illuminance on certain working plane or at other designated points due to light pipes. Till this project, no mathematical method that takes account of the effect of external and internal environmental factors and light pipe configurations has been made available. However, Carter's work [7] put forward three charts as a design tool for light pipe applications under overcast sky conditions.

3.4.1 Carter's design charts for light pipes

Using the techniques of luminous flux measurements and calculation, the relationship of pipe efficiency and aspect ratio for 25 pipes, variously of 330, 450 and 530 mm diameter was investigated. Pipe input was calculated as a function of external horizontal illuminance and pipe cross-section area. Pipe output was either measured or calculated using protometric integrator. A design chart was given by Carter to show the attenuation of light output with aspect ratio under overcast skies for vertical pipe systems including a clear light capture dome and an opal diffuser. Carter used Love et al's results as the design tool for light pipe bends under overcast sky conditions.

Experiments were undertaken to measure the luminous intensity in the vertical plane for the quadrant 0 – 90 degrees. Measurements were undertaken for two 330 mm diameter light pipes, one 610 mm in length and the other 1220 mm. Readings were taken (not continuously) through the months from September to November. It was noted however, that the sky conditions for the testing period were predominately overcast or cloudy with external horizontal illuminance only exceeding 25 000 lux for about 10% of the readings.

3.4.2 Design method based on Coefficients of Utilization

A design methods based on Coefficients of Utilization (CU) was proposed by Tsangrassoulis [23] based on the work of Tregenza [24]. This method treats the light pipe's aperture as a fixture and assumes that light pipes use perfectly diffuse emitter. The method was developed to estimate quickly the number of light pipes needed to light a room at a given level of lux. It was found by the author that CU depended on the geometric form of the light pipes (aspect ratio, area of admittance), the material properties (reflectance, specularity), the angle of incident of the solar radiation and the dimension of the room, the room's surface reflectance. It was concluded that the number of light pipe could thus be expressed as a function of CU, design illuminance, the area of the working plane and light loss factors (LLF). It was pointed out that the method was by the time still in its development stage, and it could be performed by a small piece of code quite easily.

3.4.3 Critical appraisal

Carter's design tool was tested by comparing the calculated internal illuminances due to light pipes against measured values. Good agreement has been seen between the predicted and measured values. However, it is noticed that the measured internal illuminances were mostly less than 30 lux. The maximum external illuminance for the validations were found to be 14 000 lux. The maximum internal to external illuminance ratio was found to be 0.225%, obtained 1 m under light pipe diffuser. This implies that the design tool given by Carter was only validated under heavily overcast sky conditions. In real applications, light pipes deliver more light in clear or part-overcast sky conditions. Shao et al's study [1] reported that in cases where light pipes with moderate aspect ratios were installed, good illuminance of up to 450 lux was obtained with internal/external illuminance ratios around 1%.

It is therefore made clear that the application of Carter's design tool is to a considerable extent limited to overcast sky conditions. This is due to the fact that the main design charts given by Carter were generated based on data measured under overcast sky conditions. Studies by Swift et al [5] and Edmonds et al [6] showed that, under clear sky conditions the transmission of light pipes is affected by solar altitude. According to Edmonds et al, for a light pipe of an aspect ratio of 3, the variation of transmission can be 100% when the solar altitude changes from 25 degrees to 40 degrees. Swift et al presented different curves to describe the transmission as a function of solar altitude for different aspect ratio.

It has been addressed in Section 2.4 that the transmission of sky diffuse illuminance and sunlight illuminance in light pipe system are different. Therefore, the applicability of a design guideline mainly for overcast sky conditions when sky diffuse illuminance is the dominant component of external global illuminance cannot be automatically extended to other sky conditions.

The Coefficients of Utilization (CU) method proposed by Tsangrassoulis [23] is mainly for estimating the number of light pipes that are needed to meet a certain lighting requirements. However, to put the method in to practical use, the relationship between CU and various geometrical and climatic factors has to be expressed in an explicit mathematical manner. Further substantial progress in this respect is therefore essential for the development of the CU method.

3.5 SUMMARY

In this chapter, previous works on daylighting performance of light pipes in real buildings, working mechanism of light pipes, transmission efficiency of light pipes and the design guidance for light pipe systems have been reported and critically appraised.

Previous works on daylighting performance of light pipe showed that light pipe is a complex system that requires extensive research to provide quantitative evaluations of its performance. The performance of light pipe system not only depends on the geometrical configurations of the system, but also depends on external meteorological and geographical conditions. It is therefore believed that to reveal the relationship between various internal and external factors, and the performance of light pipes, vast database that can provide necessary information on both light pipe itself and its ambient internal and external environment is needed. It is also revealed that instead of conventional daylight factor, the ratio between internal illuminance and external illuminance shall be used to measure the daylighting performance of light pipes. As the indicator of light pipe daylighting performance, the ratio shall be defined as a dimensional variety that can describe the internal illuminance distribution due to the light pipes. Due to the draw backs of measurements of light pipes performance in real applications, it is believed that mathematical modelling should be based on measurements undertaken in laboratories. Measurements on light pipes of various configurations under all weather conditions shall be undertake to enable the mathematical modelling to the purpose of generating a general performance evaluation model.

The efficiency of light pipe tube should be investigated under real sky conditions. Theoretical equations given by Zastrow et al [4], Swift et al [5] and Edmonds [6] do not take account of diffused light and due to their respect drawbacks, cannot be used in real applications. Light pipe diffuser is an integral part of light pipe system; therefore it may be more practical to assess its performance with other components as an entirety. It was also found that the transmittance of a light bend was affected by sky conditions, solar altitude and the geometrical configuration of the bend. This implies that the light transmission within light pipe bends can be complex, and it may be more practical to assess bends' performance as one integral part of the whole light pipe system.

The design tool given by Carter was only validated under heavy overcast sky conditions. It is made clear that the application of Carter's design tool is to a considerable extent limited to overcast sky conditions. The applicability of Carter's design tool, which is mainly for overcast sky conditions when sky diffuse illuminance is the dominant component of external global illuminance cannot be automatically extended to other sky conditions. Design tools should enable designers to know the values of illuminance on certain working plane due to light pipe installation under all weather conditions, especially when the sky is clear and the system delivers more daylight into buildings. As a conclusion, sophisticated mathematical performance predicting models that takes account of the effect of external and internal environmental factors and light pipe configurations is needed.

REFERENCES

1. Shao, L. (1988) Mirror lightpipes: Daylighting performance in real buildings *Lighting Research and Technology*, 30 (1), 37-44

2. Yohannes, I. (2001) *Evaluation of the Performance of Light pipes Used in Offices*, PhD Thesis, Nottingham, Nottingham University

3. Oakley, G., Riffat, S. B. and Shao, L. (1999) Daylight performance of lightpipes *Proceedings of the CIBSE National Conference*, Harrogate, London, Chartered Institution of Building Services Engineers, 159-174

4. Zastrow, A. and Wittwer, V. (1987) Daylighting with mirror lightpipes and with fluorescent planar concentrators *Proceedings of Spie - the International Society for Optical Engineering*, 692, 227-234

5. Swift, P. D. and Smith, G. B. (1995) Cylindrical mirror light pipes *Solar Energy Material and Solar Cells*, 36(2), 159-168

6. Edmonds, I. R., Moore, G. I., Smith, G. B. and Swift, P. D. (1995) Daylighting enhancement with light pipes coupled to laser-cut light-deflecting panels *Lighting Research and Technology*, 27(1), 27-35

7. Carter, D. J. (2002) The measured and predicted performance of passive solar light pipe systems *Lighting Research and Techonology*, 34 (1)

8. Whitehead, L. A. (1987) Large scale core daylighting by means of a light pipe, *Sunworld*, 11(1), 14-15

9. McCluney, R. (1990) Color-rendering of daylight from water-filled light pipes, *Solar Energy Material*, 21, 191-206

10. Edmonds, I. R. (1992) Performance of laser cut light deflecting panels in daylighting applications, *Solar Energy Materials and Solar Cells*, 29, 1-26

11. Edmonds, I. R., Reppel, J., Jardine, P. (1997) Extractors and emitters for light distribution from hollow light guides, *Lighting Research and Technology*, 29(1), 23-32.

12. Aizenberg, J. B., Aleshina, N. A., Pyatigorskii, V. M. (1996) Arched hollow light guides at the Chkalovskaya Moscow subway station, *Light and Engineering*, 4(3), 1-4.

13. Aizenberg, J. B., Buob, W., Signer, R., Korobko, A. A., Pyatigorsky, V. M. (1996) Solar and artificial lighting of a school building with hollow light guide system "Heliobus", *Light and Engineering*, 4(3), 41-54.

14. Shao, L. and Riffat, S. B. (2000) Daylighting using light pipes and its integration with solar heating and natural ventilation, *Lighting Research and Technology*, 32(3), 133-139.

15. Oakely, G., Smith, S. J., Shao, L. (2000) Triple Save – the investigation and monitoring of a combined natural daylighting and stack ventilation system, Internal report provided by Dr L. Shao, Institute of Building Technology, School of the Built Environment, University of Nottingham.

16. Smith, S. J., Elmualim, A. A., Riffat, S. B., Shao, L. (1999) Evaluation of dichroic material for enhancing light pipe/natural ventilation and daylighting in an integrated system, *CAST*, 1.

17. Surapong, C., Siriwat, C. and Liu, R. (2000) Daylighting through light pipe in the topics, *Solar Energy*, 69(4), 331-341

18. Hansen, V. G., Edmonds, I., Hyde, R. (2002), *Proceedings of the International Experts Meeting on Daylighting Conference*, CIBSE, Singapore.

19 Callow, J. M., Shao, L. (2002), Air-clad optical rod daylighting system, internal report from Institute of Building Techonology, Nottingham University, UK.

20. Loncour, X., Schouwenaars, S., L'heureux, D., Soenen, S., Voordecker, P., Wouters, P. (2000) *Performance of the Monodraught systems Windcatcher and Sunpipe*, BBRI - Belgian Building Research Institute

21. Muneer, T., Fairooz, F. and Zhang, X. (2001) Sky Luminance and Radiance Distributions - A comparison based on data from Bahrain, Japan and Europe *CIBSE Singapore Conference on Tropical Daylighting*

22. Love, J. A., Arch, D., Eng, P. and Dratnal P. (1995) Photometric comparison of mirror light pipe systems, unpublished report prepared for CF Management Calgary, The University of Calgary, Alberta, Canada

23. Tsangrassoulis, A. (2002) CIE TC 3-38 Tubular daylighting guidance systems (TDGS), internal report submitted to CIE TC 3-38.

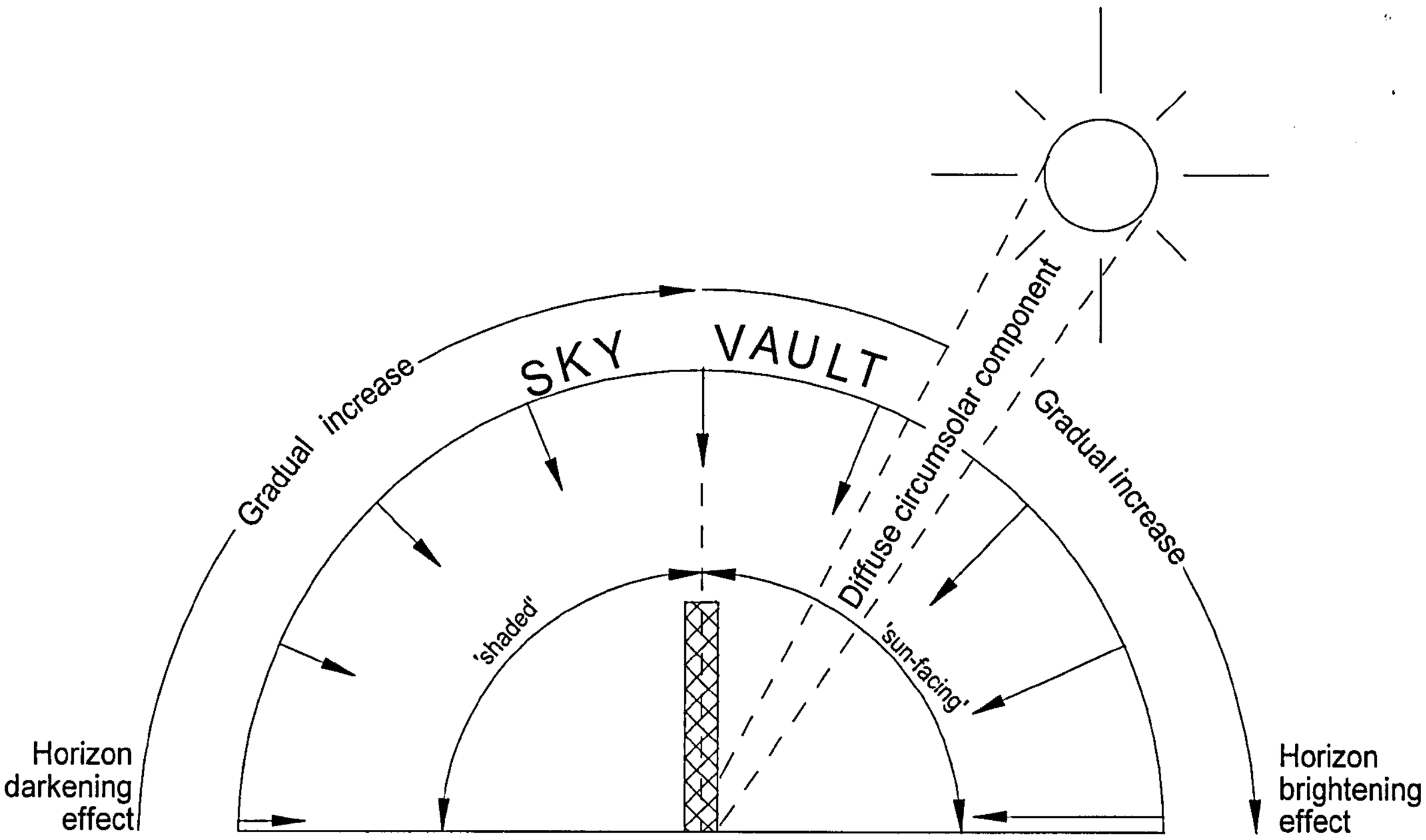

Figure 3.1 Representation of the sky luminance distribution under non-overcast conditions

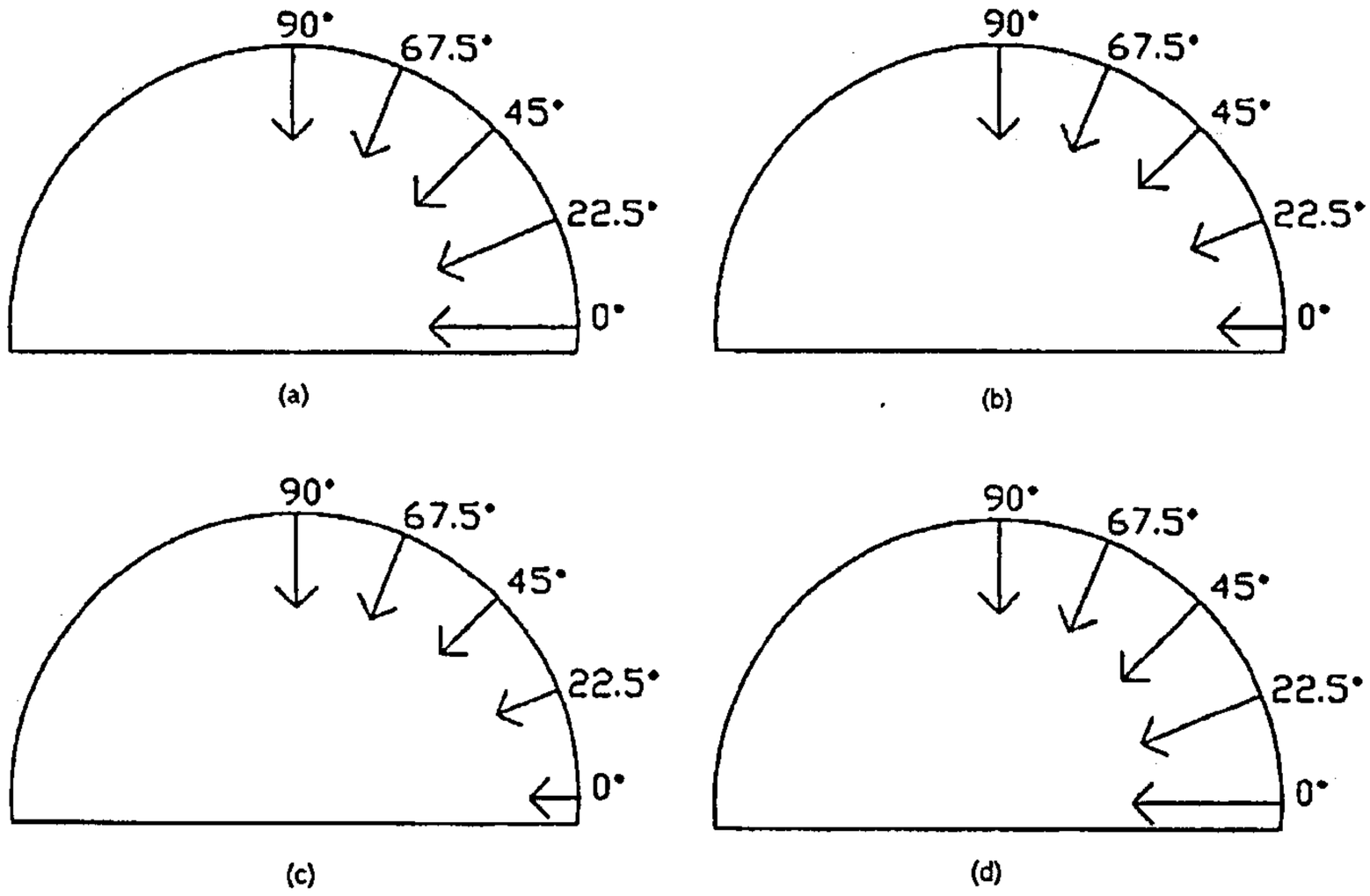

Figure 3.2 Vector presentation of Bahrain sky radiance distribution: (a) clear sky k_t=0.7, (b) part-overcast sky k_t=0.5, (c) thin overcast sky k_t=0.35 and (d) heavy overcast sky kt=0.2

4. RELEVANT THEORIES

Passive tubular solar light pipe is a daylighting device that transmits external daylight into buildings. To evaluate and predict the daylighting performance of light pipes, an explicit term that can specify its daylighting performance must be defined first. Daylight factor has been widely used as an industrial standard in daylighting design. However, because light pipes utilize both sky diffuse and sunlight radiation, the method of daylight factor is not suitable to measure the performance of light pipes. With the development of various innovative daylighting devices, it is necessary to use new concept that measures devices' performance in delivering both sky diffuse light and sunlight. Daylight penetration factor (DPF) is hence introduced in this study to specify, and as an index to evaluate the performance of light pipes.

The introduction of the concept of DPF forms the basis on which the daylighting performance of light pipes can be modelled. The proposed DPF models are built to predict the daylight delivery efficiency and the internal distribution by light pipe systems of various configurations under all weather conditions. The core task of the proposed DPF model is to predict transmission of daylight (sky diffuse light + sunlight) through light pipe systems. Light pipes use external daylight as input and produce diffused daylight as output. However, the input and output for light pipes are complex, therefore the proposed DPF model should incorporate other models so as to account for the complexity of input and output of light pipe system.

As shown in Section 3.2, daylighting performance of light pipes varies with the changing of external weather conditions. Since the proposed DPF model aims to predict the daylighting performance under all weather conditions, factors that describe the dynamic external weather condition have to be incorporated into the DPF model. Thus the input of light pipe systems can be described. Light pipes use diffusers to produce diffused light and spread it into buildings. The internal illuminance distribution resulting from light pipe's output depends on the amount of the daylight delivered by light pipe and the properties of the diffusers. The proposed DPF model aims to predict the daylight level at any points of interest. To achieve this, internal illuminance distribution models have to be produced, and incorporated into the proposed DPF model.

4.1 DAYLIGHT PENETRATION FACTOR

In design studies it has been conventional to specify interior daylighting in terms of daylight factor (DF). DF is defined as the ratio of the internal illuminance to the external diffuse illuminance available simultaneously and usually expressed as a percentage. Daylight factor is divided into three components, namely the sky component, the externally reflected component and the internally reflected components. The sky component is the ratio of illuminance at any given point that is received from a sky of known luminance distribution, to the horizontal illuminance under an unobstructed sky hemisphere. The external and internal reflected components are, respectively the ratios of the illuminance received after reflections from external and internal surfaces to the horizontal illuminance under an unobstructed sky hemisphere.

Because DF cannot specify the transmission of sunlight into buildings, light pipe daylight penetration factor (DPF) is introduced. DPF is defined as the ratio of the internal illuminance (due to light pipe daylight penetration) to the external global horizontal illuminance available simultaneously. Light pipe DPF has two components, namely the sky diffuse component ($DPF_{diffuse}$) and the sunlight (DPF_{beam}) component. When light pipe's efficiencies in transmitting sky diffuse light and sunlight are identical, DPF is a product of external global horizontal illuminance and the transmittance of light pipe (Eq. 4.1).

$$DPF = E_{internal} / E_{eg} \tag{4.1}$$

where $E_{internal}$ is the internal illuminance at a given point and E_{eg} is the total external illuminance. In general DPF can be described using Eq. 4.2:

$$DPF = (E_{vd} \times DPF_{diffuse} + (E_{vg} - E_{vd}) \times DPF_{beam}) / E_{vg} \tag{4.2}$$

The definitions of $DPF_{diffuse}$ and DPF_{beam} are shown in Eqs. 4.3 and 4.4 respectively.

$$DPF_{diffuse} = E_{internal\text{-}diffuse} / E_{vd} \tag{4.3}$$

$$DPF_{beam} = E_{internal\text{-}beam} / (E_{vg} - E_{vd}) \tag{4.4}$$

where E_{vd} is the external horizontal diffuse illuminance, $E_{internal\text{-}diffuse}$ the internal illuminance at a given point due to the sky diffuse light transmitted by light pipe, $E_{internal\text{-}beam}$ the internal illuminance at a given point due to the sunlight by light pipe.

Using DPF, the internal illuminance at a given point with coordinates (x, y, z) due to a given light pipe can be obtained, as shown in Eq. 4.5.

$$E_{internal\,(x,y,z)} = DPF_{(x,y,z)} \times E_{external} \tag{4.5}$$

where $E_{internal\,(x,y,z)}$ is the internal illuminance at the given point $P_{(x,y,z)}$, and $DPF_{(x,y,z)}$ is the light pipe Daylight Penetration Factor for the given point.

By including key parameters that present light pipe geometric and internal/external environmental factors into the proposed DPF model, the effects of these factors on light pipe daylighting performance can be taken into account. Geometric factors that may determine the performance of light pipe are the configurations of the system including the length and diameter of the light pipe tube and so on. The external irradiance captured by light pipe has two components: sky diffuse irradiance and direct beam irradiance. The split between these two components can be dictated by the numerical value of the sky clearness index k_t [1]. Sky clearness index (defined as the ratio of global to the extra-terrestrial irradiance) has been widely used to specify weather conditions. However, k_t is not an independent factor, other factors such as solar altitude (α_s) that is usually used to index the position of the sun on its track through the sky canopy can also have effect on light pipe daylighting performance. The internal illuminance distribution can also be affected by the internal geometric factors such as the position of the point of interest (due to the inverse square law and cosine law). Other factors such as the room shape, room dimensions and the internal reflection within a room lit by light pipes will also affect the internal illuminance distribution. However, because presently the main aim of the project is to evaluate light pipe's daylighting performance, internal reflection is discussed in later part of the thesis (Section 6.6.5). As a conclusion, DPF model can be expressed as a function of light pipe configurations factors (F_g), external environmental factors (F_e) and internal distribution geometric factors (F_i),

$$DPF_{(x,y,z)} = f(F_g, F_e, F_i) \tag{4.6}$$

4.2 TRANSMISSION OF SKY DIFFUSE LIGHT AND SUNLIGHT WITHIN LIGHT PIPES

It has been explained in Section 3.2 that light pipe transmits sky diffuse light and sunlight in different mechanism. This is mainly due to the different nature of sky diffuse and beam irradiance. Sky diffuse irradiance is from all angular directions within the 2π solid angle range while sunlight is parallel with its direction dependent on the position of the sun. Therefore it is logic to suppose that the transmittances of sky diffuse and beam illuminance through light pipe system can be different. The theoretical methods for calculating the transmittances of sky diffuse and beam illuminance through light pipe tube are presented in this section.

4.2.1 Transmission of sunlight within light pipe tube

Based on physical reasoning presented in Section 3.2, it is possible to show that a light pipe's transmittance is a function of the number of reflections required for a ray of light to descend the pipe and its reflectance (Fig. 4.1). If sunlight of intensity I and elevation α is incident on a light pipe tube of radius R and length L as in Fig. 4.1 then the input power is $\pi IR^2 \sin\alpha$. At each reflection the light descends a distance $2R\tan\alpha$ and the number of reflections is $L/(2R\tan\alpha)$. However, above calculation is only for a two-dimension light pipe tube. In real applications, light pipes are three-dimensional. For a three-dimension light pipe tube, most light is not incident normally to the reflection surface of the tube and therefore will require more reflections to descend the tube.

Figure 4.2 shows a projected view along the axis of a straight tubular light pipe tube. Light incident on the aperture at a distance x from the axis is incident on the reflecting surface at angle i. Then the number of reflections required to descend the light pipe tube is N,

$$N = L/(2R\cos i \tan\alpha) \tag{4.7}$$

If the reflectance of the reflecting surface is ρ then the transmission of a ray is ρ^N. The energy entering the aperture in the internal between x and $x + \Delta x$ is proportional to $\Delta x (R^2 - x^2)^{1/2}$. Therefore the

transmission of the light pipe tube for sunlight (defined as the ratio of output to input beam irradiance) can be obtained as:

$$T = \int_{x=0}^{R} [(R^2 - x^2)^{1/2} / R] \rho^{L/2R\cos i \tan\theta} dx \quad] \tag{4.8}$$

4.2.2 Transmission of sky diffuse light within light pipe tube

The transmission of sky diffuse light is more complex. However, by dividing the sky vault into a series of patches, the calculation can be carried out. Figure 4.3 shows an isotropic sky vault divided into 21 patches. Presume the radiance distribution is uniform and for a given sky patch, its azimuth angle is ψ and altitude α, then the horizontal diffuse illuminance (ΔIL) entering light pipe tube due to the sky patch can be obtained as:

$$\Delta IL = L\, d\alpha\, d\psi \sin\alpha \tag{4.9}$$

where $d\alpha$ and $d\psi$ are the span of the given sky patch in altitude and azimuth dimensions.

The total horizontal diffuse illuminance (E_{vd}) input into light pipe tube can be obtained by either summing up the contributions of all relevant sky patches or by measurements. Say IL_n is the horizontal diffuse illuminance entering light pipe tube due to a given sky patch, and T_n is the transmission of IL_n within the light pipe tube, then the total transmission of the sky diffuse illuminance ($T_{diffuse}$) can be obtained as:

$$T_{diffuse} = (\sum_{n=1}^{21} IL_n T_n) / E_{vd} \tag{4.10}$$

in which IL_n can be obtained using Eq. 4.9 and T_n can be calculated using Eq. 4.8. Above calculation on $T_{diffuse}$ in Equation is based on the consumption that the sky luminance distribution is uniform, i.e. an isotropic model is used to provide the input illuminance value for light pipes. However, it is well known that the sky illuminance distribution is not uniform. Therefore, to calculate $T_{diffuse}$ with a higher

accuracy requires the application of zenith luminance models that can describe unisotropic sky luminance distributions. This is explained in Section 4.3.

4.3 ZENITH LUMINANCE MODELS

It has been addressed in Section 4.2.2 that to calculate the theoretical transmission of sky diffuse illuminance within light pipe tube, sky luminance distribution should be made known first. Since the sky luminance distribution is not uniform, it is a more accurate procedure to apply unisotropic sky models that can describe the luminance distribution across the sky vault to the theoretical calculation.

Zenith luminance, L_{vz}, describes the luminous intensity of the circular part that is on the top of the sky vault. Using zenith luminance models, the luminance of other parts of the sky can be directly related to L_{vz}. This has two important bearing on the design of light pipes. Firstly, in real applications a light pipe can be installed in such a condition that its solar energy collector can only have a view of part of sky. The use of zenith luminance models enables lighting designers to know the estimated sky diffuse illuminance available to light pipe as input, so as to predict the internal illuminances due to the light pipe. Secondly, the transmission of the illuminance from different parts of sky that have varying elevation and luminance intensity can be calculated, leading to a more accurate result than that obtained based on an isotropic sky model.

4.3.1 Moon and Spencer's overcast sky model

Lighting designers often refer to CIE standard overcast sky condition when undertaking interior daylighting design as this sort of sky condition is regarded as a worst-case scenario. Overcast sky can be defined as the sky conditions that the sun is completely blocked by cloud. It has been found by measurements that when the sky is overcast, the zenith part of the sky vault tends to be brighter than other part of the sky whose altitude is α. The brightness of sky patches increases when its α increases. The ratio of the luminance of any sky patch, $L_{v\theta}$ to zenith luminance, L_{vz}, was found to be a function of luminance distribution index, b, and the altitude of the sky patch α. Moon and Spencer [2] described above relationship as:

$$L_{v\theta} / L_{vz} = (1 + b\sin\alpha)/(1 + b) \tag{4.11}$$

Moon and Spencer found that for overcast skies, the best value for b was 2. Commission International de Eclairage (CIE) has been using this b value of 2 as the standard reference value for overcast skies.

4.3.2 Muneer's model

Muneer [3] has used Eq. 4.11 to establish a relationship between slope diffuse irradiance and horizontal diffuse irradiance. Muneer's model is given by Eq. 4.12,

$$D_\beta/D = \cos^2(\beta/2) + [2b/\pi(3+2b)][\sin\beta - \beta\cos\beta - \pi\sin^2(\beta/2)] \tag{4.12}$$

where D_β is the hourly diffuse irradiance for a sloped surface, D is the hourly horizontal diffuse irradiance, β is the tilt of the sloped surface.

Muneer's model treats the shaded and sunlit surfaces separately and further distinguishes between overcast and non-overcast conditions. Based on his study for Bracknell, Muneer found that for a shaded surface (facing away from sun) the 'best' value of b was 5.73; for a sunlit surface under overcast sky conditions b = 1.68; and for a sunlit surface under non-overcast sky conditions b = -0.62.

Applying the b value of 2 to Eq. 4.11, it can be seen that under overcast sky conditions, the ratio of the luminance of the zenithal part of sky to that of the horizontal part is 3. Applying the b value of –0.62 for southern sky vault under non-overcast sky conditions, the ratio of the luminance of the zenithal part of sky to that of the horizontal part is 0.38. Shao et al [4] have reported the phenomenon that under overcast sky the efficiency of light pipe seems to be higher than that under clear sky conditions. This may be explained based on above brief analysis. When the sky is overcast, the direct view of the zenithal part of the sky, which has the highest luminance, is transmitted by light pipe with high efficiency. While under clear sky conditions, luminance emitting from the brightest part of sky is transmitted by light pipe with lower efficiency due to the multiple reflections, resulting in lower overall transmittance of daylight.

4.3.3 Perez all-sky model

The Perez et al model [5] computes L_v, defined as the ratio between the sky luminance at the considered point L_p and the luminance of an arbitrary reference point, as a function of the zenith angle of the considered point and the angle between the considered point and the position of the sun. The formula is given in Eq. 4.13.

$$L_v = f(\xi, \gamma) = [1 + a\exp(b/\cos\xi)][1 + c\exp(d\gamma) + e\cos^2\gamma] \tag{4.13}$$

where ξ is the zenith angle of the considered point, and γ the angle between the considered point and the position of the sun. The parameter a, b, c, d and e are adjustable coefficients, functions of insolation conditions [5]. The scheme of the parameters is represented as a 256-combination of the values of the zenith angle of sun, the isotropic correction factor, the sky's clearness index and the sky's brightness index [6].

4.3.4 Kittler, Darula and Perez's standard sky model

Based on Perez model, Kittler, Darula and Perez proposed a new range of standard skies. This is a set of mathematical formulae that are used to describe the luminance distribution under 15 different sky conditions.

The equation for relative sky luminance distribution to the zenith luminance is defined as a function of ξ, the zenith angle of the considered point and γ, the angle between the considered point and the position of the sun.

$$\frac{L_{v\theta}}{L_{vz}} = \frac{f(\gamma)\varphi(\xi)}{f(Z_s)\varphi(0)} \tag{4.14}$$

$$\frac{\varphi(\xi)}{\varphi(0)} = \frac{1 + a\exp(b/\cos\xi)}{1 + a\exp b} \tag{4.15}$$

in which the function f is the scattering index that relates the luminance at a point to its distance from the sun.

$$f(\xi) = 1 + c[\exp(d\xi) - \exp(d\pi/2)] + e\cos^2\xi \qquad (4.16)$$

4.4 INTERNAL ILLUMINANCE DISTRIBUTION

To determine the internal illuminance distribution due to light pipe using the proposed DPF model, the model must be able to predict the illuminance received by a given point from light pipe diffuser. The theoretical calculation of a given point due to a certain light source often involves two laws, which are the Inverse Square Law and the Cosine Law. According to the property of the light source, the procedure of applying Inverse Square Law and Lambert's Cosine Law differs. Particularly, when the output of light pipe is assumed to be uniform diffuse light, the approach of "radiative view factors" can also be used to determine the illuminance received at a given point from light pipe.

4.4.1 Lambertian Surface and Lambert's Cosine Law

A Lambertian surface is a surface of perfectly matte properties, which means that it adheres to Lambert's cosine law. Lambert's cosine law states that the reflected or transmitted luminous intensity in any direction from an element of a perfectly diffusing surface varies as the cosine of the angle between that direction and the normal vector of the surface. As a consequence, the luminance of that surface is the same regardless of the viewing angle. It is further illustrated by Fig. 4.4 that the intensity of radiation along a direction that has angle θ with the normal to a radiation-emitting surface is,

$$I_\theta = I_n \cos\theta \qquad (4.17)$$

where I_n is the intensity of radiation in normal direction. The intensity of radiation is defined as the rate of emitted energy from unit surface area through unit solid angle.

4.4.2 The Inverse Square Law

Distant lights appear fainter than nearby lights of the same intrinsic brightness. However, the true brightness of an object (its luminosity), must be distinguished from its apparent brightness. The term of luminosity is defined as the amount of energy radiated per second by an object. The intensity of light observed from a source of constant intrinsic luminosity falls off as the square of the distance from the object. This is known as the inverse square law for light intensity. Figure 4.5 illustrates the inverse square law. The entire light through the 1 square-foot first area goes through the second one, which is 100 times larger; hence the light intensity per square foot is 100 times smaller in the second area. The intensity drops as $1/R^2$.

4.4.3 Radiative view factor method

The view factor between any two surfaces is defined as that fraction of the radiative energy leaving an emitting surface that is intercepted by the receiving surface. The method for calculating the view factors from differential areas to spherical segments was given by Naraghi [7]. Figure 4.6 illustrates that according to the relative position of a given point to a energy emitting hemisphere surface, the calculation of view factor for the given point uses different formulae as shown below by Eqs. 4.18 (Appendix I).

4.5 STATISTICAL METHODS FOR EVALUATION OF MODEL PERFORMANCE

As noted in Section 4.1, mathematical DPF model that enables the prediction of the daylighting performance of passive solar tubular light pipe under all weather conditions will be developed in this work. In order to ensure the computational reliability of the proposed DPF model, validation methods have to be applied to assess the model's validity.

Model validation is conducted throughout this body of work with the aid of established statistical methods. In theory, data can be manipulated to produce results from which almost any conclusion can be drawn. Therefore, rather than to rely on a single statistical procedure, model evaluation is to be carried out using various statistical procedures. A summary of the statistical tools used throughout this work is presented forthwith.

4.5.1 Mean bias error (MBE)

The mean bias error (MBE) of a model indicates the model's ability to replicate data. In another word, the MBE tells whether or not a given model tends to overestimate or underestimate the measured data. In present study, the MBE is defined as:

$$Mean\ Bias\ Error,\ MBE = \frac{\Sigma(E_{estimated} - E_{actual})}{no.of\ observations} \tag{4.19}$$

where $E_{estimated}$ is the estimated internal illuminance due to light pipe, E_{actual} the measured internal illuminance, and "no. of observations" means number of data points.

A lower value of MBE indicates better model performance. A 0 value MBE indicates optimal model performance. A positive MBE indicates an overestimation of measured data. The converse applies for underestimation. Equation 4.18 shows the mean absolute value of the difference between the measured and predicted data. Therefore, the physical deviation can often be misinterpreted, particularly when it is used to describe model performance against measured data of low magnitude.

4.5.2 Root mean square error (RMSE)

Root mean square error (RMSE) is widely used to indicate the degree of scatter of the computed data compared against the actual data. In this study RMSE is defined as:

$$Root\ Mean\ Square\ Error, RMSE = \sqrt{\frac{\Sigma(E_{estimated} - E_{actual})^2}{no.of\ observations}} \tag{4.20}$$

where $E_{estimated}$ is the estimated internal illuminance due to light pipe, E_{actual} the measured internal illuminance, and "no. of observations" means number of data points.

The greater the deviation between $E_{estimated}$ and E_{actual} , the greater the sum of the square of the difference will be. A low RMSE is indicative of better model performance. A larger RMSE indicates greater dispersion of data.

4.5.3 Percentage average deviation (PAD)

As addressed in Section 4.5.1, in some cases MBE can be misinterpreted. For example, for two mathematical models A and B, when both model have the same MBE, the performance of them can be different. This is because that the magnitude of the data that the two models handle can be different. If the data that model A handles is in average several times to that of model B, then the performance of model A is actually better than model B. The value of MBE being equal to 0 does not necessarily indicate a good performance model. Suppose a model predicts largely overestimated value for half of the observations and gives heavily underestimated value for the other half, the MBE will also be found to be zero which can lead to erroneous conclusions such as the model is performing exceptionally well.

To overcome the drawback of MBE, a suitable accompanying statistical reinforcement shall be found.

PAD is therefore introduced in this study, which is defined as:

$$Percentage\,Average\,Deviation, PAD = \frac{\Sigma(100 * |E_{estimated} - E_{actual}| / E_{estimated})}{no.of\ observations} \qquad (4.21)$$

4.5.4 Slope and the value of the coefficient of determination of predicted versus measured illuminance

In case of regressional analysis, the technique used in the present work to fit models around measured data, the use of scatter plot of calculated versus actual data, and the slope of the fitted trend line and the value of the coefficient of determination are advised to provide insight into the performance of models.

The slope value is indicative of the validity of the model under test. The degree of validity increases as the slope approaches unity. In the case of present study, a slope value lower than 1 implies that the model tends to underestimate internal illuminance values due to light pipe, and the converse applies for

overestimation. However, the slope value cannot be used solely to evaluate the performance of a model. A model that produce large scatter can produce a unity slope trend line, although the performance of the model is actually not well. Therefore, the combined use of slope and the coefficient of determination (R^2) shall be applied to determine the performance. The value of R^2 ranges from 0 to 1, and it indicates the percentage of data points that the model can describe.

4.5.5 Histogram of errors

Besides scatter plot, another widely used validation method is histogram. Histogram plots of percentage deviation can be used to compare the performances of models. The histograms present graphical representations of the frequency distribution of the percentage error. A given model's performance is examined in two ways. Firstly, the histogram provides a check regarding the proportion of data points that fall within specific range of percentage error and secondly, it allows an examination of the range of errors.

$$\text{Percentage error} = 100 * \left| E_{estimated} - E_{actual} \right| / E_{actual} \quad (4.22)$$

where $E_{estimated}$ is the estimated internal illuminance due to light pipe, E_{actual} the measured internal illuminance.

REFERENCES

1. Lopez, G., Batlles, F. J., Martinez, M., Perez, M. and Tovar, J. (1998) Estimation of hourly beam solar from measured global solar irradiance in Spain, *Proceedings of the World Renewable Energy Conference*, 1998

2. Moon, P., and Spencer, D. E. (1942) Illumination from a non-uniform sky *Trans. Illum. Eng. Soc.*, 37, 707-725

3. Muneer, T. (1990) Solar Radiation Model for Europe *Building Serv. Eng. Res. Technol.*, 11(4), 153-163

4. Shao, L. (1988) Mirror lightpipes: Daylighting performance in real buildings *Lighting Research and Technology*, 30 (1), 37 - 44

5. Perez, R., Seals, R. and Michalsky, J. (1992) Modelling skylight angular luminance distribution from routine irradiance measurements, *IESNA transmission of the 1992 IESNA annual conference*

6. Muneer, T. and Zhang, X. (2002) A new method for correcting shadow band diffuse irradiance data, *Journal of Solar Energy Engineering: ASME*, 124

7. Naraghi, M. H. N. (1987) *Engineering Notes: American Institution of Aeronautics and Astronautics*

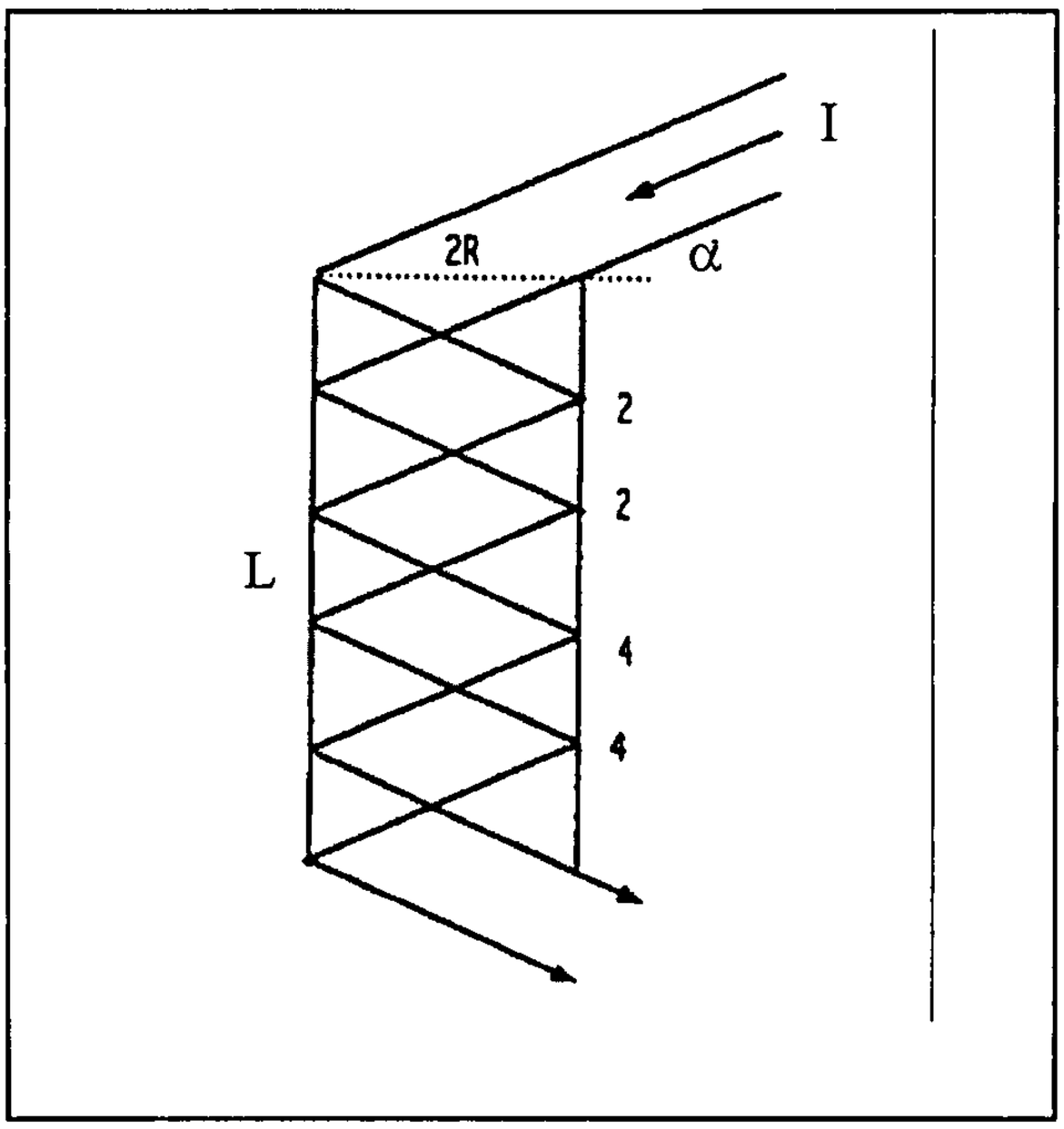

Figure 4.1 Sunlight of intensity I and elevation α descending a 2-D straight light pipe

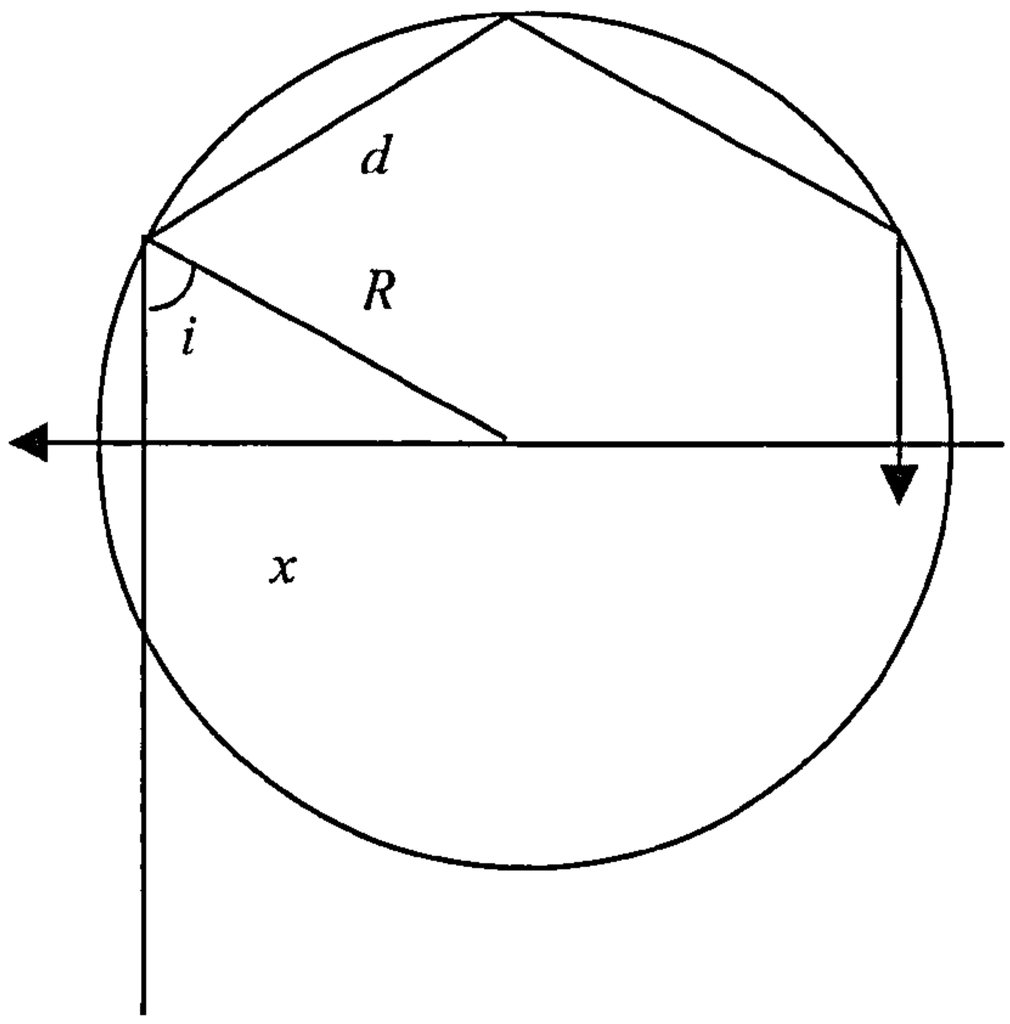

Figure 4.2 A projected view along the axis of a straight tubular light pipe tube, with light entering at distance x from the axis followed by its incident on the internal surface at projected angle I and travels distance d between reflections

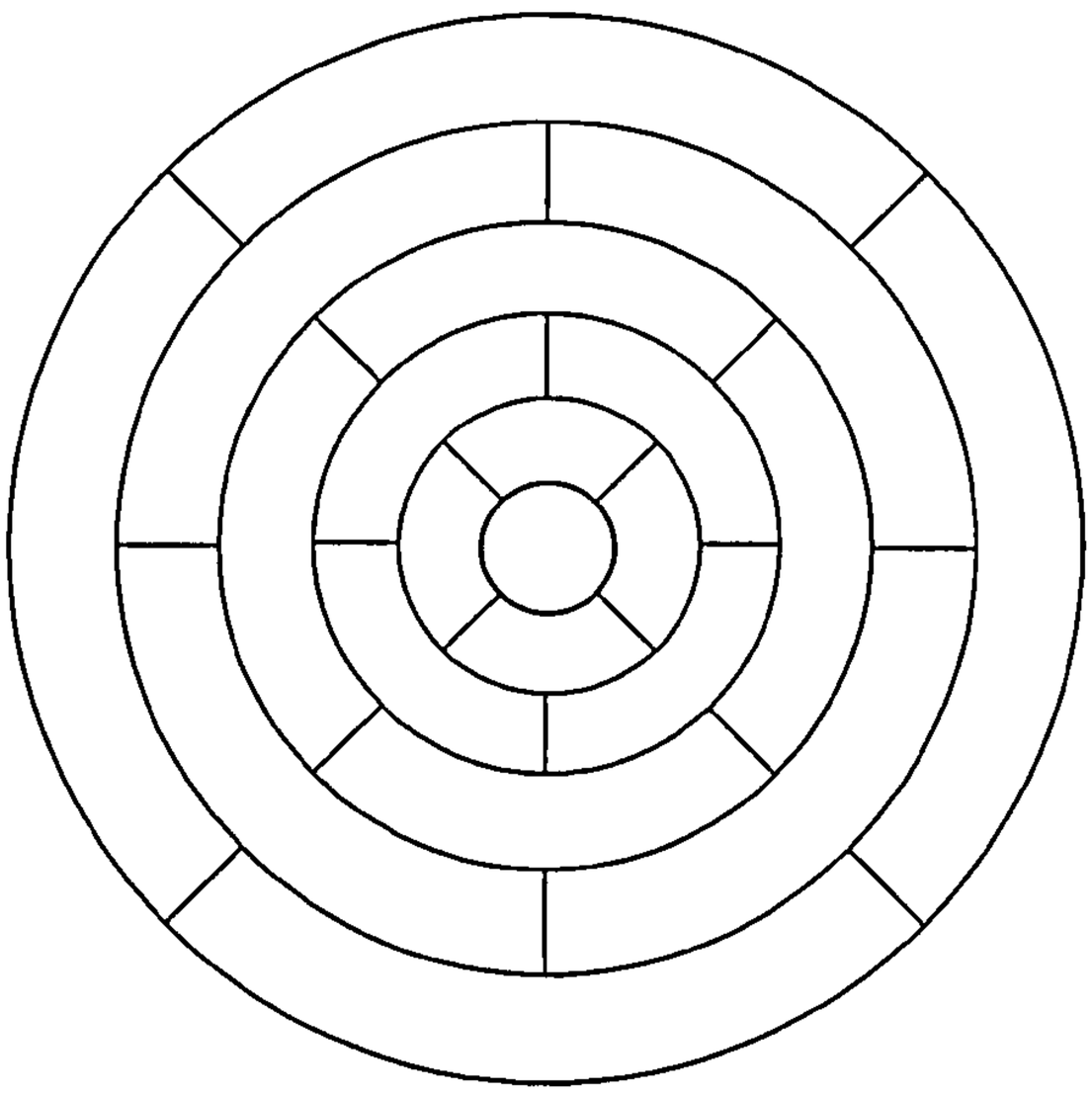

Figure 4.3 The uniform overcast sky vault devided into 21 patches

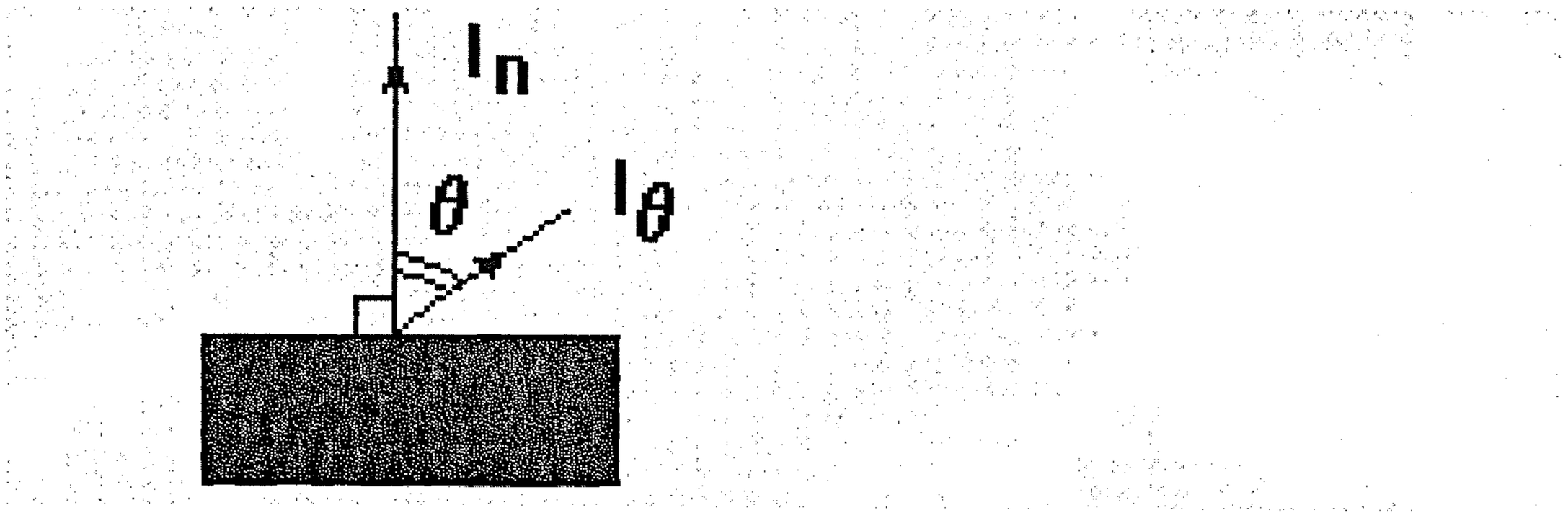

Figure 4.4 Emitted radiation from a surface

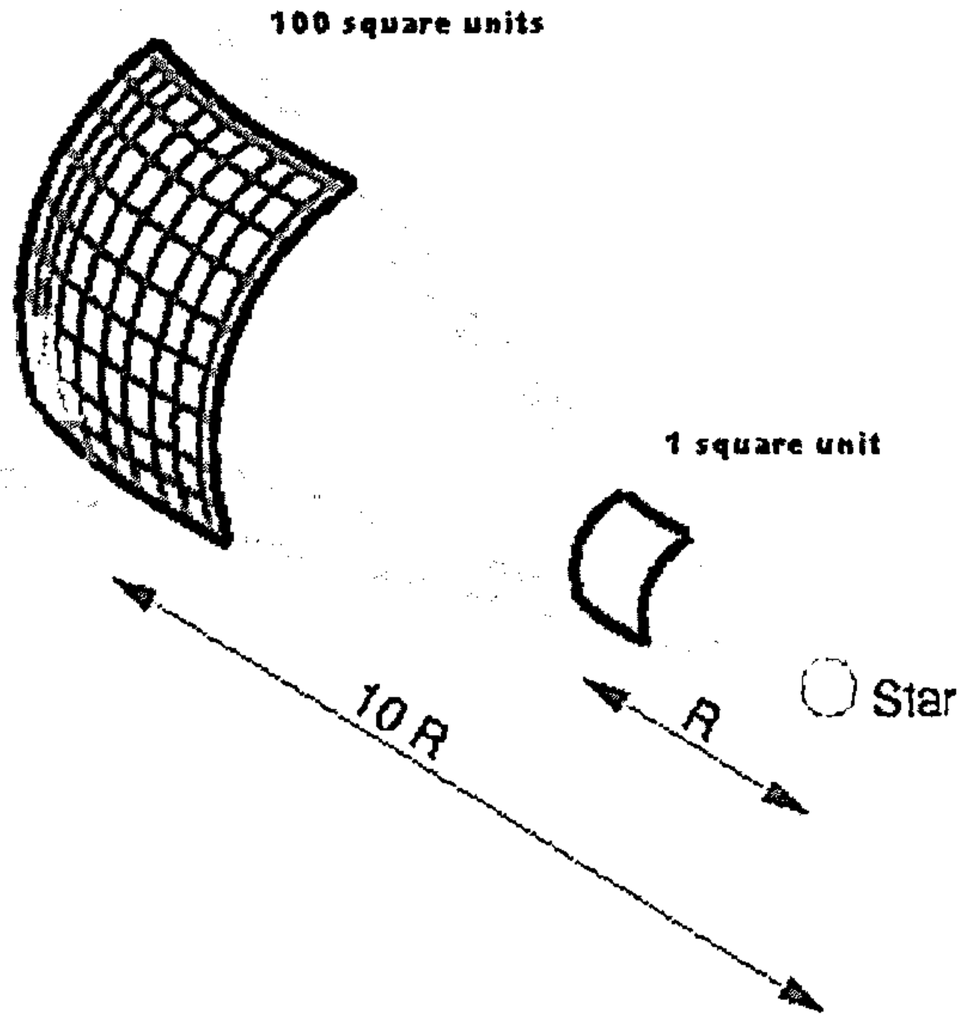

Figure 4.5 The inverse square law

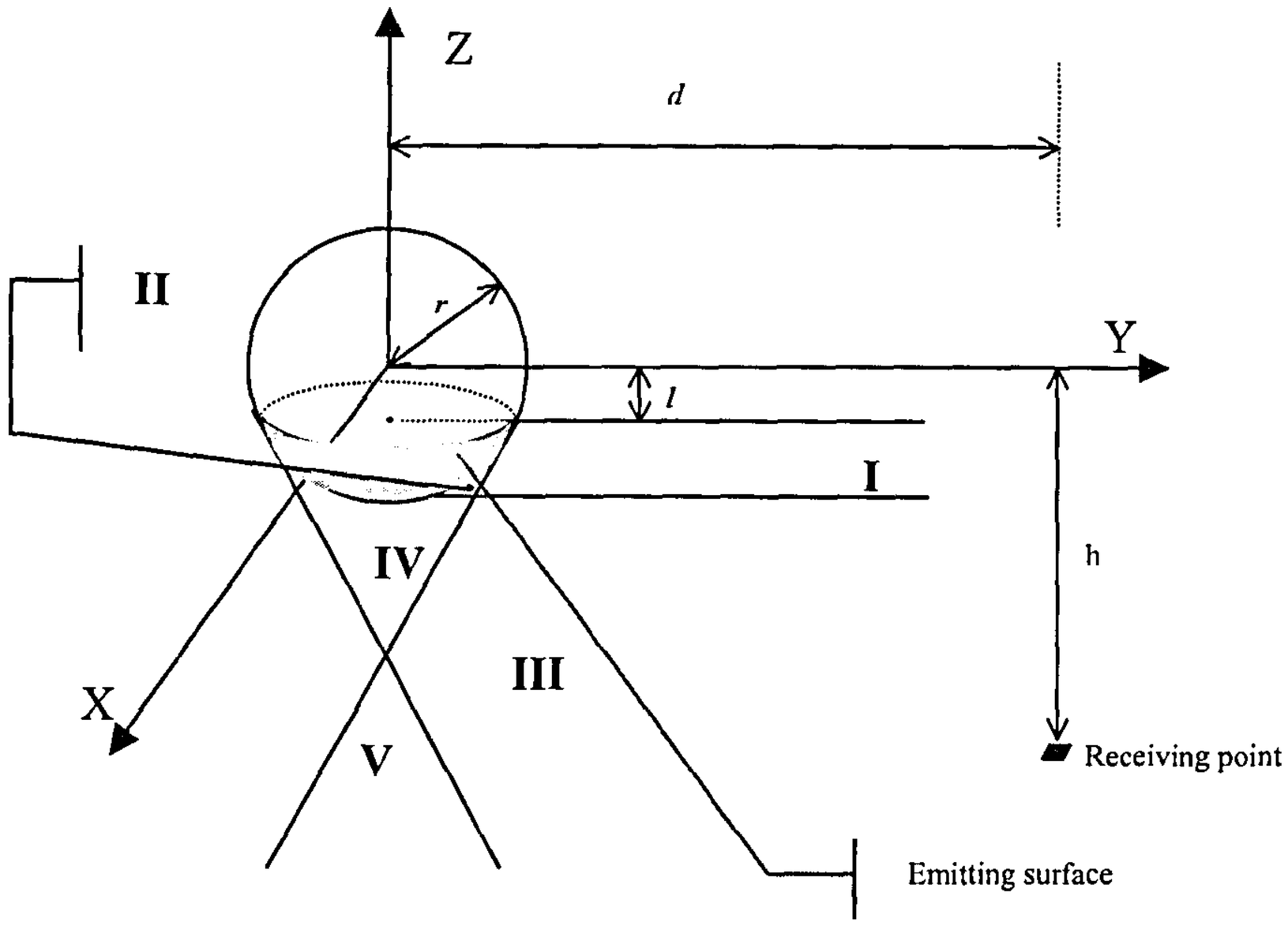

Figure 4.6 The calculation of view factors between a point and a hemisphere surface

5. MEASUREMENTS AND DATA PROCESSING

To enable the modelling of the daylighting performance of light pipes, data on the internal illuminances due to light pipes of various geometrical configurations under all weather conditions need to be obtained. The proposed DPF model (Eq. 4.6) expressed the daylighting performance of light pipes as a function of light pipe configurations factors (F_g), external environmental factors (F_e) and internal distribution geometric factors (F_i). It has been addressed in 3.5 that to build the proposed mathematical model, vast data should be measured in laboratory environment so as to eliminate the effects of other factors rather than F_g, F_e and F_i factors.

Other factors rather than F_g, F_e and F_i factors, which can affect the daylighting performance of light pipes may include the blocked sky view and shaded sunlight caused by surrounding natural or artificial objects, internal reflection related factors (e.g. the colour of the ceiling and walls), the shading caused by interior furniture layout and so on. Once a basic and general daylighting performance model of light pipes has been generated, the effects of above factors can be incorporated into or added to the model. Therefore, present study focuses on F_g, F_e and F_i factors, aiming to produce a fundamental DPF model of wide applicability.

Before the commence of large scale and long term measurements, a trial test on single light pipe was undertaken to preliminarily identify the key factors that affect the performance of light pipes. This trial test was undertaken in a real building room – the Currie test room. After the key factors being identified, daylighting performance measurements were undertaken in two sites, namely the Craighouse test room and the Merchiston test room.

The development of light pipe system has been an on-going process. More monitoring was therefore carried out to determine the performance of newly developed light pipes so as to examine the applicability and adaptability of the proposed DPF model. The latest developed light pipes (Monodraught) use a group of new diffusers, which enhances the daylight penetration into buildings. Effects of different light pipe diffusers on internal illuminance distribution were investigated and corresponding measurements were carried out in Currie test room.

5.1 NAPIER SOLAR STATION

Napier University solar station is located on the roof the main building at Merchiston campus, Napier University, Edinburgh. Edinburgh experiences a temperate climate and the average sunshine duration is 1351 hours. Merchiston campus, Napier University is situated on a main road, approximately 2 km to the south-west of Edinburgh. In a 5 km radius around the campus, 80% of land comprises of urban and suburban housing and offices whilst the remainder is a mixture of farmland and natural features [1].

Napier University solar station was built as a part of the international daylight measurement programme (IDMP) that was launched by the Commission International de l'Eclairage (CIE). The latitude and longitude of the solar station are 55.95°N and 3.20°W respectively. The height of the solar station above sea level is 110m. The local time for Edinburgh is GMT + 0.

The following instrumentation was installed at Napier University solar station. Illuminances are taken at one-minute intervals, and are recorded in a PC station. A tape recorder is installed in to the PC so as to enable the backup of massive data sets.

Illuminances

Global horizontal: PRC Krochmann 910GV

Diffuse horizontal: PRC Krochmann 910S

North-vertical: PRC Krochmann 910GV

East-vertical: PRC Krochmann 910GV

South-vertical: PRC Krochmann 910GV

West-vertical: PRC Krochmann 910GV

Shadow band specifications

Napier University solar station employs a Kipp & Zonen CM121 shadow ring with the German manufacturer Krochmann's diffuse illuminance sensor. Adjustment of the shadow ring is required for each measuring day and diffuse illuminance correction factor for the obstruction of the shade ring has to be applied. The shadow band has a radius of 31.0cm and a width of 5.5.

Figure 5.1 shows the views of the Napier University solar station. Figure 5.1(a) shows a close-up view of the installation and the relative position of the instrumentation. The sky diffuse illuminance sensor and shadow band are shown in the background and the horizontal global and vertical illuminances sensors are shown in foreground. Figure 5.1(b) represents a macro view of the station with the global horizontal and vertical illuminance sensors and sky diffuse illuminance sensor and shadow band respectively shown on the right- and left-hand side of the frame.

5.2 INTERNAL ILLUMINANCE SENSORS, DATA-LOGGER AND STANDS

One Kipp & Zonen pyranometer CM11 global irradiance sensor was used to measure the global incident energy to the light pipe installed in Currie test room. The Kipp and Zonen CM11 global irradiance sensor is classified as a "secondary standard" sensor according to the classification of the World Meterological Organization. The range the CM11 is 0 -- 1400 W/m^2 with a sensitivity of 4.6 $\mu V/Wm^{-2}$. The CM11 global irradiance sensor had been calibrated in November 1999 by the UK Meteorological Office.

Six sensors of two types were used to measure the internal illuminances due to light pipes. Three sensors of Selenium Photo-Electric Cells Type-B were supplied by Megatron Ltd, London. The active area and the sensitivity of Magetron Type-B photoelectric sensors are 3.5 cm^2 and 0.245 μA/lux. Magetron Type-B photoelectric sensors are of a dimension of 42mm diameter and 20mm high with integral cable 2m long. The advantage of selenium photovoltaic cells over other cells is that their response is very close to that of the human eye; this makes them particularly suitable for use in light measuring instruments. Their efficiency as energy converters of the total spectrum is not as high as some other photocells, and so they are not used as solar cells [2]. The three Magetron Type-B

photoelectric sensors employed in this study use amplifier that requires external 4.5 Volts AC-DC power-supply.

The other three sensors were supplied by Kipp & Zonen [3]; the actual component supplied was a Lux Lite illuminance meter, 54mm diameter × 35mm high with integral cable 3 m long. The Lux Lite consists of a photodiode, a filter, a diffuser and a housing. A resistance shunts the photodiode; this is done to generate a voltage output. The photodiode, the filter and the diffuser on top determine the spectral specifications. The diffuser ensures a field of view of 180 degrees, and that angular characteristics fulfil the so-called cosine response. The sensitivities of the three Lux Lite sensors are given as 10.32 μV/lux (±1%), 9.68μV/lux (±1%) and 10.11μV/lux (±1%) respectively. The ranges of the sensors are the same, namely 5±1klx.

A 20-channel data-logger was installed to record the measurements transmitted from the sensors. The actual component was a Squirrel SQ1000 Series data-logger supplied by Grant Instruments (Cambridge) Ltd, England [4]. Squirrel SQ1000 Series data-logger reliably measure and record inputs from a variety and member of sensors, making them suitable for a wide range of tasks in many industrial, scientific and research applications. SQ1000 Squirrel data-logger can be used as a portable meter, stand-alone data-logger or as a PC based data acquisition system.

To enable the measurement of internal illuminance achieved by various light pipes with bends, one stand on which photoelectric sensors could be mounted was used. The use of the adjustable stand ensured that photoelectric sensors measured the illuminances received by a plane that was parallel to the cross section of the light pipe tube (end section). The adjustable stand consisted of two components, a commonly available photographer's tripod and a table. The flexibility offered by the tripod made the slope and the distance of the plane where illuminance sensors were mounted adjustable. The table was manufactured from a piece of high-density polystyrene 25mm thick, 1m wide and 1.5m long. Prior to use, the table was painted with a matt black finish to eliminate any light reflection into areas within the sensors' range. This stand was used in Craighouse test room. Another stand was made to measure the internal daylight distribution due to light pipes. This stand was made similar to the one used in

Craighouse test room, but in a smaller dimension to be adaptable to Merchiston test room that is smaller than Craighouse test room.

5.3 DAYLIGHTING PERFORMANCE MONITORING IN REAL BUILDING - CURRIE TEST ROOM

A trial measurement was first carried out to determine the decisive factors that directly affect the performance of light pipe. The obtained data were to be analysed to reveal the influences of F_g, F_e and F_i factors on light pipe DPFs. A simple DPF model on the performance of a single straight light pipe can thus be built upon the data obtained in the trial measurement. The performance of this simple model was used as a pre-check of the sufficiency and validity of the large-scale measurement to be undertaken in Craighouse and Merchiston test rooms.

Since September 1999, a 330-mm diameter light pipe provided by Monodraught has been installed on the roof of a two-storey detached house in Currie, 10km south-west of City Centre, Edinburgh. The roof is free of obstructions. The light pipe is allocated in a child's bedroom on the top floor. The bedroom area is a rectangular-shaped space of 3.7 × 2.1 × 2.3 m (length × breadth × height). Figure 5.2 shows the dimensions of the room and the measurement scheme undertaken. The room has four walls, all of them covered with yellowish-white wallpaper. A small window on wall 1(Fig. 5.2 refers) has a western aspect. The sizes of the window's two panes are 32 × 71 cm^2 and 26 × 65 cm^2; and the height of the window's sight line (sill level) is 126cm from the floor. Near a corner of the room, there is a door on wall 2, which is opposite to wall 1. Two pieces of yellow wooden furniture are located along wall 3. In another corner and along wall 4, a bed is placed under the diffuser of the light pipe.

The light pipe on test was installed on a north-facing roof, which has a slope of 29° (Fig. 5.3). The length of the light pipe is 121cm (measured from the top edge to the bottom rim of the mirror pipe). The horizontal distances from the diffuser centre to wall 1, 2, 3 and 4 are 225cm, 146cm, 131cm and 79cm respectively.

From 1^{st} – 7^{th} of May and from 26^{th} – 31^{st} of May 2001, monitoring was carried out to record the external global illuminance and internal illuminance data. For this experiment, the window was

covered with a thick dark cotton towel, and the door was sealed to prevent any light entering from outdoors. One Kipp and Zonen CM11 global irradiance sensor was fixed on the ridge of the roof to measure the global incident energy of the light pipe under test. Three Megatron indoor illuminance sensors were employed to record the internal illuminance in different positions of the room. These sensors were fixed horizontally on three stands, all of height = 0.7m; and there was no obstruction between the light pipe diffuser and these sensors. During the measurement programme, positions of these sensors were changed each day and corresponding distances recorded.

External global irradiance data and internal illuminance data were recorded by a Grant (Squirrel) data-logger on a minute-by-minute basis throughout the day. In the two weeks of measurement about 23490 points of data were obtained, which provides a sufficient database for the trial mathematical modelling procedure to be carried out.

The measurement carried out included external global irradiance, internal illuminance and distances from survey points to light pipe diffuser, with corresponding date and time recorded. Sky clearness index and solar altitude were calculated using the algorithm provided by Muneer [5]. To ensure the database reliability, data were discarded for solar altitude less than 10°, or for $k_t \geq 1$. Out of the 23490 data points, 21147 data were selected to develop and validate the proposed model.

5.4 DAYLIGHTING PERFORMANCE MONITORING UNDER ALL SKY CONDITIONS - CRAIGHOUSE TEST ROOM

A purpose built test facility was established within the Craighouse campus of Napier University. Within the open grounds the test room was located on flat ground with an open southern aspect. The test room was 3.0m long × 2.4m wide with a height of 2.5m. Inside the test room all four sides and the roof had hardboard cladding nailed to the frame. All edges and the door surrounds were covered with heavy paper tape to seal the inside space from ingress of daylight. Sophisticated data-logging equipment inside the room was protected from the effects of weather. The room was equipped with power supply unit to support a PC, data-logger and multiple indoor illuminance sensors.

To enable the performance comparison between different light pipes, the test room was designed for ease of installation of light pipes with various designs. Initially, a total of eight light pipes with varied configurations (straight runs plus those with multiple bends) were supplied by the project co-sponsor. The diameters of these light pipes were 210mm, 330mm, 450mm and 530mm. All the light pipes use clear polycarbonate domes, 610mm long silverised aluminium tubes and opal polycarbonated diffusers.

Continuous performance monitoring was undertaken over a period from 10th May to 15th September, 2000. Daylighting performance of 15 light pipes of various configurations under all sky conditions were carried out during these four months. Details of all tests completed are listed in Table 5.1. The light pipe diameter, length, number of bends and length of bends, if any, were noted. Illuminance sensors were arranged on floor or on stands with their respective distances to the centre of light pipe diffuser recorded. External horizontal global irradiance data from the pyranometer (Kipp & Zonen CM11) and internal illuminance data from three photoelectric sensors (Megatron Type-B) were sampled every ten seconds and the averaged minute-by-minute data were stored by the data-logger. The desiccant of the Kipp & Zonen CM11 pyranometer had been checked before and during the measurements and changed when necessary so as to ensure the accuracy of the external global illuminance measurements. The system time of Grant Squirrel data-logger was synchronized according to solar time.

After the measurements, data obtained were processed and quality controlled. External illuminance, k_t and α_s were calculated using the algorithm provided by Muneer [5]. To ensure the database reliability, data were discarded for $\alpha_s \leq 10°$, or for $k_t \geq 1$. A total of 65 270 data points for all light pipes configuration were made available for mathematical modelling.

5.5 DAYLIGHTING PERFORMANCE MONITORING UNDER ALL SKY CONDITIONS - MERCHISTON TEST ROOM

A new test room was built upon the roof of the main building ("Main building" roof) at Merchiston campus of Napier University. The test room was located in the central part of the roof and has a complete open view to the southern sky, and 95 per cents of the whole sky hemisphere. The test room was 2m wide and 2m long with a height of 2m. Inside the test room all four sides and the roof had hardboard cladding nailed to the frame. All edges and the door surrounds were covered with heavy paper tape to seal the inside space from ingress of daylight. Internal illuminance sensors and data-logger equipment inside the room were protected from the effects of external environment. The room was not equipped with power supply, because Grant data-logger uses six AA1.5V batteries and three Kipp & Zonon Lux Lite indoor illuminance sensors do not require power supply.

The test room was designed for ease of installation of light pipes with various designs, so as to to enable the performance comparison between different light pipes. Initially, a total of four light pipes with varied diameters were installed in the test room. The diameters of these light pipes were 210mm, 330mm, 450mm and 530mm. All the light pipes use clear polycarbonate domes, 610mm long silverised aluminium tubes and opal polycarbonated diffusers.

Continuous performance monitoring was undertaken over a period from 28th May to 29th August, 2001. Daylighting performance of 10 light pipes of various configurations under all sky conditions were carried out during these three months. Details of all tests completed are listed in Table 5.2. The light pipe diameter, length, number of bends and length of bends, if any, were noted. Illuminance sensors were arranged on floor or on stands with their respective distances to the centre of light pipe diffuser recorded. The relative position of each testing point where each illuminance sensor seats to the light pipe being measured was also recorded. External horizontal global irradiance data from the pyranometer (Kipp & Zonen CM11) and internal illuminance data from three photoelectric sensors (Kipp & Zonon Lux Lite) were sampled every ten seconds and the averaged minute-by-minute data were stored by the Grant Squirrel data-logger.

External global horizontal illuminance data were measured at Napier University CIE IDMP solar station. Napier University solar station is established on the "South workshop" roof at Merchiston campus, Napier University. Both the test room on the "Main building" roof and the solar station on the "South workshop" roof have open view to the sky hemisphere. The horizontal distance between the two roofs is about 150 m. Napier University CIE IDMP solar station uses solar time as system time. The system time of the Grant Squirrel data-logger used to record internal illuminances due to light pipes within Merchiston Campus was synchronized according to the system time of Napier University CIE IDMP solar station.

After the measurements, data obtained were processed and quality controlled. External illuminance, k_t and α_s were calculated using the algorithm provided by Muneer [5]. To ensure the database reliability, data were discarded for $\alpha_s \leq 10°$, or for $k_t \geq 1$. A total of 22 270 data points for all light pipes configuration were made available for mathematical modelling.

5.6 INTERNAL DAYLIGHT DISTRIBUTION BY LIGHT PIPES – CRAIGHOUSE TEST ROOM

From 30th October 2000 to 14th January 2001, an eight-week test was carried out in Craighouse test room to investigate the internal daylight distribution due to light pipe with different configuration and type of diffuser. Eight tests were carried out in the measurements. Table 5.3 shows the composition of the tests.

Before the commence of the test, all the light pipes (Monodraught Sunpipe) installed in the Craighouse test room had their diffusers covered with black heavy plastic sheet and secured with adhensive tape. The cover was removed from the light pipe to be tested and the test equipment was placed directly beneath the light pipe diffusers.

The diameters of the light pipes were noted and six sensors (including three Kipp & Zonen Lux Lite sensors and three Megatron Type-B sensors) were arranged in an array being equispaced on the same diameter. The six sensors were fixed upon a table sustained by a tripod. The table was manufactured from a piece of high-density polystyrene 25mm thick and sky-blue in colour. Prior to use, the table was painted with a matt black finish to eliminate any light reflection into areas within the sensors' range. It

was important to have the plane where sensors were fixed perpendicular to the light pipe axis to ensure that all sensors were at an equal distance from the diffuser, the adjustable tripod was used to ensure this condition was achieved.

5.7 DIFFUSER COMPARISON – CURRIE TEST ROOM

To study the effect of light pipe diffuser type on light pipe daylighting performance, a 330 mm diameter light pipe provided by Monodraught was installed in the Currie test room. The object of these tests was to compare the performance of the opal diffuser against flat design clear diffuser. The opal diffuser takes the form of a white polycarbonate convex shape dome, which diffuses the light evenly into the interior space. The flat design clear diffuser is made of translucent plastic material with crystal effect finish and flat end. The latter type of diffuser is used to improve the daylight transmission of light pipes even further, albeit having a stronger directional component.

For three days from 28th to 30th May 2001, the daylighting performance of a 330 mm diameter light pipe with flat diffuser was monitored. The external global irradiance and internal illuminances at three points at varying distances to light pipe diffuser centre were measured simultaneously on a minute-by-minute basis. The three indoor Megatron illuminance sensors were installed corresponding to the measurements carried out on the light pipe with the older opal diffuser (see Section 5.3). A total of 4 300 data points were thus obtained. Daylight penetration factor DPF, defined as the ratio of internal illuminance to external illuminance for flat diffuser were calculated for all data points.

REFERENCES

1. Kinghorn, D. (1999) *Solar illuminance models based on other meteorological data* Ph.D. Thesis, Napier University, 64

2. http://www.megatron.co.uk/homepage.html, Megatron Ltd, London, UK

3. Kipp & Zonen B. V. (2001) *Lux Lite Instruction Manual*, Rontgenweg, Netherlands

4. Grant Instruments (Cambridge) Ltd. (2000) *Squirrel Data-logger Manual*, Cambridgeshire, UK.

5. Muneer, T., Abodahab, N., Weir, G. and Kubie, J. *Windows in buildings thermal, acoustic, visual and solar performance.* Oxford: Architectural Press, 2000.

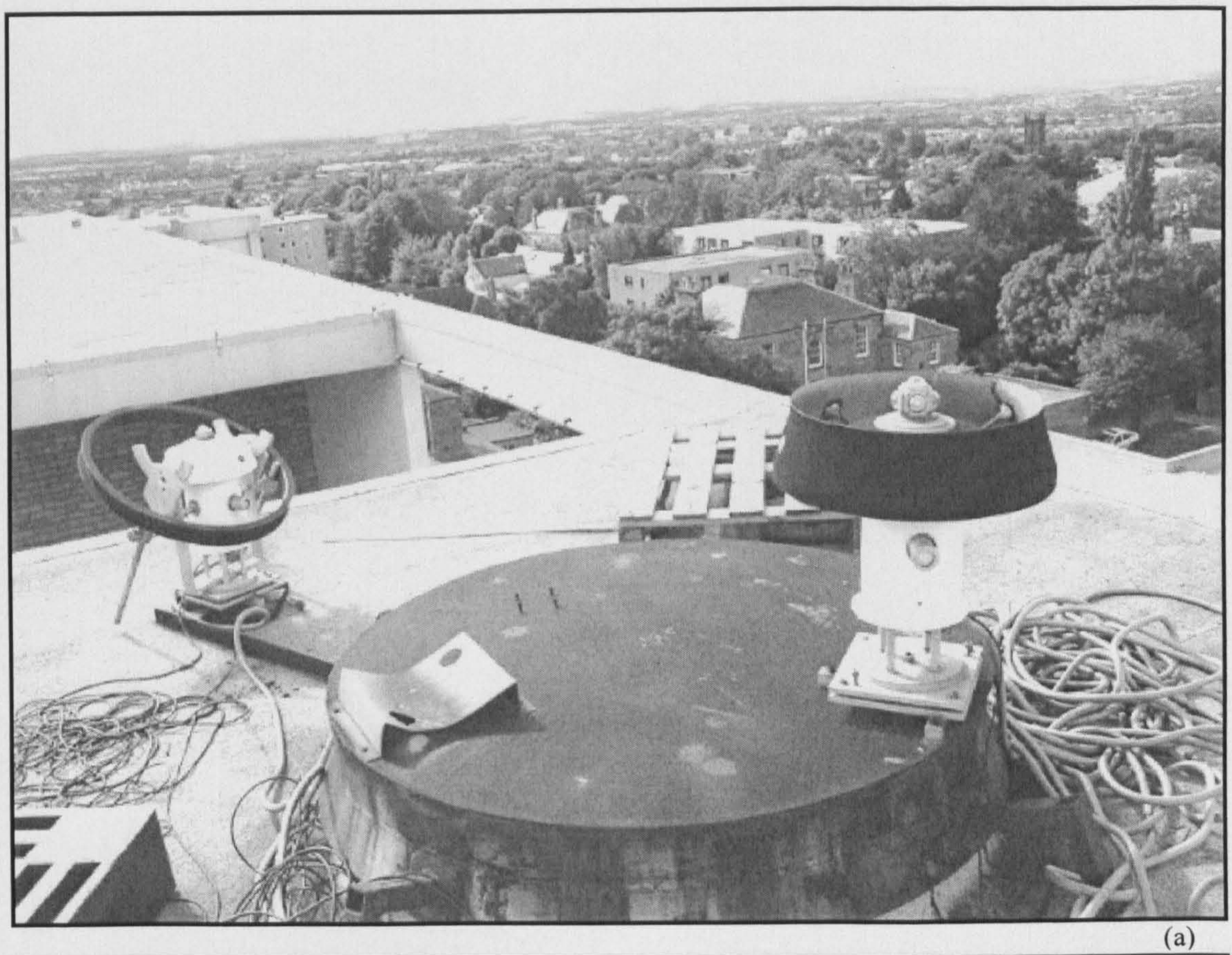

(a)

(b)

Figure 5.1 Napier University CIE First-Class solar station

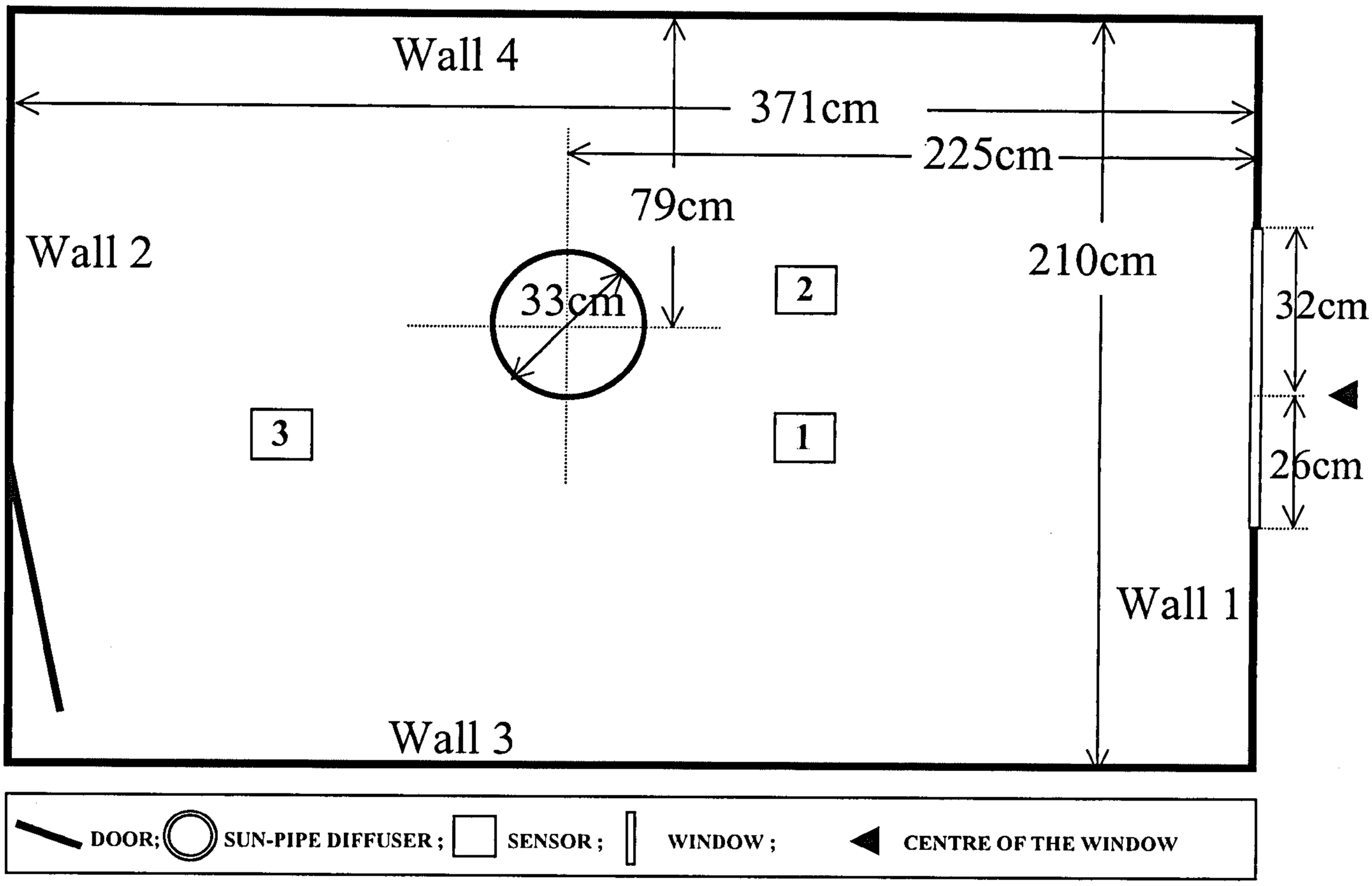

Figure 5.2 Schematic of the Currie test room and light pipe system

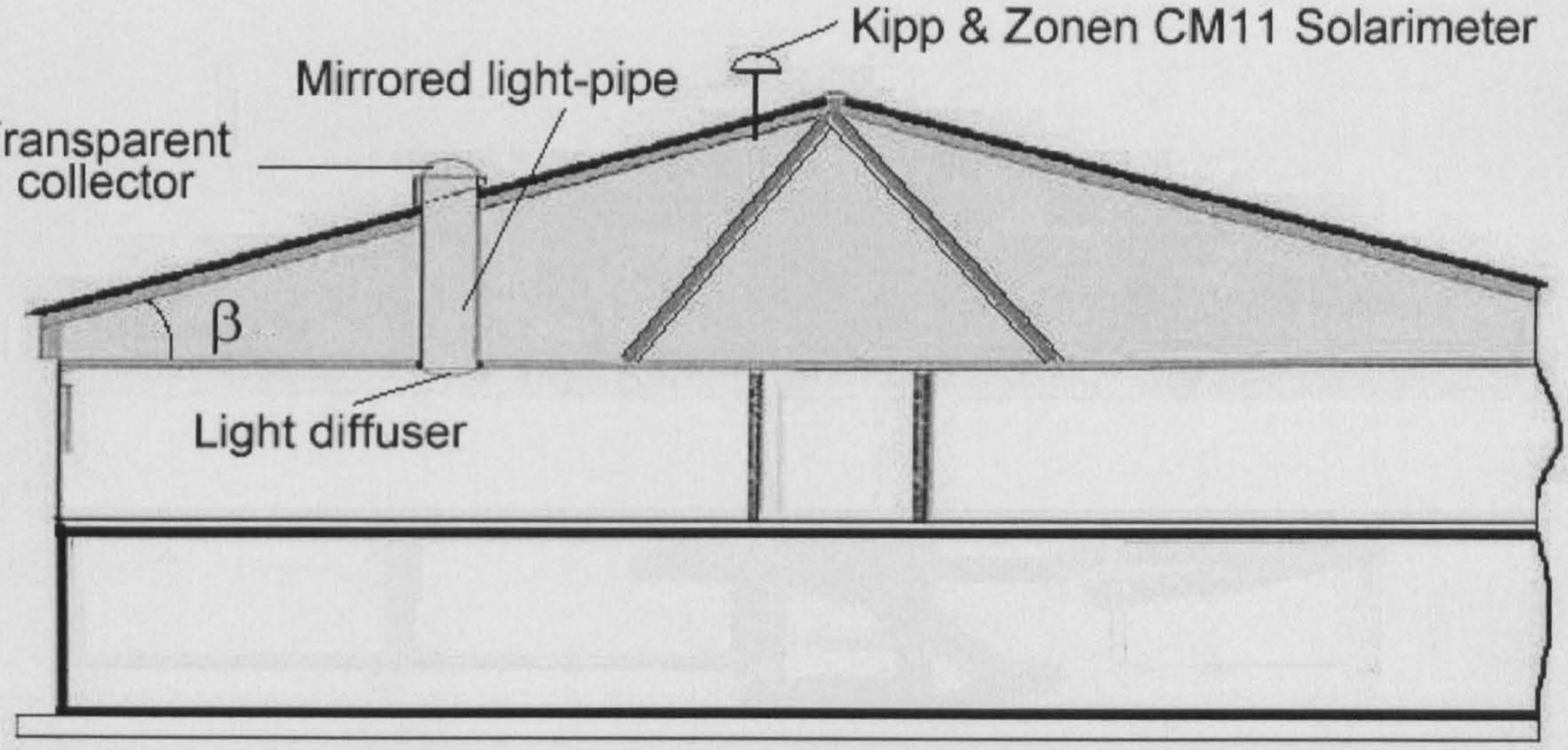

Figure 5.3 Light pipe system installation in Currie, Edinburgh (β=29°)

Table 5.1 Designs of light pipes that were monitored in Craighouse campus, Napier University

Design	Diameter, mm	Type	Length, mm	Bends number
1	210	straight	60	N/A
2	210	straight	120	N/A
3	210	elbowed	60	1
4	210	elbowed	60	2
5	330	straight	60	N/A
6	330	straight	121	N/A
7	330	elbowed	60	1
8	330	elbowed	60	2
9	330	elbowed	60	3
10	330	elbowed	60	4
11	420	straight	120	N/A
12	420	straight	60	N/A
13	530	straight	60	N/A
14	530	straight	120	N/A
15	530	elbowed	60	1

Table 5.2 Designs of light pipes that were monitored in Merchiston Campus, Napier University

Design	Diameter, mm	Type	Length, mm	Bends number
1	210	straight	60	N/A
2	210	straight	120	N/A
3	210	elbowed	60	2
4	330	straight	60	N/A
5	330	straight	121	N/A
6	330	elbowed	60	2
7	330	elbowed	60	4
8	420	straight	120	N/A
9	420	straight	60	N/A
10	530	straight	60	N/A

Table 5.3 Internal daylight distribution tests on light pipes installed in Craighous Campus, Napier University

Design	Diameter, mm	Type	Length, cm	Diffuser type
1	210	straight	60	Clear diffuser
2	330	straight	60	Opal diffuser
3	330	straight	60	Clear diffuser
4	420	straight	60	Opal diffuser
5	420	straight	120	Opal diffuser
6	420	straight	120	Clear diffuser
7	530	straight	60	Opal diffuser
8	530	straight	60	Clear diffuser

6. MATHEMATICAL MODELLING

The research strategy for the mathematical modelling of light pipe daylighting performance in terms of DPF (Daylight Penetration Factor) is straightforward and can be divided into three main blocks:

(1) Parameterisation, to identity the most decisive factors that affect the daylighting performance of light pipe systems;

(2) Framework, to choose a proper mathematical expression for proposed models;

(3) Formula fitting;

(4) Evaluation of models and modification to the models.

Figure 6.1 shows the system structure of the development of the proposed mathematical models and the procedure to validate the models.

Above research strategy treats a light pipe system as a black box and does not care the physical model of the system. The main approach to implement such a strategy is to combine an empirical mathematical expression with a set of coefficients derived from a large, high-quality and versatile experimental database. The major advantage of this strategy is that it is simple, practical and highly efficient. The possible limitation of this strategy is that it seems to be a non-physical mathematical model. To investigate the validity of the research strategy and to evade potential involved risks, a staged tactic was adopted to examine the strategy. The main aims of the two stages are outlined below:

(1) Stage I. According to the proposed strategy, a simple yet accurate mathematical model for a straight light pipe will be developed. After that, numerical error analysis will be applied to verify the validity of the straight light pipe model, DPF. The analysis results obtained in this stage will determine the sufficiency and the necessity of the proposed strategy, and hence will decide whether the research led by this strategy should go onto the second stage. Further work to improve the performance of DPF model and to extent the model to all light pipes can then lead the research into its second stage.

(2) Stage II. The second stage is a logically extending and deepening of the research carried out in stage I. It will include three main blocks, they are:

Firstly, to build general mathematical DPF model based on the methodology verified in stage I. Secondly, to target a more accurate performance prediction that takes account of the causes of system bias identified in stage I. Advanced solar radiation theories and techniques will be applied in this stage of research. It is intended that the completion of this stage of research will further improve the overall accuracy and reliability of the proposed model. Finally, validation of and modification to the general mathematical model DPF based on independent data will be undertaken.

6.1 LIGHT PIPE DESIGN AND DPF MODELLING

A precise design of light pipe system is only possible via a thorough understanding of the illuminance transmittance of the system. Light pipes are designed to collect light from both the sky and the sun. Since the external environmental factors such as sky clarity, sky-diffuse radiance distribution and sun's position change dynamically, the light pipe's overall efficiency of illuminance transmission also changes continuously.

The determination of light pipe system configuration aimed at achieving a given internal illuminance under given sky conditions would be the task of light pipe designers. It may be logical to assume that light pipe system's illuminance performance would depend on: (a) geometrical factors such as its length, diameter, number of bends, angle of bend and the diffuser type, and (b) the above mentioned external environmental factors. Thus, a mathematical model that encompasses the above factors would be desirable.

The concept of light pipe Daylight Penetration Factor (DPF) has been explained in Chapter 4, Section 4.1. $DPF_{s\,(x,\,y,\,z)}$ is defined as the ratio of a given point's internal illuminance to the total external illuminance for a given point with coordinates (x, y, z),

$$E_{internal\,(x,y,z)} = DPF_{s\,(x,y,z)} \times E_{external} \qquad (6.1)$$

where $E_{internal\,(x,y,z)}$ is the internal illuminance at the given point $P_{(x,y,z)}$, $E_{external}$ is the total external illuminance and $DPF_{(x,y,z)}$ is the light pipe Daylight Penetration Factor for the given point.

Light pipes are daylighting devices that utilise both sunlight and skylight. It has been reported that sun's position has an effect on light pipe's performance [1]. When the sky is clear, the solar altitude α_s influences the transmittance of sunlight within the light pipes. However, when the sky is overcast or part-overcast, the influence of sun's position becomes weaker since sunlight may no longer be the major component of external global illuminance. Hence in the present study the transmittance of light pipes was initially considered to be a function of α_s and the sky clearness index k_t (defined as the ratio of global to the extra-terrestrial irradiance).

According to the research strategy addressed in Section 6, DPF modelling for light pipes were undertaken in two steps. The first step is to develop a DPF_s model based on the performance modelling of a straight light pipe [4], which is described by Eq. 6.2,

$$DPF_{s\,(x,y,z)} = f(\alpha_s, k_t, D) \qquad (6.2)$$

where D is the distance from light pipe diffuser centre to a given position $P_{(x,y,z)}$. Eq. 6.2 is only applicable for straight light pipe designs and therefore cannot serve as a general DPF model for light pipes of other configurations. A generalised performance model that covers light pipes of all typical configurations ought to take account of geometrical design factors as well as environmental factors.

The second step is therefore, to build general DPF models based on the performance measurements of light pipe of various designs under all weather conditions. This requires one year's measured data to build the model and another one year's independently measured data to validate the model. The building and validation of DPF models are reported in the following sections.

6.2 THE DPF OF A STRAIGHT LIGHT PIPE

6.2.1 Parameter analysis

It may be shown from first principles [2] that the illuminance received at any given point from an elemental area of a luminous source of a finite size is proportional to the product of the luminous intensity of the elemental area (I), the respective cosines of the angles of emittance (θ_e) and incidence (θ_i) and the inverse square of the distance (D) between the elemental area and the point of incidence (see Eq. 6.3).

$$\text{Illuminance} \propto I \frac{\cos\theta_e \cos\theta_i}{D^2} \tag{6.3}$$

The area of the Currie test room (Section 5.7) was $7.8m^2$ while the light pipe luminous diffuser had a diameter of 330mm. Hence, the diffuser cannot be considered as a point source. Furthermore, observations have indicated that the diffuser was of non-uniform luminosity.

Therefore to obtain a precise estimate of the luminance environment of the test room under discussion, one has to integrate Eq. 6.3 point-by-point within the room, taking account of the variation of luminous intensity of the diffuser. However, a detailed procedure such as this is impracticable and unwarranted for design purposes, in particular by an industry that is in a stage of infancy. In view of the above discussion and as a first approximation the relationship between $DPF_{s\,(x, y, z)}$ and the distance D is presently proposed as that given by Eq. 6.4,

$$DPF_{s\,(x, y, z)} = A*(1/D)^2 \tag{6.4}$$

where $DPF_{s\,(x, y, z)}$ is the light pipe daylight penetration factor at the point $P_{(x, y, z)}$, due to the particular straight light pipe in test, A is a parameter that is dependent on sun's position and sky clarity, D is the distance from point $P_{(x, y, z)}$ to light pipe diffuser. Note that the integral calculation suggested via Eq. 6.3 is subsumed in Eq. 6.4 by adapting an empirical approach.

Figure 6.2 shows the scatter plot of measured DPF_s against D. Although the general trend seems to be in order, the percentage deviation for any given distance of the daylight penetration factor may be very large. Figure 6.2 therefore suggests that other non-geometry factors may be involved. Presently the role of k_t and α_s in improving the prediction of DPF has been investigated.

To explore the relationship between DPF_s and α_s, data sets recorded by sensors at a distance of 155cm for different time frames were selected. A total of 258 data points were employed to plot DPF_s as a function of solar altitude. Figure 6.3 shows this scatter plot. It is evident that for any given α_s a large scatter is generated, e.g. the percentage deviation of DPF is 120% when $\alpha_s \approx 41.5°$. This behaviour suggests that weather parameters additionally affect the daylight penetration factor. A further demonstration of the influence of weather condition's on DPF_s is shown by plotting DPF_s against sky clearness index k_t for $48.5° \leq \alpha_s \leq 49.5°$. Figure 6.4 shows such a scatter plot for D=155cm. A strong relationship between the two variables is evident.

6.2.2. Modelling and validation

It was demonstrated in the above section that DPF_s is influenced by D, α_s and k_t. Presently, a model given by Eq. 6.5 is proposed:

$$DPF_s = (a_{00} + a_{01} * \alpha_s + a_{02} * \alpha_s^2 + a_{03} * k_t + a_{04} * k_t^2 + a_{05} * \alpha_s * k_t + a_{06} * \alpha_s^2 * k_t + a_{07} * \alpha_s * k_t^2 + a_{08} * \alpha_s^2 * k_t^2) / D^2 \quad (6.5)$$

Equation 6.5 was further simplified and its validity evaluated. The simplified model is:

$$DPF_s = (a_{10} + a_{11} * \alpha_s + a_{12} * \alpha_s^2 + a_{13} * k_t + a_{14} * k_t^2 + a_{15} * \alpha_s * k_t) / D^2 \quad (6.6)$$

Values for the coefficients used in Eqs. 6.5 and 6.6 are listed in Table 6.1.

Equations 6.5 and 6.6 present a generic procedure to associate DPF to the two widely known parameters, namely α_s and k_t that influence daylight receipt. The equations cover the entire range of k_t, i.e. from heavy overcast when $k_t \approx 0.2$ to clear skies when $k_t > 0.6$. Further precision may be obtained by selecting specific formulations for overcast and clear skies. In this respect recommendation is made herein for more research work.

Model validation was undertaken via estimation of Mean Bias Error (MBE), Root Mean Square Error (RMSE) and Percentage Average Deviation (PAD):

$$Mean\ Bias\ Error,\ MBE = \frac{\Sigma(E_{estimated} - E_{actual})}{no.of\ observations}$$

$$Root\ Mean\ Square\ Error, RMSE = \sqrt{\frac{\Sigma(E_{estimated} - E_{actual})^2}{no.of\ observations}}$$

$$Percentage\ Average\ Deviation,\ PAD = \frac{\Sigma(100 * |E_{estimated} - E_{actual}| / E_{estimated})}{no.of\ observations}$$

Equation 6.7 is used to obtain estimated internal illuminance $E_{estimated\,(x,\,y,\,z)}$ for a given position $P_{(x,\,y,\,z)}$, where G is the instantaneous external global irradiance, and K_G is the global luminous efficacy (lumen/Watt). K_G is computed from a formulation provided by Muneer and Kinghorn (Eq. 6.8) [3]:

$$E_{estimated\,(x,\,y,\,z)} = DPF_{s\,(x,\,y,\,z)} * G * K_G \qquad (6.7)$$

$$K_G = 136.6 - 74.541k_t + 57.3421k_t^2 \qquad (6.8)$$

Based on above procedure using Eq. 6.5 calculated internal illuminance were plotted and regressed against corresponding measured data to determine the model's performance. Results of this comparison

are shown in Fig. 6.5. The slope of the fitted trend line is 0.973, and the coefficient of determination R^2 is 0.929. The MBE was found to be -2lux and RMSE 27lux which is 5% of the maximum value of measured illuminance (512lux) and 20% of mean illuminance (138lux). Percentage average deviation was noted as 21%. Calculated internal illuminance data were once again plotted against measured values for 11 different positions within the test room. 'D' for these positions range from 154cm to 212cm. Figure 6.6 shows this plot for D = 194cm. Table 6.2 shows the slope of the regressed line and other error statistics for six values of D.

Similar validation procedures were applied to Eq. 6.6 to examine its performance. In this case the slope of the fitted trend line was found to be 0.970, and the coefficient of determination R^2 was 0.930. The MBE was -2lux and the RMSE 28lux, which is 5% of the maximum value of measured illuminance (512lux) and 20% of mean illuminance (138lux). Percentage average deviation was once again found to be 21%. Thus, the simple model represented by Eq. 6.6 has comparable performance to the more involved model (Eq. 6.5). Table 6.3 shows the validation results for 7 positions at which internal illuminance were recorded.

6.2.3 Summary

Measurements of a single straight light pipe installed in a detached house in Edinburgh has been undertaken. Experimental analysis on the effects of different factors that influence the daylighting performance of light pipe system has been carried out. Based on the comparative analysis, the most decisive factors have been identified and a "best" form of mathematical expression has been determined. A DPF_s model for a particular light pipe has been established. Two articles, one on the DPF_s model and the other on light pipe performance monitoring have been published on the journal of Lighting Research and Technology (CIBSE) and on the international Renewable Energy for Housing Conference Proceeding [4, 5].

It has been concluded that the internal illuminance at a given point in a room where light pipes are the only lighting system can be estimated using Eqs. 6.5 and 6.6. Reasonably good agreement has been obtained between the predicted internal illuminance and experimental measurements. The Root Mean Square Error (RMSE) of calculated internal illuminance, the Mean Bias Error (MBE) and the

percentage average deviation have been found to be 27lux, -2lux and 21% respectively. The slope of the best fitted trend line was noted as 0.97 and the coefficient determination R^2 was found to be 0.93.

It is hence confirmed that the proposed research method is effective and valid. Similar measurements and modelling procedure will be applied to all types of light pipes available to obtain a general mathematical model.

6.3 STRAIGHT LIGHT PIPE DPF MODEL (S-DPF)

Since the DPF_s model has been verified, DPF modelling for all straight light pipes were carried out. It was thought that an appropriate model for straight light pipes with differing geometrical configurations should take account of the contribution of light pipe's length and diameter as well as α_s and k_t. The proposed generalised formulation that includes 12 coefficients ($a_0 - a_{10}$ and m) is given by Eq. 6.9,

$$S-DPF_{(x,y,z)} = (a_0 + a_1 k_t + a_2 \alpha_s + a_3 k_t \alpha_s + a_4 k_t^2 \alpha_s + a_5 k_t \alpha_s^2 + a_6 k_t^2 \alpha_s^2) \rho^{(a_7 + a_8 A_p + a_9 \cot \alpha_s + a_{10} A_p \cot \alpha_s)} R^2 (H/D)^m / D^2 \quad (6.9)$$

R is the radius of the light pipe, ρ the light pipe surface reflectance, A_p the aspect ratio (defined as the ratio of light pipe length to diameter) and H the vertical height of light pipe diffuser above the working plane. Values for the coefficients used in Eq. 6.9 are given in Table 6.4.

It may easily be shown that $DPF_{(x,y,z)}$ is proportional to the light pipe's sectional area and this accounts for the inclusion of the R^2 term in Eq. 6.9. It may be recalled that the inclusion of α_s and k_t and D^2 terms has already been discussed with reference to Eq. 6.5.

What follows now is a justification of the remainder of the terms included within Eq. 6.9. As a daylight reflecting device, the light pipe's transmission is affected by the reflectance of its interior coating material. Based on physical reasoning presented in Section 2.4, it is possible to show that a light pipe's transmittance is a function of the number of reflections required for a ray of light to descend the pipe and its reflectance (Fig. 6.7). The higher the reflectance of the pipe's interior surface (ρ), the higher the

light pipe's daylight transmittance. Edmonds *et al.* [1] reported that for sunlight of any given intensity, the number of reflections required is proportional to A_p and $\cot\alpha_s$, where A_p is aspect ratio defined as the ratio of light pipe length to its diameter and α_s the solar altitude. Therefore, a linear function that combines A_p and $\cot\alpha_s$ has been presently employed to account for the number of inter-reflections occurring within the light pipe. This explains the second factor in Eq. 6.9,

namely $\rho^{(a_7+a_8A_p+a_9\cot\alpha_s+a_{10}A_p\cot\alpha_s)}$.

A consideration of the manner of the spread of daylight by light pipe diffusers within interior spaces led to the adoption of the last factor in Eq. 6.9, i.e. $(H/D)^m/D^2$, where $1\leq m\leq 2$. For a given point in space, to obtain its illuminance resulting from a point or finite light source, the inverse square law and the cosine law must hold. However, if a light pipe diffuser is to be considered as a point light source, the cosine law should be applied only once and hence m=1; while on the other hand if the diffuser could be treated as a finite light source, then the cosine law must be applied twice, once for the emanation of light and the other for its incidence (or projection) on the horizontal plane. This requires m to be equal to 2. Thus a compromise was achieved by using a variable m. The "$1/D^2$" term embodies the application of the inverse square law.

Using the Craighouse data set, Eq. 6.9 was fitted. Good agreement between the measured data and calculated values was obtained and in this respect Fig. 6.8 shows the scatter plot of the predicted internal illuminance against measured data. The trend line was found to have a slope of 0.98 and the coefficient of determination was noted to be 0.95.

Model validation was also undertaken by estimation of the Mean Bias Error (MBE), the Root Mean Square Error (RMSE) and the Percentage Average Deviation (PAD). The MBE was found to be -1lux. The RMSE was 27lux which was 2% of the maximum illuminance (1187lux) and 15% of the mean illuminance (177lux). The PAD was found to be 12%. Results are summarized in Table 6.5.

To facilitate the use of the S-DPF model, Eq. 6.9 was further simplified and its validation was undertaken by estimation of MBE, RMSE and PAD. The simplified S-DPF model is,

$$S-DPF_{(x,y,z)}=(a_0+a_1k_t+a_2\alpha_s)\rho^{(a_3+a_4A_p+a_5\cot\alpha_s+a_6A_p\cot\alpha_s)}R^2(H/D)^m/D^2 \qquad (6.10)$$

Values for the coefficients used in Eq. 6.10 are listed in Table 6.4. Calculated internal illuminance based on the procedure using Eq. 6.10 were plotted and regressed against corresponding measured data. The slope of the best-fit trend line is 0.98, and the coefficient of determination R^2 is 0.95. The MBE, RMSE and PAD for the simplified S-DPF model were found to be –3lux, 29lux and 13% respectively (Table 6.5).

6.4 ELBOWED LIGHT PIPE DPF MODEL (E-DPF)

To predict the $DPF_{(x,y,z)}$ of elbowed light pipe systems (30-degree bends), the energy loss due to each bend has to be considered. The length of each bend (L_b) and the number of bends (N) have been accounted for by the use of an equivalent-length factor (f_{len}) and the energy-loss factor (f_{loss}) within Eq. 6.11. L_b and f_{len} are subsumed within a modified expression for A_{pe}. The factor $(1-f_{loss})^N$ used in Eq. 6.11 accounts for the overall transmittance efficiency of the N bend(s),

$$E-DPF_{(x,y,z)}=(a_0+a_1k_t+a_2\alpha_s+a_3k_t\alpha_s+a_4k_t^{\,2}\alpha_s+a_5k_t\alpha_s^{\,2}+a_6k_t^{\,2}\alpha_s^{\,2})\rho^{(a_7+a_8A_{pe}+a_9\cot\alpha_s+a_{10}A_{pe}\cot\alpha_s)}R^2(1-f_{loss})^N(H/D)^m/D^2 \qquad (6.11)$$

where $A_{pe}=(L+f_{len}L_b)/2R$ and L is the length of straight light pipe, f_{len} the equivalent-length factor, L_b the sum of the linear lengths of all bends and R the radius of light pipe. f_{loss} is the energy-loss factor for each 30-degree bend, most commonly used in a light pipe system. Values for the coefficients used in Eq. 6.11 are listed in Table 6.4.

Using an optimisation procedure, regressed coefficients in Eq. 6.11 were determined. The "best" value for f_{len} was found to be 0.65 and the value for f_{loss} was found to be 0.2, which is in good agreement with Cater's study [6].

The performance of the E-DPF model was then evaluated using MBE, RMSE and PAD. The MBE was found to be -2lux. The RMSE was 23lux which was 2% of the maximum illuminance (931lux) and

22% of the mean illuminance (103lux). The PAD of the estimated internal illuminance was found to be 25%. A scatter plot of the calculated against measured internal illuminance is shown in Fig. 6.9. The slope of the trend line was found to be 0.97 and the coefficient of determination was noted as 0.97.

Eq. 6.11 was further simplified and the simplified E-DPF is given below,

$$E-DPF_{(x,y,z)} = (a_0 + a_1 k_t + a_2 \alpha_s)\rho^{(a_3 + a_4 A_{pe} + a_5 \cot\alpha_s + a_6 A_{pe}\cot\alpha_s)} R^2 (1 - f_{loss})^N (H/D)^m / D^2 \quad (6.12)$$

Values of the coefficients used in Eq. 6.12 are shown in Table 6.4. The MBE, RMSE and PAD for the simplified E-DPF model are –3lux, 25lux and 24% respectively. The calculated internal illuminance due to Eq. 6.12 were regressed against measured data. The slope of the best-fit trend line was found to be 0.97 and the coefficient of determination was noted as 0.97. Results are shown in Table 6.5.

6.5 Light pipe View Factor DPF Model (V-DPF)

The presently proposed S-DPF and E-DPF models describe the internal illuminance distribution of light pipes using the factor $(H/D)^m / D^2$. The "best-fit" value for parameter m was obtained as 1.3. To validate the sufficiency of the expression $(H/D)^m / D^2$ in describing the light pipe internal illuminance distribution characteristics, another approach, namely the "radiative view factors" method has been applied to enable a performance comparison between the two different approaches.

The view factor between any two surfaces is defined as that fraction of the radiative energy leaving an emitting surface that is intercepted by the receiving surface. A V-DPF model is defined herein as a DPF model that uses view factor method to describe internal illuminance distribution within room. The proposed view factor model V-DPF of a straight light pipe is shown in Eq. 6.13, where $F_{v(x,y,z)}$ is the view factor between the ceiling mounted light diffuser and the given point $P_{(x,y,z)}$.

$$V-DPF_{(x,y,z)} = (a_0 + a_1 k_t + a_2 \alpha_s + a_3 k_t \alpha_s + a_4 k_t^2 \alpha_s + a_5 k_t \alpha_s^2 + a_6 k_t^2 \alpha_s^2) \rho^{(a_7 + a_8 A_p + a_9 \cot\alpha_s + a_{10} A_p \cot\alpha_s)} R^2 F_{v(x,y,z)} \quad (6.13)$$

The method for calculating the view factors from differential areas to spherical segments is given by Naraghi [7]. The entire formulation has been provided in Section 4.4.3. However, only case numbers III and V are of interest within the present context.

Using the Craighouse test room database for all straight light pipes, the view factor $F_{v(x,y,z)}$ for each data point has been calculated and the value of the coefficients in Eq. 6.13 have been re-fitted. Fig. 6.10 shows the scatter plot of the estimated internal illuminances due to the V-DPF model against the measured data. The RMSE and MBE for the V-DPF model were found to be 52lux and -9lux, corresponding to 27lux and -1lux for the V-DPF model (Eq. 6.13). The slope of the trend line for a plot of calculated versus measured data was found to be 0.94 and the coefficient of determination was 0.86. The corresponding figures for the V-DPF model (Eq. 6.9) were 0.98 and 0.95. Results are shown in Table 6.5.

6.6. PARAMETRIC ANALYSIS

In the modelling process, a number of environmental and geometrical factors that influence the daylight transmission of light pipes have been identified. In this section a parametric analysis of those factors is presented.

6.6.1 Effect of α_s and k_t

It was shown above that α_s affects the DPF by altering the number of inter-reflections within light pipes. When α_s increases, the number of inter-reflections decreases which results in a higher transmittance. However, when k_t changes, the extent to which α_s affects DPF also changes. Figure 6.11 shows the variation of S-DPF and E-DPF against α_s for varying weather conditions. It was noted that DPF shows an increasingly stronger trend with α_s for clear sky conditions.

6.6.2 Effect of R and L

For any given α_s and k_t, the square of the radius of a light pipe, R^2 affects the light pipe's external illuminance admittance. Furthermore, the aspect ratio of light pipe A_p (=L/2R) and α_s influence the light pipe's transmittance. Figure 6.12 presents this functional variation.

6.6.3 Effect of distance D and diffuser height H

The DPF model shows that light pipe's performance strongly depends on D, namely the distance between light pipe diffuser centre to the given point $P_{(x,y,z)}$ and H, the vertical distance between the diffuser centre to the working plane. In Eqs. 6.9, 6.10, 6.11 and 6.12, the best-fit value for the coefficient m was found to be 1.3. This indicates that in real applications, light pipes work more like a point light source rather than a source of a finite area. The internal illuminance achieved by a light pipe system with an opal diffuser is proportional to $(H/D)^{1/3}$ and inversely proportional to D^2.

6.6.4 Effect of light pipe bends

In Eqs. 6.11 and 6.12, the best fitted value for f_{loss} was found to be 0.20, which means that each 30-degree bend looses 20% of energy during daylight transmission. For a light pipe with N bends, the total energy transmittance of light pipe bends is therefore $(1-f_{loss})^N$, where $f_{loss} = 0.2$. The use of bends increases the value of the aspect ratio and thus it reduces the daylight transmittance. Figure 6.13 shows the comparison of DPF for a 600mm-long, 520mm-diameter straight light pipe with an increasing number of bends.

6.6.5 Effect of internal reflection

The internal surfaces (ceiling, roof and floor) of the Craighouse test room were painted white which has a high reflectance, the assessment of the contribution of internal reflected illuminance is therefore necessary to enable an assessment of the contribution of internal reflection on DPF. In the absence of any other information regarding the inter-reflection of diffuse as well as beam illuminance within rooms and also bearing in mind the fact that light pipes are primarily providers of diffuse illuminance,

the internal reflection characteristics of light pipes were treated as being of similar order as windows. Therefore, for the Craighouse test room, the contribution of internal-reflected illuminance to the total illuminance that is received at survey points can be qualitatively assessed by comparing it to that of a window operating under similar conditions.

The surface reflectance of the test room has been matched using the CIBSE Lighting Guide [8] and was found to be 0.74. By abbreviated analysis, the contribution of internal reflection to the light pipe DPF of largest diameter (0.53m) light pipe was obtained as only 5% of the total DPF using the chart given by Muneer [9]. Presently undertaken analysis shows that the maximum contribution of internal reflection to the total internal illuminance measured on each survey point in Craighouse test room will not exceed the level of 5%. In summary, for the present DPF model, the effect of internal reflection is of a low order.

6.6.6 Effect of diffuser type

During 2001-2002 two new types of light pipe diffuser have been introduced into the market, namely new opal diffuser and clear diffuser. Performance assessment of the new opal diffuser was not carried out due to its short life span. Figure 6.14 presents the daylighting performance of two light pipe diffuser designs: old opal and clear diffusers. The DPFs that were achieved by the light pipe with a flat clear diffuser were higher than those achieved by an old opal diffuser. The performance gain ratio ranges from 2 (8am, 31st May 2001) to 4 (2pm, 29th May 2001), and the average value has been found to be 2.9. This factor is herein called the Diffuser Factor (f_D). By applying the average f_D factor to the internal illuminances values given by Eqs. 6.9, 6.10, 6.11 and 6.12, the internal illuminances that can be achieved by a flat diffuser fitted light pipe can be determined.

Due to the irregular knurling finishing of the clear diffuser, it produces apparently different internal daylight distributing property from that of an old opal diffuser. Figures 6.15 and 6.16 show the difference between the two types of diffusers in terms of their reflectivity and transparency properties. The pictures presented in Figs. 6.15 and 6.16 were taken in Edinburgh, Currie at about 3pm on 28th April 2002. Figure 6.15(a) shows that bright sunlight penetrates the clear diffuser creating a glare effect, while the sunlight goes through old opal diffuser appears to be much weaker and dimmer.

Another obvious phenomenon is that opal diffuser produces much more uniform diffused light than clear diffuser. The latter one produces multi-directional and irregularly distributed light. Figure 6.16 shows the reflected light from of a point source due to the two types of diffuser.

Due to the improved transparency property of the new clear diffuser, the transmission of daylight by light pipe has been improved. As shown in Fig. 6.14, the total amount of light delivered by light pipe with new clear diffuser is much more than that delivered by old opal diffuser light pipe. However, at the same time, it was found that the uniformity of the internal light due to former kind of diffuser seemed to be poorer than the latter one. This becomes obvious when the light pipes are applied in areas where sunshine is abundantly available. Figure 6.17 shows that certain kind of light ring pattern was observed when light pipes with new clear diffusers were installed in Bahrain. Pictures in Fig. 6.17 show that in noontime in Bahrain, clear diffuser light pipe seem to delivery pools of light instead of uniformly distributed internal light. This "pools of light" pattern is so strong that it causes certain discomforts such as glare and undesired light ring on the ground. The problem was eventually resolved by replacing the new clear diffusers with old opal diffusers. Occupants are satisfied with both the amount of daylight that old opal diffuser light pipe delivers and the way the pipe distributed the internal daylight.

The Dubai project hence shows that, for sites where sunlight are abundant, the application of light pipe with old opal diffuser can not only bring sufficient daylight into buildings but also ensure the uniformity of the internal daylight distribution, which is very desirable. However, for sites where the weather is dominantly part-overcast or medium overcast sky, the influence of light pipe diffusers to the performance of light pipe is more complicated. Measurements carried out in Merchiston test room revealed that the position and size of the ring of light due to light pipe varies during the day. By simply physical analysis, it was found that the presentation of the ring pattern of light due to clear diffuser light pipe is dependent on sky condition, external sunlight intensity, the geometrical factors of light pipe tubes, the optical property of light pipe diffusers and the sun's position. Although by applying the Diffuser Factor (f_D) of value of 2.9 to DPF models for old opal diffuser light pipes, an averaged evaluation of the performance of clear diffuser light pipes can be obtained, considering the complex

decisive factors that affect the performance, the evaluation can only be regarded as a rough estimation. Further work need to be carried out to attack the problem.

6.7 A COMPARISON BETWEEN WINDOWS DF AND LIGHT PIPE DPF

In design studies it has become customary to specify interior daylighting in terms of Daylight Factor. The Daylight Factor (DF) is the ratio of the internal illuminance to the external diffuse illuminance, available simultaneously. The Daylight Factor is divided into three components, the direct skylight (sky component), SC, the externally reflected component, ERC, and the internally reflected component, IRC. It must be borne in mind that by far the SC is the dominant component of DF. In present analysis only the SC is considered as the contributing factor for the make-up of DF.

The CIBSE Lighting Code suggests that when the average DF exceeds 5 per cent in a building, which is used mainly during the day, electricity consumption for lighting should be too small to justify elaborate control systems on economic grounds, provided that switches are sensibly located. When the average DF is between 2 and 5 per cent, the electric lighting should be planned to take full advantage of available daylight. Localised or local lighting may be particularly advantageous, using daylight to provide the general lighting. When the average DF is below 2 per cent, supplementary electric lighting will be needed almost permanently.

DPF is the ratio of the internal illuminance to the corresponding total external illuminance. Hence when comparing the performance of windows and light pipes the above fundamental difference ought to be borne in mind, i.e. in the main, the former exploits only the sky-diffuse, whereas the latter exploits total (sky-diffuse + solar beam) illuminance. In this analysis an attempt is made to relate the window DF to its counterpart, i.e. an equivalent DF for light pipes with the view to compare the performance of the two possible sources of daylight.

For UK sites, Muneer and Saluja [12] and Muneer [13] have presented the relationship between the above two quantities (sky-diffuse and solar beam). This type of relationship is developed using observed hourly diffuse ratio (sky-diffuse to total (global) horizontal illuminance) data. A validated regression between the above ratio and sky clarity has been given in the above-cited references. It is

obvious that as the sky clarity reduces with increasing cloud cover, the diffuse ratio would tend to become 1. Under such conditions a light pipe with an area equal to that of a vertical window would receive at least double amount of illuminance due to its exposure to the whole sky hemisphere. As the sky clarity increases, the light pipe would gain in performance on two counts - whole sky exposure plus receipt of beam illuminance. Note that with increasing sky clarity the diffuse ratio decreases and hence vertical windows would only receive a fraction of a light pipe illuminance. Table 6.6 shows the ratio of the internal illuminance achieved by a light pipe with a DPF of 1% to that achieved by a window with a DF value of the same.

Due to their very nature light pipes have exposure to the whole sky hemisphere (2π steradian solid angle) and thus have an advantage over their vertical counterparts, i.e. windows within vertical facades. The latter can, at best, have exposure to π steradian solid angle. Furthermore, windows are most often not in receipt of sunlight, whereas the light pipe can exploit both components of daylight – sunlight and skylight. Table 6.6 is based on the assumption that the window and the light pipe have equal areas. In practice, however, a light pipe will have much smaller area than a window.

6.8 Cost and value analysis of tubular light pipes

Prior to the analysis of cost and value analysis of light pipes, it is essential to give definitions of 'cost' and 'value' in this context. Cost is the price paid for a thing, object, service or utility. Value is the worth, desirability of a thing, object, service or utility or the qualities on which these depend. In most cases value can at best be estimated in an approximate manner. On the other hand, cost is a much more accurate measure. In this section a discussion on the cost and value of daylight delivered by light pipes is presented. The material on both cost and value ought to be taken as an indicative assessment owing to the infancy of this technology. Using light pipes in buildings as daylighting devices can bring multi-fold benefit. The application of light pipes produces good value in terms of energy conservation, environment protection, maintaining health (physical and psychological) and improving productivity and work performance.

6.8.1 Energy conservation

- Improvements in daylight penetration to the indoor environment, where better design can significantly lessen energy consumption on artificial lighting systems, and where lighting control strategies can improve building performance [14].
- Negative impacts by environmental change due to global warming. Official report to be published by the UK Government's Energy Saving Trust says some five million people living in 1.8 million homes – one in every 13 in the UK – risk being inundated by rising seas and increased rainfall in the starkest official assessment yet of the human cost of climate change in Britain [15].
- An economic cost comparison is to be carried out for light pipes and electrical lighting for an office environment. The following data are available:

Condition:

Office area = $15m^2$

Location: London

Design illuminance for electrical lights = 425lux [16]

Design illuminance for natural lighting = 330lux [16]

Capital cost of electric lights and devices = £35/m^2 [17]

Cost of replacement electric: Fluorescent lamps (30W×5) = £89 [18]

Life expectancy of Fluorescent lamps = 7500 hours [18]

Number of fluorescent lamps = 5

Utilisation factor for lamps = 0.8

Design electrical lighting load = 15W/m^2 [16]

Price of electricity including VAT = 7.22p/kwh [19]

<u>Environmental impacts</u>

CO_2 emissions = 1030g/kwh-electricity

SO_2 emissions = 5.32g/kwh-electricity

NO_2 emissions = 3.51g/kwh-electricity

Additional Environmental levy on electricity use = 15%

Light pipes

Minimum external illuminance required to provide an internal illuminance of 330lux via use of light pipe = 39klux [4];

Daylight ability = 10×365×8×0.3 = 8760 hrs [3];

Required light pipe dimensions (2-off): 1.2m long with 0.45m diameter [20]

Solution (based on a ten-year cycle):

Case I - Only electrical lighting:

Annual capital cost of electrical light fitting = £52.5

Annual running cost of electricity = £109.0

Annual Co_2 Penalty = £8.3 (see UK Emissions Trading Scheme, Section 6.8.3)

Total ≈ £170/year

Case II - Electrical lighting with light pipe:

Annual capital cost of light pipe fitting = £88.4

Annual running cost of electricity = £86.0

Total ≈ £174/year

Conclusions:

Cost comparison: The costs for Case I (only electrical lighting) and Case II (electrical lighting with light pipe) are at the same level with a minute difference of £4/year;

Emissions saved in 10 years due to the use of light pipes (Case II) are significant:

CO_2 emission = 1555 kg

SO_2 emission = 8 kg

NO_2 emission = 5 kg

Emission saved per hour due to the use of light pipes (Case II):

CO_2 emission = 177 g

SO_2 emission = 0.9 g

NO_2 emission = 0.6 g

6.8.2 Health

Research has shown that daylight has an important bearing on the human brain chemistry. Light entering via eyes stimulates the nerve centres within brain that controls daily rhythms and moods.

- People prefer environments with daylight conditions [21], and may recover from operations and illness more quickly in environments which are daylit, and which afford an exterior view [22].
- Buildings with low daylight factor create environments with homogenous lighting, having little contrast and holding limited interest for the occupant, whereas buildings with high daylight factor transmit more quality daylight, creating conditions likened to those found externally, maintaining optimal mood conditions for longer [23].
- Typically people who are exposed total daylight levels of greater than 2000 lux for only 90 minutes each day [24] show positive mood symptoms. Light exposure is important to the inner time keeping of humans. Through evolution, man has adapted to rhythms such as body temperature to provide him with explicit knowledge of external time [25]. The loss of this connection can contribute to fatigue, insomnia, and Seasonal Affected Disorder (SAD).
- It was concluded that light is an important factor in the wellbeing of building occupants and lack of it can have a deleterious effect on them [26].
- It has been reported that students within class rooms do benefit from higher dosages of daylight in terms of increased performance and better general health [27].
- Research was carried out to reveal the relationship between SAD and light levels. Seasonal Affective Disorder (SAD) is a disturbance of mood and behaviour that resembles some seasonal changes seen in lower mammals. SAD is thought to be related to decreased sunlight during winter months. SAD affected patients have been successfully treated with exposure to bright artificial light of higher intensity than is usually found in the home or in the work place.

An open trial of bright environmental light reversed many of these symptoms and improved mood and social functioning in the winter months [28].

6.8.3 Work performance and productivity

- The average person receiving more than 1000 lux from natural daylight for less than one hour per day, is not receiving sufficient levels to maintain optimal mood. A typical office worker could spend 50% or more of their time in environments of 0.1 – 100 lux [29].
- It is recognised that a holistic approach to lighting design is required to provide environments which are pleasing to the eye, comfortable for the occupant, and which do not limit work productivity [22].
- Daylight, a full-spectrum light source, most closely matches the visual response that, through evolution, humans have come to compare with all other light. Daylight provides continually changing values, brightness and contrasts to the workplace, allowing the human eye to constantly adjust. This adjustment reduces eye fatigue. The human eye is capable of adjusting to high levels of luminance without producing discomfort [25].
- Research by Alberta Department of Education concluded that: exposure to full-spectrum light resulted in better attendance – 3.5 fewer days-absent a year. Students in full-spectrum rooms had better dental records – nine times less tooth decay; students in full-spectrum classrooms grew more – more than 20-mm in two years; daylit libraries had significantly less noise; a result of students increases concentration levels; full-spectrum lighting induced more positive moods in students and caused them to perform better scholastically [30].
- Research results by Rudolph and Kleiner argued that most office environments are detrimental to productivity because they ignore the requirements of those who work in them. Office layout can be improved by considering changes to office furniture, lighting and noise control [31].
- Research carried out by Heschong Mahone group concluded that: 1) Overall, elementary students in classrooms with the most daylight showed a 21% improvement in learning rates compared to students in classrooms with the least daylight. 2) A teacher survey and teacher bias analysis found no assignment bias that might have skewed the original results. 3) A grade level analysis found that the daylighting effect does not vary by grade. 4) An absenteeism

analysis found that physical classroom characteristics (daylighting, operable windows, air conditioning, portable classrooms) do not have an effect on student absenteeism. These findings may have important implications for the design of schools and other buildings [32].

- Heschong Mahone group [33] revealed a clear relationship between skylighting and increasing sale. A number of mechanisms that can explain the effect of daylighting on sale have been put forward as following: a) high customer loyalty to a daylit store, b) more relaxed customers in a daylit store, c) better visibility, d) more attractive products and e) better employee morale. A study on the effect of daylighting to students' performance in school was also carried out the by the same group. It was concluded that a uniformly positive and statistically significant correlation exists between the presence of daylighting and better student test scores. Possible explanations for this phenomenon were given as: i) improved visibility due to higher illumination levels; ii) improved visibility due to improved light quality, iii) Improved health, iv) improved mood, v) higher arousal level and vi) improved behaviour.

In this section the value of daylight has been categorised. An example was also presented to compare the costs associated with tubular daylighting and electrical lighting devices. It would be desirable to translate the itemised value of daylight into costs so that a 'complete' picture may emerge. Towards this end the environmental impact of using electric light have been expressed in monetary cost via the Climate Change Levy [34] announced by one European government, and Emissions Trading Scheme by UK government [35]. However, not all of the associated value of daylight can easily be converted into cost data. For example, only rough cost estimates may be provided for the health and productivity benefits obtained through daylight exploitation. Hence, no attempt has presently been made within the present document to 'go all the way'. The authors feel that such value-to-cost conversions are best left for the judgement of the reader. The analysis presented are however conducive to the research on the value and cost engineering study on all natural daylighting techniques.

6.9 SUMMARY

Mathematical modelling activities aiming at predicting the daylighting performance achievable by light pipes with various configurations under all weather conditions have been undertaken. Two DPF models, one for straight light pipes and the other for elbowed light pipes were built. The models enable

estimation of daylight provision of the light pipes with a high degree of accuracy, i.e. R^2 values of 0.95 and 0.97 for regression between predicted and measured illuminance were respectively obtained for the above models. The maximum Mean Bias Error (MBE) and Root Mean Square Error (RMSE) were – 2lux and 27lux.

REFERENCES

1. Edmonds, I. R., Moore, G. I., Smith, G. B. and Swift, P. D. (1995) Daylighting enhancement with light-pipes coupled to laser-cut light-deflecting panels. *Lighting Research and Technology*, 27(1), 27-35

2. Siegel, R. and Howell, J. R. (1981) *Thermal radiation heat transfer*, McGraw Hill, New York

3. Muneer, T., Abodahab, N., Weir, G. and Kubie, J. (2000) *Windows in buildings thermal, acoustic, visual and solar performance*, Architectural Press, Oxford

4. Zhang, X. and Muneer, T. (2000) A Mathematical Model for the Performance of Light-pipes, *Light Research and Technology*, 32(3)

5. Zhang, X. and Muneer, T. (2000) Light pipes for Daylight Penetration Indoors, *Proceedings of Renewable Energy for Housing Conference*, The International Solar Energy Society, ISBN: 1-873640-32-3

6. Carter, D. J. (2001) The Measured and Predicted Performance of Passive Solar Light Pipe Systems. *Lighting Research and Technology*, 34(1), 39-52

7. Naraghi, M. H. N. (1987) *Engineering Notes: American Institution of Aeronautics and Astronautics*

8. The Society of Light and Lighting (2001) *CIBSE Lighting Guide 11: Surface Reflectance and Colour*, The Society of Light and Lighting, London

9. Muneer, T. (1997) *Solar radiation & daylight models for the energy efficient design of buildings*, Architectural Press, Oxford

10. Loncour, X., Schouwenaars, S., L'heureux, D., Coenen, S., Voordecker, P. H. and Wouters, P. (2000) *Performance of the Monodraught systems windcatcher and sunpipe: A case study*, Belgian Building Research Institute

11. Muneer, T. (2002) Brief report on the performance of Napier's Daylight Penetration Factor (DPF) and its comparison against other published work, internal report, Napier University

12. Muneer, T. and Saluja, G. S. (1986) Correlation between hourly diffuse and global irradiance for the UK, *Building Serv. Eng. Res. Techo*l. 7(1), 37–43

13. Muneer, T. (1987) Hourly diffuse and global solar irradiation, further correlation *Building Serv. Eng. Res. Technol.* 8(4), 85–90

14. Zeguers, J. D. M. and Jacobs, M. J. M. (1997) Energy saving and the perception of visual comfort, *Proceedings of Lux Europa*

15. The Independent (2002), The Independent 15 September 2002 No.658, UK

16. CIBSE (2001) *Building Service Journal*, December 2001, 22

17. Glenigan (1998) *Griffiths Electrical Installations Price Book*, Glenigan Cost Information Service, Bournemouth, UK

18. Goodoffices (2002) www.goodoffices.com

19. Scottish Power (2002) www.scottishpower.co.uk

20. Zhang, X. and Muneer, T. (2002) A Design guide for performance assessment of solar Light-pipes *Lighting Research and Technology*, 34 (2), 149-169

21. Wyon, D. P. and Nilsson, I. (1980) Human experience of windowless environments in factories, offices, shops and colleges in Sweden, Building Resources Worldwide, *Proceedings of the 18th CIB conference*, 234-239

22. Loe, D. and Davidson, P. (1996) A holistic approach to lighting design, *Energy Management*, Sep/Oct 16-18

23. Cawthorne, D. (1991) Buildings, lighting and the biological clock, The Martin Centre for Architectural and Urban Studies, University of Cambridge

24. Savides, T. J., Messin, C., Senger, C. (1986) Natural light exposure of young adults, *Physical Behavior*, 38, 571-574

25. AIA, Franta, G., Anstead, K. (1993) Daylighting Offers Great Opportunities, Daylight American Institute of Architects, Building Connections, Energy and Resource Efficiencies, Washington, DC, U.S.A

26. Steemers, K. (1993) The role of lighting in the environmental performance of buildings *Facilities*, 11(5)

27. Plympton, P., Conway, S., Epstein, K. (2000) Daylighting in schools: Improving student performance and Health at a price schools can afford, National Renewable Energy Laboratory, U.S.A, report presented in American Solar Energy Society Conference Madison, Wisconsin, 2000

28. Truesun (1987) http://www.truesun.com/main/articles.htm, Seasonal Affective Disorder: A Review of the Syndrome and it's Public Health Implications, *American Journal of Public Health*, 77(1), 57-60

29. Espiritu, R. C. (1994) Low illumination experienced by San Deigo adults: association with atypical depressive symptoms, *Biological Psychiatry*, 35, 403-407

30. ADE - Alberta Department of Education (1992) Study into the effects of Light on Children of Elementary School Age: A Case of Daylight Robbery, Alberta Department of Education, Source: http://www.huvco.com/studies.htm

31. Rudolph, P. A. and Kleiner, B. H. (1990) Building an Effective Office Space, *Work Study*, 39(3)

32. Heschong Mahone Group (1999a) Daylighting in school: An investigation into the relationship between daylighting and human performance (condensed report)

33. Heschong Mahone Group (1999b) Skylighting and retail sales: An investigation into the relationship between daylighting and human performance (condensed report)

34. EEBPP (Energy Efficiency Best Practice Programme) 2002, http://www.energy-efficiency.gov.uk/

35. *Professional Engineering*, 27 November 2002, UK, pp32

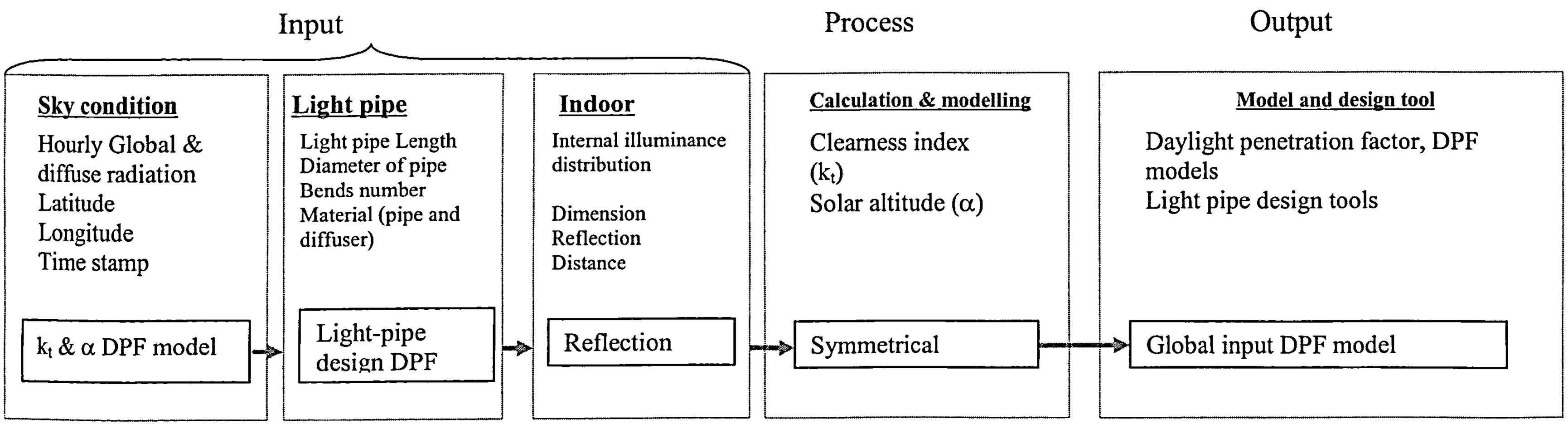

(a) The modelling of the daylighting performance of light pipe systems

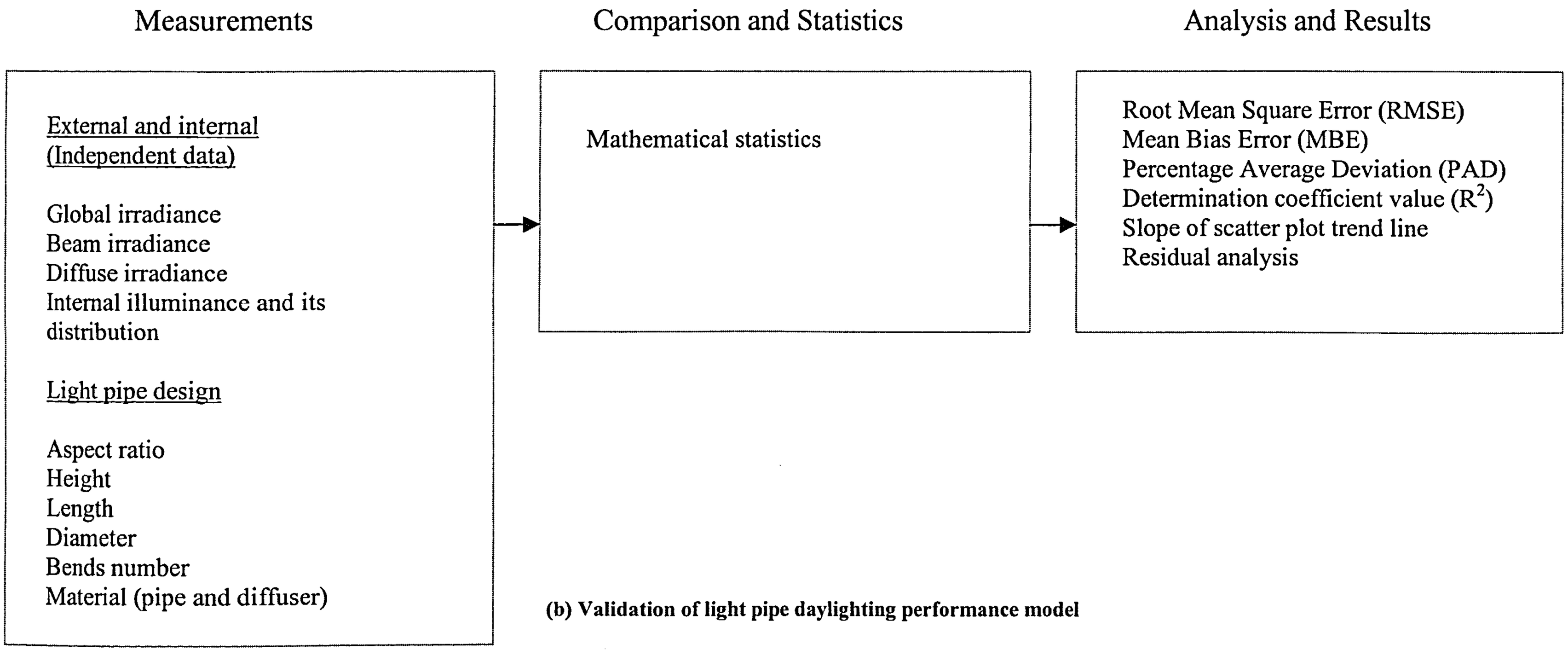

(b) Validation of light pipe daylighting performance model

Figure 6.1 The development of the proposed DPF model: system structure of the development of DPF model (a) and the procedure to validate the model (b)

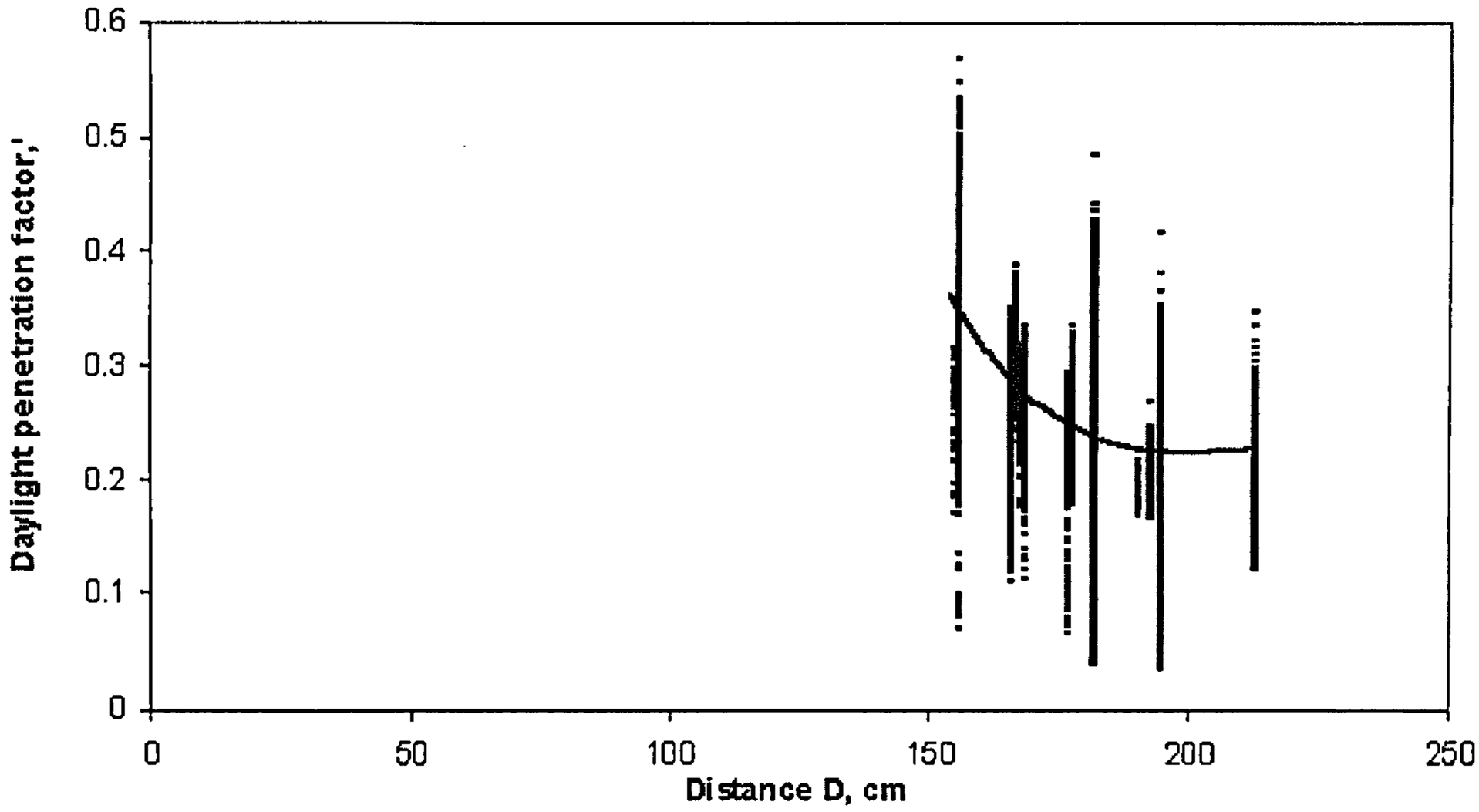

Figure 6.2 Variation of daylight penetration factor as a function of distance, D

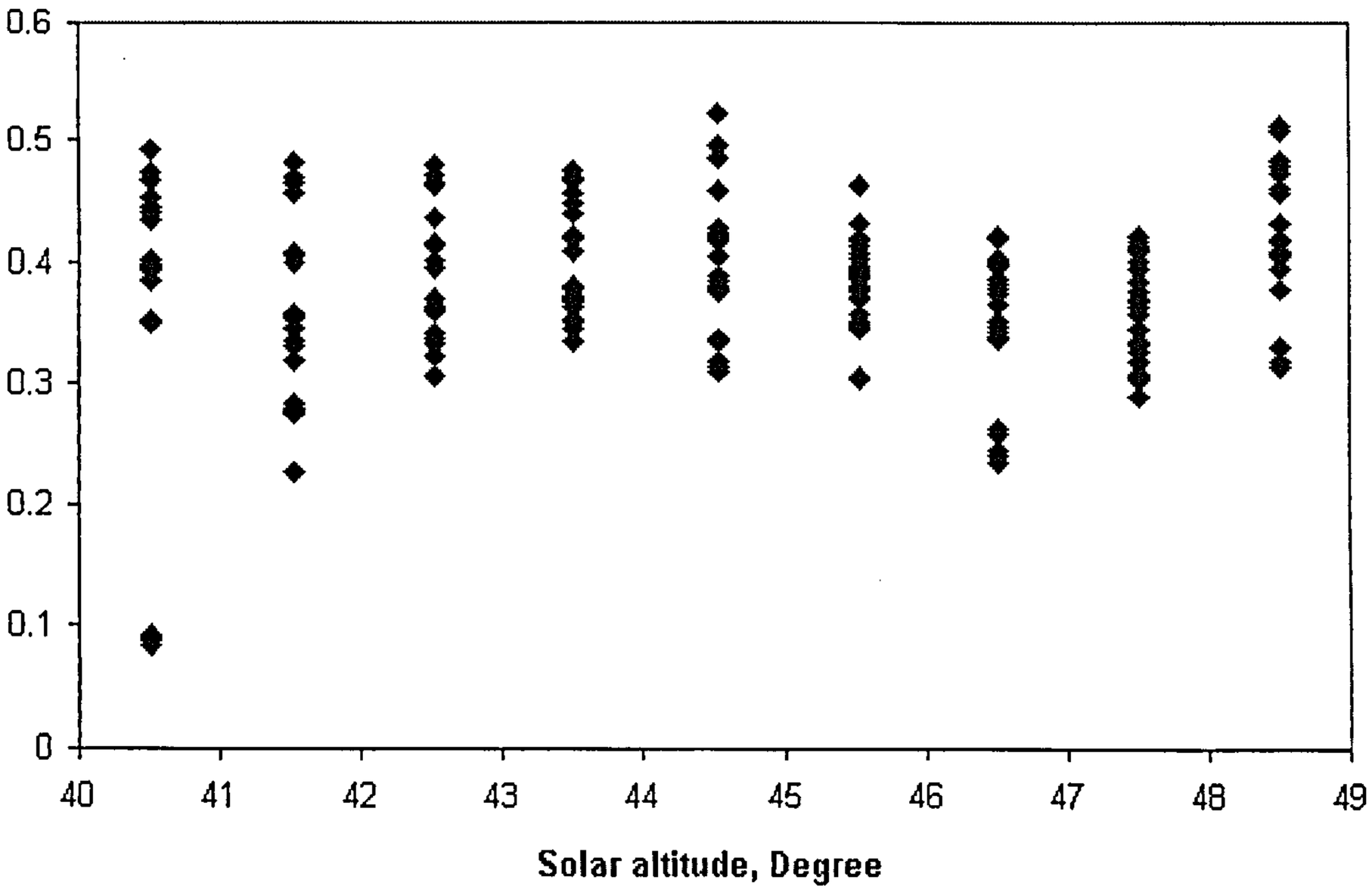

Figure 6.3 Daylight penetration factor variation as a function of solar altitude (D=155cm)

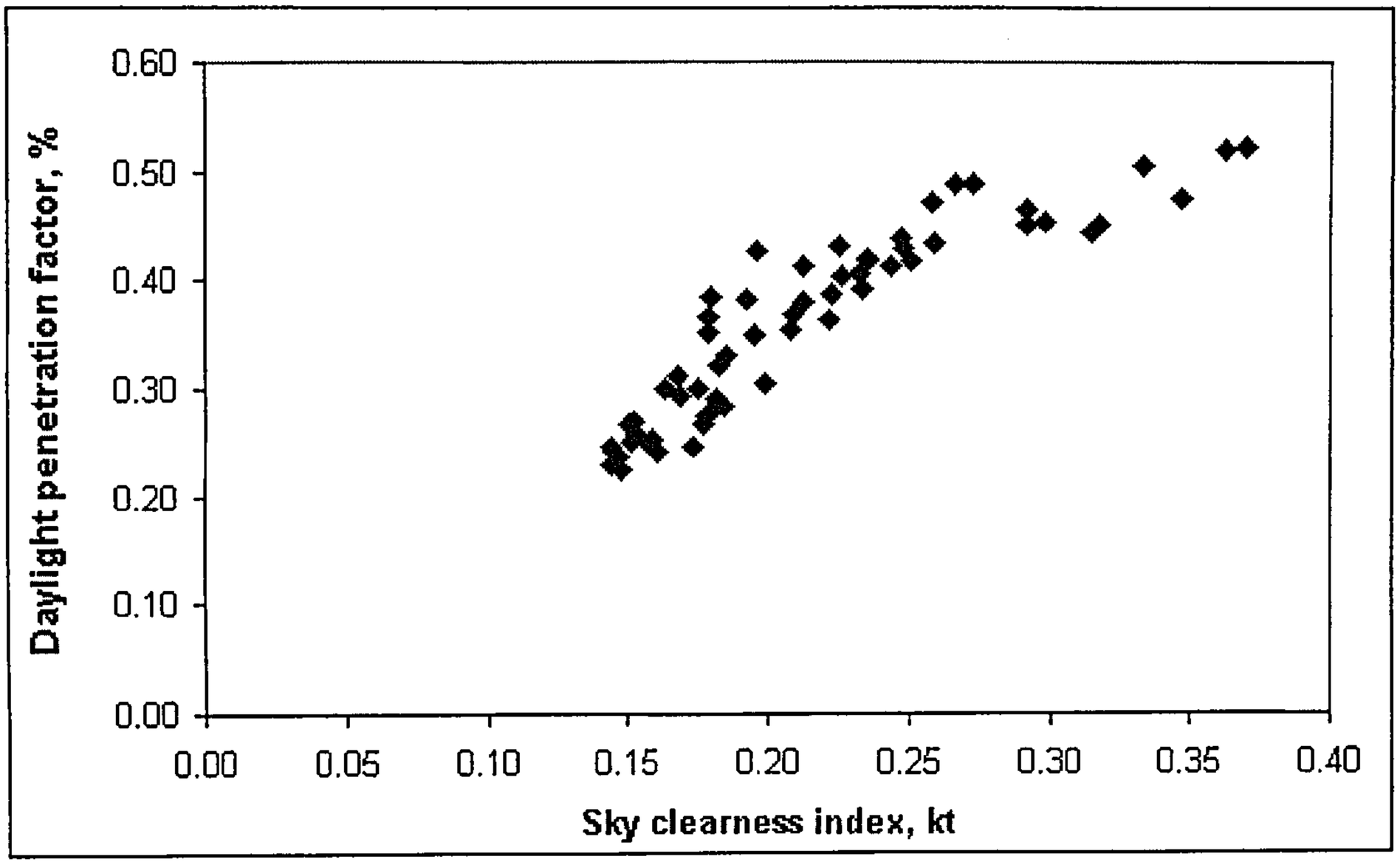

Figure 6.4 Daylight penetration factor as a function of sky clearness index, k_t (D = 155cm; solar altitude = 49±0.5°, light pipe sees only Northern part of sky vault)

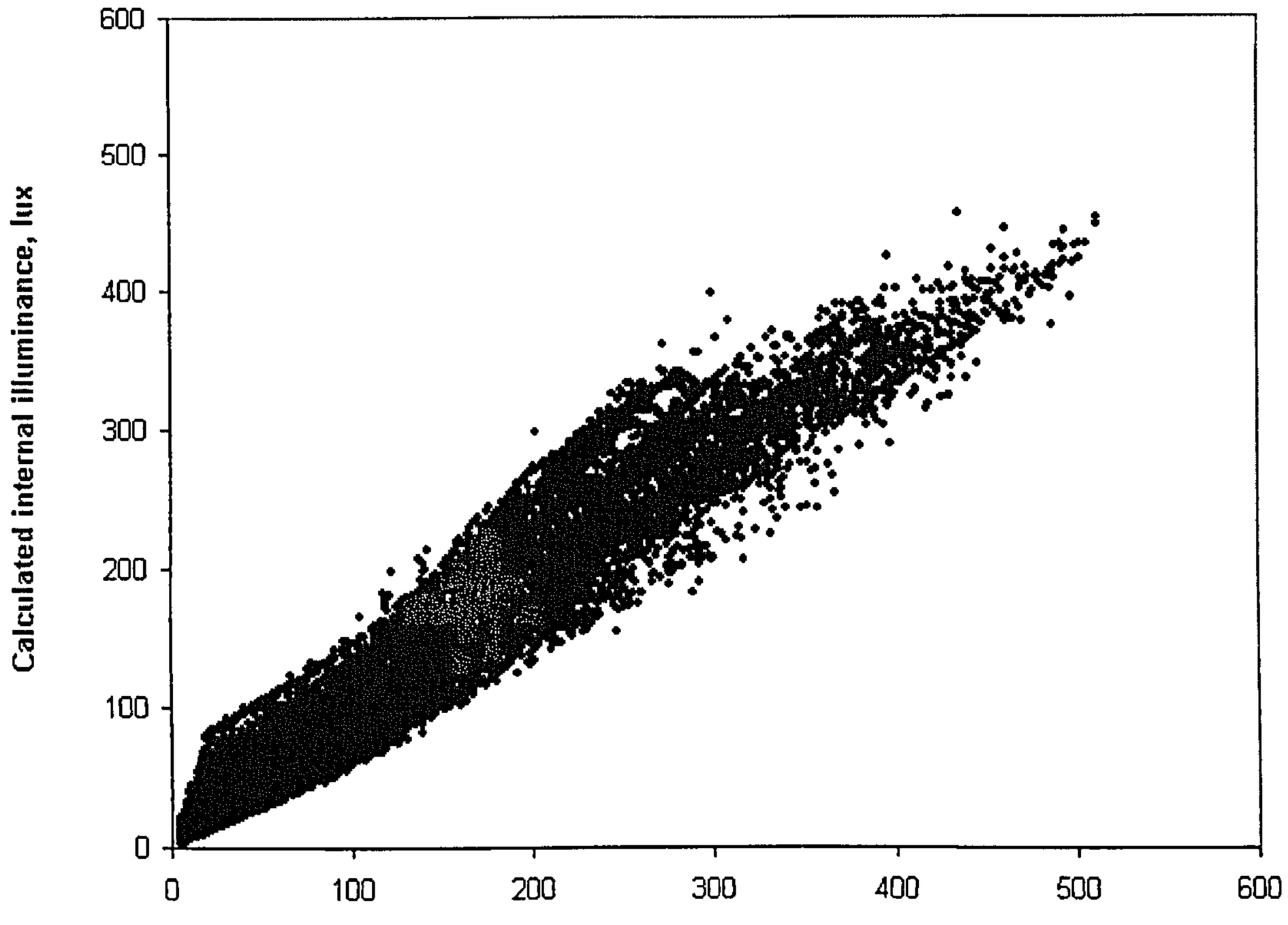

Figure 6.5 Plot of calculated internal illuminance against measured internal illuminance for all distances

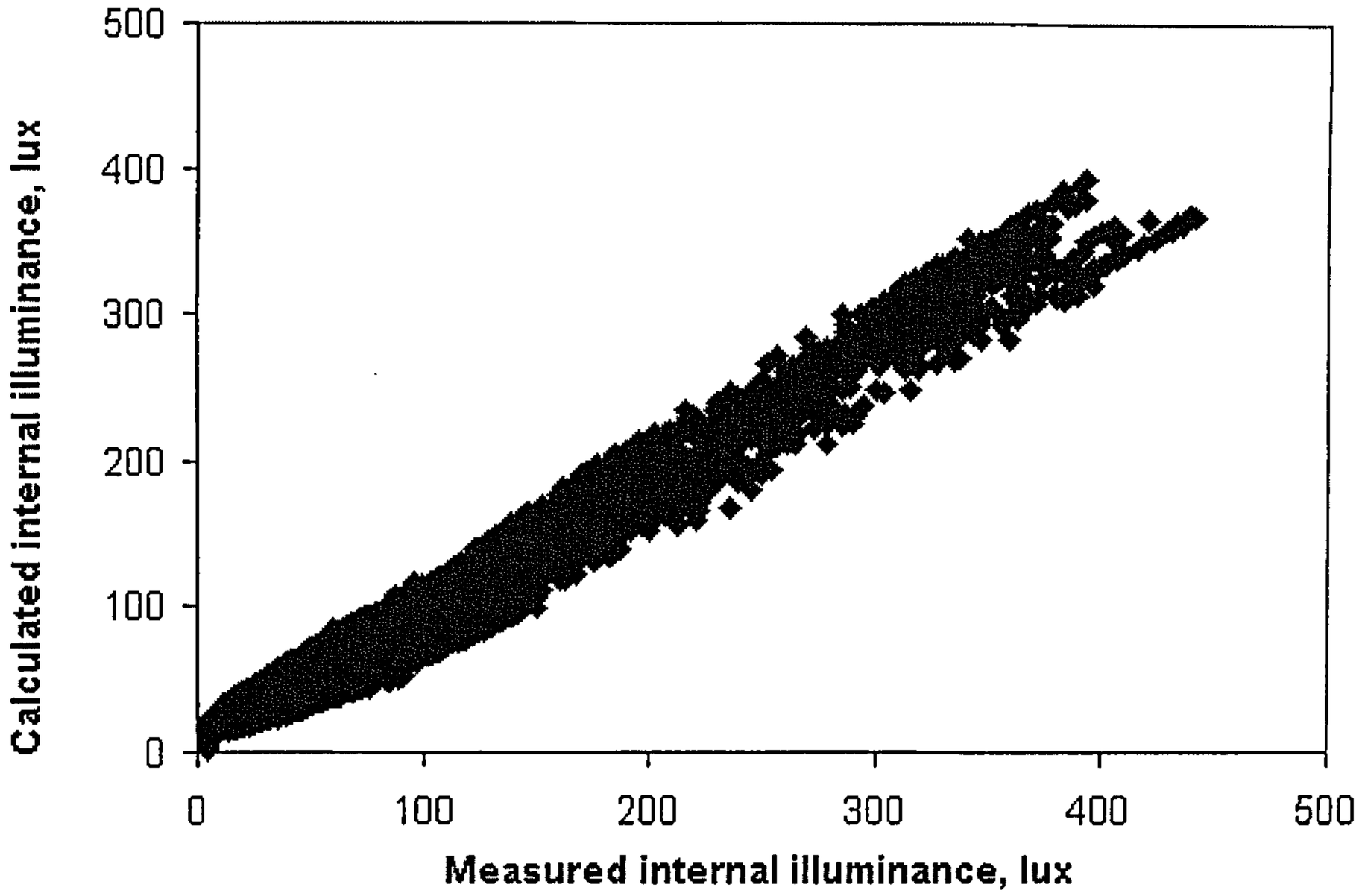

Figure 6.6 Plot of calculated internal illuminance against measured internal illuminance for D=194cm

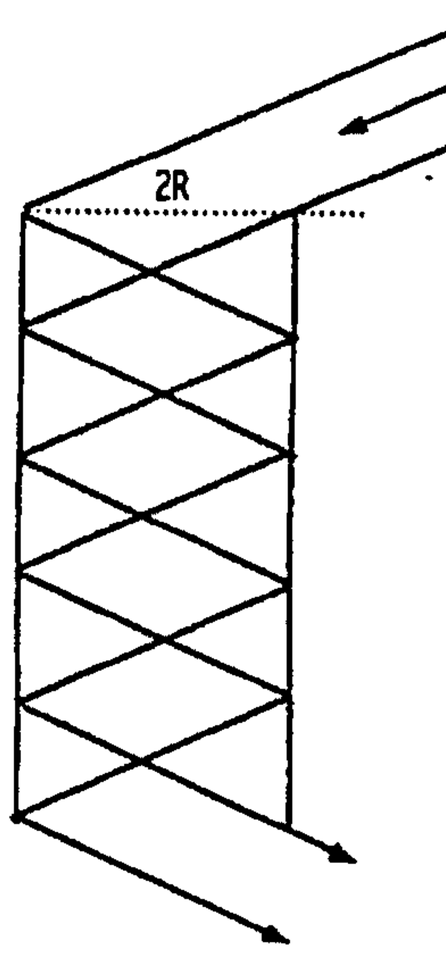

Figure 6.7 Light entering a light pipe descends via a series of inter-reflections

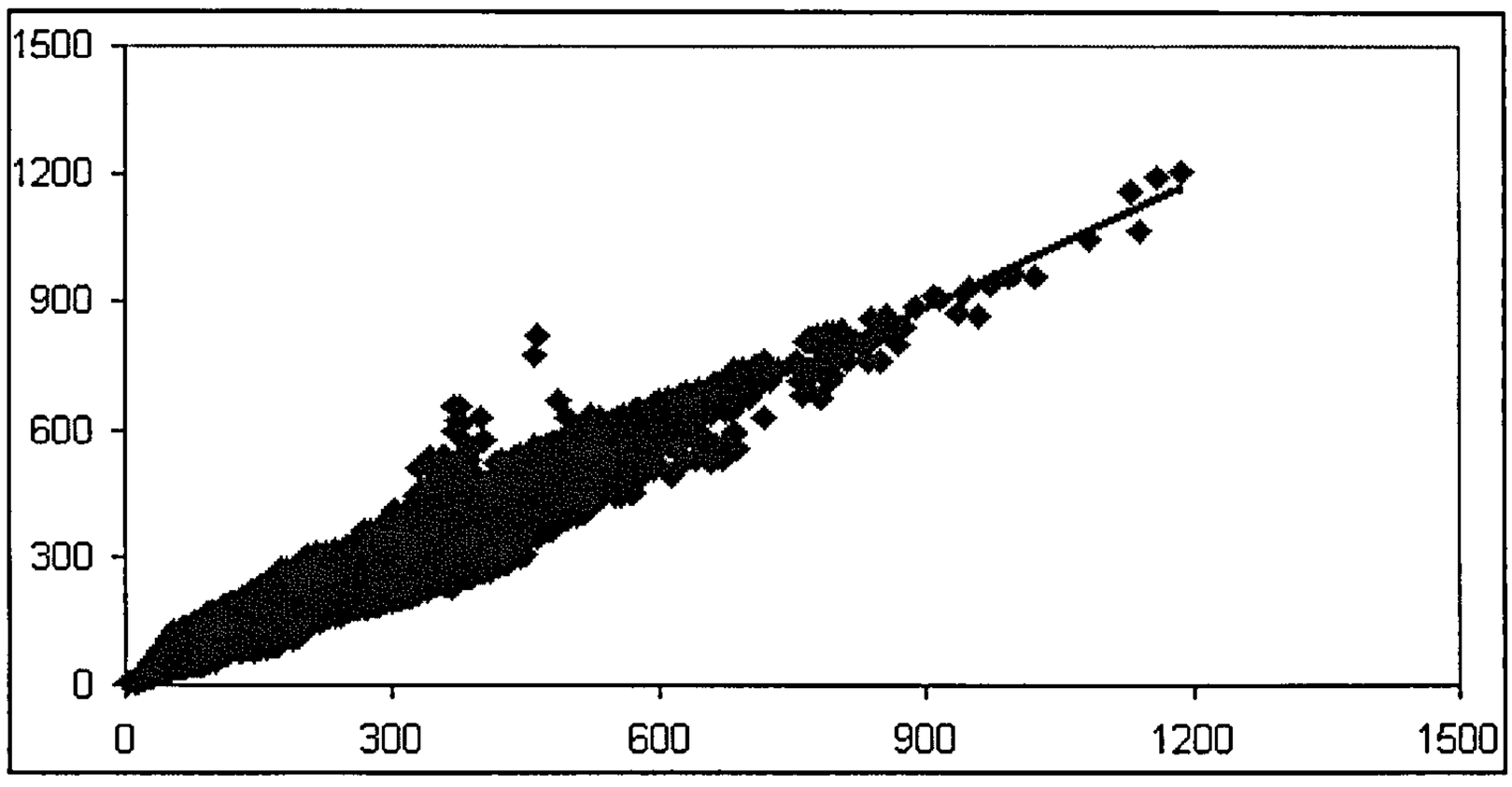

Figure 6.8 Scatter plot of calculated due to Eq. 6.9 (Y-axis) against measured internal illuminance (X-axis) for straight light pipes (units = lux)

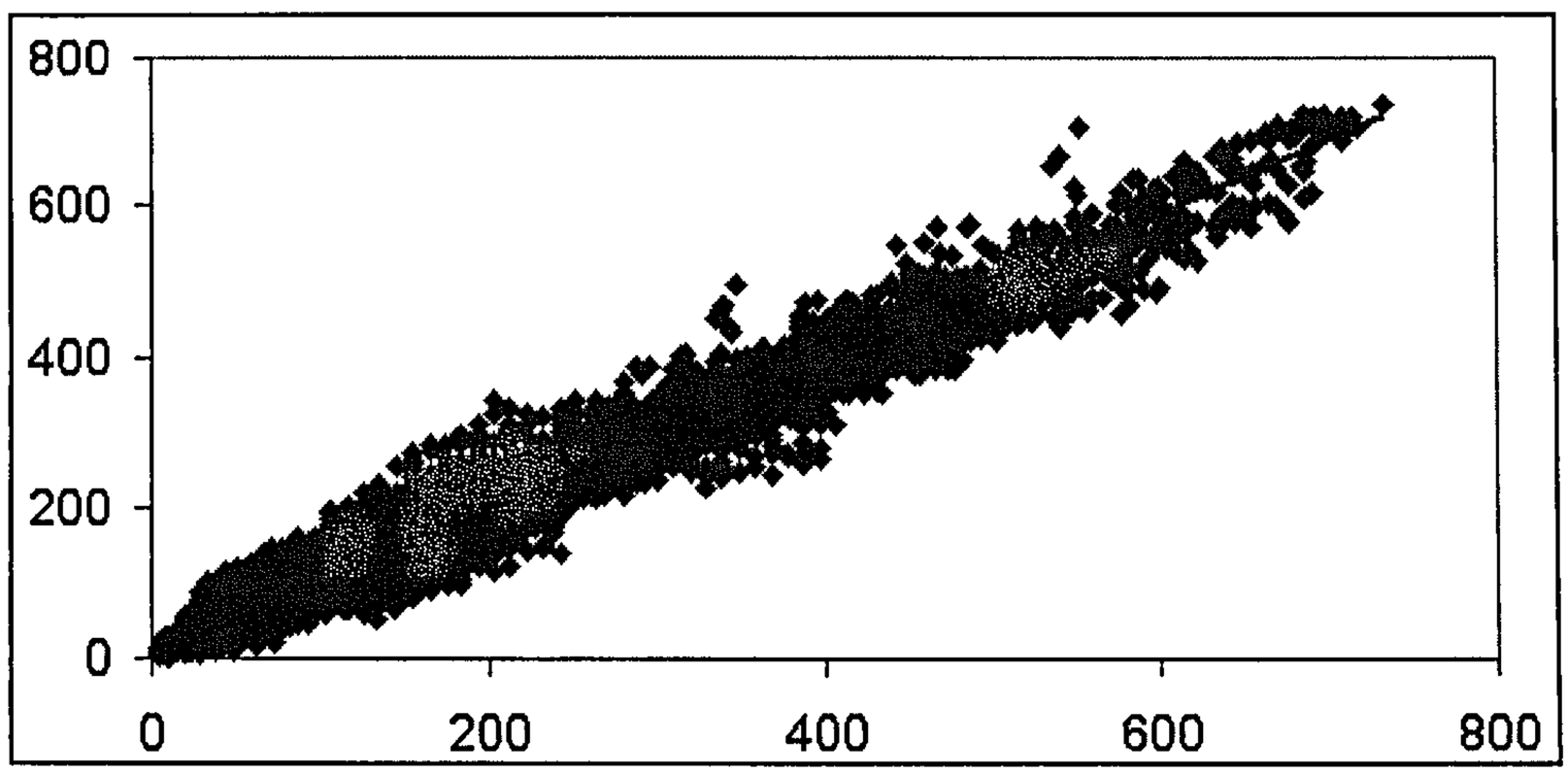

Figure 6.9 Scatter plot of calculated due to Eq. 6.11 (Y-axis) against measured internal illuminance (X-axis) for elbowed light pipes (units = lux)

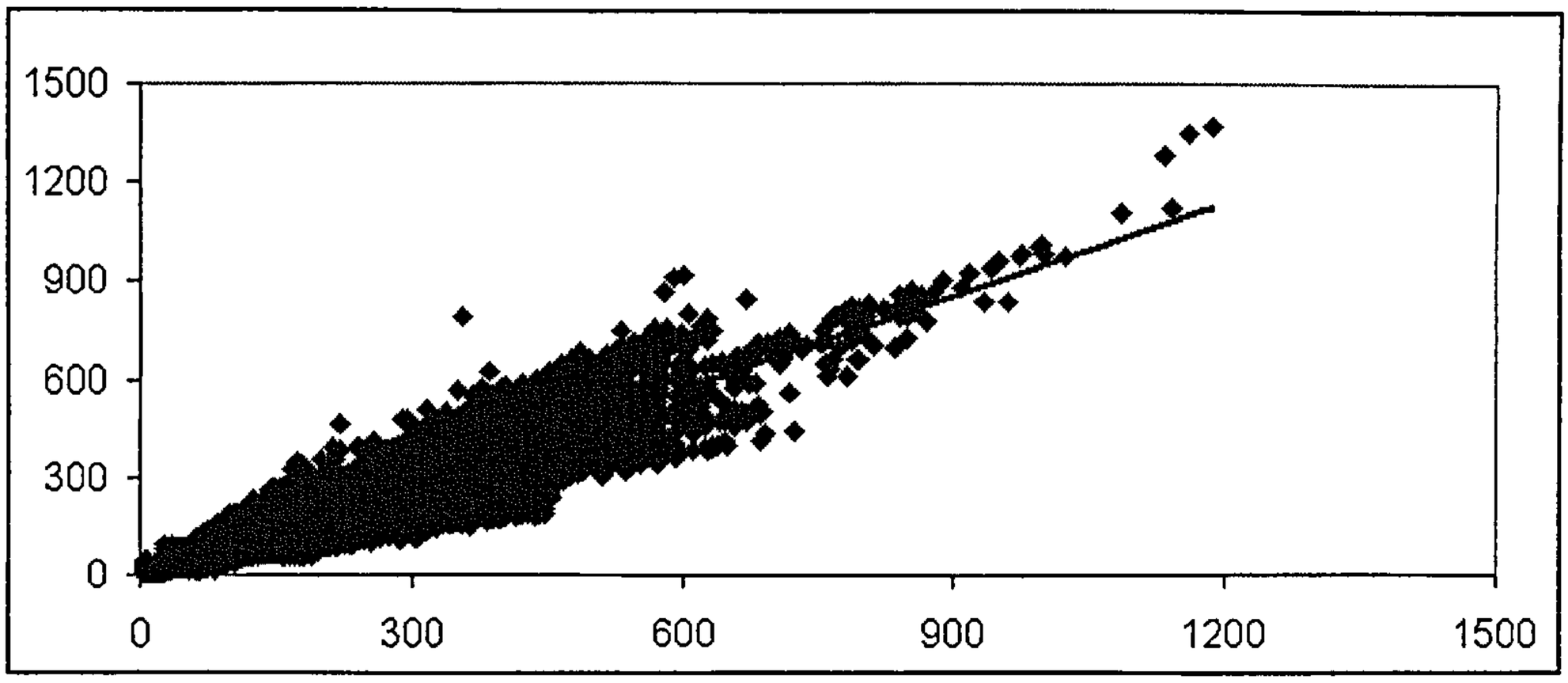

Figure 6.10 Scatter plot of calculated due to Eq. 6.13 (Y-axis) against measured internal illuminance (X-axis) for straight light pipes (units = lux)

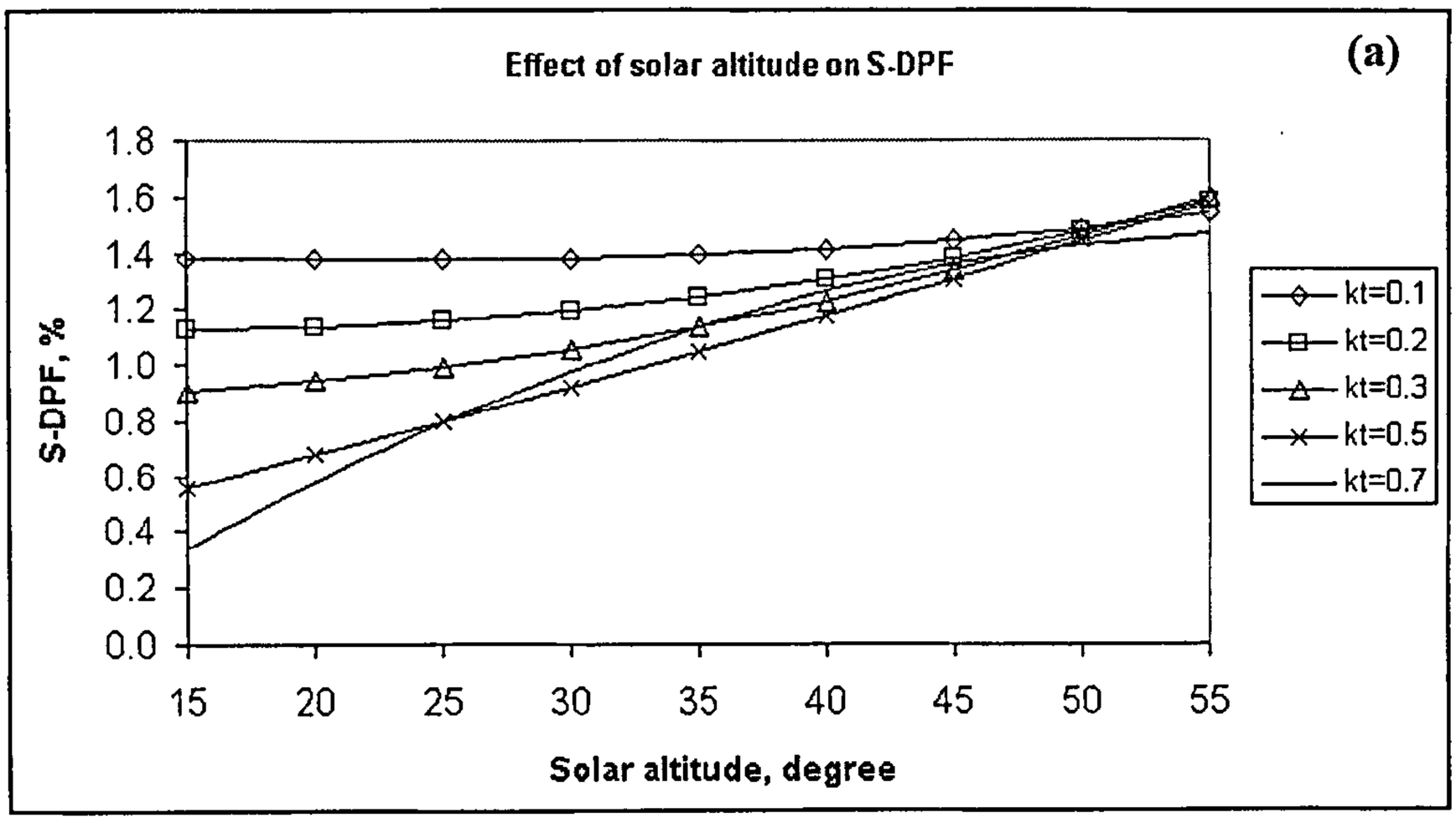

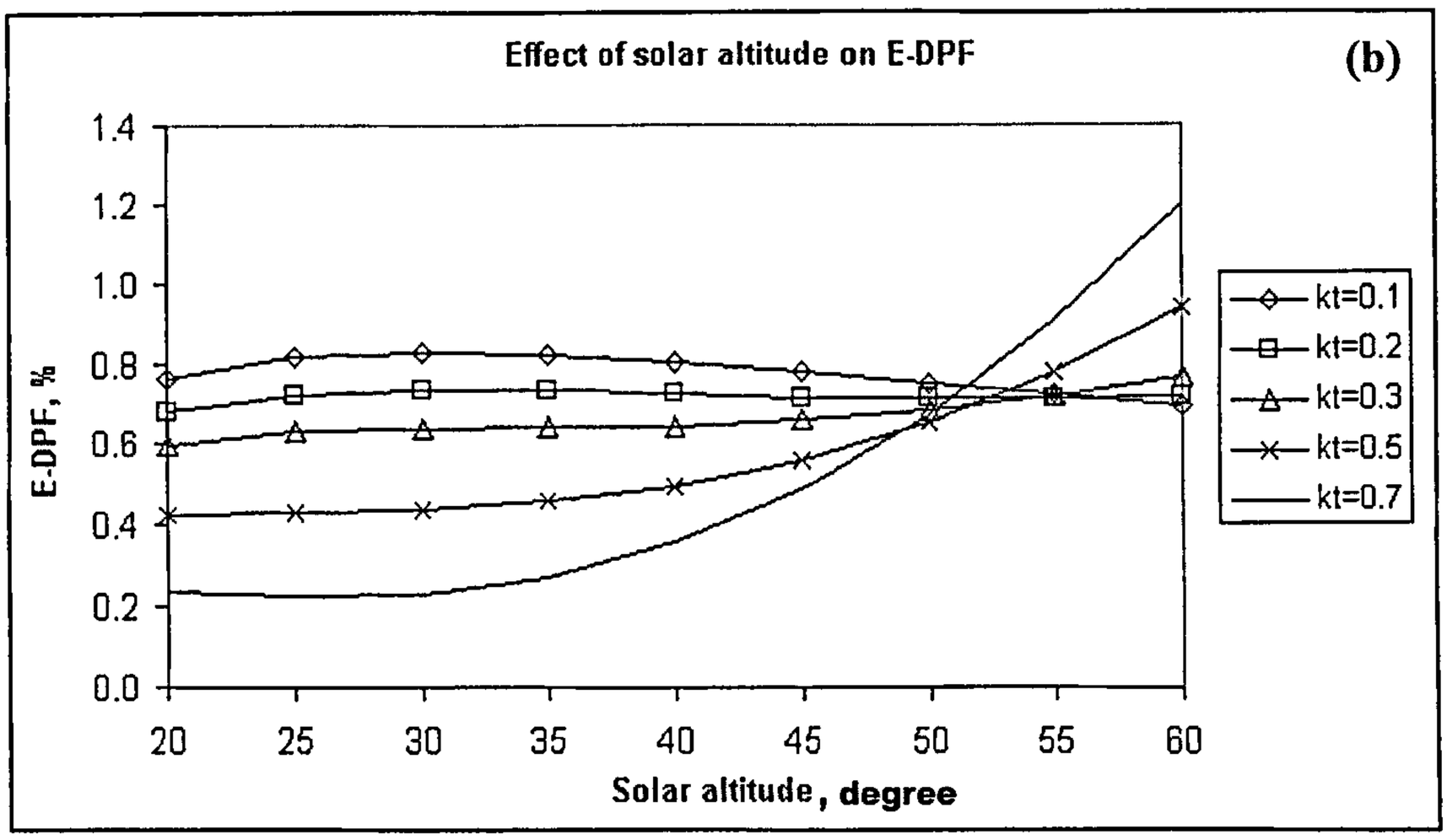

Figure 6.11 DPF for 420mm-diameter light pipe as a function of α_s and k_t ,(a) for straight light pipe and (b) for light pipe with two bends (D=H=1.2m)

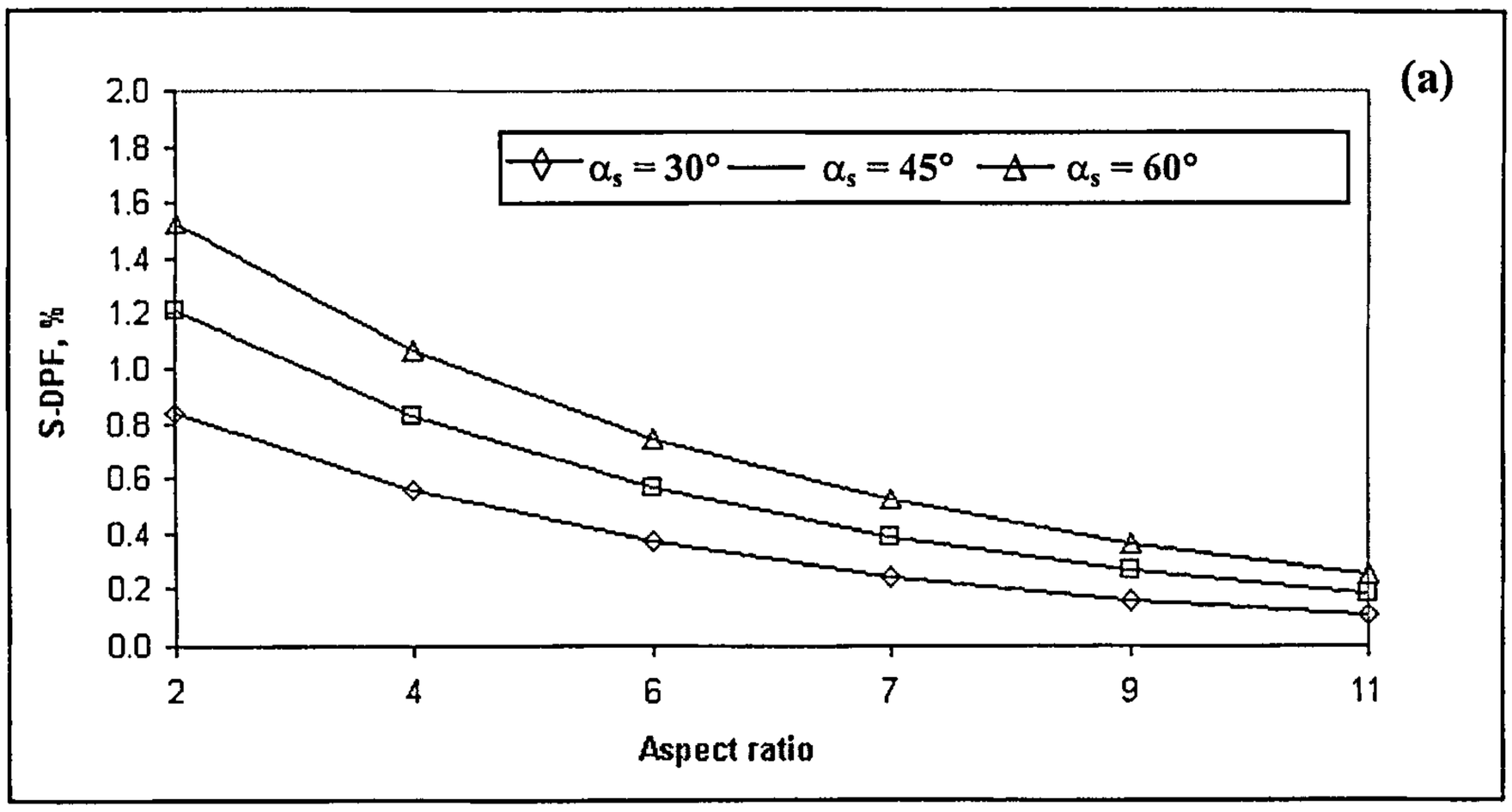

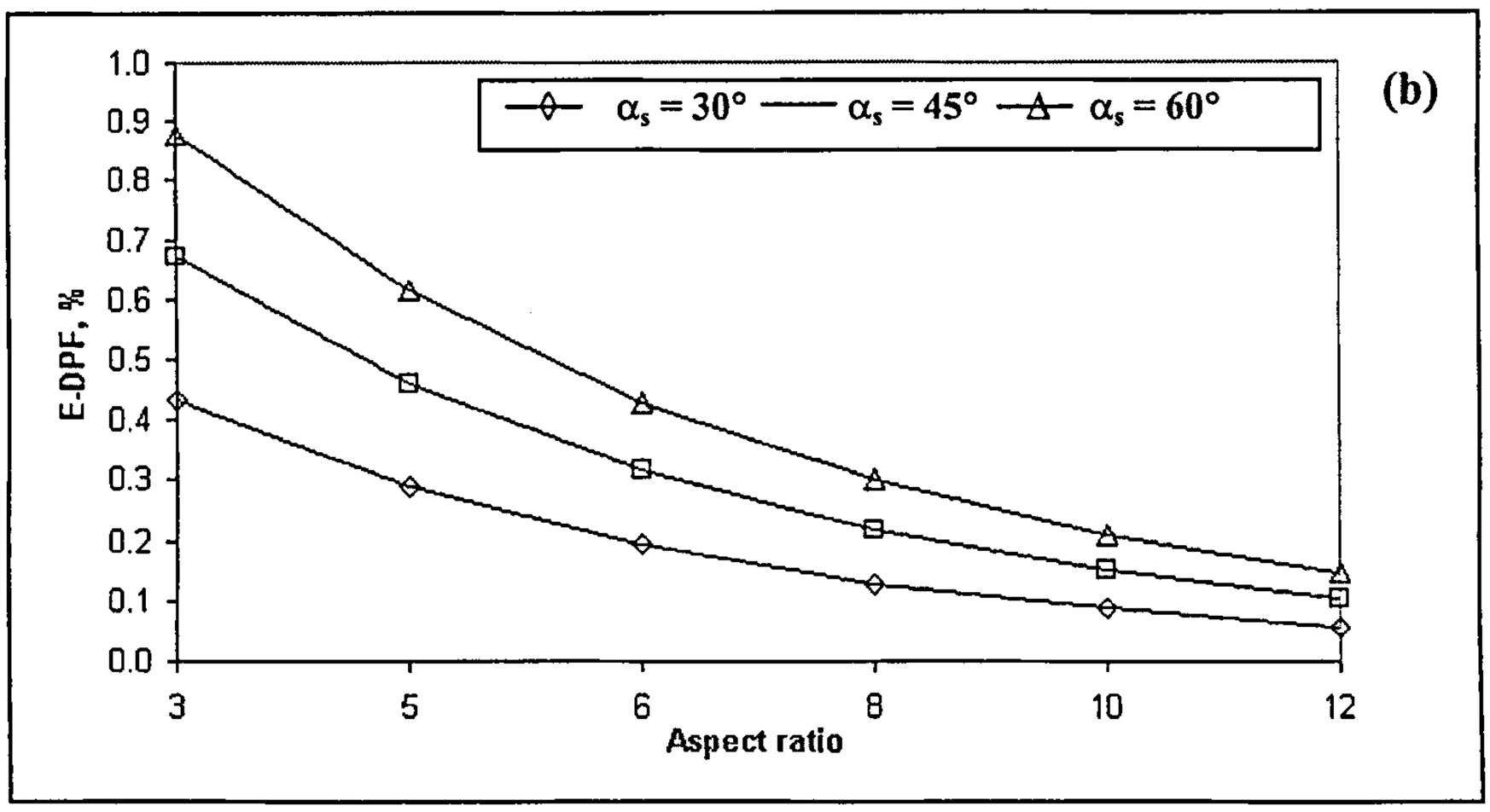

Figure 6.12 Effect of aspect ratio on DPF, (a) for straight light pipe and (b) for light pipe with one bend (420mm-diameter, D=H=1.2m)

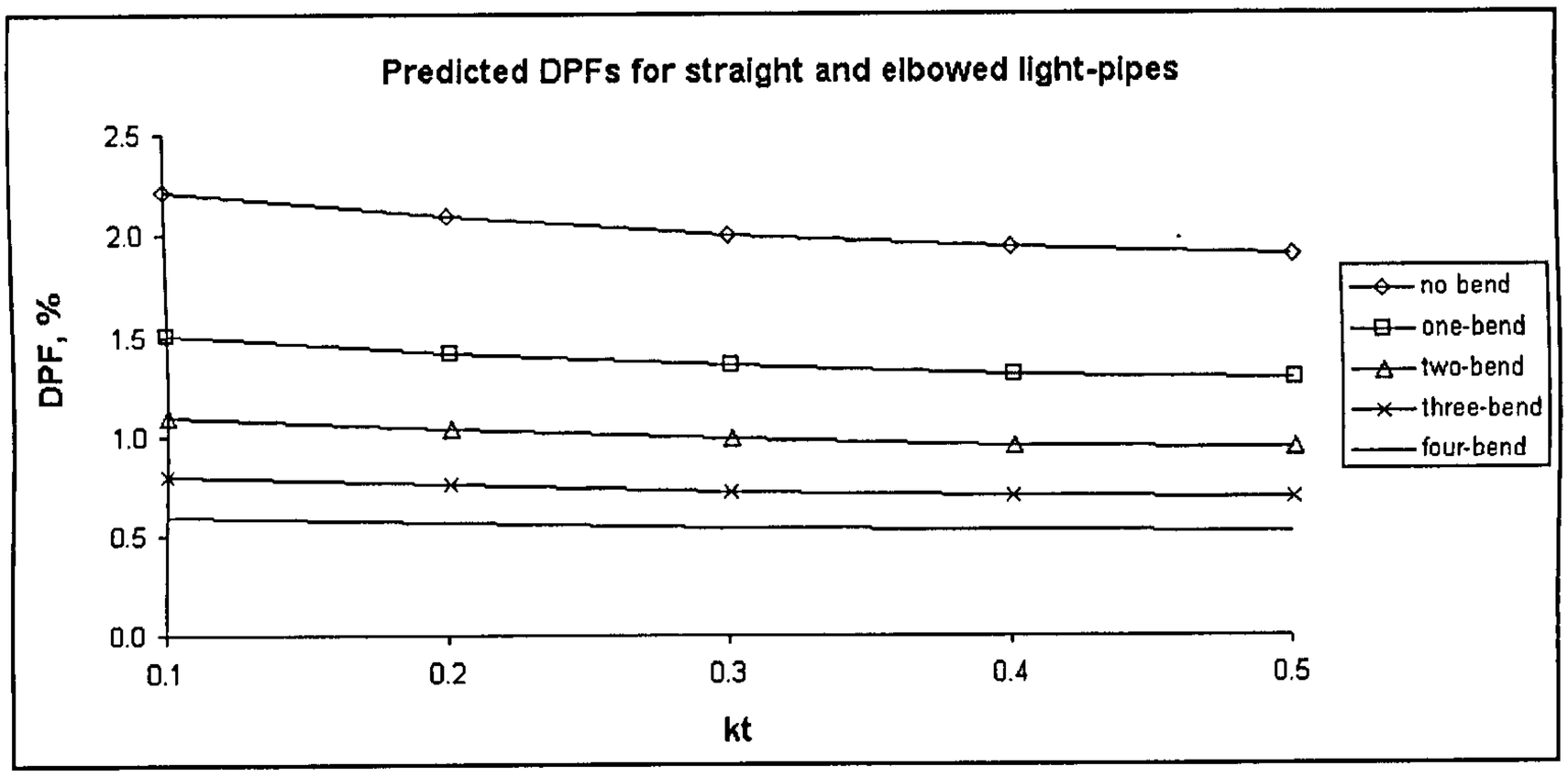

Figure 6.13 Comparison of the predicted DPFs for straight light pipe and elbowed light pipes with one, two, three and four bends (530mm-diameter, α_s=45°, D=1.2m, H=1m)

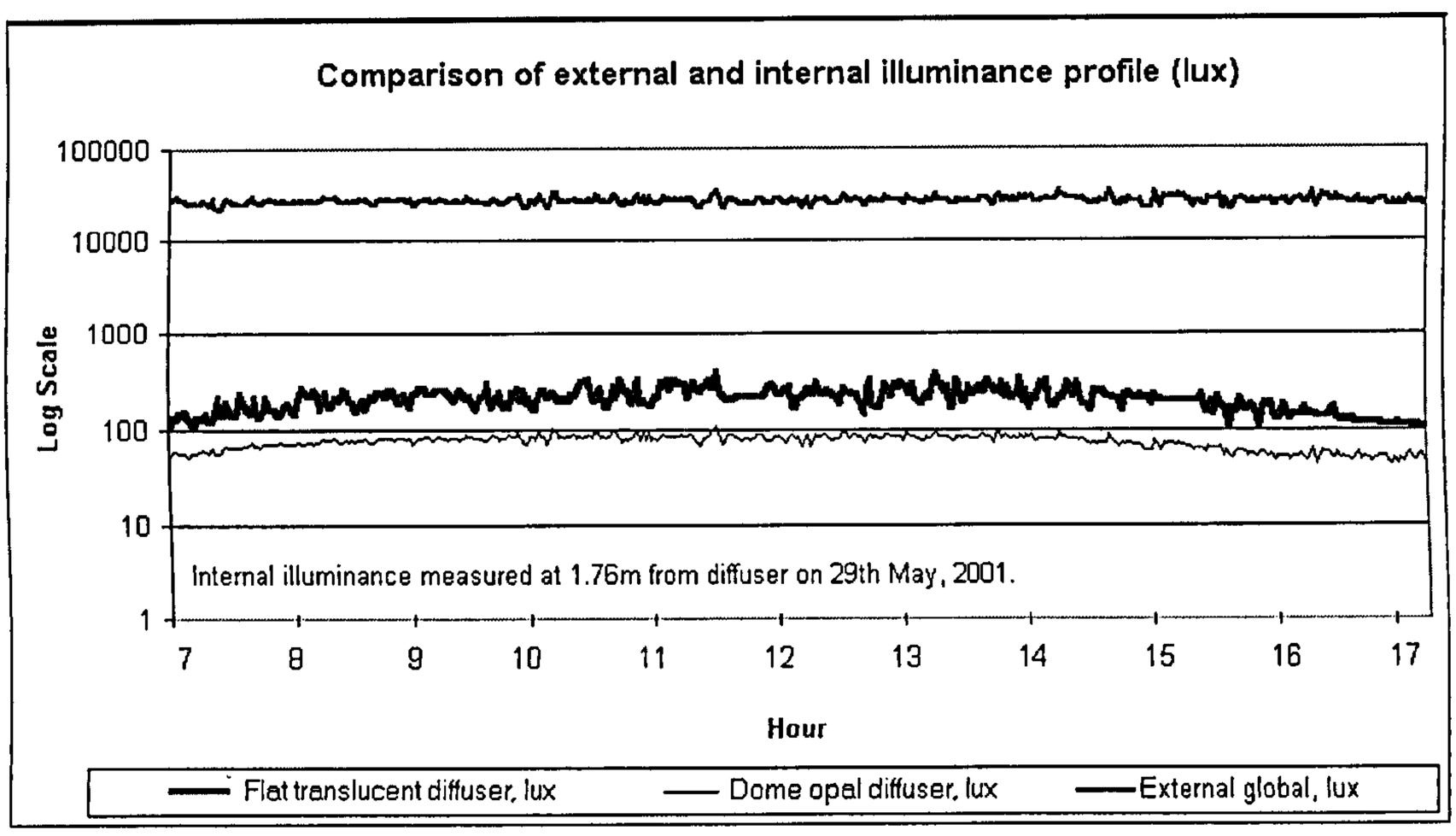

Figure 6.14 Comparison between external and internal illuminance due to different diffusers

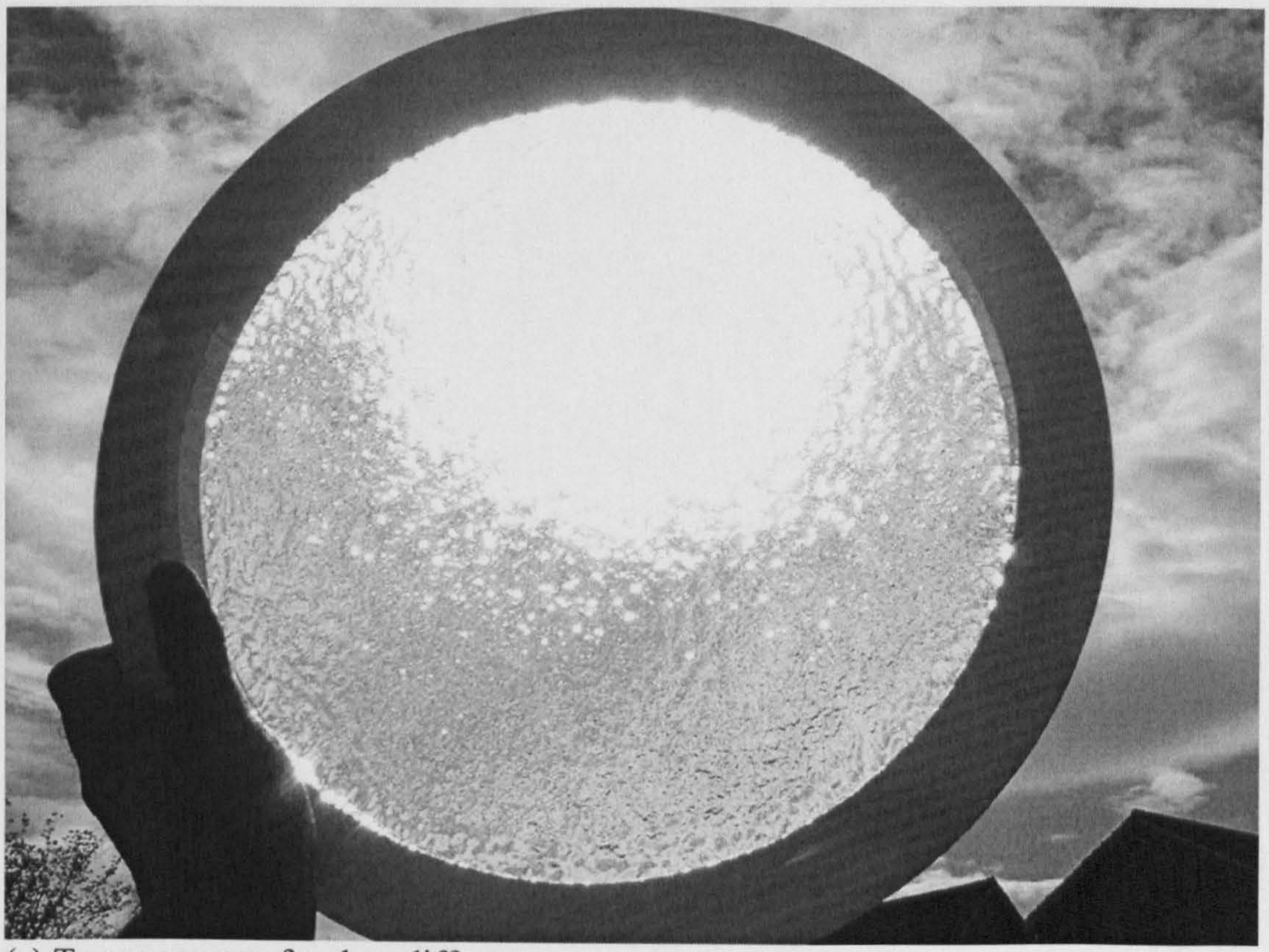

(a) Transparency of a clear diffuser

(b) Transparency of an old opal diffuser

Figure 6.15 The comparison of an old opal against a clear diffuser (transparency property)

(a) Light of a point light source reflected from the clear diffuser inner surface

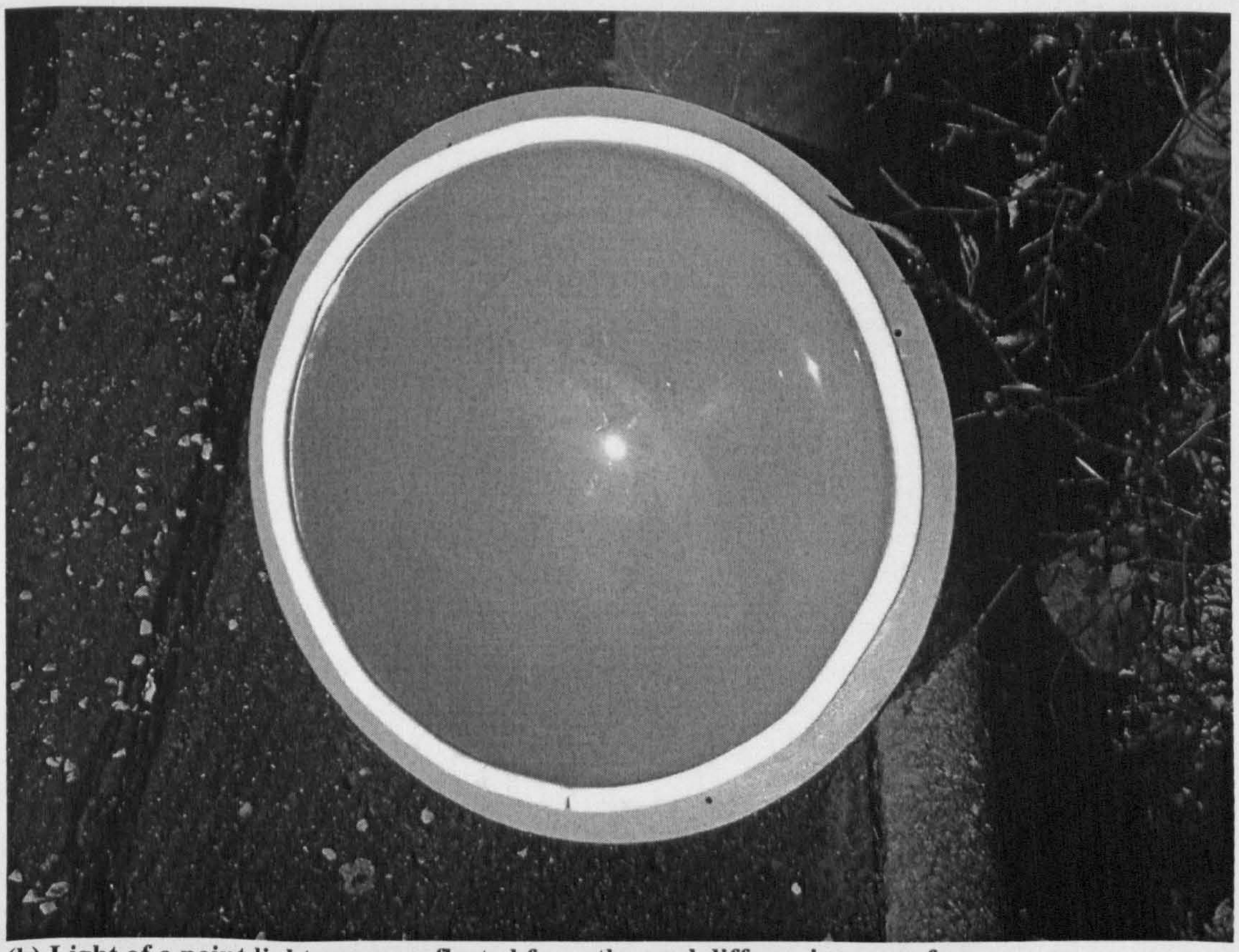

(b) Light of a point light source reflected from the opal diffuser inner surface

Figure 6.16 The comparison of an old opal against a clear diffuser (reflectivity property)

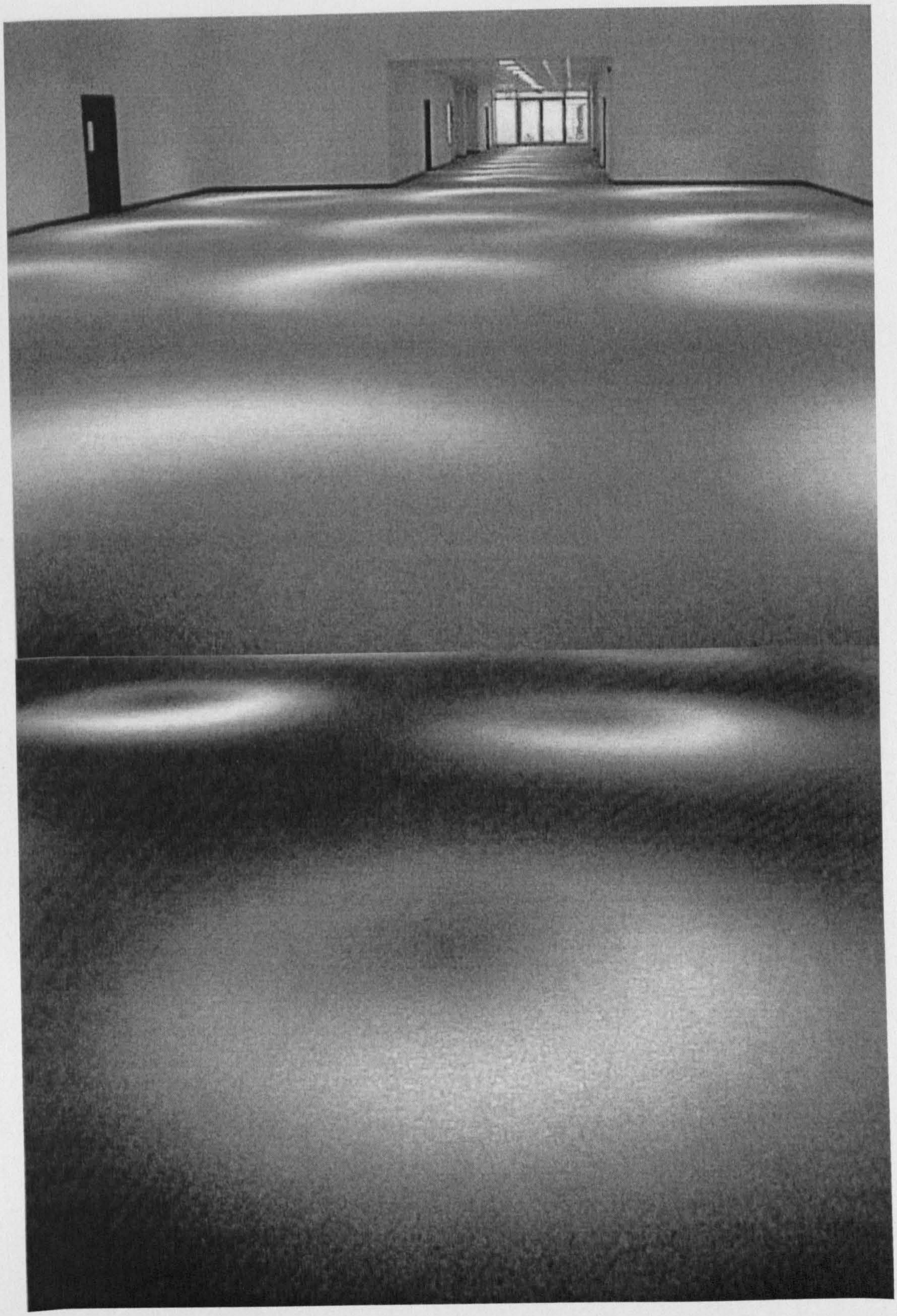

Figure 6.17 Ring pattern and "pools of light" phenomenon seen in Bahrain light pipe project

Table 6.1Coefficients used in Eqs. 6.5 & 6.6

a_{00}	a_{01}	a_{02}	a_{03}	a_{04}	a_{05}	a_{06}	a_{07}	a_{08}
0.053	0.032	-0.000	1.952	-1.878	-0.140	0.002	0.146	-0.002
a_{10}	a_{11}	a_{12}	a_{13}	a_{14}	a_{15}			
0.407	0.008	0.000	-0.149	0.266	0.002			

Table 6.2 Validation results for the model represented by Eq. 6.5

Distance(cm)	155	167	176	181	191	212
Slope	0.96	1.13	1.16	0.90	1.15	0.90
R^2	0.93	0.96	0.95	0.95	0.92	0.96

Table 6.3 Validation results for the model represented by Eq. 6.6

Distance(cm)	155	167	176	181	191	194	212
Slope	0.96	1.13	1.16	0.89	1.16	0.91	0.90
R^2	0.93	0.96	0.94	0.94	0.92	0.97	0.96

Table 6.4 Coefficients used in Eqs. 6.9 – 6.13

Models	a_0	a_1	a_2	a_3	a_4	a_5	a_6	a_7	a_8	a_9	a_{10}
Eq. 6.9	356.7	-572.4	-1.2	-10.2	42.8	0.5	-0.9	137.7	3.5	-0.5	0.5
Eq. 6.10*	62.5	-17.2	2.6	136.0	4.3	1.1	-0.4				
Eq. 6.11	305.0	-190.5	-2.9	-5.3	-5.8	0.2	0.2	133.8	4.0	7.1	-2.1
Eq. 6.12**	192.5	-108.8	-0.3	132.4	4.4	8.6	-2.6				
Eq. 6.13	356.7	-572.4	-1.2	-10.2	42.8	0.5	-0.9	137.7	3.5	-0.5	0.5

*** Equation 6.10 is the simplified model of Eq. 6.9**
**** Equation 6.12 is the simplified model of Eq. 6.11**

Table 6.5 Error statistics for Eqs. 6.9 – 6.13

Models	MBE	RMSE	RMSE/$Max_{measured}$[×]	RMSE/$Mean_{measured}$[#]	PAD	Slope	R^2
Eq. 6.9	-1lux	27lux	2%	15%	12%	0.98	0.95
Eq. 6.10[*]	-3lux	29lux	2%	16%	13%	0.98	0.95
Eq. 6.11	-2lux	23lux	2%	22%	25%	0.97	0.97
Eq. 6.12[**]	-3lux	25lux	3%	24%	25%	0.97	0.97
Eq. 6.13	-9lux	52lux	18%	29%	25%	0.94	0.86

×$Max_{measured}$: The maximum value of measured internal illuminance due to light pipes, lux
#$Mean_{measured}$: The mean value of measured internal illuminance due to light pipes, lux
* Equation 6.10 : the simplified model of Eq. 6.9
** Equation 6.12 : the simplified model of Eq. 6.11

Table 6.6 Relationship between a 'conventional' window daylight factor and an equivalent daylight factor for a light pipe

Sky type	Sky Clarity	Ratio of external global to diffuse illuminance	DF (%)	DPF (%)	Ratio of internal illuminance achieved by a light pipe to that by a window
Heavy overcast	0.2	1.00	1	1	2.0
Thin overcast	0.3	1.06	1	1	2.1
Part overcast	0.5	1.46	1	1	2.9
Clear	0.7	2.80	1	1	5.6

7. SHADOW BAND DIFFUSE MEASUREMENTS CORRECTION

For solar energy applications designs, global and diffuse horizontal irradiance and beam normal irradiance are the three most important quantities. Global horizontal irradiance can be easily measured using a pyranometer. As to the measurement of diffuse horizontal irradiance, the most common approach is to use a shadow band aided pyranometer to intercept beam irradiance. To study the effect of sky diffuse radiation to the daylighting performance of light pipe installed on horizontal roofs, horizontal diffuse irradiance measurements have to be made available. Moreover, considering in real applications light pipes are often installed on slope roofs where the total input illuminance is not horizontal global illuminance. For the latter case, true slope illuminance has to be calculated so as to predict the performance of light pipes. Slope illuminance has two major components, name direct sun illuminance and sky diffuse illuminance. Horizontal diffuse illuminance measurements are being carried out throughout the world, therefore the method for calculating slope illuminance from horizontal illuminance has to be used for light pipe design. In this chapter, a new method of obtaining more accurate horizontal diffuse illuminance than the prevailing method being used around is reported.

7.1 BACKGROUND

Global (G) and diffuse (D) horizontal irradiance and beam normal irradiance (B_n) are the three most important quantities for solar energy applications design. The important role that diffuse irradiance plays in a solar system design cannot be overemphasised. It was reported by Drummond [1] and others that the ratio of diffuse component to the global irradiance can be as high as 0.65. Therefore, to provide a precise estimation of the solar energy available for a given application, a more accurate measurement of diffuse irradiance is required.

A simple relationship exists between G, D and B_n (see Eq. 7.1).

$$D = G - B_n \sin\alpha \tag{7.1}$$

Therefore, diffuse irradiance can either be calculated from measurement of G and B_n or measured directly. However, in the first instance, the beam normal irradiance measurement device

(pyrheliometer) has to be installed on an equatorial mount with active tracking of the sun's trail. As this is expensive, this method has not been widely adopted. The more common approach has therefore been to use a pyranometer aided by a shadow band to intercept beam irradiance. The beam irradiance is then obtained via subtraction of the diffuse component from global irradiance.

Unfortunately, the shadow band that is used to block the sunshine also shades some diffuse irradiance as well. It can lead to the monthly averaged error of horizontal diffuse irradiance measurement of up to 24% of the true value [1]. Hence it is necessary to correct the measured diffuse irradiance obtained using the shadow band instrument.

The inner surface of a shadow band is usually painted black so as to eliminate any reflected irradiance from the inner surface to the pyranometer. If the sky-diffuse irradiance distribution is assumed to be isotropic and the irradiance that is reflected by inner surface of shadow band negligible, the correction factor of the diffuse irradiance can be calculated by using the simple geometric method given by Drummond [1]. This geometric method calculates the proportion of the sky area that is subtended by the shadow band, P, and then derives the correction factor as 1/(1-P).

However, as the real sky-diffuse distribution is not isotropic, an anisotropic factor must be taken into consideration to obtain a correction factor. The necessity of applying an anisotropic correction factor has been widely investigated. Kudish [2] has reported that, for Beer Sheva, Israel, the anisotropic correction factor varies from 2.9% to 20.9%, whereas the geometric (isotropic) correction factor varies only from 5.6% to 14.0%. Painter [3], compared the diffuse irradiance measured by both an occulting disc and a shadow band pyranometer. He concluded that the anisotropic correction factor has a significant seasonal deviation. Eero's study [4] showed that the deviation of the monthly isotropic correction factor with respect to total correction factor ranges from 1% for December to 7.5% for August.

Work relating to the development of an anisotropic diffuse irradiance correction method has been undertaken by several investigators during the past decade. Ineichen [5] reported his method of combining two simple models to determine the total correction factor: one was the isotropic geometric

model and the other was based on the diffuse radiation as a function of solar altitude. Kasten et al[6] considered the influence of three parameters that were most relevant in determining the anisotropic correction factor, namely: the ratio of the diffuse to global radiation, the solar declination and the coefficient for beam radiation transmission. Siren's investigation and evaluation [7] , based on a two-component sky radiation model, showed that the total correction factor appeared to be a function of the shadow band geometry, location of the shadow band, and the sky radiation distribution. LeBaron et al. [8] presented a model employing the parameter scheme method put forward by Perez. This parameter scheme is represented as a 256-combination of the values of the zenith angle of sun, the isotropic correction factor, the sky's clearness index and the sky's brightness index.

The common character of the above anisotropic methods is that they employ different radiation distribution models to obtain the ratio of diffuse irradiance subtended by shadow band to the total diffuse irradiance. However, the use of a complex function and parameter scheme within such a model makes it more difficult to apply the model in practise. The purpose of this article is to develop a relatively simple yet accurate anisotropic model that can be applied widely across the global.

In this article, the development of a new model based on the radiance distribution index formulation introduced by Moon and Spencer [9] is presented. Investigation of the relationship between the radiance distribution index and sky clearness index, k_t, is reported. The model is validated using data from two sites with disparate climate conditions. Drummond's isotropic model is examined through physical reasoning and numerical analysis. A comparison of the performance of the proposed model, and Drummond's isotropic model is illustrated through the use of error histograms and statistical analysis. The proposed model has been derived based on non-site specific parameters, namely: radiance distribution index, b and clearness index k_t, and hence should be applicable for all sites.

7.2 DRUMMOND'S METHOD

7.2.1 Theory

Drummond [1] gave the following formula based on geometrical analysis to calculate the isotropic shadow band diffuse correction factor F_D:

$$F_D = 1/(1-f) \tag{7.2}$$

where F_D is the correction factor and f is the proportion of diffuse irradiance obstructed by the shadow band. Note that F_D is to be multiplied with the uncorrected value of diffuse irradiance as measured with shadow band to provide the corrected diffuse irradiance. f can be calculated using Eq. 7.3:

$$f = X/T = 2(W/\pi)\cos^3\delta\,(t_0 \sin\varphi \sin\delta + \cos\varphi\ \cos\delta \sin t_0) \tag{7.3}$$

where X is the diffuse irradiance shaded by shadow band, T is the total diffuse irradiance. Eq. 7.3 is derived from the integration of Eqs. 7.4 and 7.5 below, based on the assumption that the sky-diffuse radiance distribution is uniform:

$$X = I\,W\ \cos^3\delta \int_{t=sunrise}^{t=sunset} \sin\alpha\, dt \tag{7.4}$$

$$T = \pi\, I \tag{7.5}$$

where I is the radiation intensity of the sky. However as real sky-diffuse irradiance distribution is anisotropic, to get a more accurate correction factor, the I value must be treated as a variant. Such a procedure is given below.

7.2.2 Examination of 'measured' diffuse correction factor

Measurements of the global and diffuse sky irradiance along with beam normal irradiance were used to examine the validity of Drummond's method [1]. To reveal the inadequacy of Drummond's isotropic method, comparison of the correction factor range obtained using Drummond's method and the range of measured correction factor has been undertaken.

One complete year's data (1995) for Bracknell (51.4°N, 0.8°W) in England are used to examine Drummond's method. The data consists of hourly horizontal global, beam normal and diffuse

irradiance measured by shadow band. Hourly irradiance on vertical surfaces facing north, east, south, west and a tilted surface facing south at the local latitude angle were also available. These data were provided by the UK Meteorological Office, Bracknell.

To ensure data reliability, data are discarded if they do not satisfy simultaneously the following quality control conditions:

$G - B_n \sin\alpha > D_{uncorrected}$;

$B_n \sin\alpha < G$;

$B_n < E_n$ * earth-sun distance correction;

$\alpha > 10$ degree

The earth-sun distance correction = 1+0.033cos(0.0172024 DN), where DN is the Julian day number. $D_{uncorrected}$ is the uncorrected diffuse irradiance. E_n, the extra-terrestrial irradiance, is taken as 1367 W/m^2. A total of 3583 hours data were thus chosen to examine Drummond's correction factor against the true correction factor.

The true correction factor, F_{true}, is obtained using Eq. 7.6:

$$F_{true} = (G - B_n \sin\alpha)/D_{uncorrected} \quad (7.6)$$

Figure 7.1 shows that Drummond's isotropic correction factor ranges from 1.010 to 1.128, whereas the true correction factor ranges from 1.001 to 1.480. It is therefore confirmed that, in the case of hourly diffuse irradiance measurement, Drummond's method underestimates the correction factor by up to 24%.

7.3 NEW MODEL BASED ON SKY-DIFFUSE DISTRIBUTION INDEX

7.3.1 Theoretical analysis

A radiance distribution index, b, based on the work of Moon and Spencer [9] is introduced herein to facilitate the present modelling exercise. The model is given in Eq. 7.7,

$$L_\theta = L_z (1 + b \sin\theta) / (1 + b) \tag{7.7}$$

where L_θ is the radiance of a given sky patch with an altitude = θ, L_z is the zenith radiance and b is the radiance distribution index.

Muneer [10] has used the above model to establish a relationship between slope diffuse irradiance and horizontal diffuse irradiance. Muneer's model is given by Eq. 7.8,

$$D_\beta/D=\cos^2(\beta/2) + [2b/\pi(3+2b)] [\sin\beta - \beta \cos\beta - \pi \sin^2(\beta/2)] \tag{7.8}$$

where D_β is the hourly diffuse irradiance for a sloped surface, D is the hourly horizontal diffuse irradiance, β is the tilt of the sloped surface. Muneer's model also treats the shaded and sunlit surfaces separately and further distinguishes between overcast and non-overcast conditions. Based on his study for Bracknell, Muneer found that for a shaded surface (facing away from sun) the 'best' value of b is 5.73; for a sunlit surface under overcast sky conditions b = 1.68; and for a sunlit surface under non-overcast sky conditions b = -0.62.

As reported above, measured vertical and slope surface irradiance data for Bracknell, England were made available to the authors. Using these data an assessment of the variation of 'b' against k_t can be made using Eq. 7.8. The presently developed mathematical relationship between b and k_t is given in Eq. 7.9,

For $k_t > 0.2$,

$$\frac{2b_1}{\pi(3+2b_1)} = 0.382 - 1.11\,k_t \qquad \text{(for southern half of sky hemisphere)} \qquad (7.9a)$$

$$\frac{2b_2}{\pi(3+2b_2)} = 0.166 + 0.105\,k_t \qquad \text{(for northern half of sky hemisphere)} \qquad (7.9b)$$

For $k_t \leq 0.2$, $b_1 = b_2 = 1.68$ (after Muneer [10]).

A point worth mentioning here is that, strictly speaking the sky radiance distribution is two-dimensional , a function of any given sky patch geometry (sky patch altitude and azimuth) and the position of sun. Eq. 7.9 represents a compromise between simplicity (represented by an isotropic model) and complexity (represented by a two-dimensional model such as the one described above). Another feature of Eq. 7.9 is that due to its relative simpler formulation it also tends to be robust (covering all-sky conditions) and of general applicability, as shall be demonstrated herein via validation undertaken for disparate sites, i.e. Bracknell, England (51.4°N, 0.8°W) and Beer Sheva, Israel (31.3°N, 34.8°E).

7.3.1.1 Total sky-diffuse irradiance

The total sky-diffuse irradiance can be obtained through a numerical integration based on Moon and Spencer's sky-diffuse distribution model. If the zenith radiance is termed L_Z, then the horizontal diffuse irradiance D can be calculated using Eq. 7.10,

$$D = \int_0^{\pi/2} (\pi \sin\theta \cos\theta)(L_{\theta 1} + L_{\theta 2})d\theta \qquad (7.10)$$

where $L_{\theta 1} = L_Z(1+b_1\cos\theta)/(1+b_1)$, and $L_{\theta 2} = L_Z(1+b_2\cos\theta)/(1+b_2)$. $L_{\theta 1}$ is defined as the sky-diffuse radiance emanating from any given patch of the southern half of the sky vault, and $L_{\theta 2}$ the corresponding radiance from the northern half of the sky hemisphere. Thus,

$$D = \pi L_Z\{[\int_0^{\pi/2} (\sin\theta \cos\theta + b_1 \sin\theta \cos^2\theta)/(1+b_1)d\theta] +$$

$$[\int_0^{\pi/2} (\sin\theta \cos\theta + b_2 \sin\theta \cos^2\theta)/(1+b_2)d\theta]\} \qquad (7.11)$$

So,

$$D = (\pi L_Z/6)\,[(3+2b_1)/(1+b_1) + (3+2b_2)/(1+b_2)] \tag{7.12}$$

Moon and Spencer [9] showed that using $b_1=b_2=2$ in Eq. 7.12 adequately describes the radiance distribution of an overcast sky, and leads to the relationship, $D = 7\pi L_Z/9$.

7.3.1.2 The new correction factor based on b_1 and b_2 functions (Eq. 7.9)

If F_Δ is defined as the diffuse irradiance that is obscured by shadow band, then F_Δ may be calculated using Eq. 7.13:

$$F_\Delta = W \cos^3 \delta \int_{t=sunrise}^{t=sunset} L_{\theta_1} \sin\alpha \, dt \tag{7.13}$$

The result of the above integration is,

$$F_\Delta = 2W\, L_Z \cos^3 \delta\ (I_1 + b_1 I_2) / (1 + b_1) \tag{7.14}$$

$$I_1 = \cos\varphi\ \cos\delta \sin t_0 + t_0 \sin\varphi \sin\delta$$

$$I_2 = t_0 \sin^2\varphi \sin^2\delta + 2\sin t_0 \sin\varphi \cos\varphi\ \sin\delta \cos\delta + \cos^2\varphi \cos^2\delta\ [\, t_0/2 + (\sin 2t_0)/4]$$

Now, using Eqs.7.12 and 7.14, the proposed shadow band diffuse irradiance correction factor, F_P, can be obtained,

$$F_P = 1/(1-F_\Delta / D) \tag{7.15}$$

7.3.2 Validation

The validity of the proposed model was tested by plotting the corrected hourly diffuse irradiance against the true diffuse irradiance as obtained via Eq. 7.1. Databases of two different sites, namely:

Bracknell, England and Beer Sheva, Israel were used to validate the proposed model. These two sites provide diverse variation in climatic conditions and latitude separation.

7.3.2.1 Validation using Bracknell database

7.3.2.1.1 Scatter plots and statistical analysis

The proposed model was applied to the culled Bracknell database which was previously used to examine the performance of the Drummond's method (see section 2). Corrected diffuse irradiance ($D_{corrected}$) data were regressed against true values of 'measured' diffuse irradiance (D) obtained via Eq. 7.1 to determine the model's performance. Results of this comparison are shown in Fig. 7.2. The slope of the fitted trend line is 0.99, and the coefficient of determination, R^2, is 0.98. Drummond's method was also applied to this database. The result is shown in Fig. 7.2. The slope of the fitted trend line is 0.95, and the coefficient of determination R^2 is 0.97. The slope of the fitted trend line is indicative of the validity of the model under test. The degree of validity increases as the slope approaches unity. The proposed method thus offer a better accuracy.

To enable further insight into the validation of the above models the mean bias error (MBE) , the root mean square error (RMSE) and the Percentage Average Deviation (PAD) have been obtained. Results are shown in Table 7.1.

$$\text{Mean Bias Error, MBE} = \frac{\Sigma(D_{corrected} - D)}{no.of\ data\ points}$$

$$\text{Root Mean Square Error, RMSE} = \sqrt{\frac{\Sigma(D_{corrected} - D)^2}{no.of\ data\ points}}$$

$$\text{Percentage Average Deviation, PAD} = \frac{\Sigma(100 * |D_{corrected} - D| / D_{corrected})}{no.of\ data\ points}$$

7.3.2.1.2 Histograms

Histogram plots of percentage error were also made to compare the proposed model's performance against that of Drummond's method. The histograms present graphical representations of the frequency distribution of the percentage error. A given models' performance is examined in two ways. Firstly, the histogram provides a check regarding the proportion of data points that fall within specific range of percentage error and secondly, it allows an examination of the range of errors.

Histograms of the proposed model for all-sky conditions, and for $0 < k_t \leq 0.2$ (heavy overcast), $0.2 < k_t \leq 0.6$ (part-overcast) and $0.6 < k_t < 1$ (clear-sky) are shown in Fig. 7.3 respectively. Corresponding histograms for Drummond's method are given in Fig. 7.4. The results of these analyses are presented in Table 7.2 as the number of data points that fall in percentage error ranges of -3% — -1%, -1% — +1%, and +1% — +3%. For the proposed model and for all-sky conditions, 70% of corrected diffuse value fall in the -3% — +3% percentage error range, while for Drummond's method the corresponding figure is 58%. Under clear-sky condition ($0.6 < k_t < 1$), when solar energy has the greatest impact the proposed model is significantly better. Generally speaking, the proposed model displays a normal distribution for errors, while Drummond's model is heavily skewed, especially under clear-sky conditions.

7.3.2.2 Validation using Beer Sheva database

Nearly two years of measured data (February, 1998 — December, 1999) for Beer Sheva (31.4°N, 34.8°E) in Israel were used for further evaluation of the models under discussion. The data consist of hourly horizontal diffuse (measured using shadow band pyranometer) and global, beam normal irradiance and irradiance on a south facing sloping surface with tilt = 40 degree. These data were provided by the Chemical Engineering Department at Ben-Gurion University. Again, the data sets were culled using the combination of the four conditions given in Section 2.

7.3.2.2.1 Scatter plots and statistical analysis

Diffuse irradiance data respectively corrected via proposed model and Drummond's method, were regressed against true diffuse irradiance values. The results of this comparison are shown in Fig. 7.5. The slope of the fitted trend line for proposed method is 1.00, and the coefficient of determination, R^2 is 0.99. The result obtained from the application of Drummond's method is shown in Fig. 7.5. The slope of the fitted trend line in this case is 0.96, and the coefficient of determination R^2 is 0.99. Table 7.3 shows the MBE, RMSE and PAD statistics for Beer Sheva database. The proposed model produces an RMSE of 17 W/m^2, an MBE of $2W/m^2$ and a PAD of 5%. The corresponding figures for Drummond's method are 23 W/m^2, $-5W/m^2$ and 7% respectively.

7.3.2.2.2 Histograms

Figure 7.6 and 7.7 show the histograms for different sky conditions obtained through application of the proposed and Drummond's method to Beer Sheva's database. The results of this analysis are presented in Table 7.4. For all-sky conditions, 41% of diffuse values corrected by the proposed method fall in the ±3% percentage error range, while for Drummond's method, the corresponding figure is 21%. Once again, the proposed model displays a normal error distribution behaviour, while Drummond's method is considerably skewed, especially under clear-sky conditions.

7.4 SUMMARY

A new anisotropic model to correct diffuse irradiance measured by shadow band has been developed. This method is based on the use of a single diffuse radiance distribution index, b, introduced after the work of Moon and Spencer [9]. Clearness index, k_t, is used as a parameter to determine the value of b, and b is then used to obtain the correction factor to account for the diffuse irradiance obscured by shadow band. The proposed method is validated using databases from sites with disparate sky conditions. The Drummond's isotropic method, which is based solely on geometric calculation is compared against the proposed method that uses an anisotropic radiance distribution. Results show that for the case of Bracknell, England the RMSE , MBE and PAD of corrected diffuse irradiance obtained using the proposed method are $12W/m^2$, -0.7 W/m^2 and 3% respectively. Corresponding RMSE, MBE and PAD due to Drummond's method are 16 W/m^2 , -5.6 W/m^2 and 4% respectively. For the case of Beer Sheva, Israel, the proposed model produces an RMSE of 17 W/m^2, an MBE of $2W/m^2$ and a

PAD of 5%. The corresponding figures for Drummond's method are 23 W/m^2, -5W/m^2 and 7% respectively.

REFERENCES

1. Drummond, A. J. (1956) On the Measurement of Sky Radiation *Arch. Meteor. Geophys. Bioklim.* 7, 413-436

2. Kudish, A. I. and Ianetz, A. (1993) Analysis of Diffuse Radiation Data for Beer Sheva: Measured (Shadow Ring) Versus Calculated (Global-Horizontal Beam) Values *Solar Energy*, 51, 495-503

3. Painter, H. E. (1981) The Shade Ring Correction for Diffuse Irradiation Measurements *Solar Energy*, 26, 361

4. Vartiainen, E. (1998) An anisotropic Shadow Ring Correction Method for the Horizontal Diffuse Irradiance Measurements *Renewable Energy*, 17, 311-317

5. Ineichen, P., Gremaud, J. M., Guisan, O. and Mermoud, A. (1984) Study of the corrective factor involved when measuring the diffuse solar radiation by using the ring method *Solar Energy*, 32, 585

6. Kasten, F., Dehne, K. and Brettschneider, W. (1983) Improvement of measurement of diffuse solar radiation *Solar radiation data*, F.2, 221

7. Siren, K. E. (1987) The shadow band correction for diffuse irradiation based on a two-component sky radiance model *Solar Energy*, 39, 433

8. LeBaron, B. A., Michalsky, J. J. and Perez, R. (1990) A simple procedure for correcting shadow band data for all sky conditions *Solar Energy*, 44, 5, 249-256

9. Moon, P. and Spencer, D. E. (1942) Illumination from a non-uniform sky *Trans. Illum. Eng. Soc.*, 37, 707-725

10. Muneer, T. (1990) Solar Radiation Model for Europe *Building Serv. Eng. Res. Technol.*, 11(4), 153-163

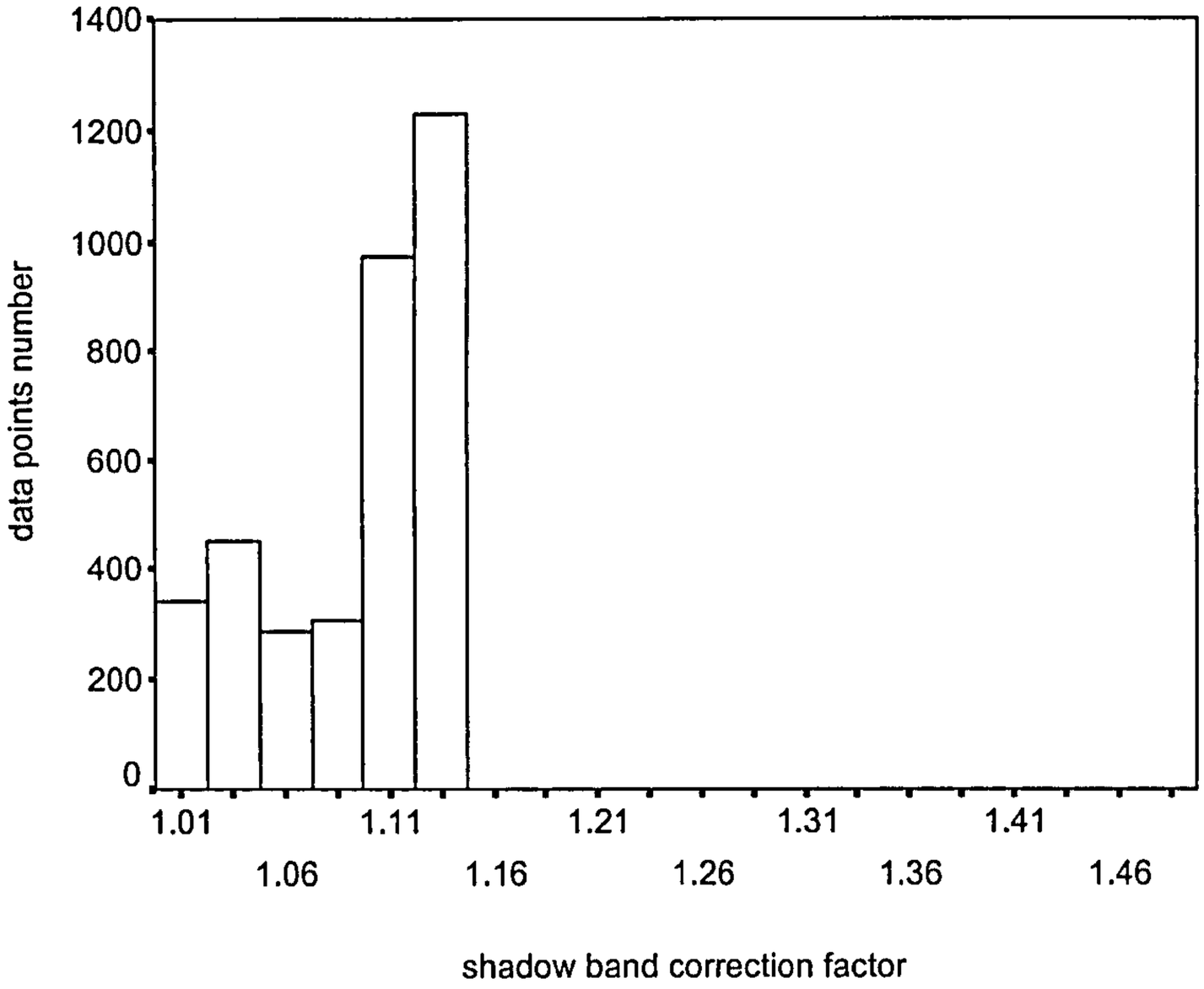

(a) Drummond's correction factor range

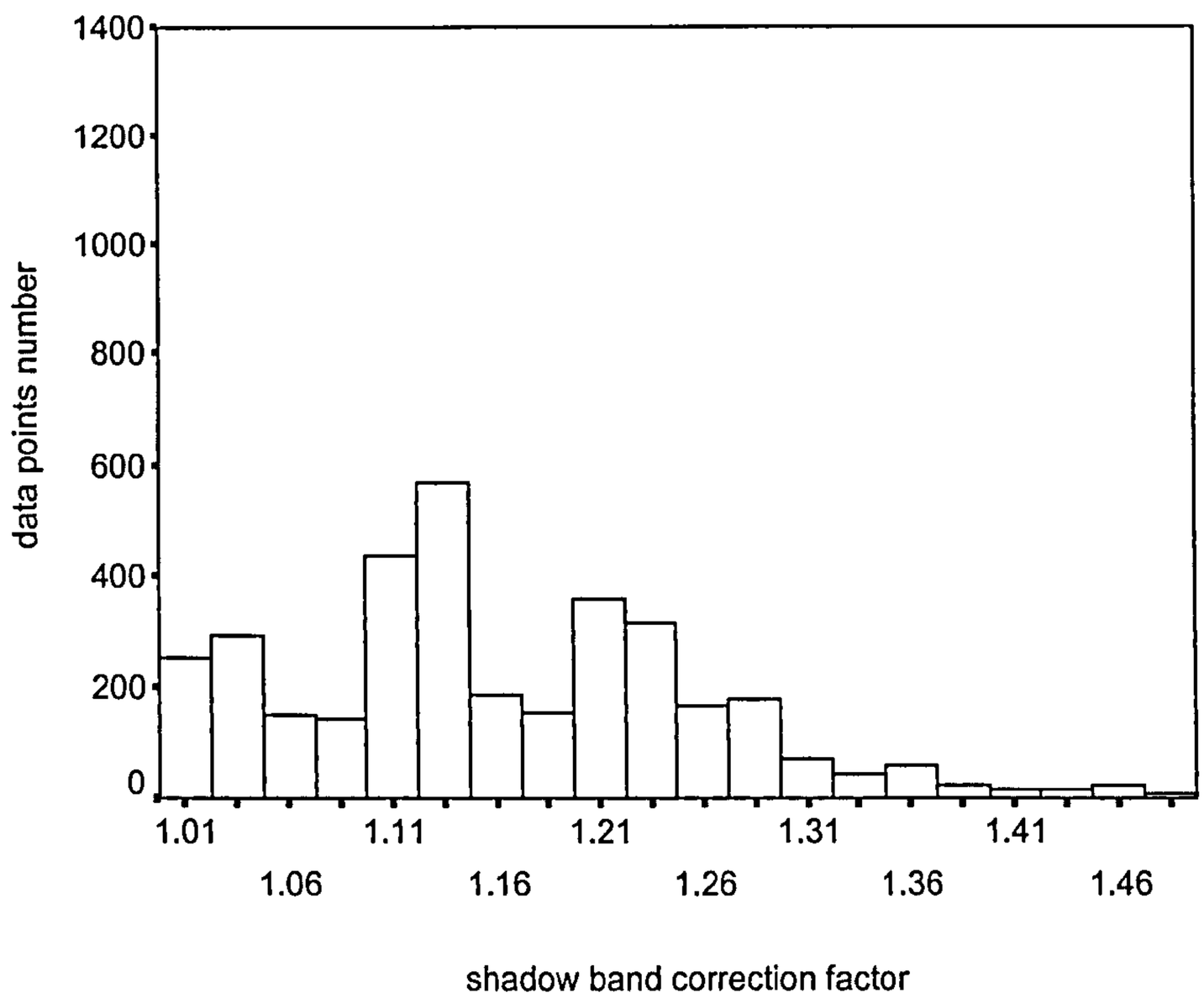

(b) Actual results

Figure 7.1 Comparison of the range of diffuse irradiance correction factor given by Drummond's method and actual results

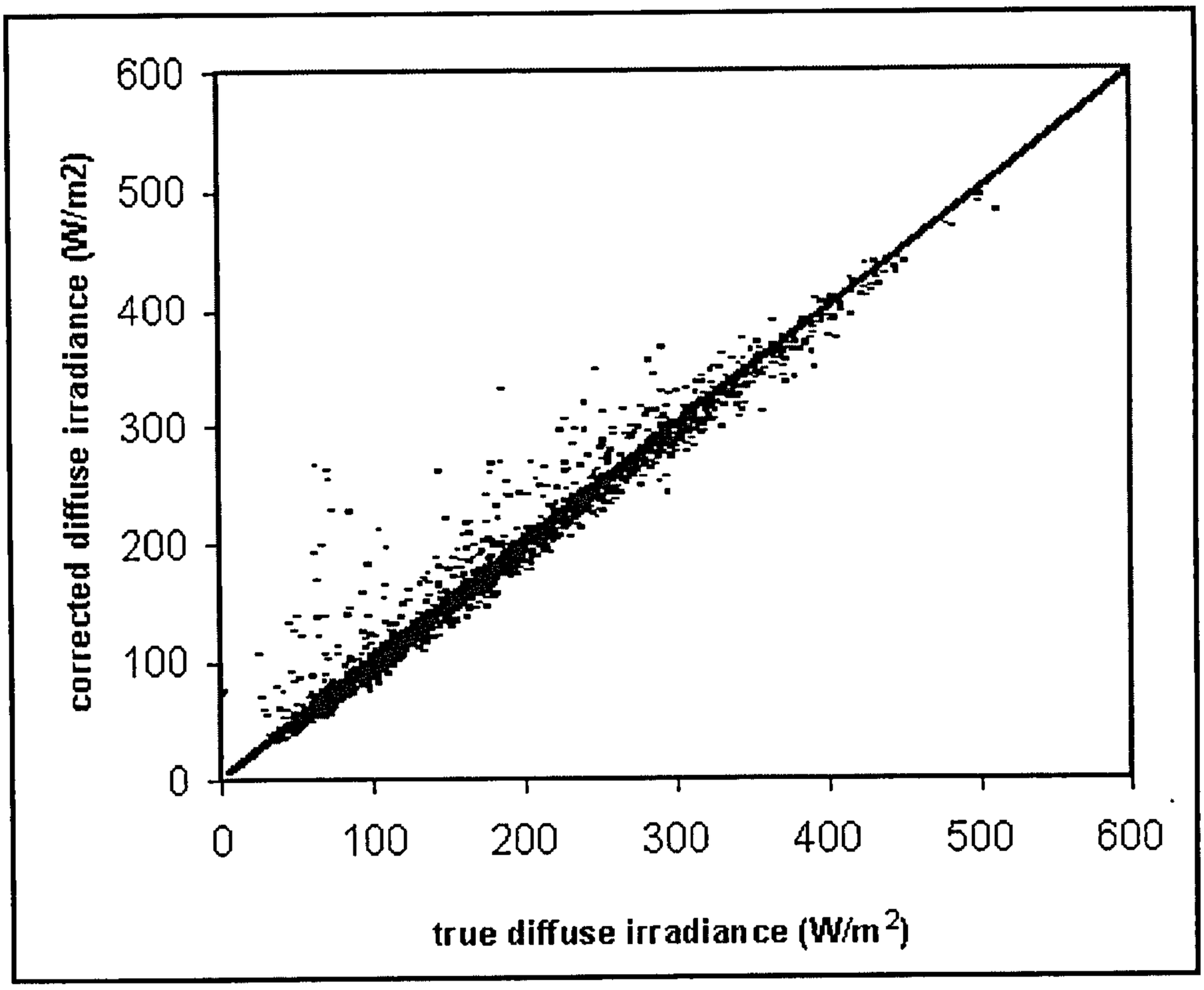

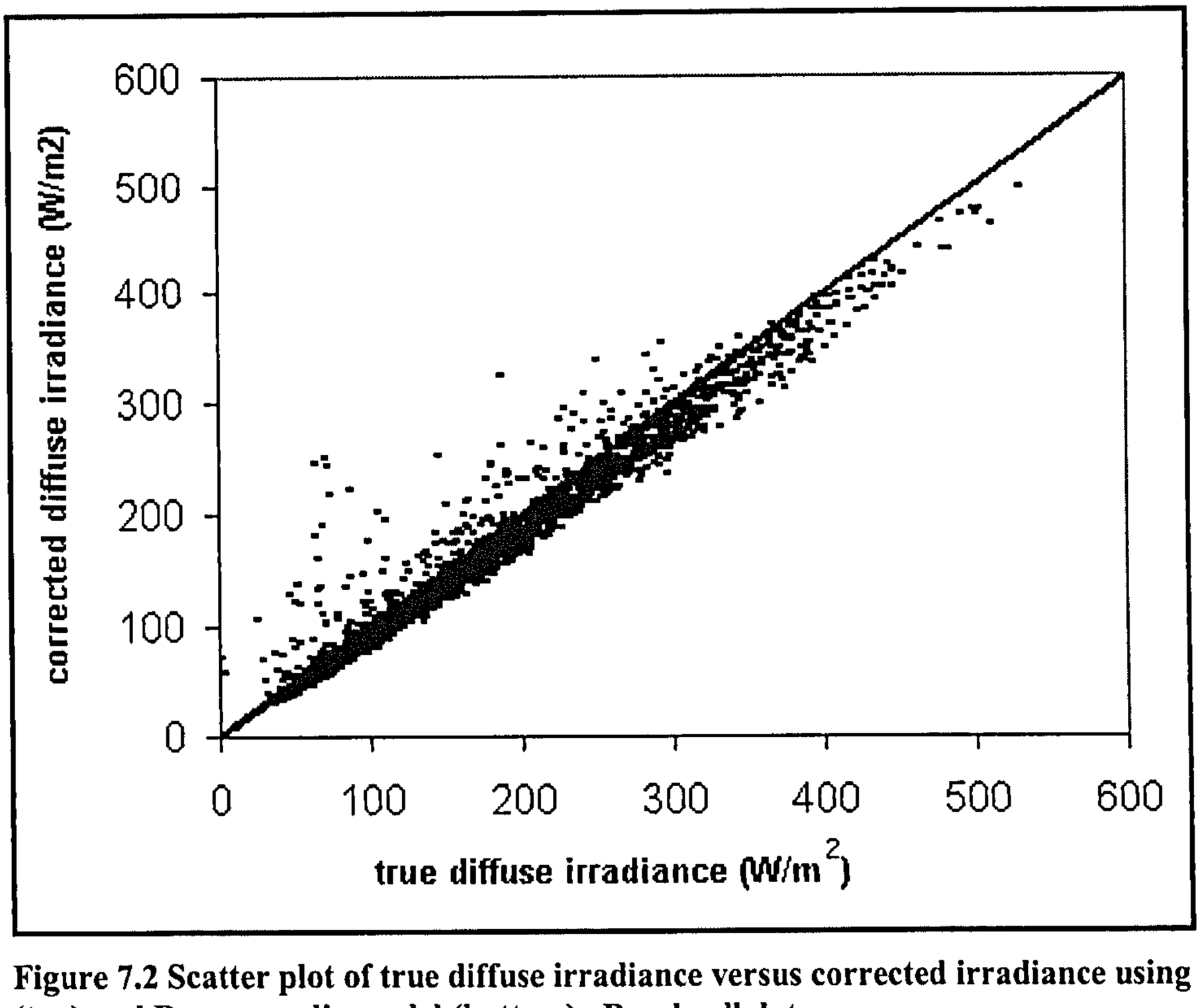

Figure 7.2 Scatter plot of true diffuse irradiance versus corrected irradiance using the proposed (top) and Drummond's model (bottom) –Bracknell data

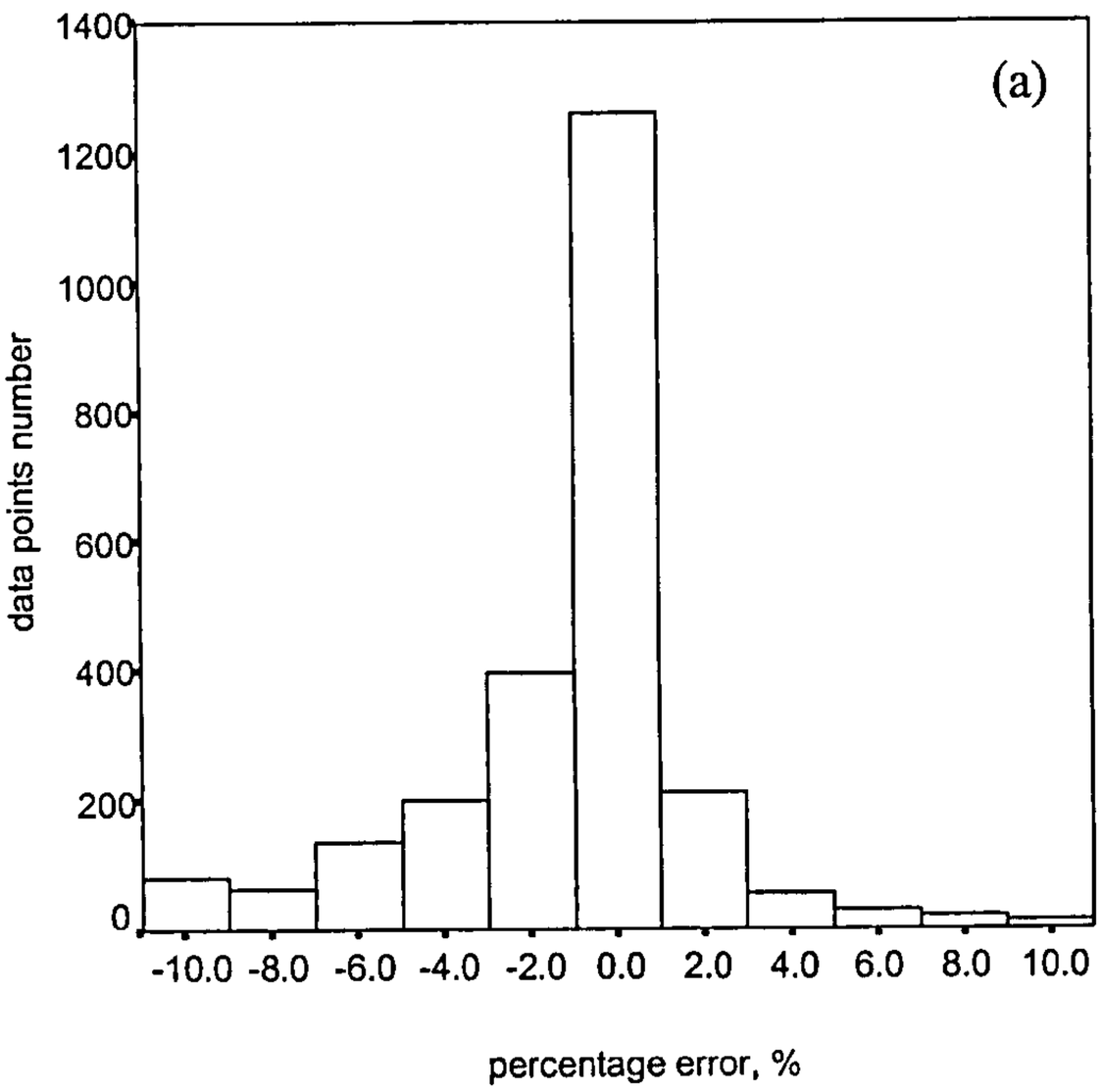

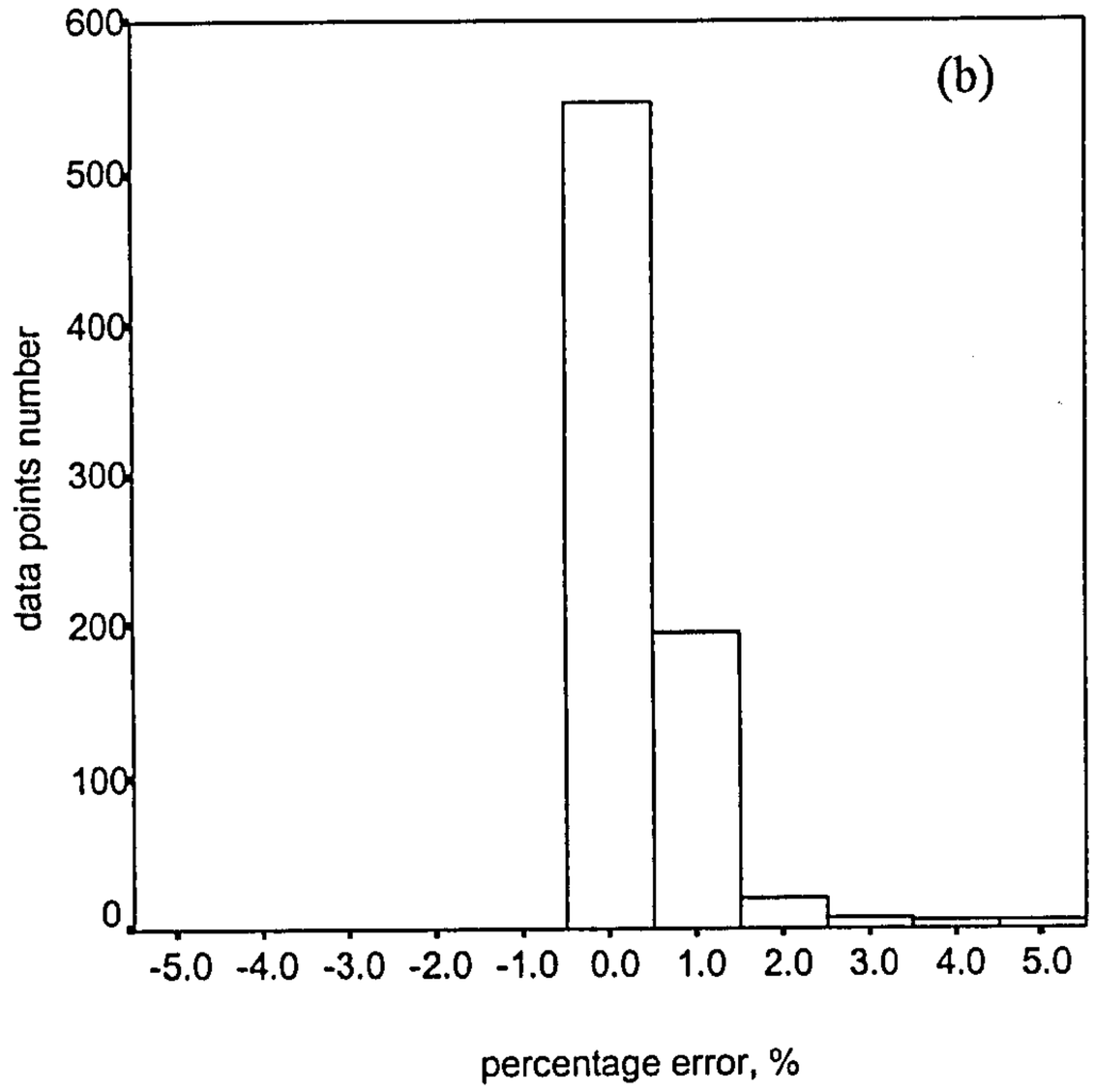

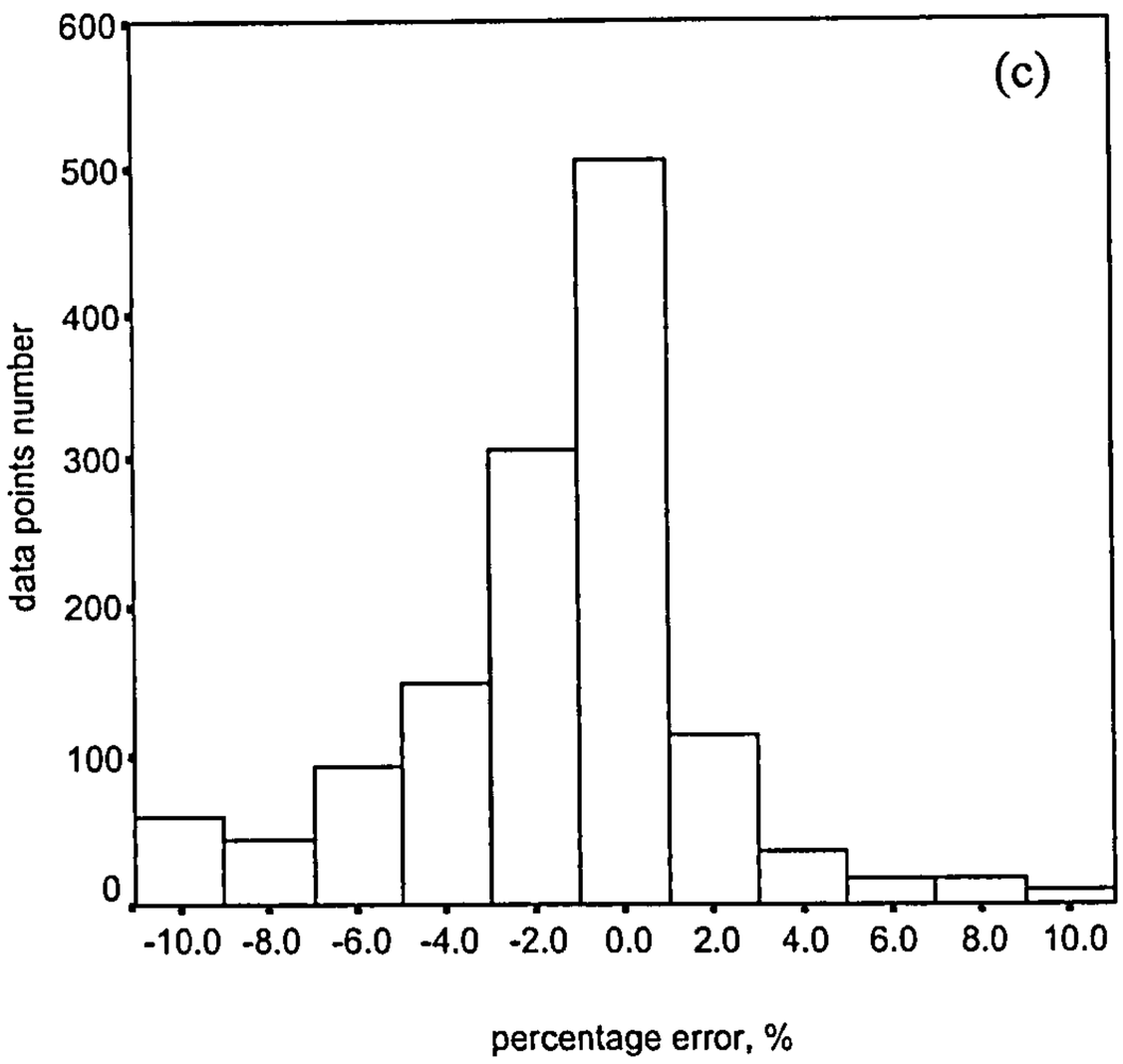

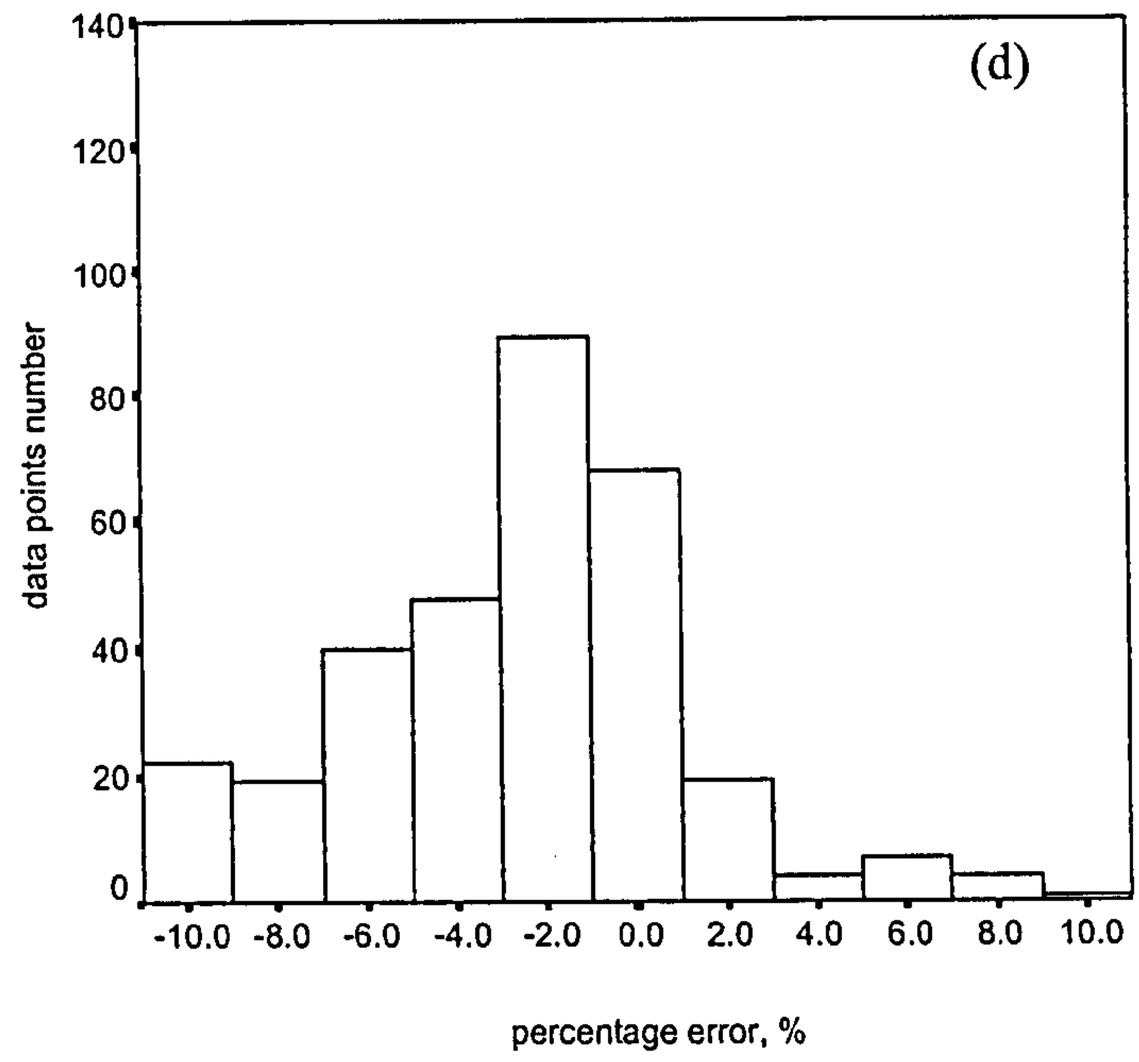

Figure 7.3 Proposed model's error histogram under all-sky (a), heavy overcast ($0 < k_t \leq 0.2$) (b), part-overcast ($0.2 < k_t \leq 0.6$) (c) and clear-sky ($0.6 < k_t < 1$) (d) conditions – Bracknell data

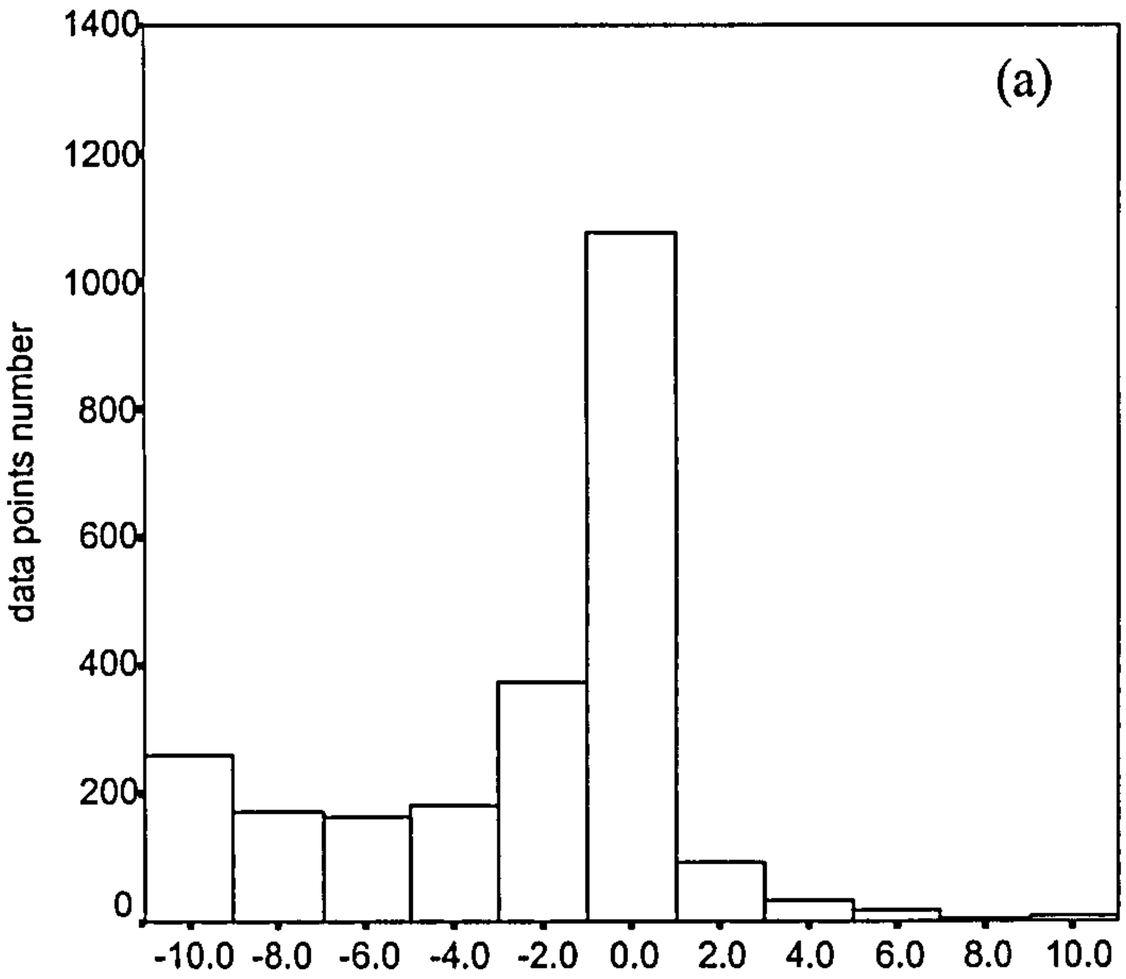

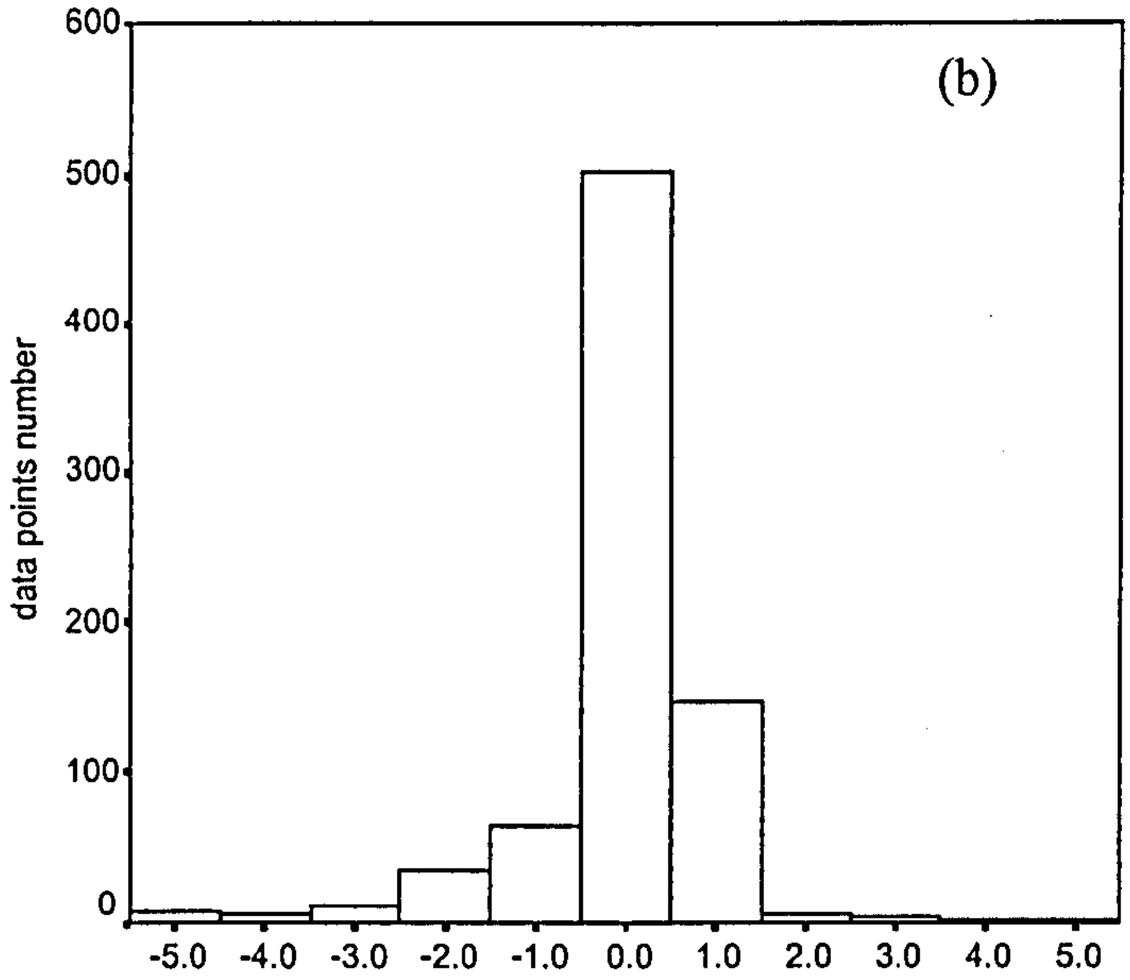

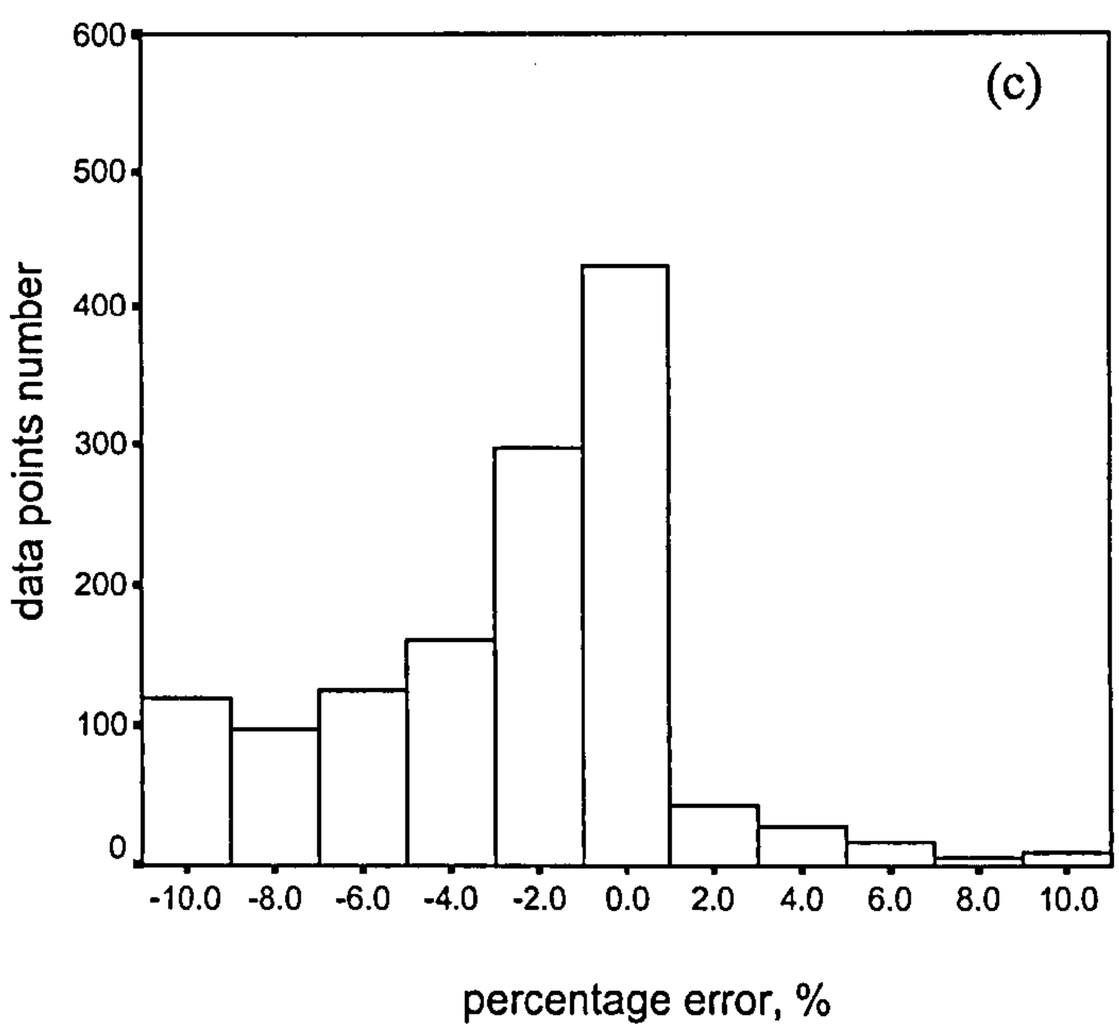

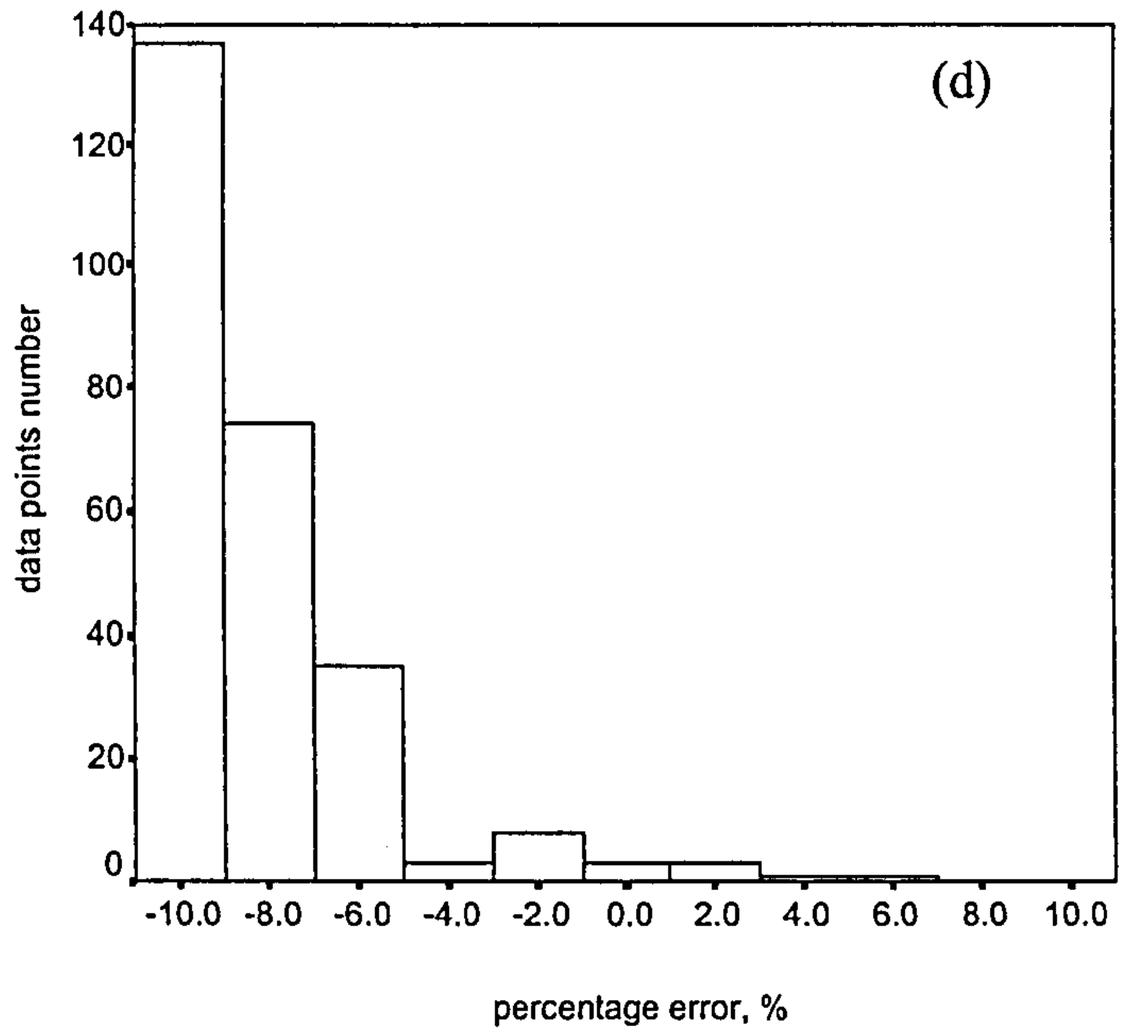

Figure 7.4 Drummond model's error histogram under all-sky (a), heavy overcast ($0 < k_t \leq 0.2$) (b), part-overcast ($0.2 < k_t \leq 0.6$) (c) and clear-sky ($0.6 < k_t < 1$) (d) conditions – Bracknell data

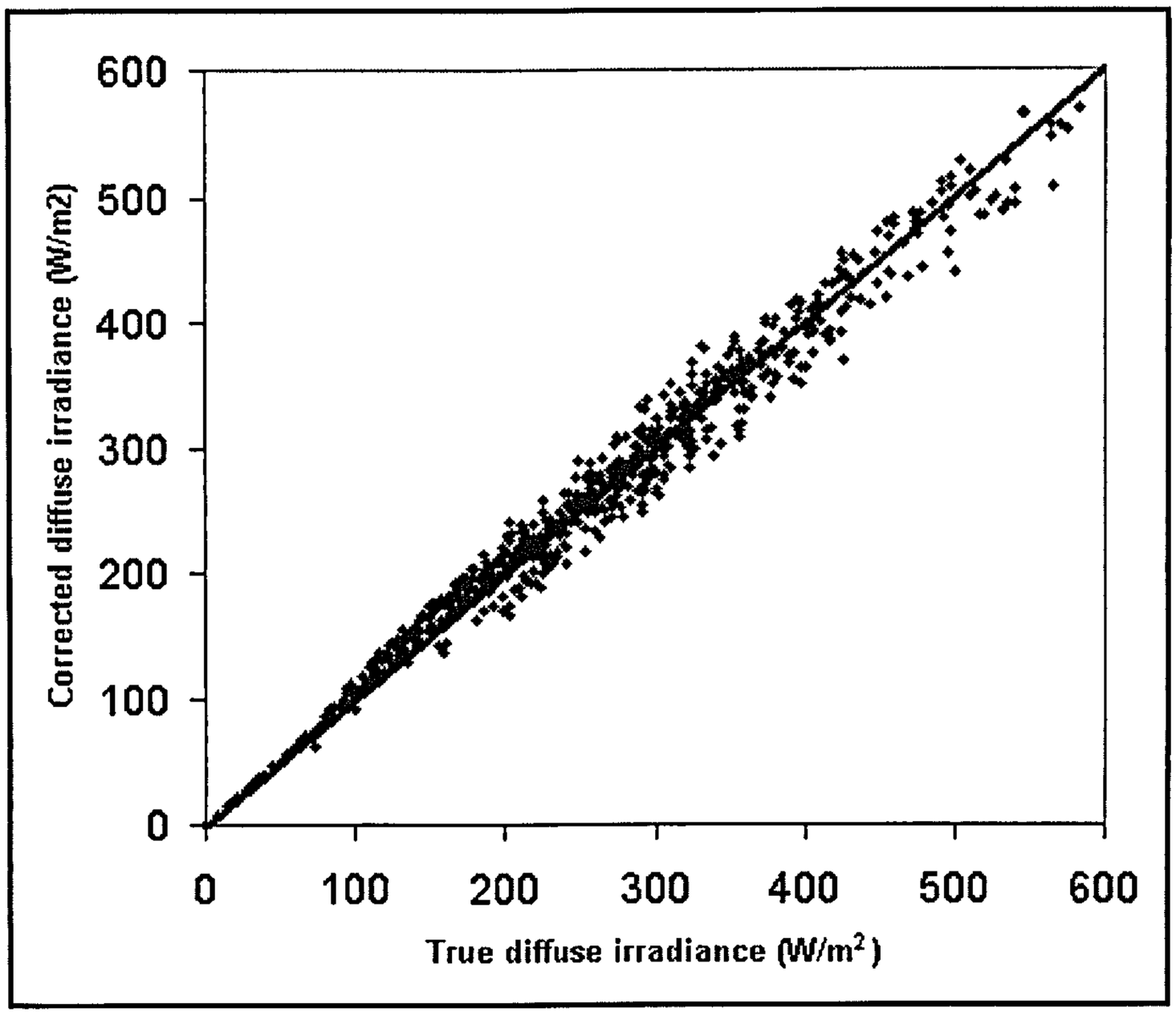

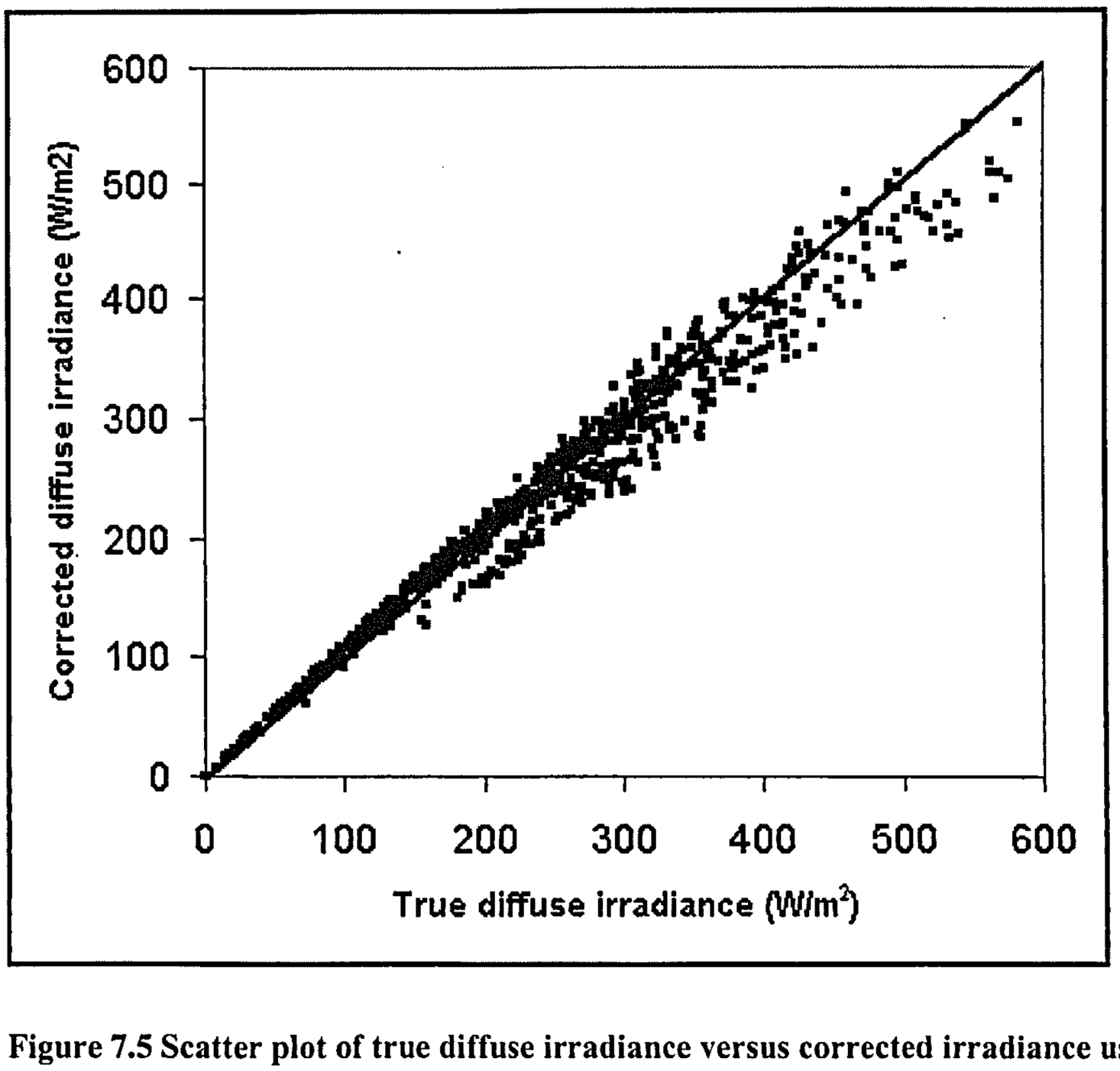

Figure 7.5 Scatter plot of true diffuse irradiance versus corrected irradiance using the proposed (top) and Drummond's model (bottom) – Beer Sheva data

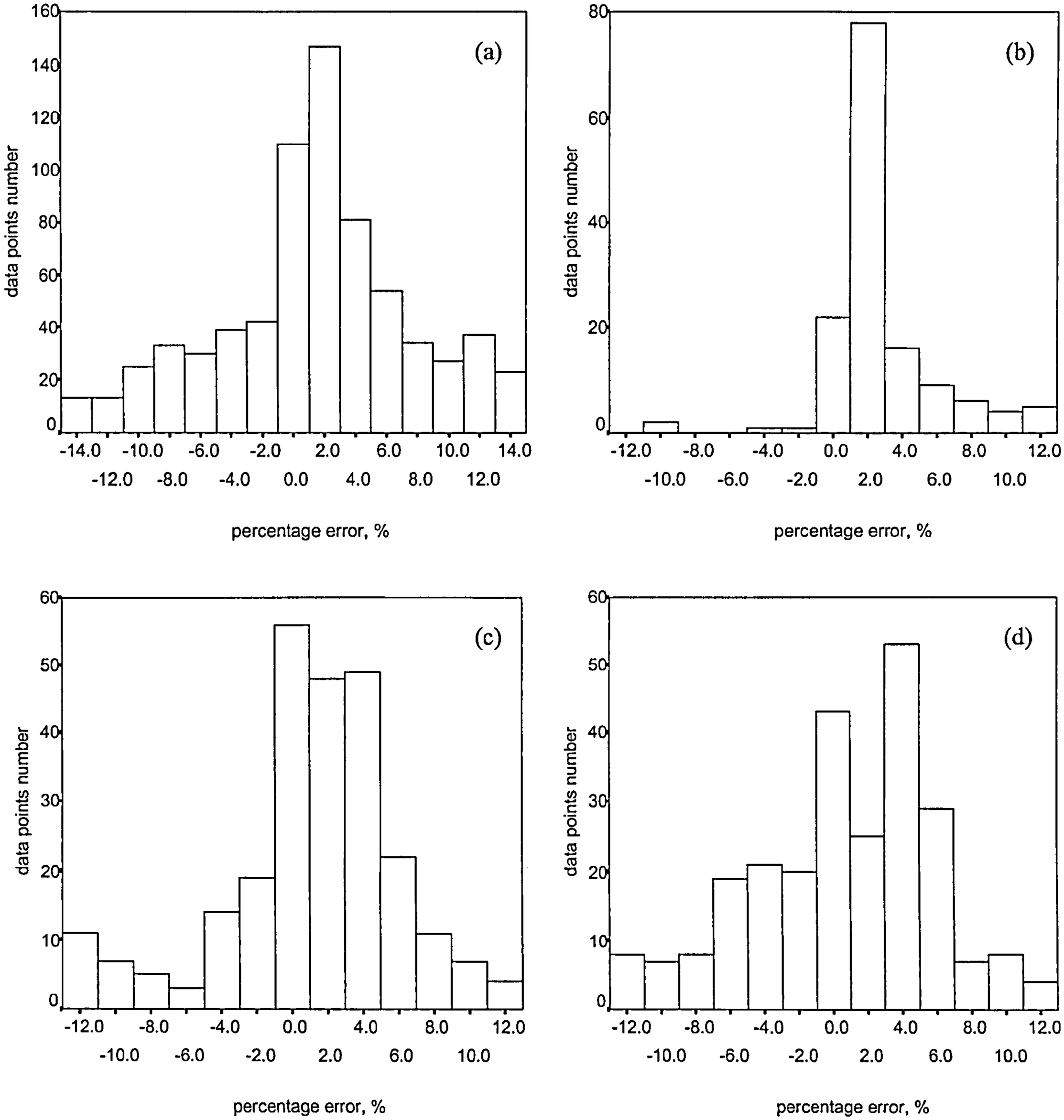

Figure 7.6 Proposed model's error histogram under all-sky (a), heavy overcast ($0 < k_t \leq 0.2$) (b), part-overcast ($0.2 < k_t \leq 0.6$) (c) and clear-sky ($0.6 < k_t < 1$) (d) conditions – Beer Sheva data

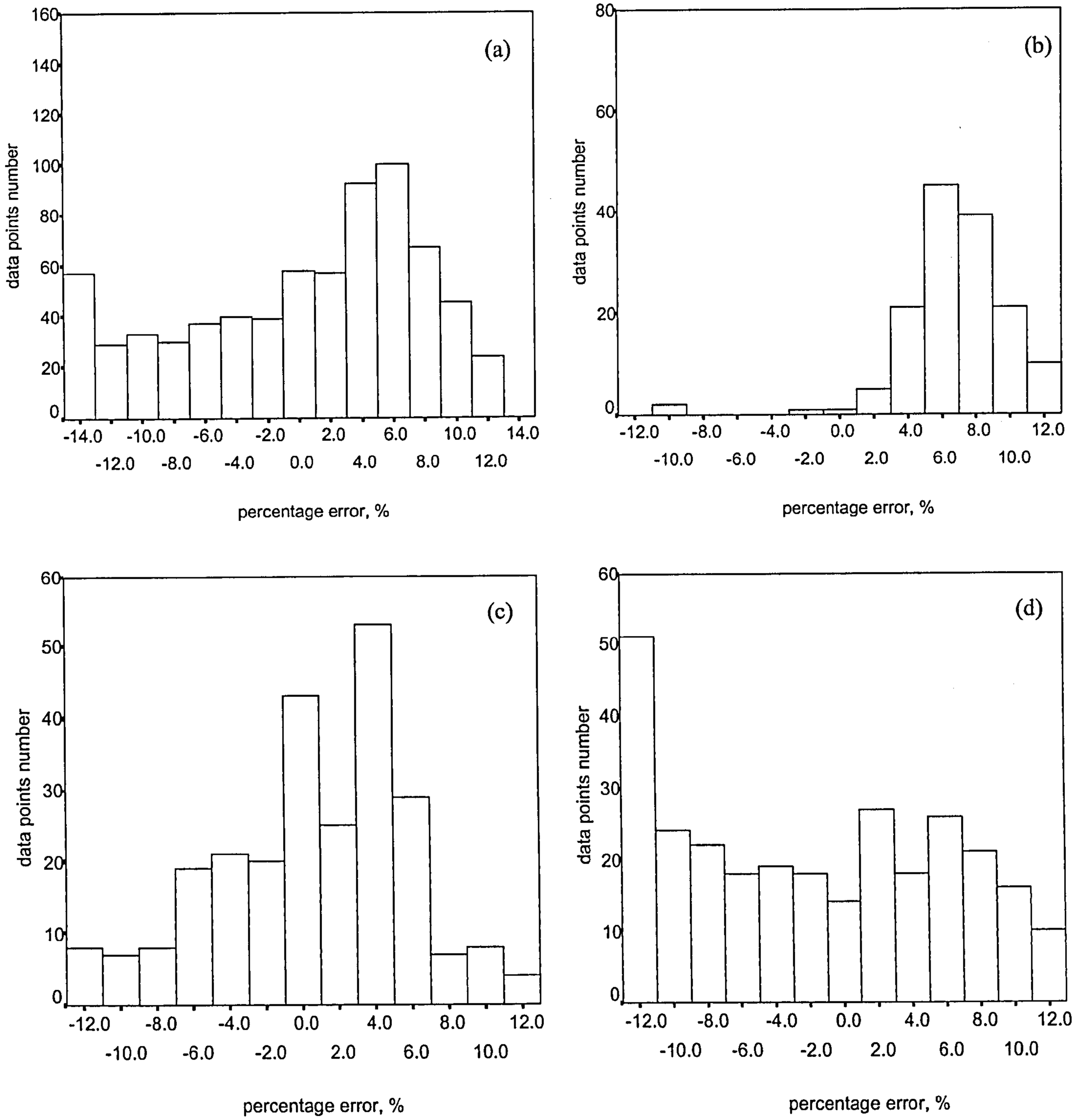

Figure 7.7 Drummond model's error histogram under all-sky (a), heavy overcast ($0 < k_t \leq 0.2$) (b), part-overcast ($0.2 < k_t \leq 0.6$) (c) and clear-sky ($0.6 < k_t < 1$) (d) conditions – Beer Sheva data

Table 7.1 Mean Bias Error (MBE), Root Mean Square Error (RMSE) and Percentage Average Deviation (PAD) comparison of the proposed model versus Drummond's method, Bracknell

	All-sky conditions			$0 < k_t \leq 0.2$			$0.2 < k_t \leq 0.6$			$0.6 < k_t < 1$		
	MBE (W/m^2)	RMSE (W/m^2)	PAD (%)	MBE (W/m^2)	RMSE (W/m^2)	PAD (%)	MBE (W/m^2)	RMSE (W/m^2)	PAD (%)	MBE (W/m^2)	RMSE (W/m^2)	PAD (%)
Proposed Model	-0.7	12.0	2.8	0.4	1.6	0.7	-0.3	15.1	3.9	-5.2	12.4	3.4
Drummond Model	-5.6	15.7	4.2	0.0	1.4	0.7	-4.8	16.7	4.9	-24.5	27.4	10.7

Table 7.2 Histogram percentage error analysis results, Bracknell. Figures given below are the number of data points in each category

	All-sky conditions			$0 < k_t \leq 0.2$			$0.2 < k_t \leq 0.6$			$0.6 < k_t < 1$		
	-3 - -1 (%)	-1 - 1 (%)	1 - 3 (%)	-3 - -1 (%)	-1 - 1 (%)	1 - 3 (%)	-3 - -1 (%)	-1 - 1 (%)	1 - 3 (%)	-3 - -1 (%)	-1 - 1 (%)	1 - 3 (%)
Proposed Model	393	1259	211	0	547	195	304	504	114	89	68	19
Drummond Model	374	1081	94	65	503	148	297	429	44	8	3	3

Table 7.3 Statistical comparison of the two models under discussion - Bracknell data.

Month	RMSE (W/m^2)		MBE (W/m^2)		Percentage Average Deviation (%)	
	Proposed Model	Drummond model	Proposed Model	Drummond model	Proposed model	Drummond Model
January	4	5	-1.5	-1.6	2.0	2.0
February	6	7	-0.6	-1.0	1.7	1.8
March	9	15	-1.8	-6.5	3.2	5.0
April	12	19	-2.5	-10.0	3.0	5.3
May	18	20	4.3	-4.4	3.7	5.2
June	10	14	-0.3	-6.0	2.0	3.8
July	18	20	3.7	-3.7	3.2	4.8
August	10	19	-4.9	-14.0	2.9	6.7
September	11	16	-3.9	-8.0	3.0	4.4
October	10	13	-6.0	-7.6	3.8	4.7
November	4	4	-1.2	-1.3	2.2	2.1
December	2	2	-0.5	-0.6	1.5	1.7

Table 7.4 Mean Bias Error (MBE), Root Mean Square Error (RMSE) and Percentage Average Deviation (PAD) comparison of the proposed model versus Drummond's method, Beer Sheva

	All-sky conditions			$0 < k_t \leq 0.2$			$0.2 < k_t \leq 0.6$			$0.6 < k_t < 1$		
	MBE (W/m^2)	RMSE (W/m^2)	PAD (%)	MBE (W/m^2)	RMSE (W/m^2)	PAD (%)	MBE (W/m^2)	RMSE (W/m^2)	PAD (%)	MBE (W/m^2)	RMSE (W/m^2)	PAD (%)
Proposed Model	2.1	17.1	5.2	3.2	5.1	3.0	5.0	17.2	4.4	-0.7	20.3	6.9
Drummond Model	-5.3	23.4	7.3	4.7	8.5	7.0	0.5	18.4	5.2	-15.6	30.4	9.0

Table 7.5 Histogram percentage error analysis results, Beer Sheva. Figures given below are the number of data points in each category

	All-sky conditions			$0 < k_t \leq 0.2$			$0.2 < k_t \leq 0.6$			$0.6 < k_t < 1$		
	-3 - -1 (%)	-1 - 1 (%)	1 - 3 (%)	-3 - -1 (%)	-1 - 1 (%)	1 - 3 (%)	-3 - -1 (%)	-1 - 1 (%)	1 - 3 (%)	-3 - -1 (%)	-1 - 1 (%)	1 - 3 (%)
Proposed Model	42	110	147	2	22	78	19	56	48	22	32	21
Drummond Model	39	58	57	2	2	5	20	43	25	18	14	27

Table 7.6 Statistical comparison of the two models under discussion - Beer Sheva data.

Month	RMSE (W/m^2)		MBE (W/m^2)		Percentage Average Deviation (%)	
	Proposed model	Drummond model	Proposed model	Drummond model	Proposed model	Drummond model
January	17	27	-4.5	-13.6	4.7	8.1
February	16	23	-1.0	-8.0	3.9	6.7
March	17	24	5.5	-2.2	4.3	6.5
April	17	23	2.8	-3.6	4.7	6.3
May	17	19	5.5	0.7	4.7	5.2
June	21	22	11.7	6.6	4.8	7.3
July	15	13	10.8	6.5	7.0	6.3
August	20	18	13.4	10.9	7.4	8.4
September	23	31	-0.5	-13.9	7.3	10.1
October	16	29	-5.9	-20.5	5.8	10.5
November	18	28	-10.0	-21.6	6.9	11.7
December	17	27	-8.9	-18.1	5.7	9.5

8. VALIDATION OF DPF MODELS

The validation of DPF models has been carried out by three approaches. The first approach was to apply the DPF models to independently measured data in Merchiston test room, and compare the measured internal illuminance data against those predicted due to DPF models. The second approach was to check the DPF models using one of the most established statistical techniques: residual analysis. The third approach was to compare the DPF models against results due to independent researches.

8.1 CHECKING THE LINEAR MODEL BY STATISTICAL TECHNIQUE – RESIDUALS PLOT

The adequacy of a fitted regression model can be carried out by the method of checking the residual plots due to the model. The residual method applies generally "whenever a linear model is fitted, no matter how many predictors there are" [1]. The procedure is to produce a graph of the residual e (the difference between observed Y_o and calculated Y_c values of the dependent variable) plotted against the independent variables X_i or the observed value Y_o [2].

A satisfactory residuals plot is one that shows a (more or less) horizontal band of points giving the impression of Fig. 8.1. There are many possible unsatisfactory plots. Three typical ones appear in Fig. 8.2. The first of these three (the funnel) displays the band of residuals widening to the right showing non-constant variance. The second is a downward trend and the third is a curve. For the funnel type of plot, it indicates a lack of constant variance of the residuals. The corrective measure in this case is a transformation of the Y variable. A plot of the residuals such as Fig. 8.2(2) indicates the absence of an independent variable in the model under examination. If however, a plot such as Fig. 8.2(3) is obtained, a linear or quadratic term would have to be added.

Because the residuals and the Y_o values are usually correlated but the residuals and the Y_c are not. Therefore, $e_i = (Y_o - Y_c)_i$, i=1, 2, …, n is usually plotted against $(Y_c)_i$. A slope in the e_i and $(Y_c)_i$ indicates that something is wrong. It is possible to evaluate test statistics on residuals, but it is often difficult to know if they are sufficiently deviant to require action. In practical regression situations, a detailed examination of the corresponding residuals plots is usually far more informative, and the plot

will almost certainly reveal any violations of assumption serious enough to require corrective action [1].

The residuals due to the S-DPF model (Eq. 6.9) were calculated for each data points from Craighouse data. It is defined that,

S = Predicted internal illuminance – measured internal illuminance, lux;

Y_{cl}= Predicted internal illuminance, lux;

X_1= Solar altitude, degree;

X_2= sky clearness index, ratio;

Absolute error = S = Predicted internal illuminance – measured internal illuminance, lux

The residuals plot of S versus Y_{cl} is shown in Fig. 8.3. It can be seen in Fig. 8.3 that the residual plot shows pattern of a horizontal band. This indicates that generally speaking, the S-DPF model being examined is adequate. Figure 8.4 shows the histogram of the absolute error (residual) due to the S-DPF model. It is shown in Fig. 8.4 that the distribution of absolute error is a normal distribution with a mean value of –2.3 lux. The standard deviation of the absolute error was found to be σ=28.31 lux. This implies that the S-DPF model can predict the daylighting performance of straight light pipes with a quite high accuracy, namely more than 99 per cent of all predictions given by the model are found within the error range of ±50lux. The mean value of measured internal illuminance was found to be 177lux, the percentage of prediction due to S-DPF model that fall in the error range of ±17.7lux (10 per cent of mean value 177lux) was then found to be 75%. Considering that the sensitivity of human eyes to illuminance at the level of 50lux is in a low order, it is therefore concluded that the prediction given by the S-DPF can be used with high confidence in practical light pipe design.

The residual plots of S versus X_1 and X_2 are shown in Figs. 8.5 and 8.6 respectively. Figure 8.5 shows that the residual due to S-DPF model is generally constant, independent to the change of solar altitude. Figure 8.6 shows a similar trend and presents a profile of horizontal band, which confirms that the S-DPF model is adequate. For solar energy applications, especially for light pipe daylighting project, sun's position and sky conditions are the most significant variables to be considered. Figures 8.5 and

8.6 confirm that the S-DPF model has adequately described the effect of above two factors to the daylighting performance of light pipes. It is also worthy here to point out that since S-DPF model uses only non-site specific factors, it is therefore expected to be applicable for global sites.

8.2 VALIDATION OF S-DPF MODEL USING MERCHISTON TEST ROOM DATA

As addressed in Section 5.5 that a total of 22 270 Merchiston test room data points for straight light pipes of seven configurations under all weather conditions had been made available for S-DPF model validation. Merchiston test room data were further divided into three groups to reveal the performance of the S-DPF model under different sky conditions. The whole data set were divided into three groups according to sky clearness index, namely measurements taken under non-heavy-overcast sky conditions (k_t>0.2), under heavy overcast sky conditions ($k_t \leq 0.2$) and under all-sky condition. The performance assessment of S-DPF model under above different sky conditions were conducted and reported in the following three sub-sections.

8.2.1 Case-by-case assessment of the S-DPF model under non-heavy-overcast sky conditions (k_t>0.2)

The S-DPF model was applied to seven cases of straight light pipe configurations to examine its performance. The seven cases are:

Case 1: light pipe in 0.21m diameter and 0.6m long,

Case 2: light pipe in 0.21m diameter and 1.2m long,

Case 3: light pipe in 0.33m diameter and 0.6m long,

Case 4: light pipe in 0.33m diameter and 1.2m long,

Case 5: light pipe in 0.45m diameter and 0.6m long,

Case 6: light pipe in 0.45m diameter and 1.2m long, and

Case 7:light pipe in 0.53m diameter and 0.6m long.

Internal illuminance predictions due to S-DPF model for each of above seven cases were calculated respectively. Scatter plot of calculated internal iluminances against measured illuminances were then obtained to assess the performance of S-DPF model based on independent data. The scatter plots were

generated within Excel environment, and after that the best-fit trend lines were generated by the Excel to examine the accuracy of the model. By linear regression, equations and slopes of the best-fit lines were obtained and corresponding coefficient of determination R-Square values were reported. Results are presented below.

Case 1: Figure 8.7 shows the scatter plot of predicted internal illuminance against measured internal illuminance for a light pipe 0.21m in diameter and 0.6m in length. The vertical distance between light pipe diffuser and the working plan was 1.68m. The distances between three testing points and the light pipe diffuser centre ranged between 1.68 and 2 meters. The sky clearness index varied between 0.2 and 0.8. The slope of the best-fit trend line was found to be 0.96 and the R-Square value was noted as 0.87. The mean error was found to be 0lux and the RMSE was noted as 10 lux. In this case it can be seen that the prediction of S-DPF is quite good. A RMSE value of 10 lux means that at least about two thirds of predicted data given by S-DPF is within an error band that is negligible (±10lux).

Case 2: Figure 8.8 shows the scatter plot of predicted internal illuminance against measured internal illuminance for a light pipe 0.21m in diameter and 1.2m in length. The vertical distance between light pipe diffuser and the working plan is 1.12m. The distances between three testing points and the light pipe diffuser centre ranged between 1.28 and 2.10 meters. The sky clearness index varied between 0.2 and 0.8. The slope of the best-fit trend line was found to be 0.96 and the R-Square value was noted as 0.96. The mean error was found to be -4lux and the RMSE was noted as 9 lux. In this case it can be seen that the prediction of S-DPF is also good. A RMSE value of 9 lux means that at least about two thirds of predicted data given by S-DPF is within an error band that is negligible (±18lux). The R-Square value is as high as 0.96 which means that 96% of data is described by the S-DPF model. It is found however, that for this case, the S-DPF model seems to slightly underestimate the internal illuminance, with a mean error of –4 lux. This might be due to the fact that when the light pipe was longer, to test the internal illuminance at distances about 1 and 2 meters, sensors were put further near to the corner of the test room where internal reflection played a more significant role and led to a higher reading of measured illuminance.

Case 3: Figure 8.9 shows the scatter plot of predicted internal illuminance against measured internal illuminance for a light pipe 0.33m in diameter and 0.6m in length. The vertical distance between light pipe diffuser and the working plan was 1.68m. The distances between three testing points and the light pipe diffuser centre ranged between 1.74 and 2.14 meters. The slope of the best-fit trend line was found to be 1.0 and the R-Square value was noted as 0.88. The MBE was found to be -6lux and the RMSE was noted as 55 lux. In this case, according to the figure of R-Square, MBE and RMSE, which are both larger than those of previous cases, the performance seems less satisfactory. However, it is noted that for this case, the averaged measured internal illuminance was found to be 200lux, while the figures for Cases 1 and 2 are 44lux and 51lux respectively. The percentage of RMSE to mean measured illuminance for Cases 1, 2 and 3 were found 23%, 18% and 27% respectively. Therefore, the values of RMSEs of cases 1, 2 and 3 are basically comparable and in the same order. It is also noted that the averaged external illuminance for the third case was found to be 46835lux, which is 35% higher than Case 1 and 32% higher than Case 2. The maximum external illuminance recorded during the measurement for the third case was found to be as high as 110klux, and correspondingly the sky clearness index monitored during the day ranged from 0.2 to 0.8. The reason why the third case produces a larger RMSE may therefore be due to the quite dramatic variance of external conditions.

Case 4: Figure 8.10 shows the scatter plot of predicted internal illuminance against measured internal illuminance for a light pipe 0.33m in diameter and 1.2m in length. The vertical distance between light pipe diffuser and the working plan was 0.9 m. The distances between three testing points and the light pipe diffuser centre ranged between 1.32 and 1.71 meters. The slope of the best-fit trend line was found to be 1.04 and the R-Square value was noted as 0.82. The mean error was found to be 1lux and the RMSE was noted as 55 lux. It is also noted that the averaged external illuminance for the third case was found to be 47219lux, which is 36% higher than Case 1 and 33% higher than Case 2. The maximum external illuminance recorded during the measurement for the third case was found to be as high as 115klux, and correspondingly the sky clearness index monitored during the day ranged from 0.2 to 0.8. The maximum and minimum internal illuminances were found to be 600lux and 20lux respectively.

Case 5: Figure 8.11 shows the scatter plot of predicted internal illuminance against measured internal illuminance for a light pipe 0.45m in diameter and 0.6m in length. The vertical distance between light

pipe diffuser and the working plan was 1.74m. The distances between three testing points and the light pipe diffuser centre ranged between 1.74 and 2.06 meters. The slope of the best-fit trend line was found to be 0.93 and the R-Square value was noted as 0.74. The mean error was found to be -25lux, which was 10% of averaged measured internal illuminance. Corresponding figures for RMSE was noted as 65lux and 26% respectively. In this case it seems that the S-DPF model underestimates the internal illuminance.

Case 6: Figure 8.12 shows the scatter plot of predicted internal illuminance against measured internal illuminance for a light pipe 0.45m in diameter and 1.2m in length. The vertical distance between light pipe diffuser and the working plan was 1.18m. The distances between three testing points and the light pipe diffuser centre ranged between 1.30 and 1.62 meters. The slope of the best-fit trend line was found to be 1.00 and the R-Square value was noted as 0.86. The MBE was found to be -17lux and the RMSE was noted as 75 lux. The MBE was found to be 6% of the averaged internal illuminance of 289lux, and RMSE was 26% of the averaged internal illuminance.

Case 7: Figure 8.13 shows the scatter plot of predicted internal illuminance against measured internal illuminance for a light pipe 0.53m in diameter and 0.6m in length. The vertical distance between light pipe diffuser and the working plan was 1.18m. The distances between three testing points and the light pipe diffuser centre ranged between 1.30 and 1.62 meters. The slope of the best-fit trend line was found to be 0.95 and the R-Square value was noted as 0.82. The MBE was found to be -33lux and the RMSE was noted as 106 lux. The MBE was found to be 8% of the averaged internal illuminance of 403lux, and RMSE was 26% of the averaged internal illuminance.

8.2.2 Performance assessment of the S-DPF model under heavy-overcast sky conditions ($k_t \leq 0.2$)

A total of 7,200 data points of seven light pipe configuration cases were measured under heave-overcast sky conditions ($k_t \leq 0.2$). S-DPF model was applied to predict the internal illuminance values due to the light pipes. Scatter plots of the measured internal illuminance versus values predicted by S-DPF model for all heavy-overcast sky condition data and for each of the seven cases are shown in Figs. 8.14 – 8.21. Statistics results are shown in Table 8.1.

Figure 8.14 shows that the slope of the best-fit trend line for all heavy-overcast sky condition scatter plot was found to be 1.12 and the R-square value was 0.94. The RMSE and MBE were found to be 31lux and 9lux respectively. The mean value of measured internal illuminance was 106lux with a maximum value of 519lux and a minimum value of 10lux. The PAD (averaged percentage deviation) was noted as 20%.

Figure 8.14 shows that under heave-overcast sky conditions, generally speaking the S-DPF model tends to overestimate the internal illuminance due to light pipes. This can be due to two main reasons.

First, the measurements undertaken in Merchiston test room was one year later than that carried out in Craighouse test room. The very same light pipes (Monodraught) were tested in the two measurements. During the two years' time, light pipes have been transported from sites to sites, and during the tests they were also installed and removed quite frequently according to the test schedules. It is therefore logical to assume that certain aging effect may have taken place during the course, which can lead to slight changes of the reflectance of internal surface of light pipe tube. Swift et al [3] pointed out that in the mathematical modelling of light pipe's transmittance of light, the reflectance of the internal surface of light pipe tube plays an important role. Swift found that "the theoretical calculations are sensitive to the choice of reflectivity, with changes in R (reflectivity, author) of 0.001 resulting in noticeable differences in the calculated curve". This therefore suggests that the method of applying the internal reflectivity value of 0.95 that was obtained based on Craighouse data, to Merchiston data may produce noticeable system bias.

The second possible reason that can contribute to the overestimate is that under low illuminance levels the measurements by Kipp and Zonon sensors are subject to more errors. It was found that under heavy overcast sky conditions, the mean value of measured internal illuminance was as low as 106lux. The ranges of the sensors are all 5±1klux. The sensitivities of the three Lux Lite sensors were given as 10.32 μV/lux (±1%), 9.68μV/lux (±1%) and 10.11μV/lux (±1%) respectively by the manufacturer (Section 5.2). Therefore under heavily overcast sky conditions, the measurement error due to the sensors can reach as high as ±50lux (equals to about 1% of the range), which accounts for almost 50% of the mean internal illuminance value.

However, it shall be pointed out that as an innovative device that utilizes sunlight, light pipe contributes most to the daylighting when the sky is clear and sunlight is available. Unfortunately, when the sky is heavy-overcast ($k_t \leq 0.2$), light pipes provide a lower level of daylight, though which is sufficient enough to form a good background internal illuminance. Nevertheless, artificial lighting is required under such a condition if any sophisticated work that requires detailed information on objects is to be carried out. Bearing this in mind, it can be seen that the performance of S-DPF model under heavy-overcast sky conditions is adequate enough for general lighting design purposes.

8.2.3 Performance assessment of the S-DPF model under all-sky conditions

To reveal the over all performance of S-DPF model, it is applied to the whole data set from Merchiston test room. Internal illuminance predictions due to S-DPF model for all seven cases presented above in Sections 8.2.1 and 8.2.2 were calculated. Scatter plot of calculated internal iluminances against measured illuminances was shown in Fig. 8.22. The slope of the best-fit trend line was found to be 1.03 and the R-Square value was noted as 0.90. The MBE was found to be -5lux, the RMSE 76 lux, and the PAD was found to be 22%. The maximum of the internal illuminance was found to be 1986lux and the minimum found 10lux. The high R-Square value of 0.90 suggests that the S-DPF model built using Craighouse data represents most of the independently measured data from Merchiston test room. The slope value of 1.03 suggests that the S-DPF model can estimate the mean values of internal illuminances due to light pipes quite precisely. It is however noticed that for Merchiston data set the RMSE was found to be 76 lux, which is higher than the RMSE value of 27 due to Craighouse data. This can be mainly own to following three reasons.

First, the external environment for the two tests in Craighouse and Merchiston test rooms were not absolutely the same. The Merchiston test room was build on the roof of a 7- storey building with an almost complete view to the sky (more than 95% of the hemisphere). However, the view angle of the test room in Craighouse to the sky was not the whole vault. Trees and buildings within a distance of 20 meters blocked about 20% of the sky although the southern hemisphere was clear. Therefore, the coefficients developed for one site may not be the best-fit value for the other. This can be the main reason for the higher value of RMSE due to Merchiston data set.

The second main reason that may contribute to the up-rise of RMSE may be due to the different geometry of the two test rooms. To enable an almost complete view of the sky hemisphere, Merchiston test room was built upon the roof of a 7- storey building within Merchiston campus. However, on the other hand it was afterwards found that the wind speed on the top of the building was so strong that the size of the test room had to be minimized so as to meet the safety requirements. The dimension of the Merchiston test room was therefore chosen as $2 \times 2 \times 2$ m^3, which was less than half of the size of the Craighouse test room ($3.0 \times 2.4 \times 2.5$ m^3). Therefore, although the internal surfaces of the two huts have the some colour (colour of wood), the smaller Merchiston test room caused more significant internal reflection than that occurred within the Craighouse test room. The application of the S-DPF model developed based on Craighouse data to the Merchiston data was thus inevitably subject to more chance of prediction error.

The third possible factor that may contribute to the higher RMSE value of 67lux is the asymmetrical distribution of internal daylight due to light pipes. The S-DPF model assumes that the internal illuminance distribution on a working plan below the light pipe diffuser is symmetrical to the diffuser centre and is a function of the vertical and total distances of one point to the diffuser centre. From 30th October 2000 to 14th January 2001, a purposed measurement was undertaken in Craighouse test room to test this assumption (see Section 5.6).

Light pipes of four configurations were tested, which were light pipe 0.21m in diameter and 0.6m in length, 0.33m in diameter and 0.6m in length, 0.45m in diameter and 0.6m in length and 0.45m in diameter and 1.2m in length. Unfortunately it was found that the test for the 0.21m-diameter light pipe was faulty due to the leakage of rainwater into the pipe. The rest of the tests produced good data and a sum of about 900 data points were obtained. Results are shown in Tables 8.2 and 8.3. Table 8.2 shows one day's data measured for the 0.33m-diameter light pipe on 18th Dec 2000. It can be seen that the standard deviations of the five measurements (one Magetron sensor was found faulty) taken at different positions surrounding the centre point of diffuser are averaged at a value of 86lux. For the 0.33m-diameter light pipe, the averaged ratio of the standard deviations to the averaged illuminance underneath light pipe diffuser was found to be 14%. The corresponding figures for the 0.45m-diameter light pipes 0.6m and 1.2m in length were found to be 12% and 13% respectively (Table 8.3). Therefore

the asymmetrical distribution of internal illuminance although not very significant, has a substantial effect on the daylighting performance of light pipe. It is worthy however to point out that in real applications, especially for large rooms, usually a group of light pipes need to be installed to provide an even distribution of daylight within the space. For occasions where multi-light pipes are installed symmetrically to the room layout, the effect of asymmetrical distribution of internal illuminances can be reduced, and the predictions given by S-DPF model tends to be more accurate.

8.3 COMPARISON OF DPF MODELS AGAINST RESULTS DUE TO INDEPENDENT RESEARCHES

In this section the performance of DPF models are evaluated by comparing it against other independent research results.

The first comparison is made with the study carried out by Loncour et al [4] on behalf of Monodraught Ltd. Figures. 8.23 and 8.24 present their findings that state that:

(a) the actual, measured light transmission within straight run of pipe was 48% as compared to 93% that was claimed by the manufacturer;

(b) the diffuser had a loss of 44% of the incident energy; and

(c) the straight-length energy loss was found to be 29% with an extra 5% loss for pipe-junction. Thus for each metre pipe-length with a pipe-junction the loss would be 29 + 5 = 34%. This figure does not include the effect of loss due to diffuser.

To compare the DPF models against the findings by Loncour et al [4], the drop of the daylight penetration factor on one point in room due to the light pipe (with a 2-meter distance from the point to the diffuser centre), as a function of the length of light pipe tube (not including dome and diffuser) has been calculated. It is found that the per meter DPF drop depends on the solar altitude, sky clearness index and the aspect ratio of light pipe tube. The average values of per meter DPF drop for 0.33m, 0.45m and 0.53m diameter light pipes are 0.42, 0.34 and 0.29 respectively.

Thus the figures given by DPF model for 0.33-m pipe diameter are comparable to the results given by Loncour et al [4]. Note that the per cent drop of 42% includes the effect of energy loss through the diffuser and hence shows slightly higher figure than 34% for a comparable aspect ratio of 3.6 (pipe diameter 0.33m).

Most scientific literature is based on a more objective approach for reporting energy loss in light pipes and that is to divorce from a per metre loss and instead report in terms of loss (or transmission) as a function of aspect ratio (light pipe length to diameter ratio). Such a plot is shown in Fig. 8.25, produced by a Liverpool based researcher, Carter [5]. Note that Carter's loss factor of 60% for an aspect ratio of 3.6 is higher than Napier's result of 42% (average figure). Note that Carter's data are within close proximity to the study undertaken by Love et al (1995) in Canada. Carter has taken a figure of ±10% difference between datasets as being acceptable. A point of further note in Fig. 8.25 is that there can be variations (scatter) in the illuminance readings – internal as well as external. Figure 8.26 shows that Carter's estimate of energy loss in a 30-degree bend is 20% [5]. This is very close to Napier-based measurements that were found to give this value as 21%. David Jenkins [6] undertook further comparative work between Napier and Liverpool studies and two such plots are shown in Fig. 8.27. Once again this plot enables validation of the DPF models.

Figure 8.28 shows the light transmission plot of a light pipe. The point that is worthy of note here is that daylight is a very variable resource. Even at a one-minute frequency there is a significant change. This must be borne in mind whenever measurements related to light pipe performance are undertaken. For short pipes DPF produces similar results to those found by Shao [7] and Oakley et al [8]. Note that Oakley quotes DPF values of 0.48%, 0.38% and 0.18% respectively for aspect ratios of 2.1, 4.6 and 8.4.

The Napier DPF has NOT been evaluated for long pipes. Early indications based on abbreviated analysis suggest that a higher loss of energy takes place within the entrance length of the light pipe (see the shape of the asymptotic curve produced by Carter, Fig. 8.25). This is analogous to a well-known phenomenon within fluid flow in pipes. Figures 8.29 and 8.30 demonstrate this concept, i.e. two sources of energy loss are shown – entrance to the pipe and developing flow within the starting length.

At this stage it is difficult to explain this phenomenon for light flow but further research in this respect to compare the performance of longer light pipes against that of shorter pipes could lead to new discovery.

8.4 THE DESIGN TOOLS

The proposed model S-DPF (Eq. 6.9) enables the prediction of the internal illuminances that are achievable by opal diffuser light pipes of various configurations and under different sky conditions. As a set of guidelines for practical engineering design, Tables 8.4 – 8.9 provide the internal illuminances at various distances that can be achieved by opal diffuser light pipes of varying geometrical configurations operating under a set of three weather conditions for Kew, London [9]. The tables also cover a set of three seasonal variations: summer, winter, and autumn and spring together.

Based on E-DPF (Eq. 6.11), it has been found that light pipe's daylight transmission reduction factor due to the use of one 30-degree bend is around 0.2. This factor can be used as a simple guideline for elbowed light pipe design. It has also been noted that the efficiency loss due to the introduction of bends is a function of solar altitude, which means that for different weather conditions and different times of the year, the actual transmission reduction factor differs. The more sophisticated mathematical model E-DPF (Eq. 6.11) should therefore be applied where more accurate design for elbowed light pipes is required.

To predict the achievable internal illuminance by straight light pipes with flat diffusers, a multiplicative factor f_D is used to obtain the internal illuminances values indicated in Tables 8.4 – 8.9. For elbowed light pipes with flat diffusers, combining the use of f_D with the factor f_{loss} =0.2 may be used as a simpler guideline. However, by applying the f_D to the results given by E-DPF model (Eq. 6.11) a more accurate performance assessment may be made.

Additionally, within the Excel Visual Basic Application environment, lux plot [Courtesy: David Jenkins, Monodraught] that can visually describe the internal illuminance distribution due to light pipes has been constructed based on DPF models. The lux plot can be used by building or lighting designers

in both of their initial and final stages of design of light pipes. Figure 8.31 shows an example of such lux plot.

8.5 LIMITATIONS OF THE DPF MODELS

Any model has its own limitations; DPF model is not an exception. It is therefore worthy here to address the envelop of the S-DPF and E-DPF models, so as to guide the application of the models in real designs.

S-DPF and E-DPF models were developed and validated using measurements on 17 different light pipes configurations and measurement settings. Since as the basis of the models the measurements have boundaries in various dimensions, it is believed that the DPF models have an envelope too. The envelope stipulates the condition under which a given model can perform with its accuracy coherent to the statistical evaluation of the model. The envelop of the DPF models is decided by the boundaries of measurement conditions. However, in developing the DPF models, empirical mathematical formulae and physical reasoning have been applied, which forms the basis on which DPF models can be expected to work well in a broader range of conditions.

Table 8.10 shows the measurement settings for all performance monitoring on the daylighting performance of light pipes with opal diffuser. Geometrically, there are mainly five dimensions of boundaries, which are the diameter, length, number of bends of light pipes, and the vertical and total distances (see Fig. 8.32) between a given point and the centre of a light pipe diffuser. On the other hand, the external weather condition produces other three boundaries including the solar altitude (α_s), sky clearness index (k_t) and the global illuminance (E_{vg}). According to Table 8.10 and the limitations of external weather conditions of α, k_t and E_{vg}, the envelop of the DPF models can be clarified, as shown in Table 8.11.

The boundary of DPF models is constrained by the facility availability of the project. However, the applicability of DPF modes is not only limited to the configurations and external conditions given in Table 8.11. When there is an attempt to apply the DPF models to a broader range that is beyond the boundary being given in Table 8.11, an estimated result that is of a right order is expectable and

achievable. But at the same time, it is also worthy here to clarify that the accuracy of the model, where it is applied to a condition that is out of the boundary, has not been well validated.

REFERENCES

1. Norman, R., Draper and Smith, H. (1998) *Applied Regression Analysis (Third Edition)*, Wiley-Interscience Publication, USA and Canada.

2. Muneer, T. (1997) *Solar radiation & daylight models for the energy efficient design of buildings*, Architectural Press, Oxford

3. Swift, P. D. and Smith, G. B. (1995) Cylindrical mirror light pipes, *Solar Energy Material and Solar Cells*, 36(2), 159-168

4. Loncour, X., Schouwenaars, S., L'heureux, D., Soenen, S., Voordecker, P., Wouters, P. (2000) *Performance of the Monodraught systems Windcatcher and Sunpipe*, BBRI - Belgian Building Research Institute

5. Carter, D. J. (2001) The Measured and Predicted Performance of Passive Solar Light Pipe Systems. *Lighting Research and Technology*, 34(1), 39-52

6. Muneer, T., Zhang, X. and Jenkins, D. (2002) Brief report on the performance of Napier's Daylight Penetration Factor (DPF) and its comparison against other published work, Report submitted to Training Company Program Meeting

7. Shao, L. (1988) Mirror lightpipes: Daylighting performance in real buildings *Lighting Research and Technology*, 30 (1), 37 - 44

8. Oakley, G., Riffat, S. B. and Shao, L. (1999) Daylight performance of lightpipes *Proceedings of the CIBSE National Conference*, Harrogate, London, Chartered Institution of Building Services Engineers, 159-174

9. Hunt, D. R. G. (1979) *Availability of daylight*, Building Research Establishment, Watford

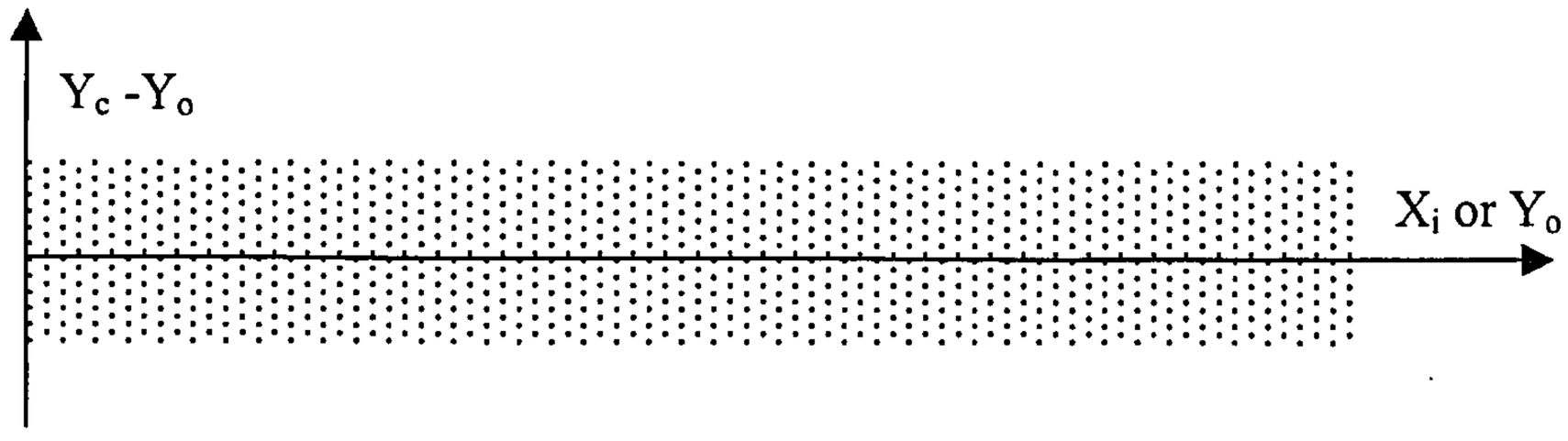

Figure 8.1 A satisfactory residuals plot

(1)

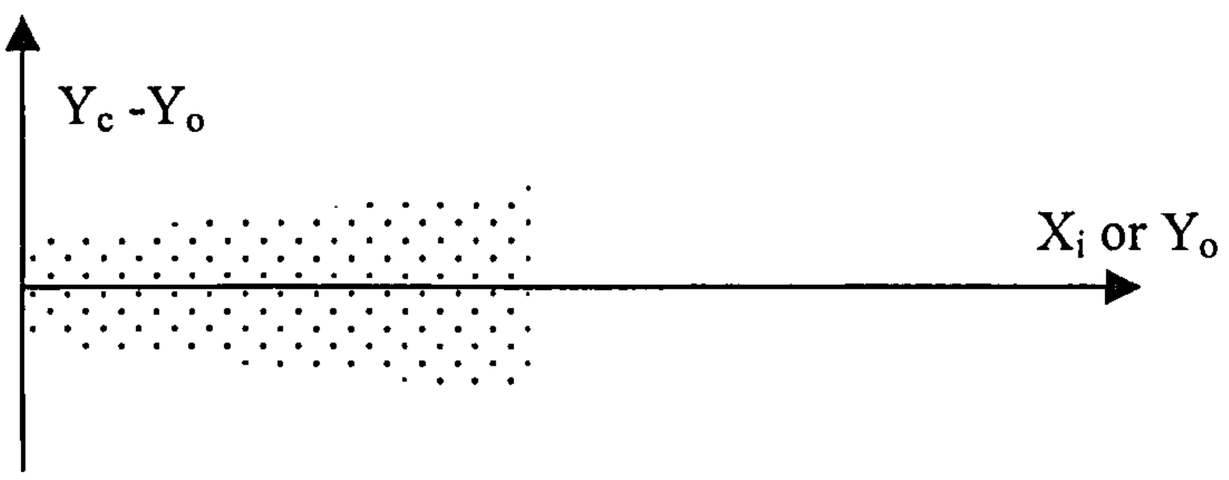

(2)

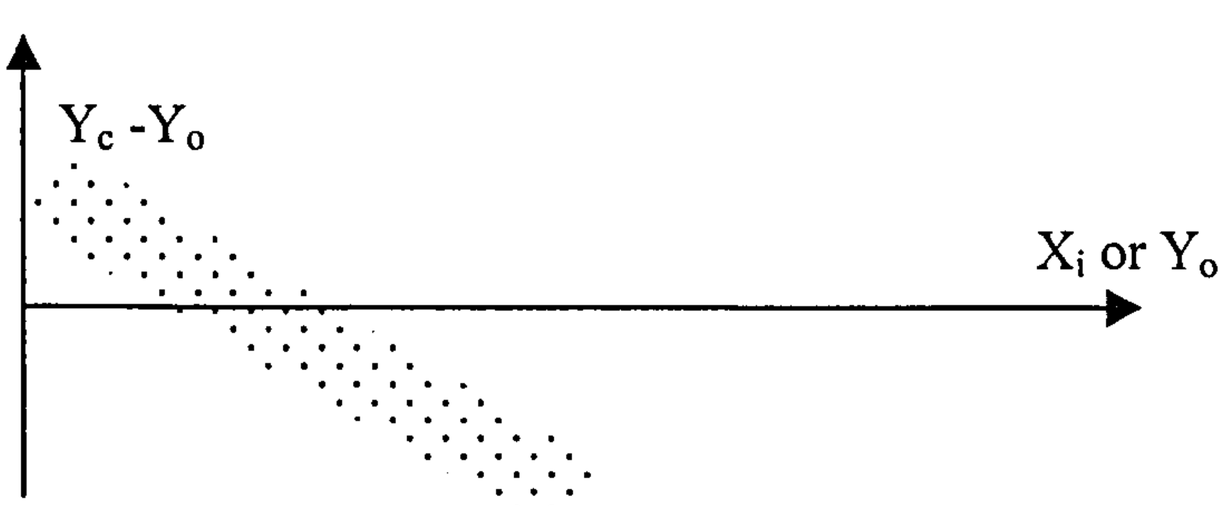

(3)

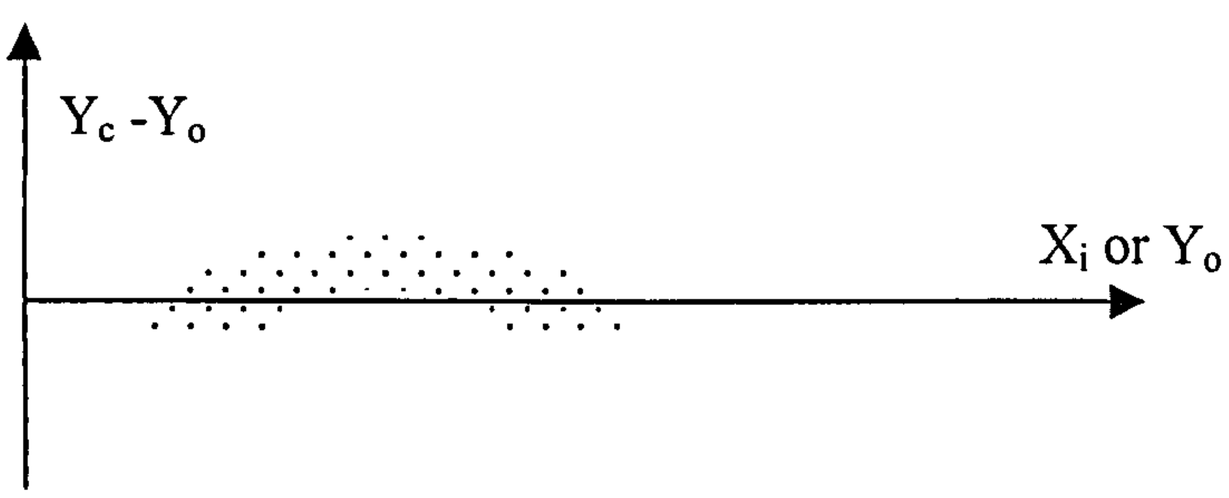

Figure 8.2 Examples of characteristics shown by unsatisfactory residuals behaviour

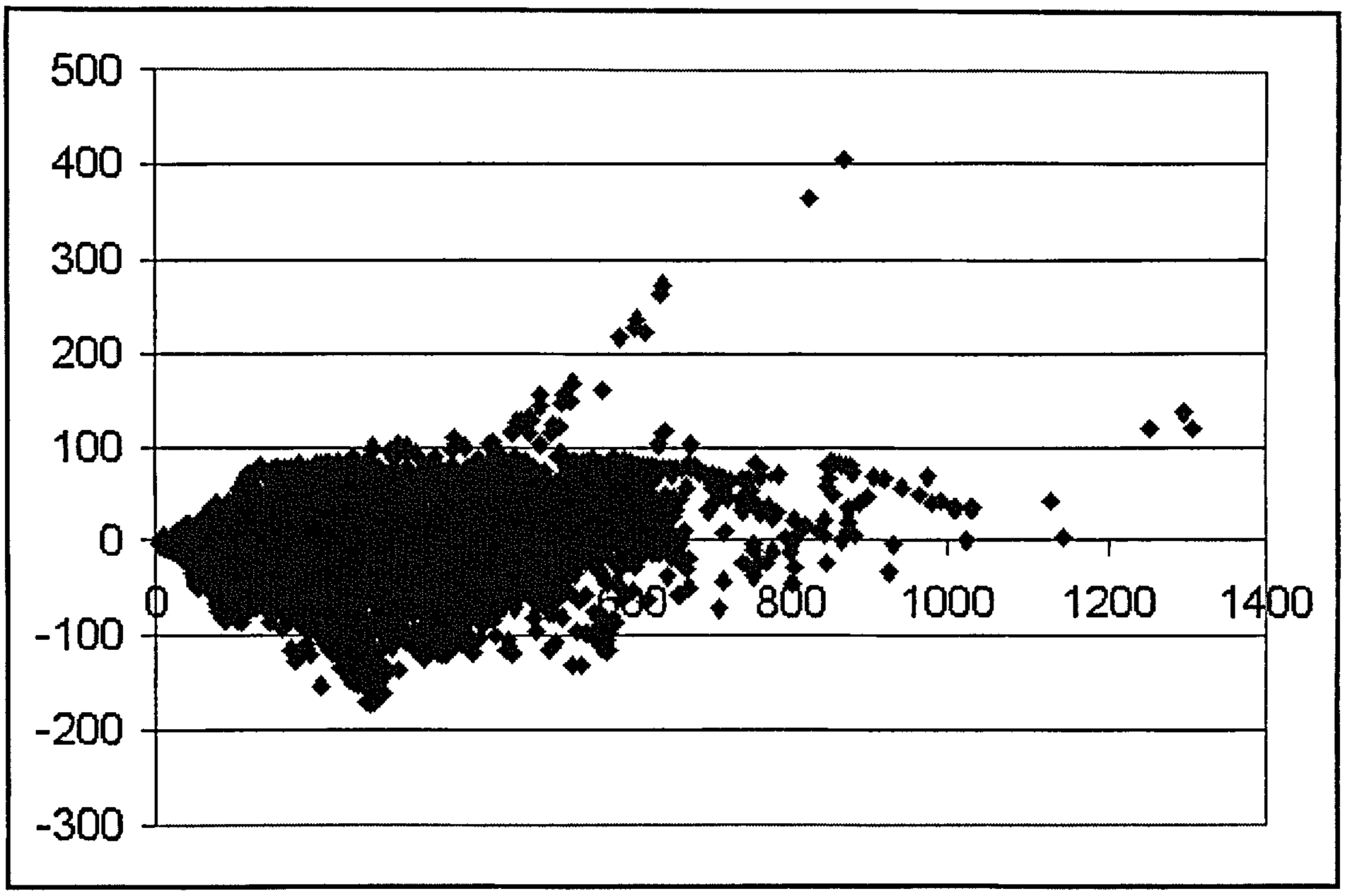

Figure 8.3 The residual plot of the difference between predicted and measured internal illuminances (Y-axis) versus predicted values (X-axis) for S-DPF model, Unit: lux

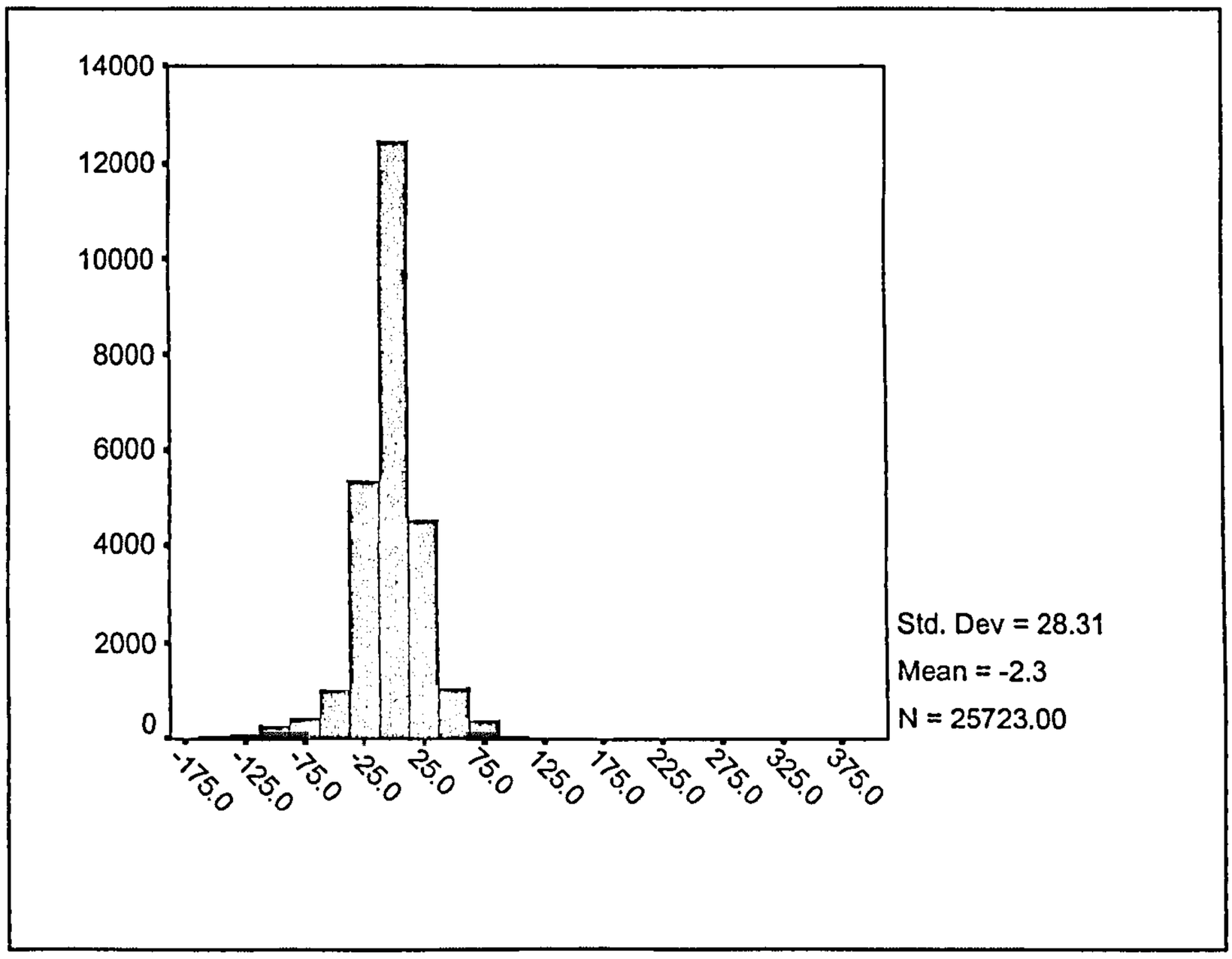

Figure 8.4 Histogram of absolute error due to S-DPF model, Unit for X-axis: lux, Y-axis: number of data points

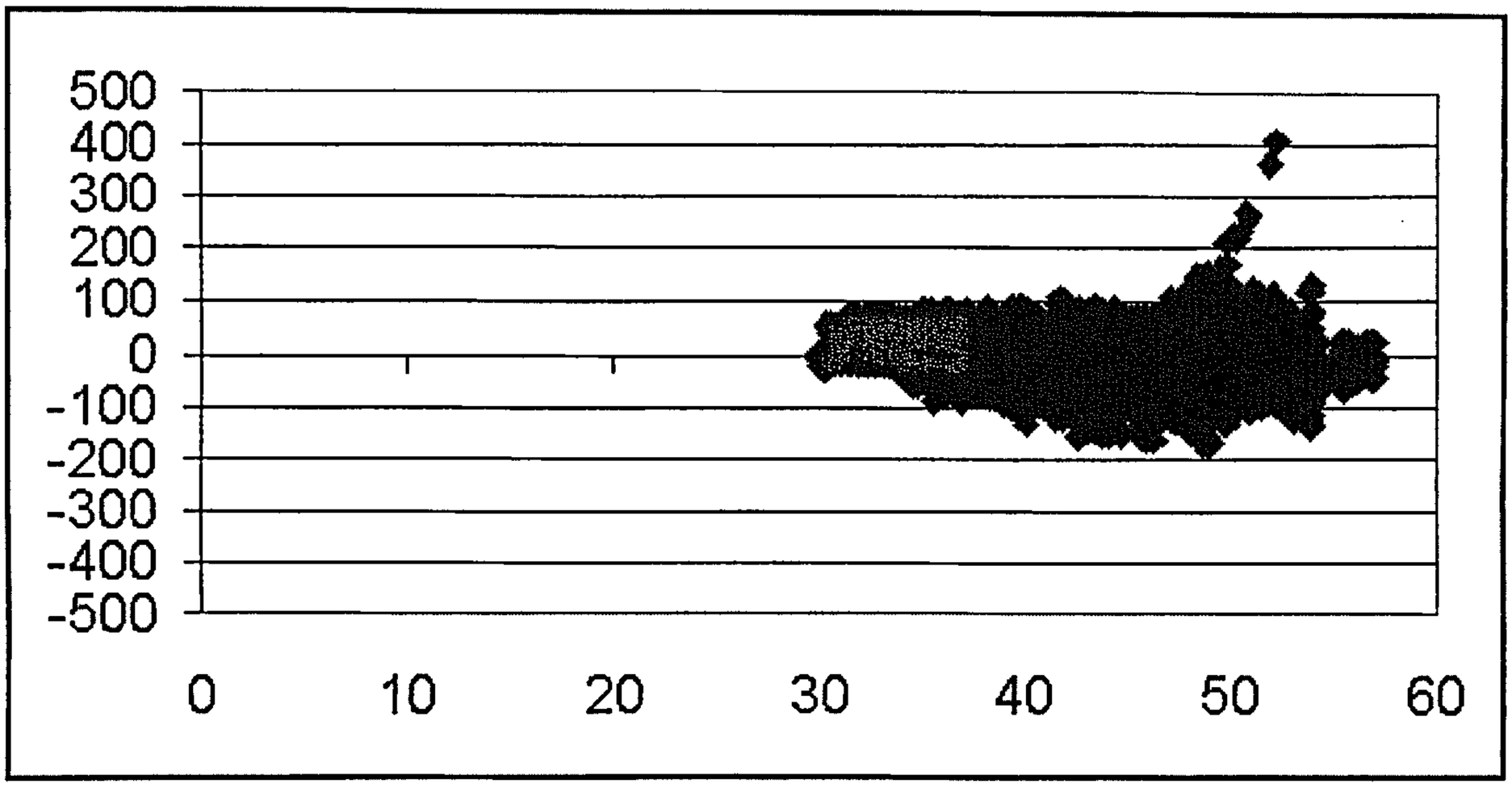

Figure 8.5 The residual plot of the difference between predicted and measured internal illuminances (Y-axis, Unit: lux) versus solar altitude (X-axis, Unit: degree) for S-DPF model

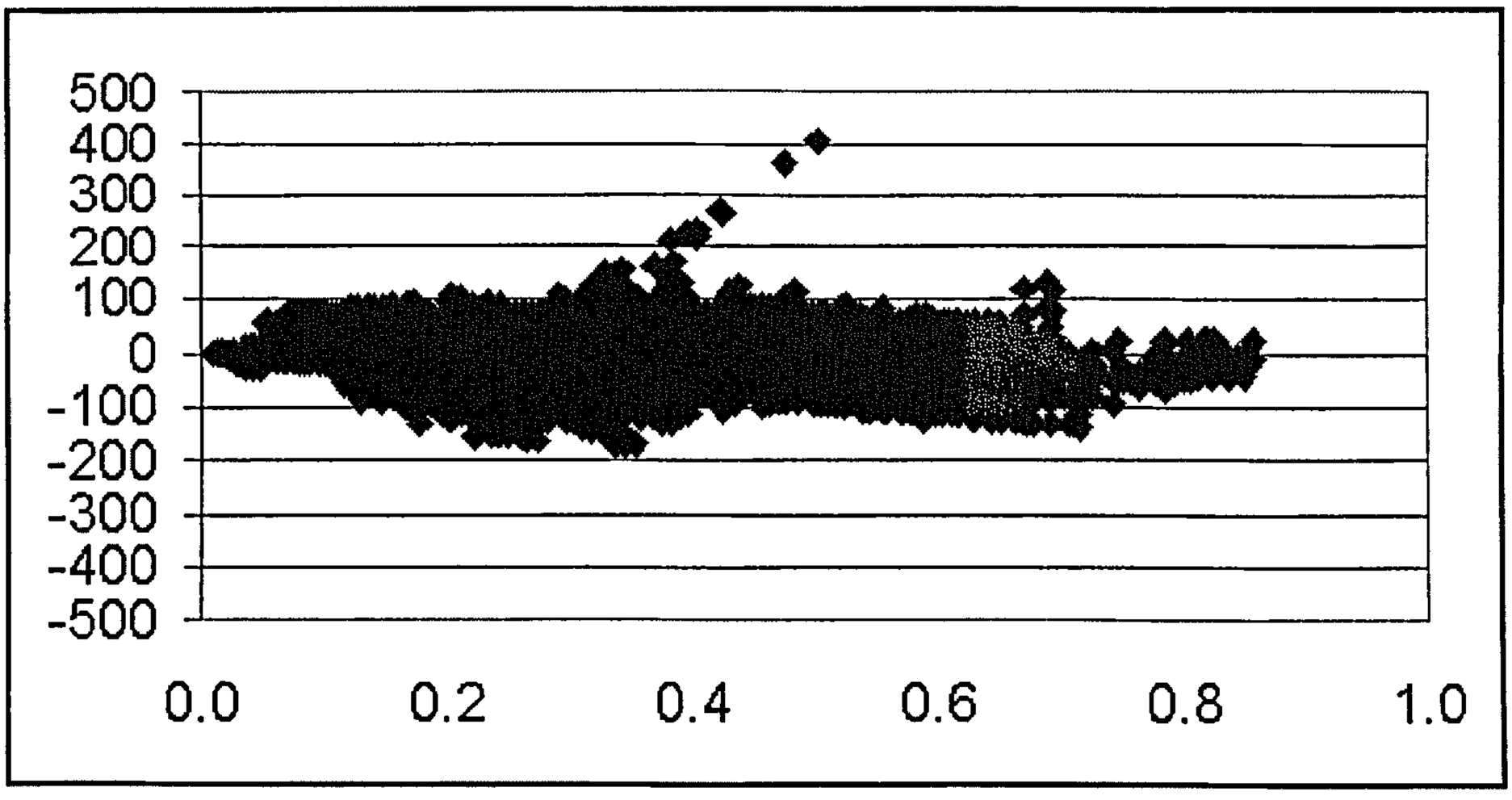

Figure 8.6 The residual plot of the difference between predicted and measured internal illuminances (Y-axis, Unit: lux) versus sky clearness index (X-axis) for S-DPF model

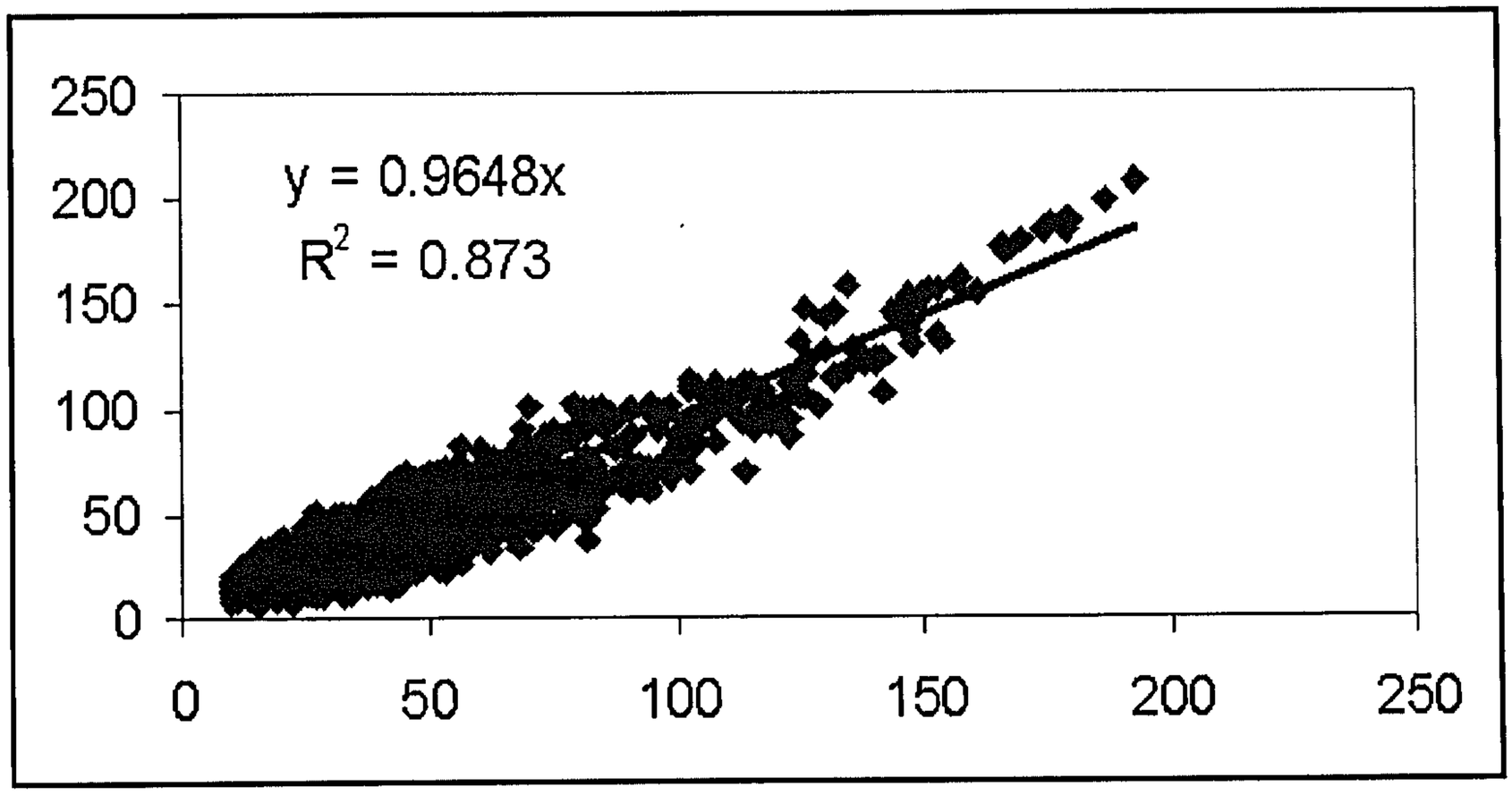

Figure 8.7 Scatter plot of predicted internal illuminance against measured internal illuminance (light pipe 0.21m in diameter and 0.61m in length), Unit: lux

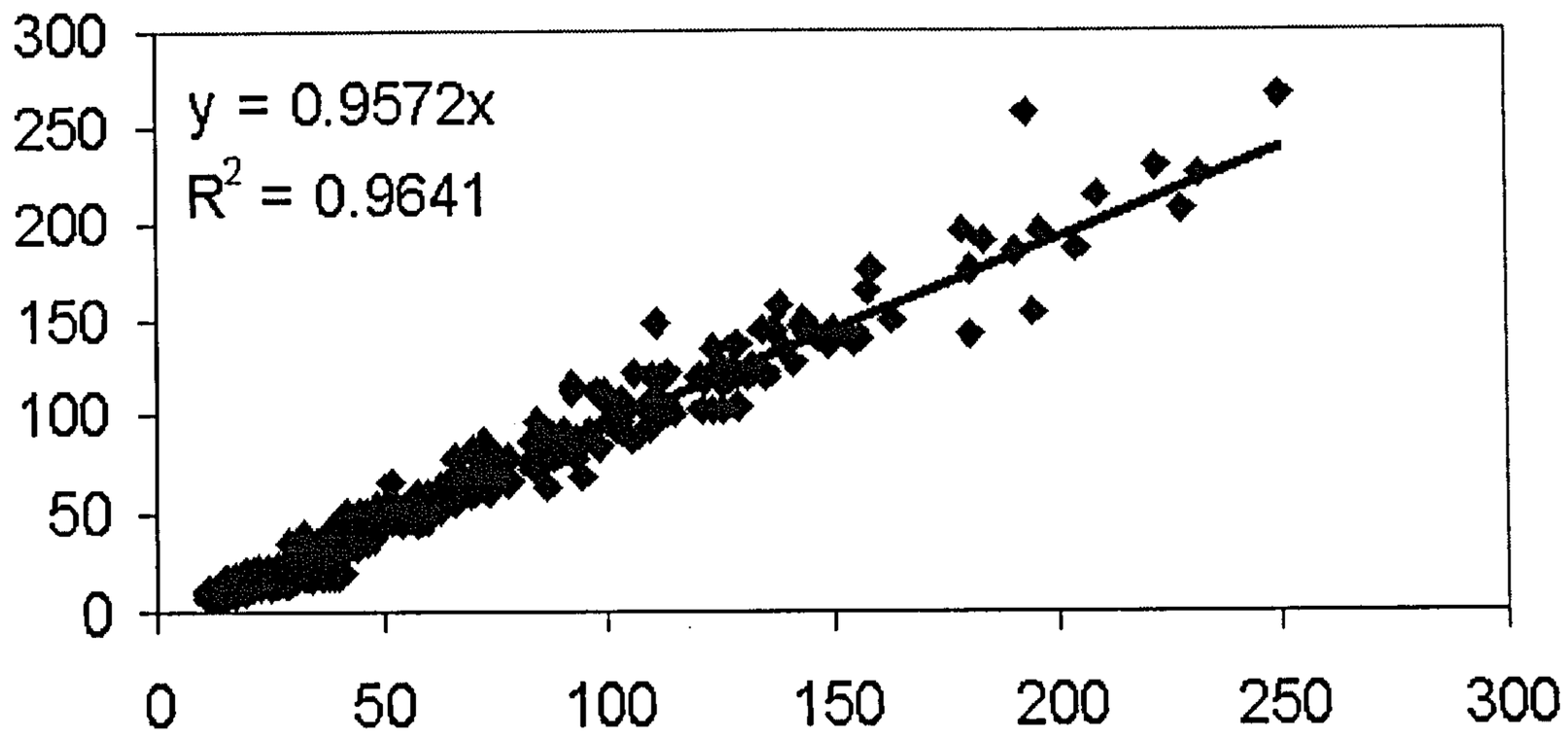

Figure 8.8 Scatter plot of predicted internal illuminance against measured internal illuminance (light pipe 0.21m in diameter and 1.22m in length), Unit: lux

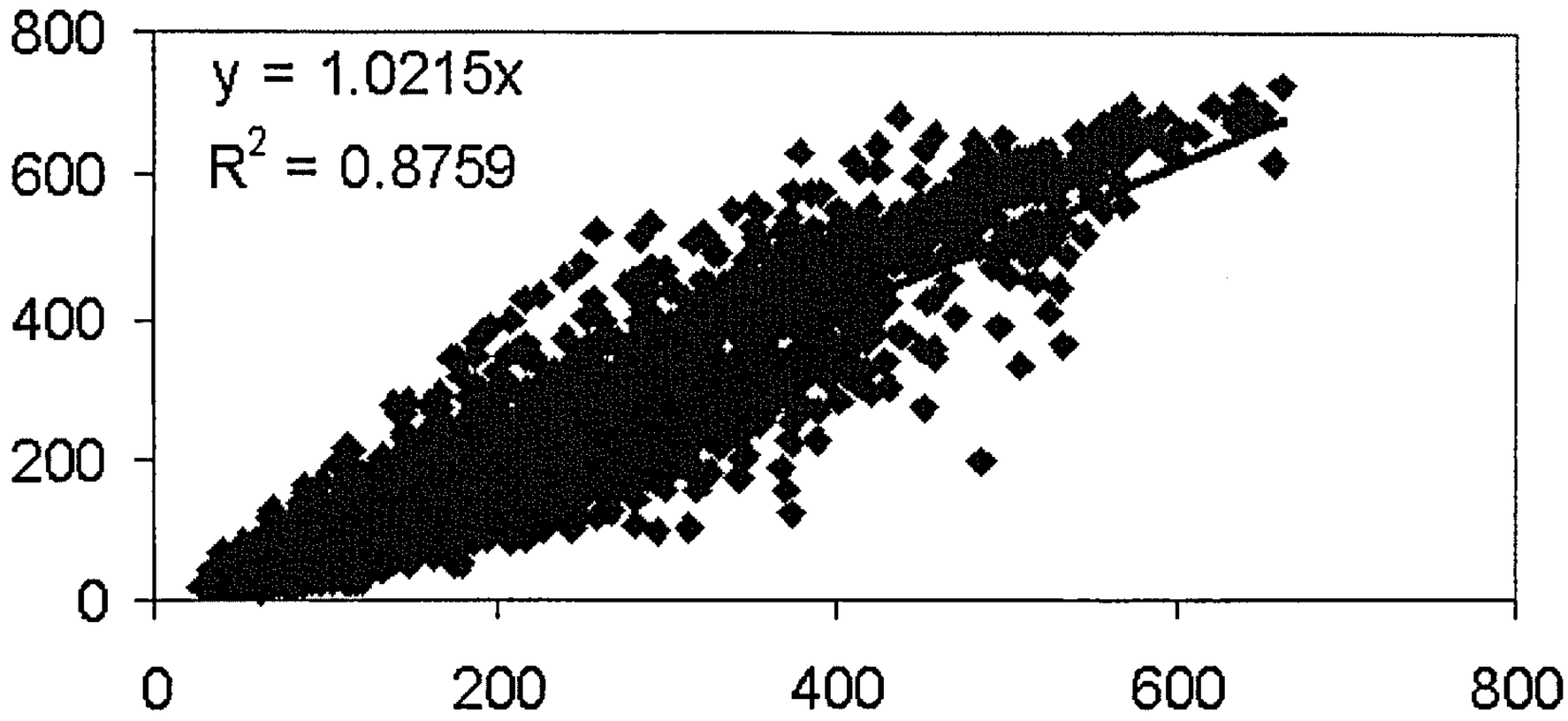

Figure 8.9 Scatter plot of predicted internal illuminance against measured internal illuminance (light pipe 0.33m in diameter and 0.61m in length), Unit: lux

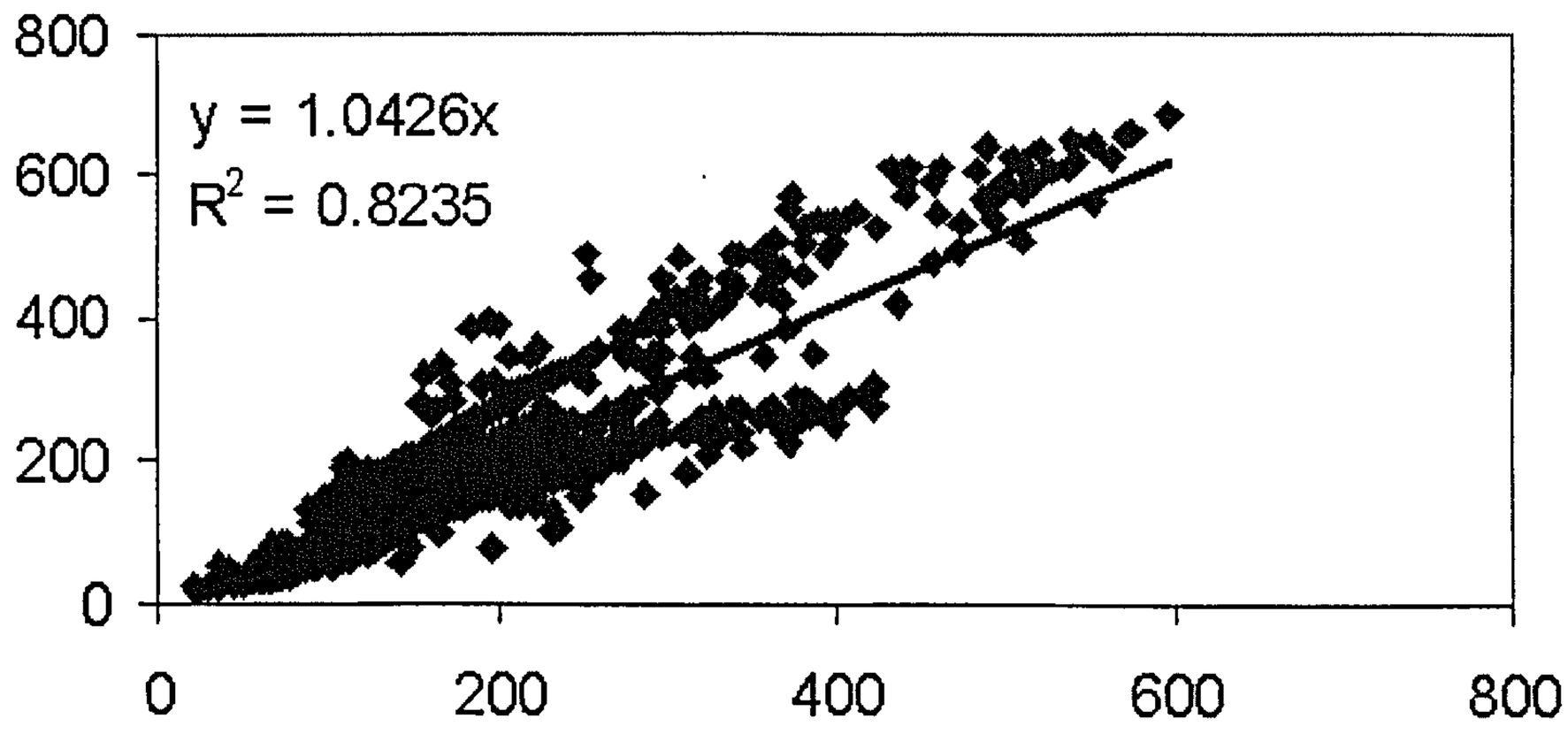

Figure 8.10 Scatter plot of predicted internal illuminance (Y-axis) against measured internal illuminance (X-axis), (light pipe 0.33m in diameter and 1.22m in length), Unit: lux

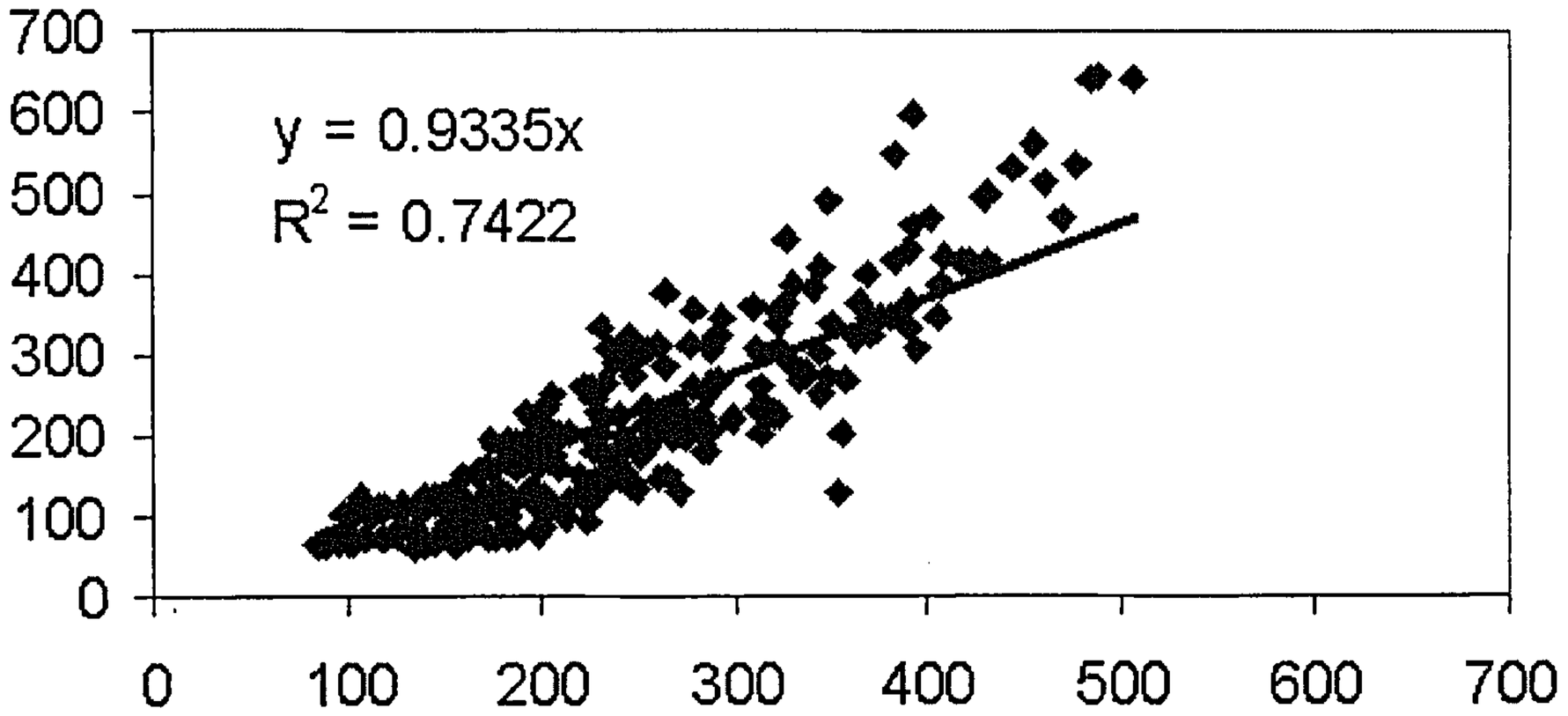

Figure 8.11 Scatter plot of predicted internal illuminance against measured internal illuminance (light pipe 0.45m in diameter and 0.61m in length), Unit: lux

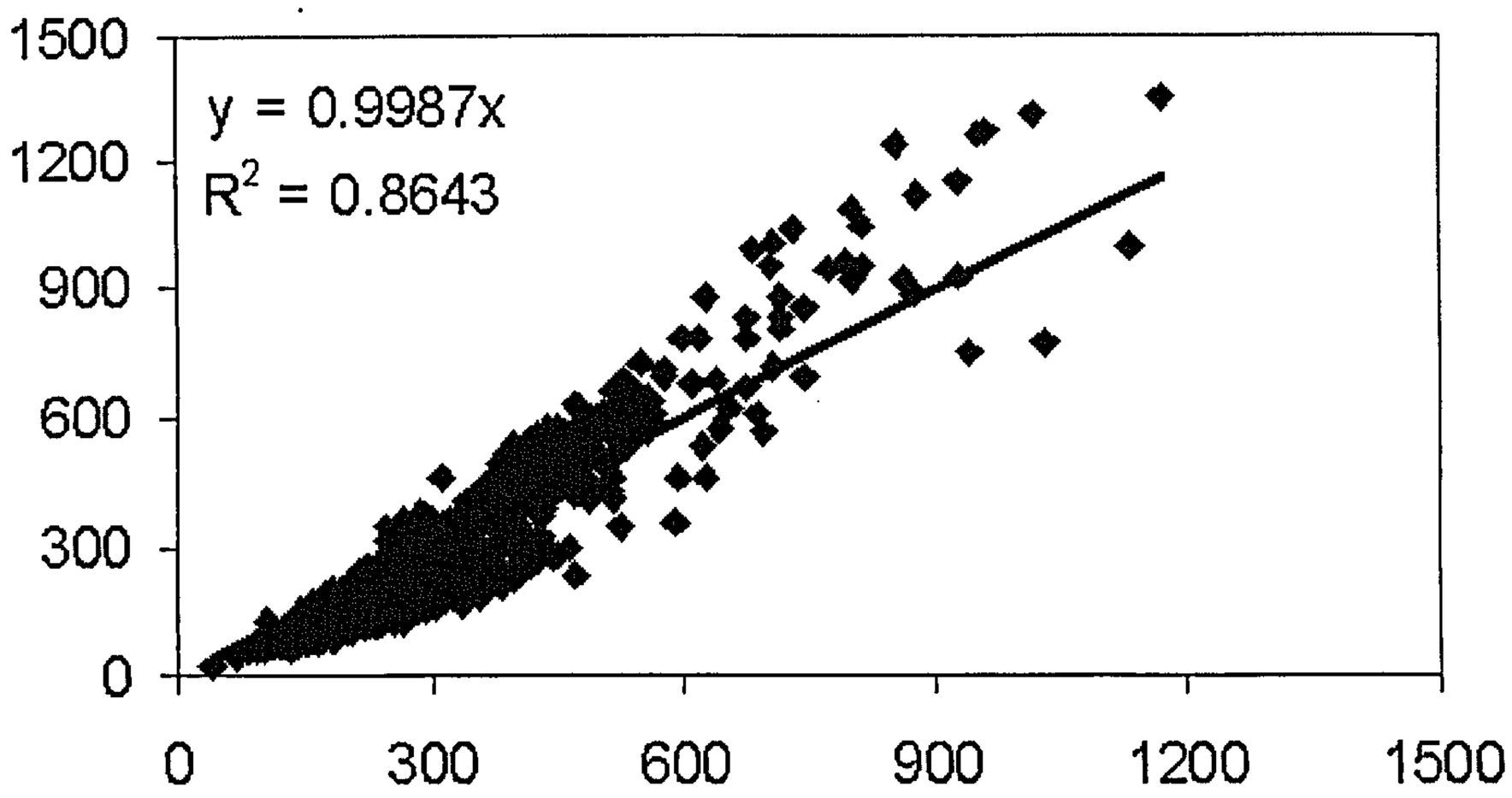

Figure 8.12 Scatter plot of predicted internal illuminance against measured internal illuminance (light pipe 0.45m in diameter and 1.22m in length), Unit: lux

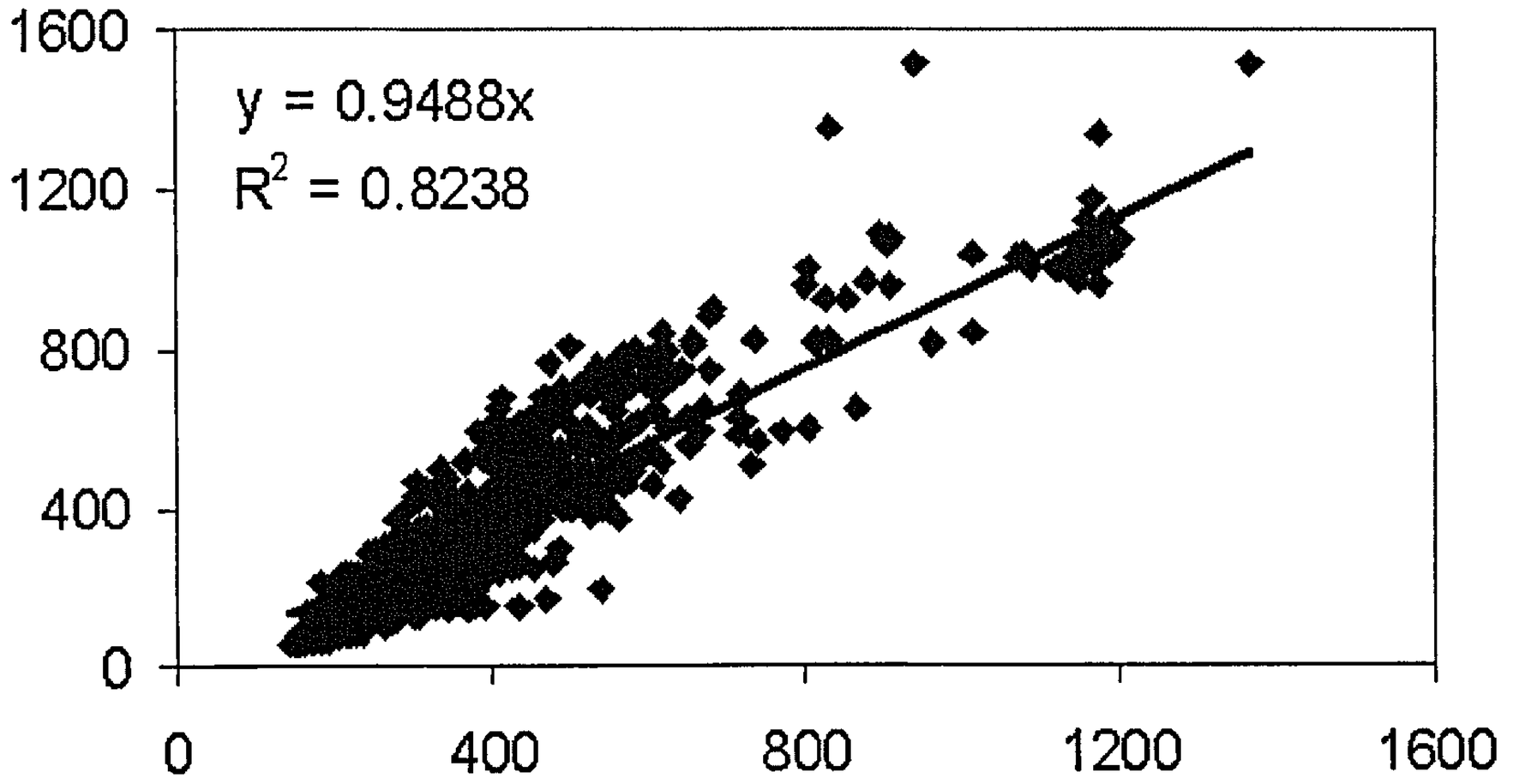

Figure 8.13 Scatter plot of predicted internal illuminance against measured internal illuminance (light pipe 0.53m in diameter and 0.61m in length), Unit: lux

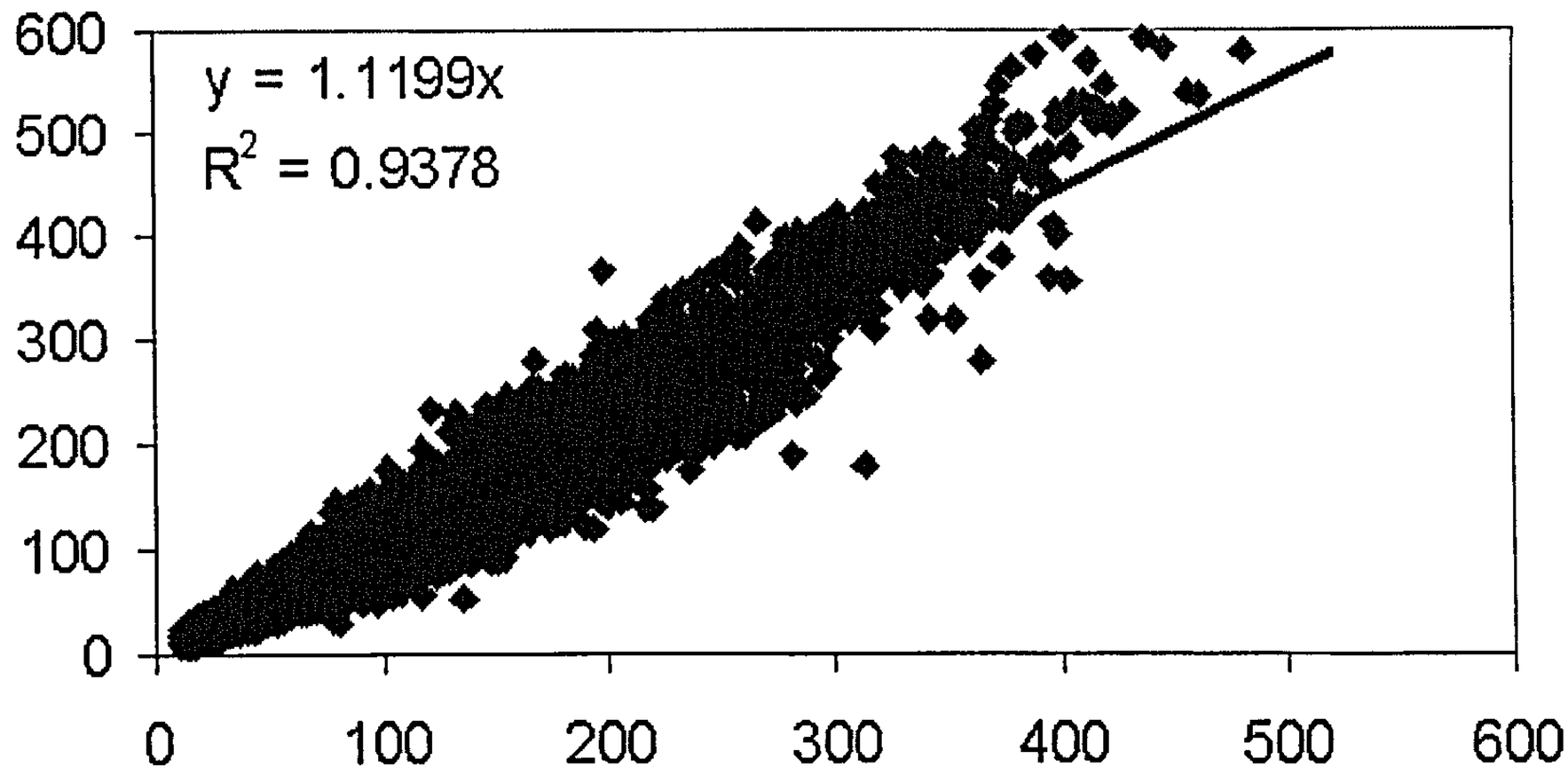

Figure 8.14 Validation: scatter plot of measured (X-axis) internal illuminance versus predicted values (Y-axis) due to S-DPF model (Merchiston data, heavy-overcast sky), Unit: lux

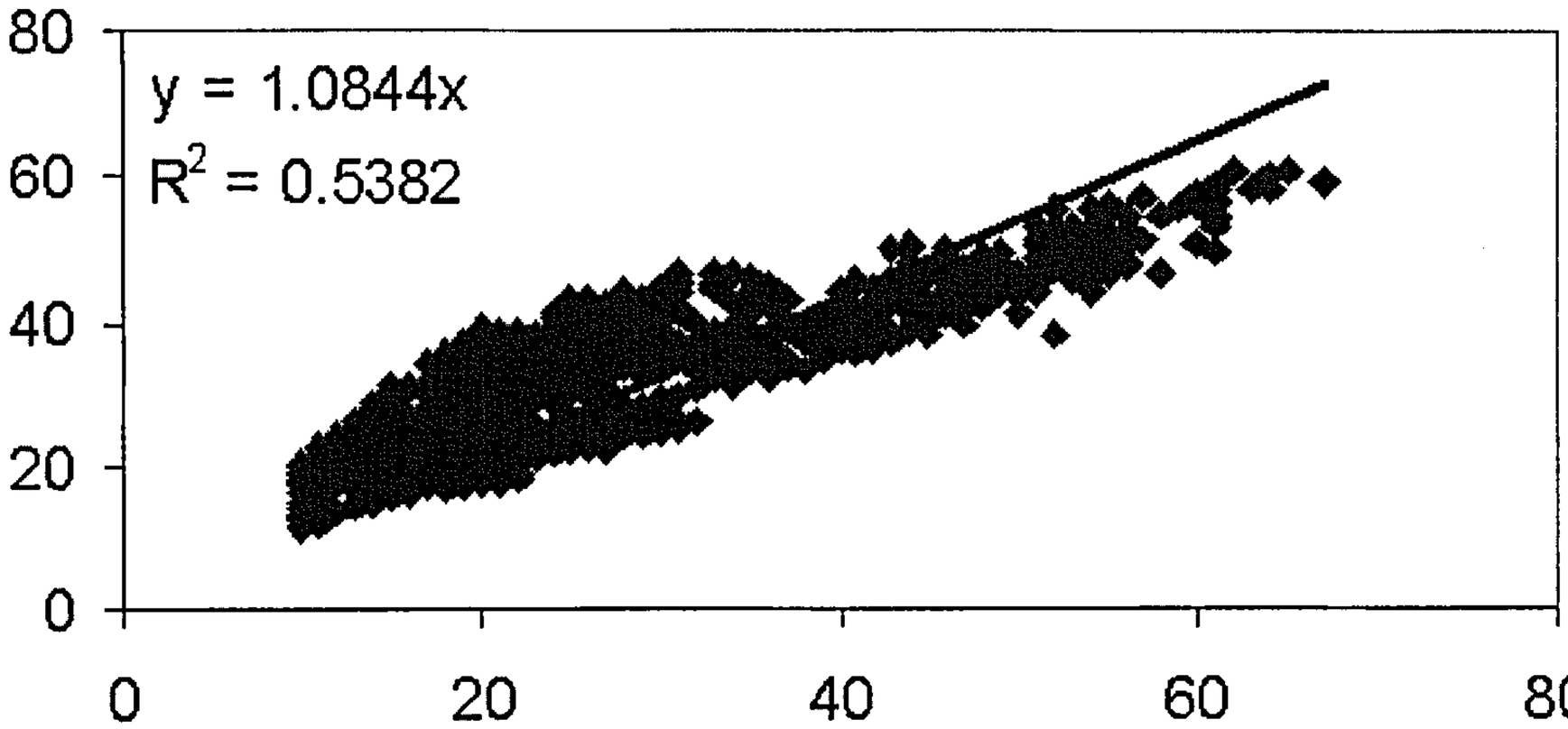

Figure 8.15 Validation: scatter plot of measured internal illuminance (X-axis) versus predicted values (Y-axis) due to S-DPF model (Merchiston data, heavy-overcast sky, 0.21m in diameter and 0.61m in length), unit: lux

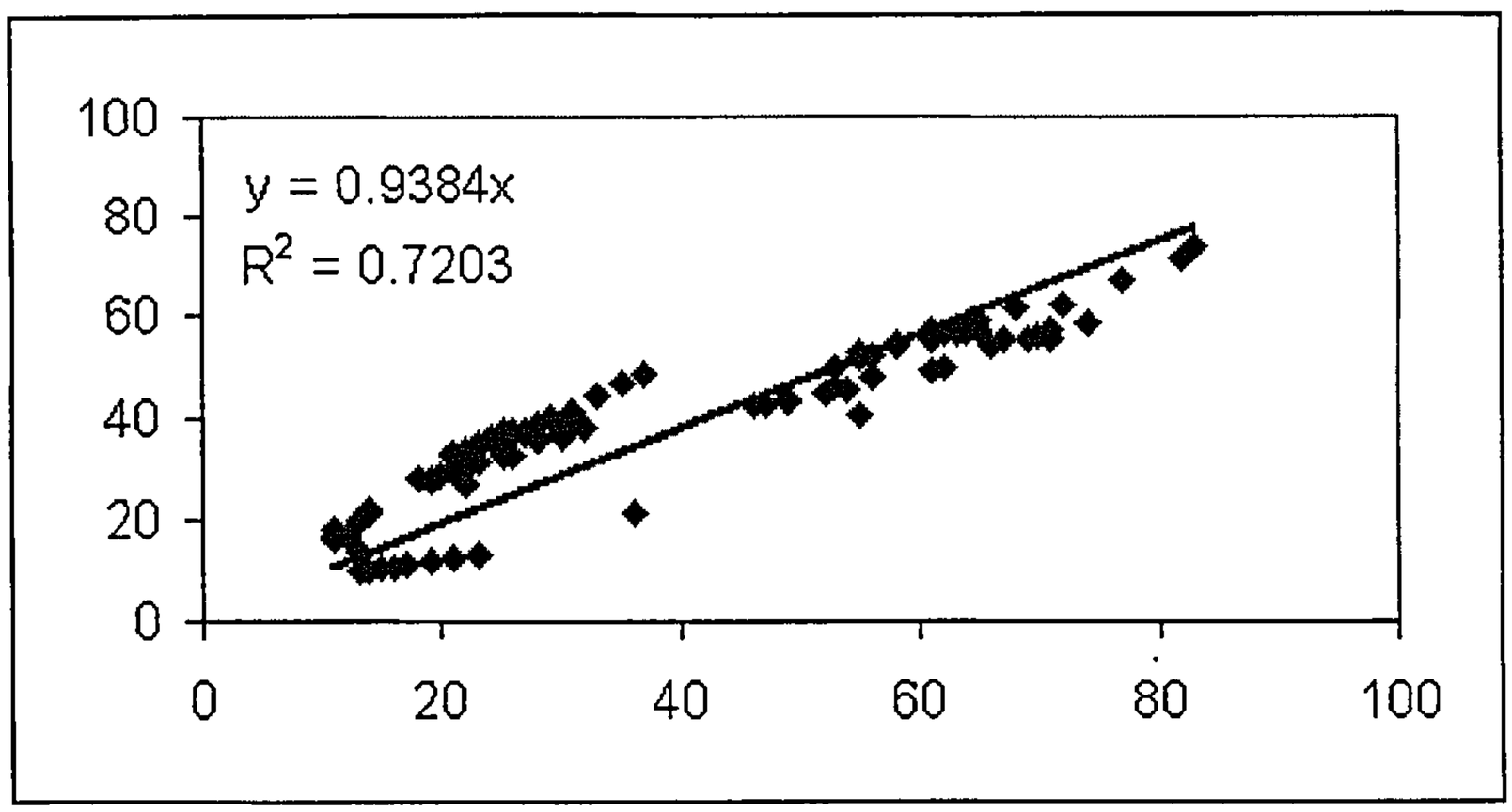

Figure 8.16 Validation: scatter plot of measured internal illuminance (X-axis) versus predicted values (Y-axis) due to S-DPF model (Merchiston data, heavy-overcast sky, 0.21m in diameter and 1.22m in length), unit: lux

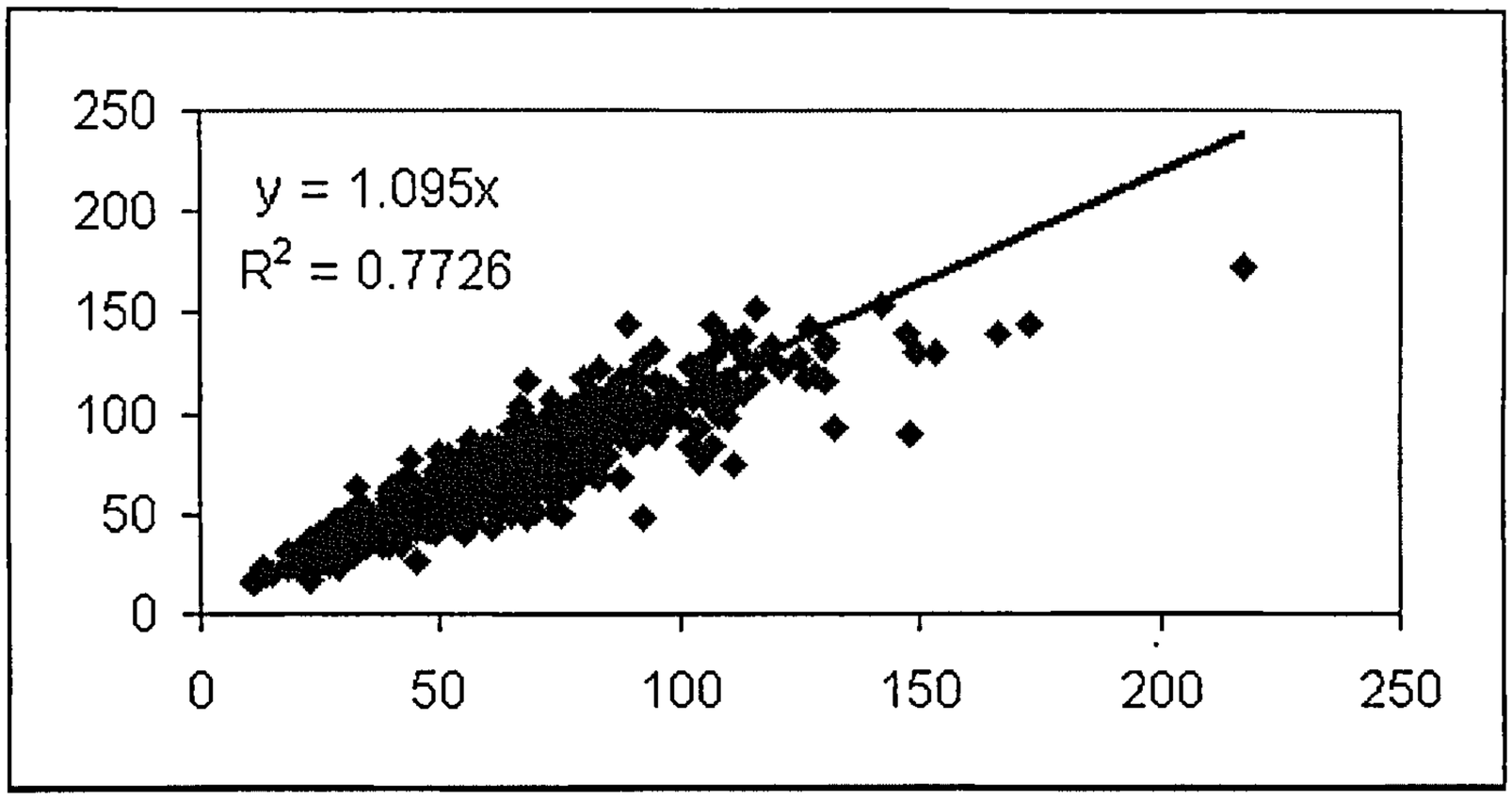

Figure 8.17 Validation: scatter plot of measured internal illuminance (X-axis) versus predicted values (Y-axis) due to S-DPF model (Merchiston data, heavy-overcast sky, 0.33m in diameter and 0.61m in length), unit: lux

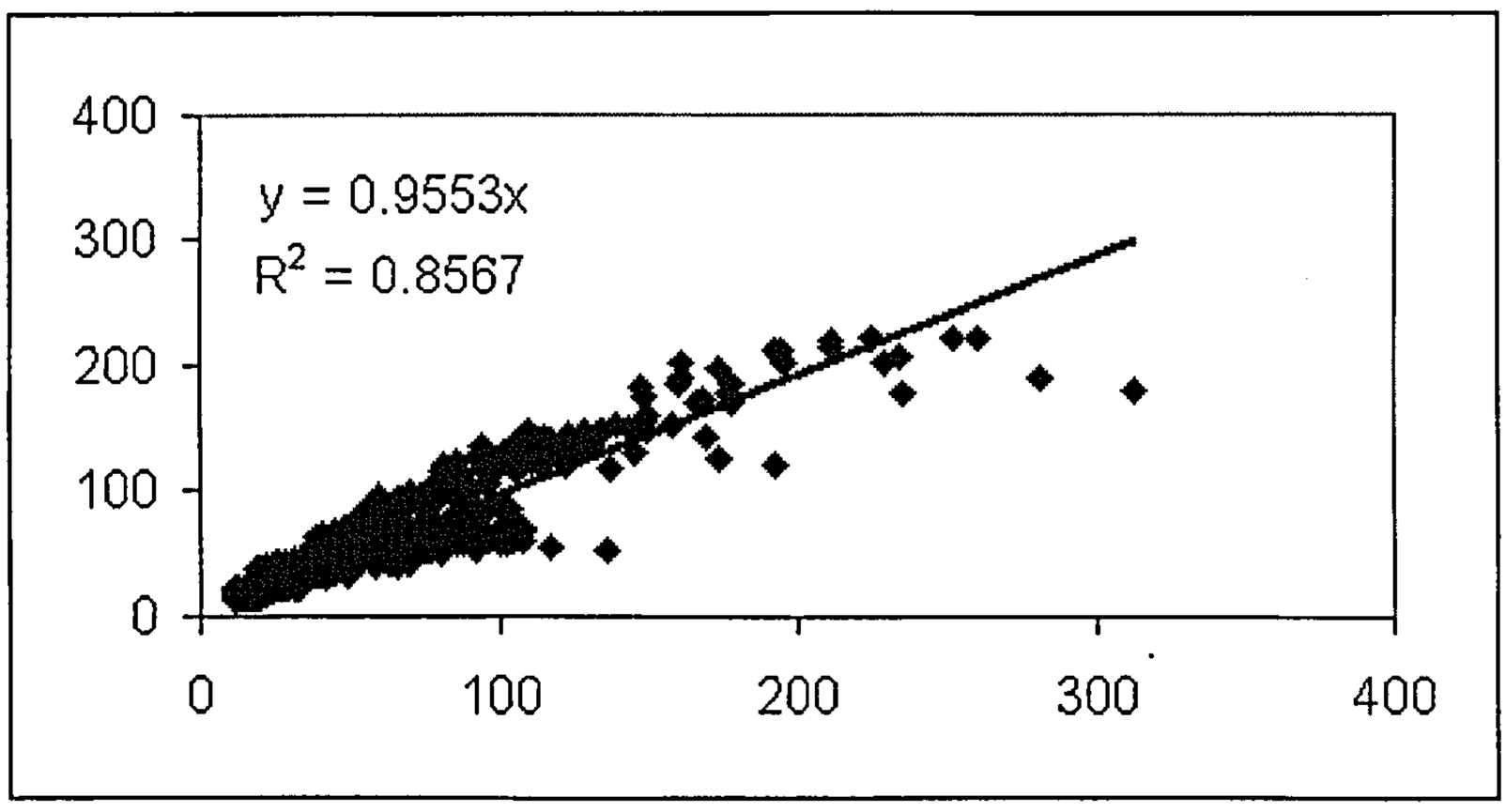

Figure 8.18 Validation: scatter plot of measured internal illuminance (X-axis) versus predicted values (Y-axis) due to S-DPF model (Merchiston data, heavy-overcast sky, 0.33m in diameter and 1.22m in length), unit: lux

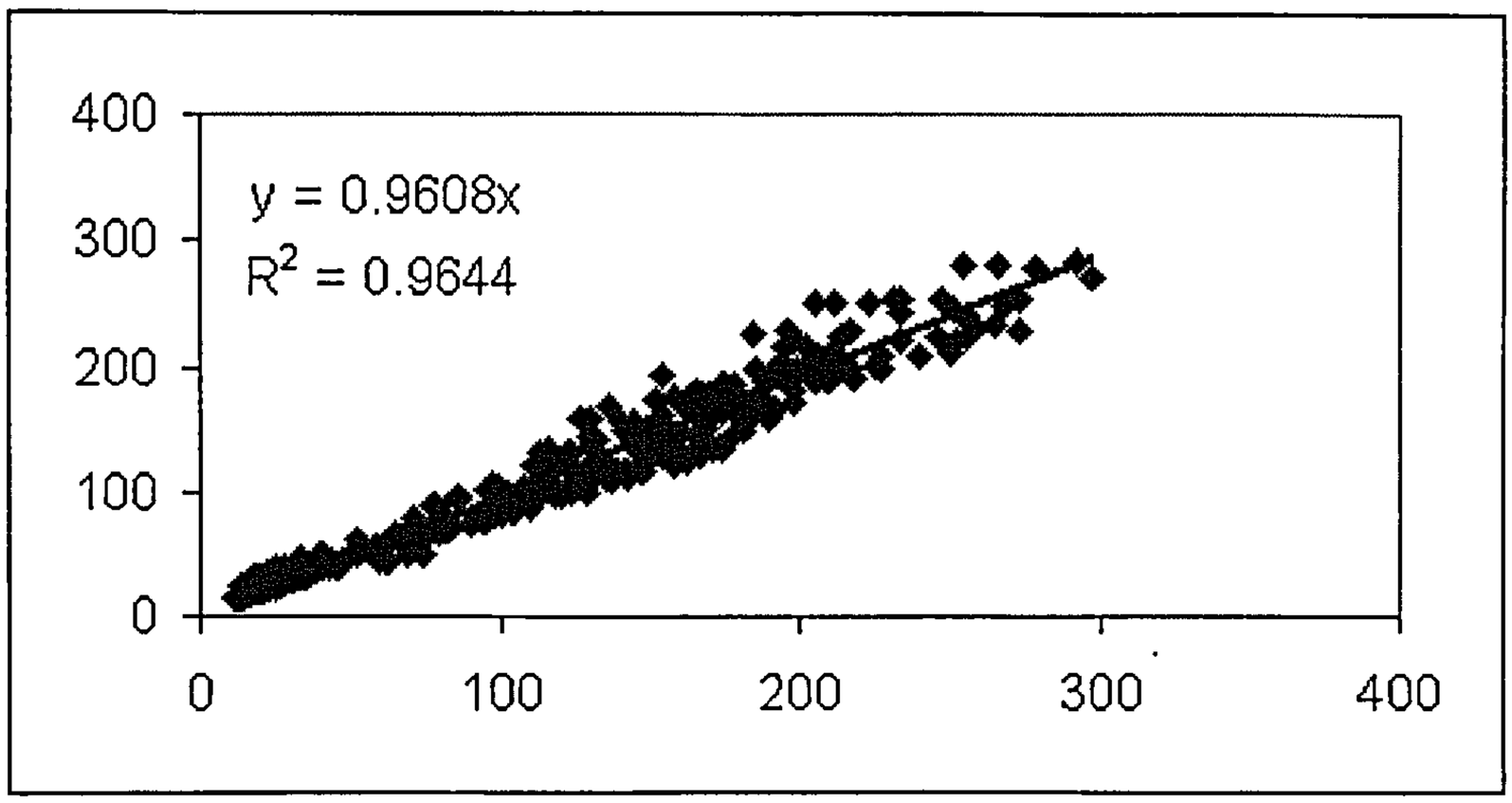

Figure 8.19 Validation: scatter plot of measured internal illuminance (X-axis) versus predicted values (Y-axis) due to S-DPF model (Merchiston data, heavy-overcast sky, 0.42m in diameter and 0.61m in length), unit: lux

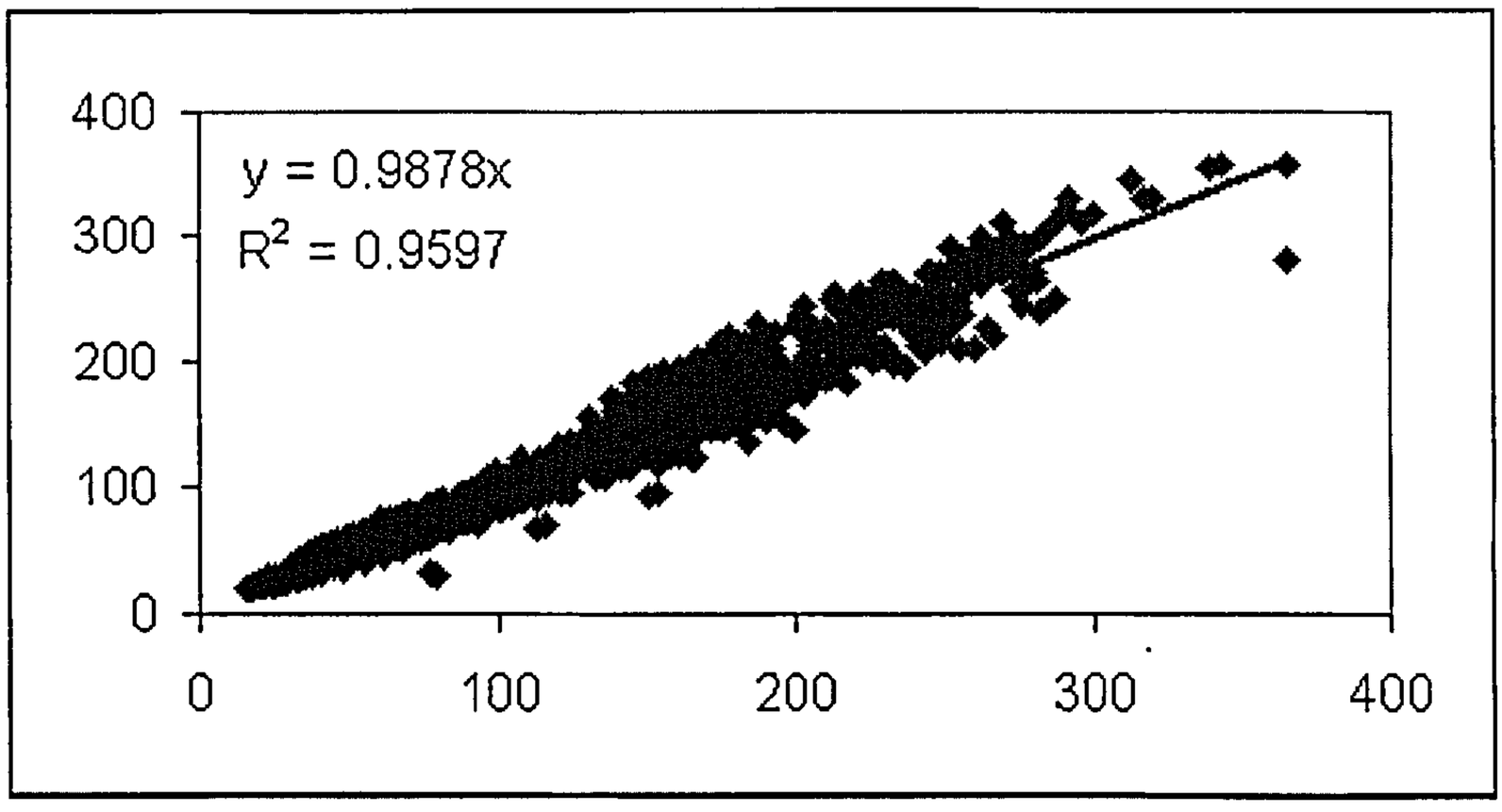

Figure 8.20 Validation: scatter plot of measured internal illuminance (X-axis) versus predicted values (Y-axis) due to S-DPF model (Merchiston data, heavy-overcast sky, 0.42m in diameter and 1.22m in length), unit: lux

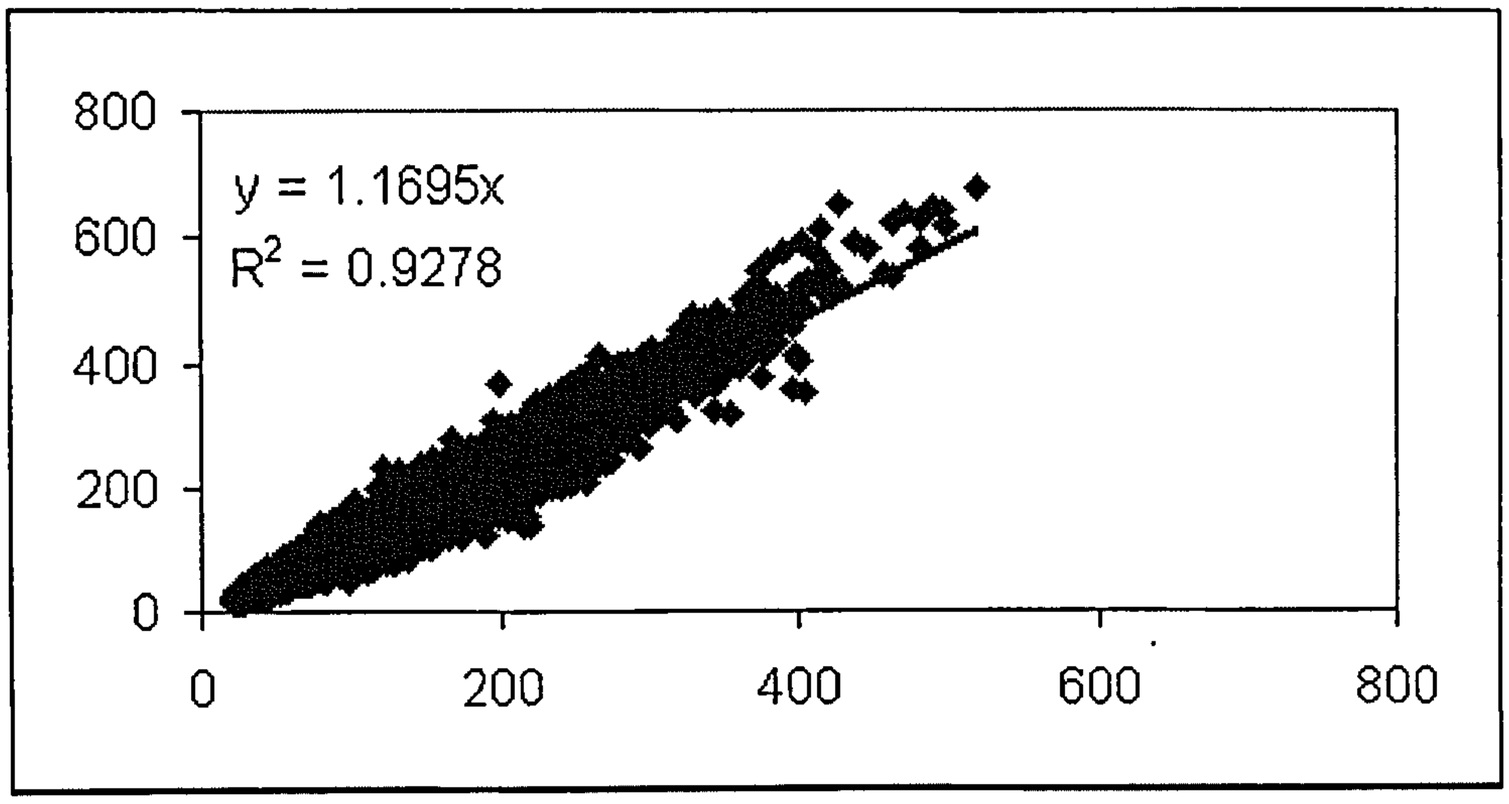

Figure 8.21 Validation: scatter plot of measured internal illuminance (X-axis) versus predicted values (Y-axis) due to S-DPF model (Merchiston data, heavy-overcast sky, 0.53m in diameter and 0.61m in length), unit: lux

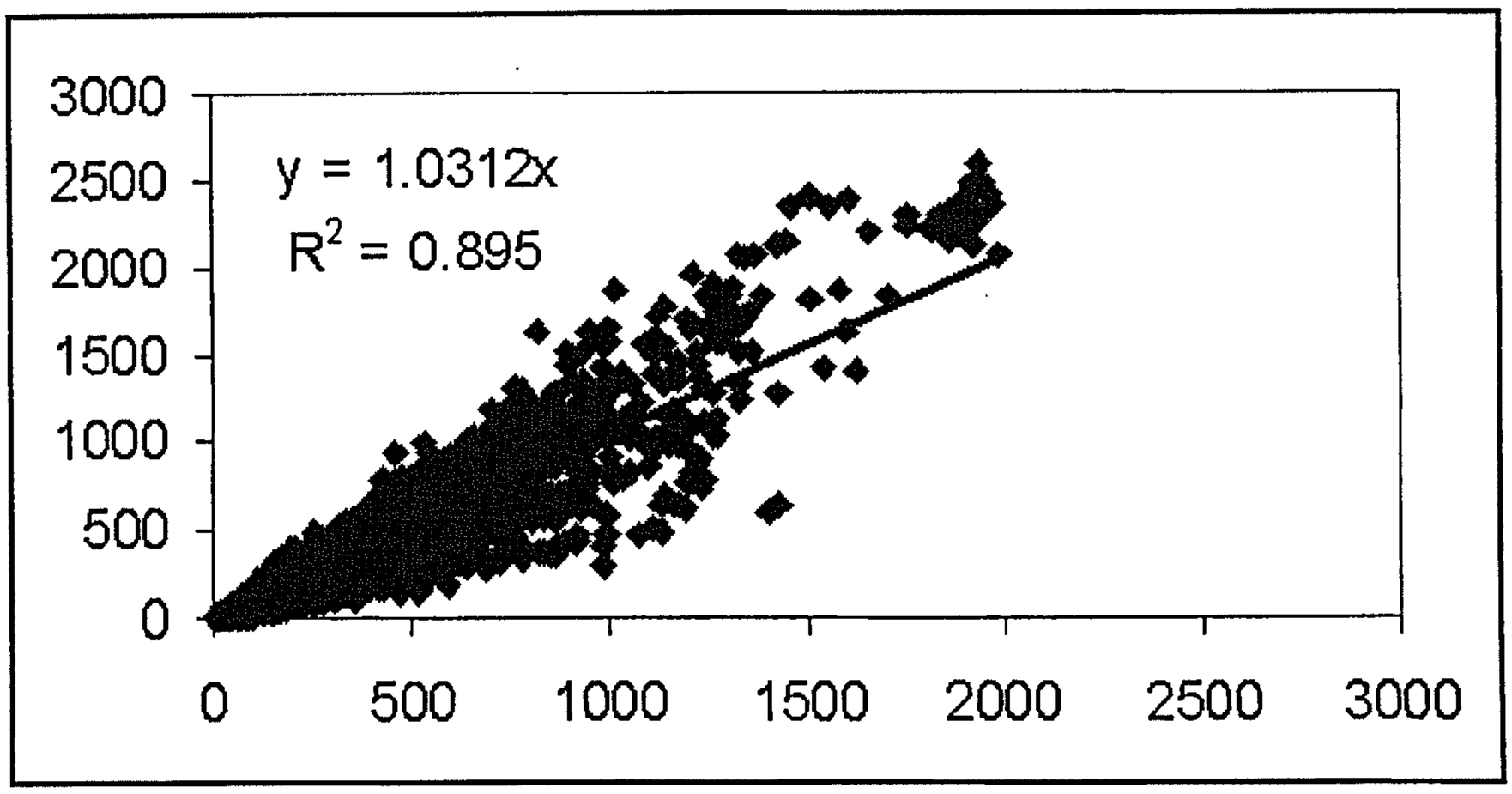

Figure 8.22 Validation: scatter plot of measured internal illuminance (X-axis) versus predicted values (Y-axis) due to S-DPF model (Merchiston data, all weather), unit: lux

3.3 Optical efficiency

The optical system can be split up into three parts:

- The transparent top dome
- The highly reflective aluminium ducts
- The end diffuser

3.3.1 The manufacturer stated performance of the aluminium ducts

Light losses in the ducts amount to 8 % per bend and 3 % per meter of straight duct according to documentation (Data Sheet No. 1, Monodraught, 1999). The light transmission of the two installed systems can as a consequence be calculated. To control these values the light level at the beginning and at the ending of Sunpipe 2 were measured, giving the real light transmission of the duct.

	Theoretical		Measured
	Sunpipe 1	Sunpipe 2	Sunpipe 2
Light transmission duct	74%	93%	48 %
Global light transmission	33%	42%	22 %

Table 3: Light transmission through the Sunpipe system

For the calculation of the light transmission of the global system the top dome and the diffuser are taken into account.

For the theoretical values the normal light transmittance were used properties (measured at BBRI, results are given in Appendix A). These amount to about 50 % for the diffusers and about 90% for the top domes. These were chosen because they are typically the values that would be included in product specifications (although not yet included in the product data sheet).

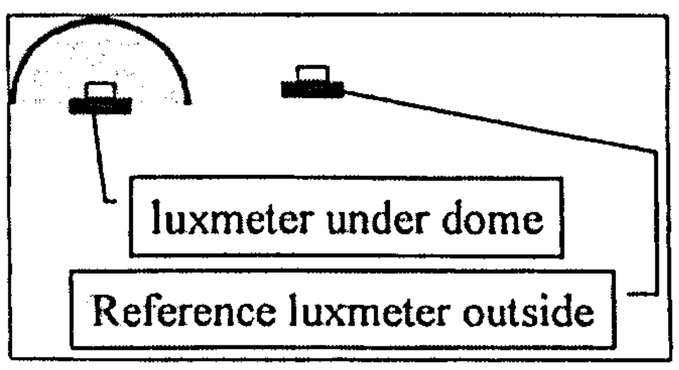

Figure 21: Determination of the hemispherical transmittance

For the measured value a test was performed to determine the hemispherical transmittance (Figure 21) of the top dome and the diffuser. These amount to 56 % for the diffuser and 80 % for the top dome.

In this particular case, the use of the normal values instead of the hemispherical values does not lead to a different result.

Remark:

These manufacturer specified values seem to be quite idealistic and lead to a performance that is almost twice as good as the real performance. Again, more prudence in product specifications would be recommendable.

Figure 8.23 Scanned copy of page 15 of report by Loncour et al [4]

3.3.2 Detailed analysis of light decrease in the aluminium duct

To get a better insight in how the light flux diminishes in the duct, a detailed measurement campaign was set-up. The decrease of light flux through the duct was determined by on-site measurements in Sunpipe 2. The illuminance in the duct was measured along the length of the duct and compared with the reference luxmeter outdoors, under an overscast sky.

The set-up (Figure 22) is comparable to a daylight factor measurement. Figure 23 shows how much light is left at every point of the duct with respect to the duct entrance.

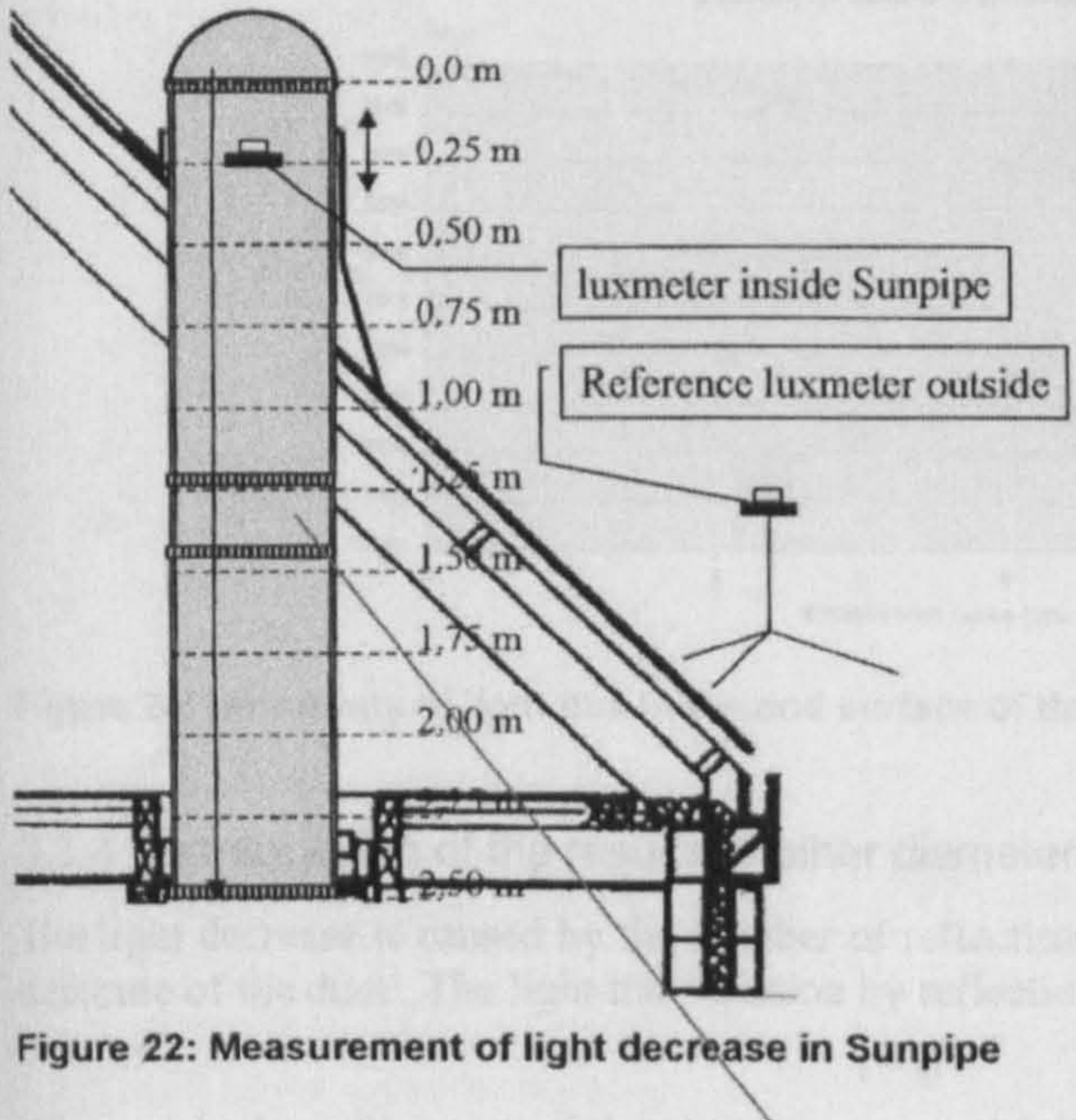

Figure 22: Measurement of light decrease in Sunpipe

The effect of the direct view of the sky can be determined. As can be seen it decreases very quickly from 100 % to only 1 % after 1 meter.

The remainder of the light is the interreflected part, which increases steeply in the beginning of the duct and after 0.75 m decreases slowly with the absorption of light by the duct. An extra light loss of about 5% is noticed between 1.25 and 1.5 m, right at the point where two junctions were made.

The average decrease per meter of duct, based on the values where the direct part is almost completely gone (starting from 75 cm), is in this case 29 %, meaning that we have a light transmission per meter of 71 %. This is a lot worse than the stated 3% per meter.

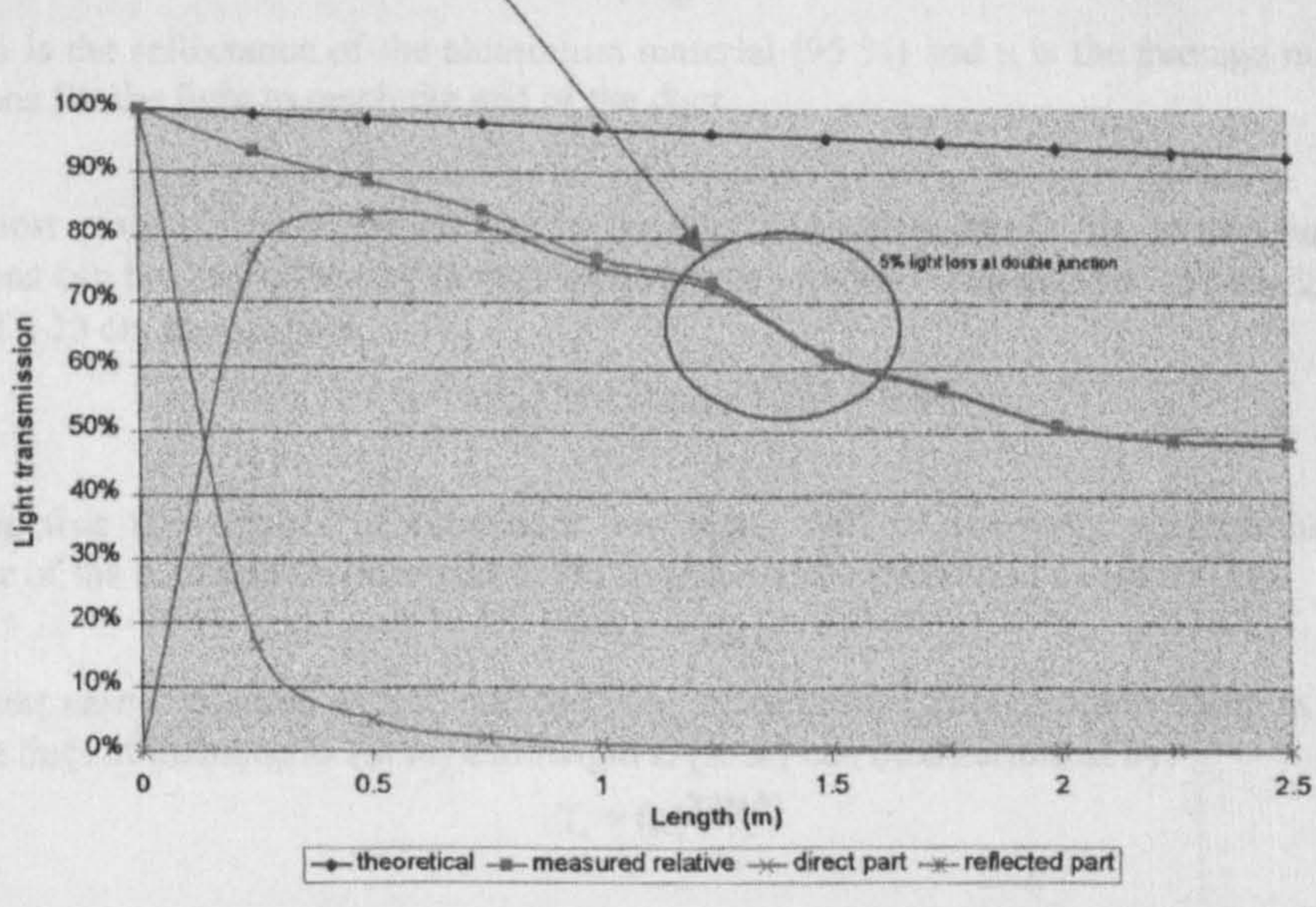

Figure 23: Light decrease along the length of the Sunpipe

Figure 8.24 Scanned copy of page 16 of report by Loncour et al [4]

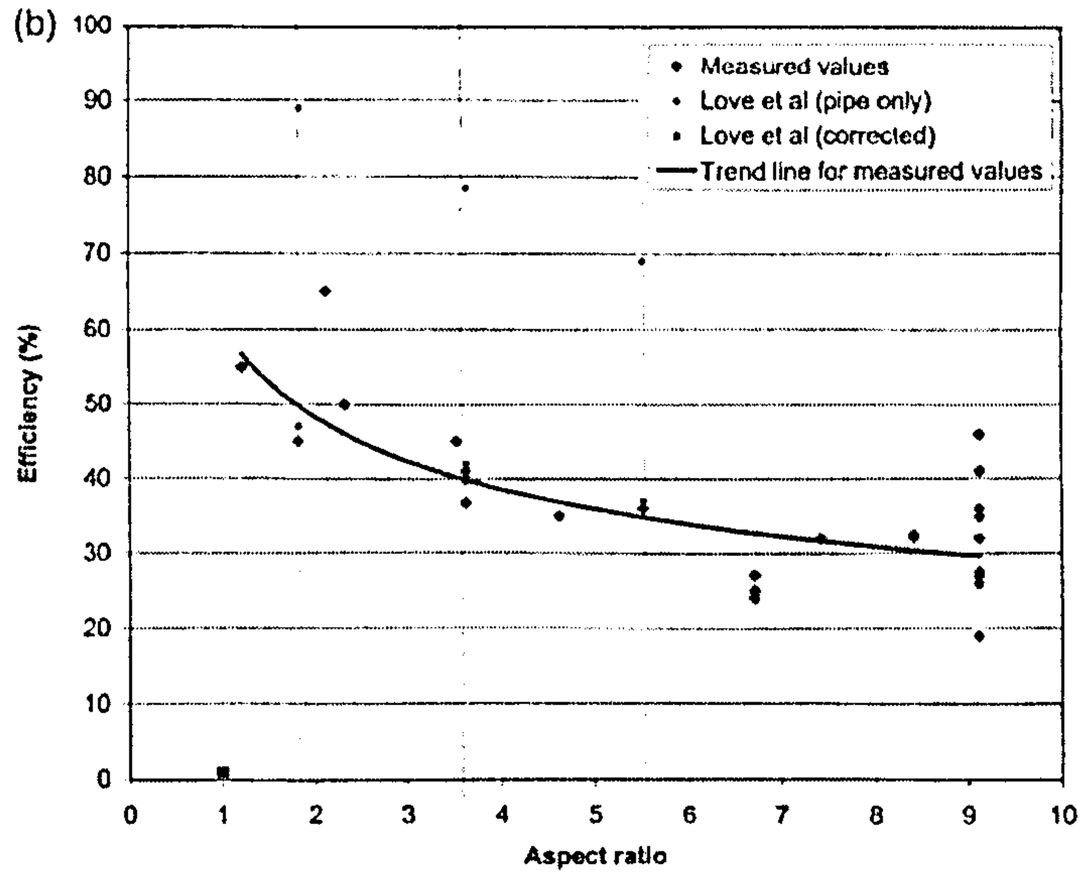

Figure 5 (a) Graph of pipe efficiency against aspect ratio. (b) Graph of pipe efficiency against aspect ratio

Figure 8.25 Scanned copy of Figure 5 of Carter [5]

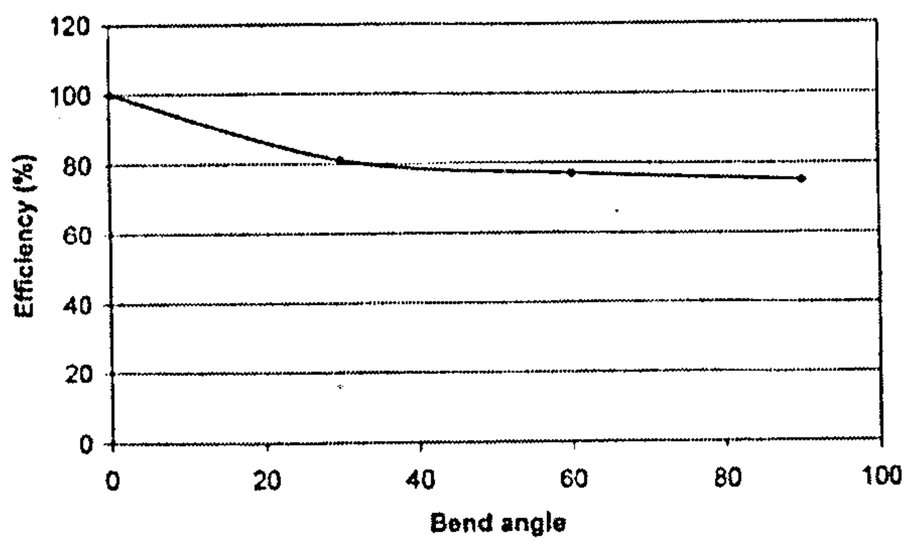

Figure 6 Graph of efficiency against bend angle for bend length equal to pipe diameter

Figure 8.26 Scanned copy of Figure 6 of Carter [5]

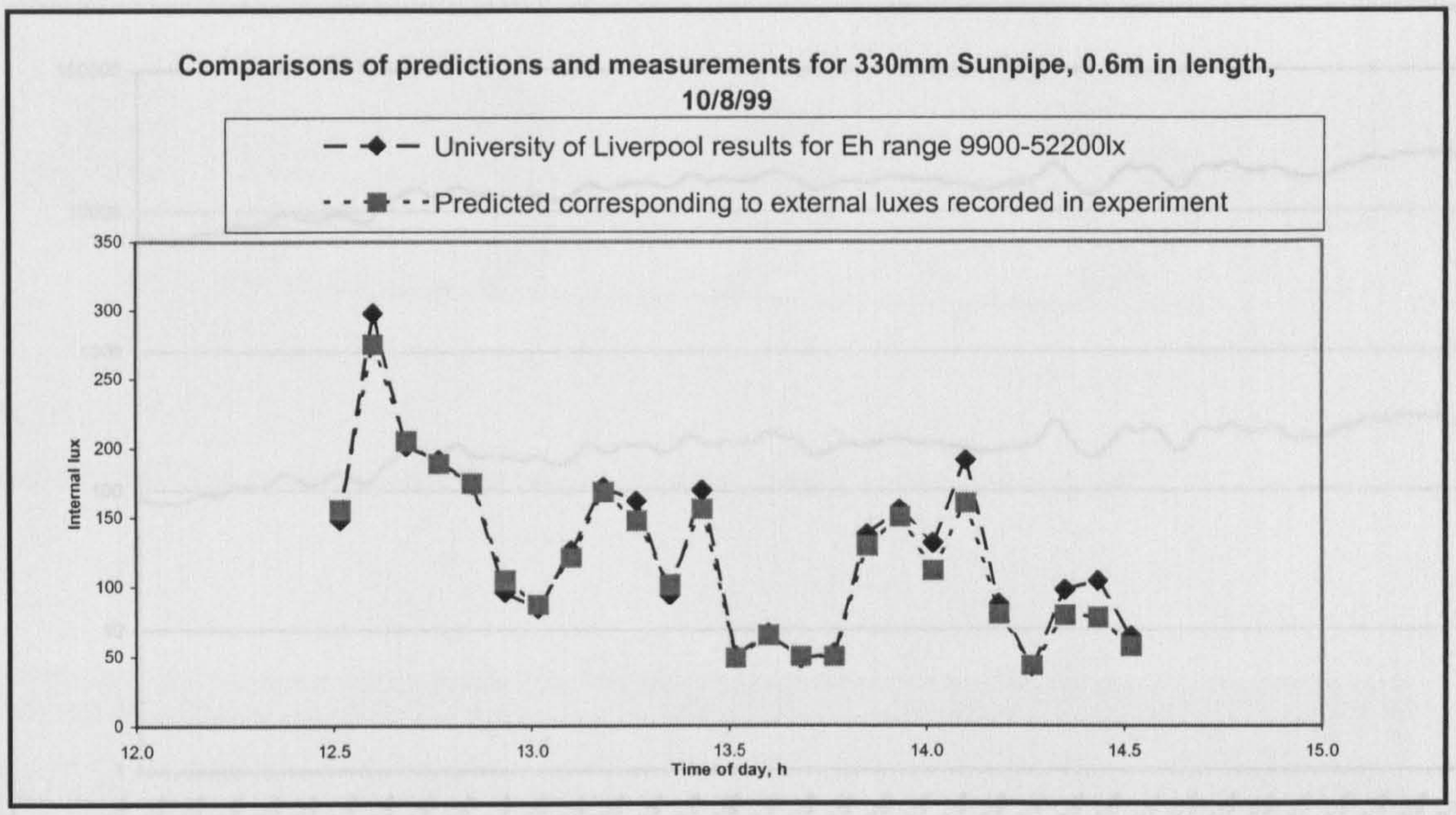

Figure 8.27 Comparative plots showing close conformance between Liverpool measurements and Napier's DPF model estimates

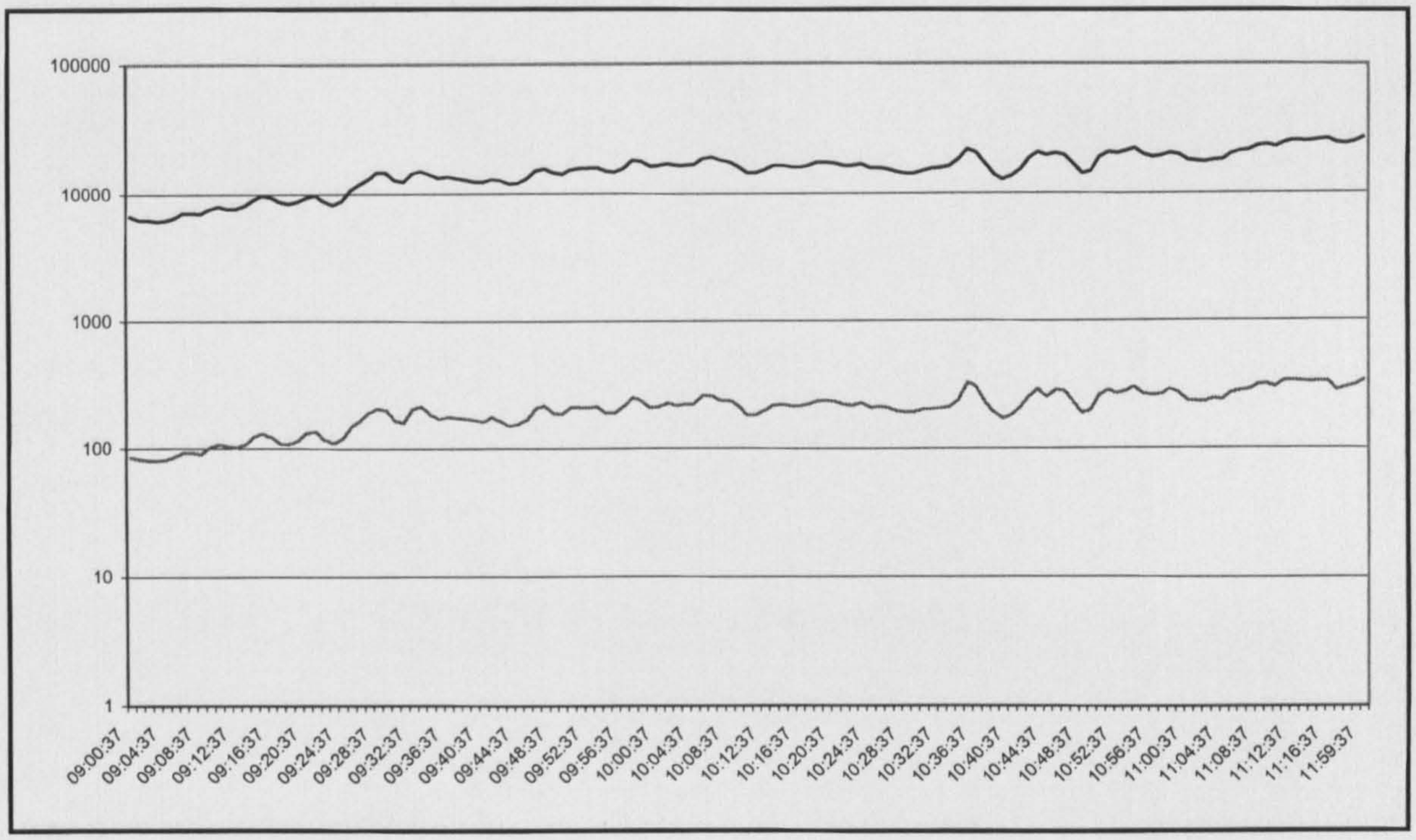

Figure 8.28 Plot showing measured external and internal illuminance at Napier University, unit: lux

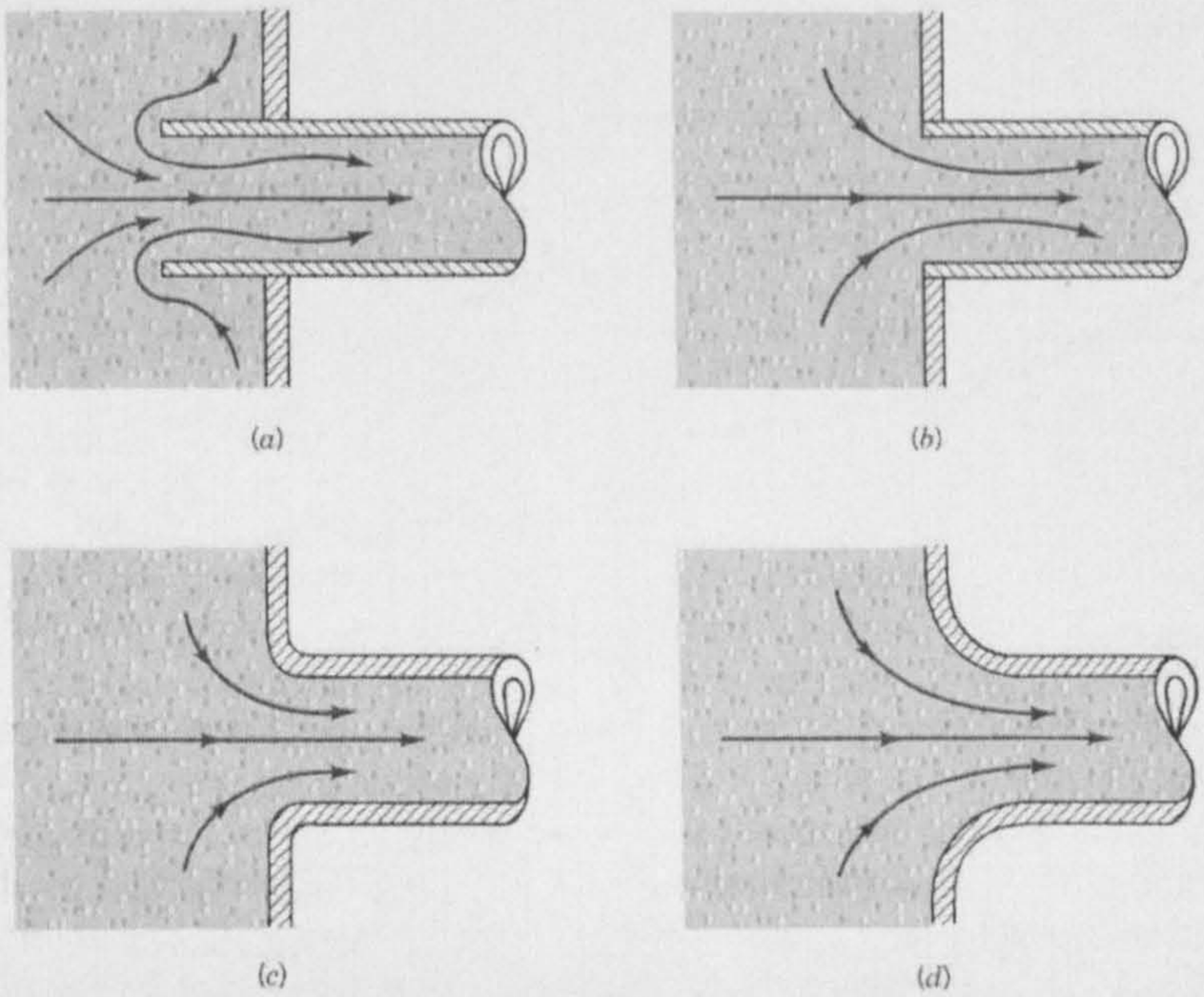

FIGURE 8.25
Entrance flow conditions and loss coefficient (Refs. 28, 29). (*a*) Reentrant, K_L = 0.8; (*b*) Sharped edged, K_L = 0.5; (*c*) Slightly rounded, K_L = 0.2 (see Fig. 8.27). (*d*) Well rounded, K_L = 0.04 (see Fig. 8.27).

Figure 8.29 Loss of flow energy at entrance to a conduit

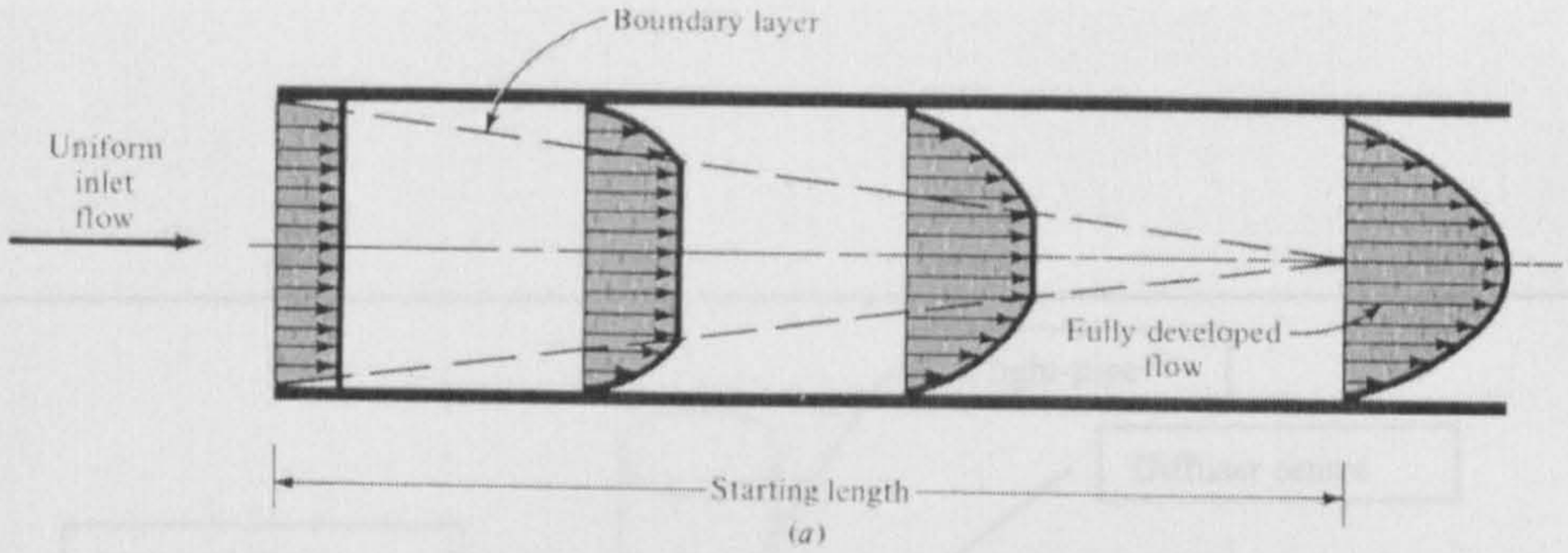

Figure 8.30 Loss of flow energy during the 'starting-length' within the conduit

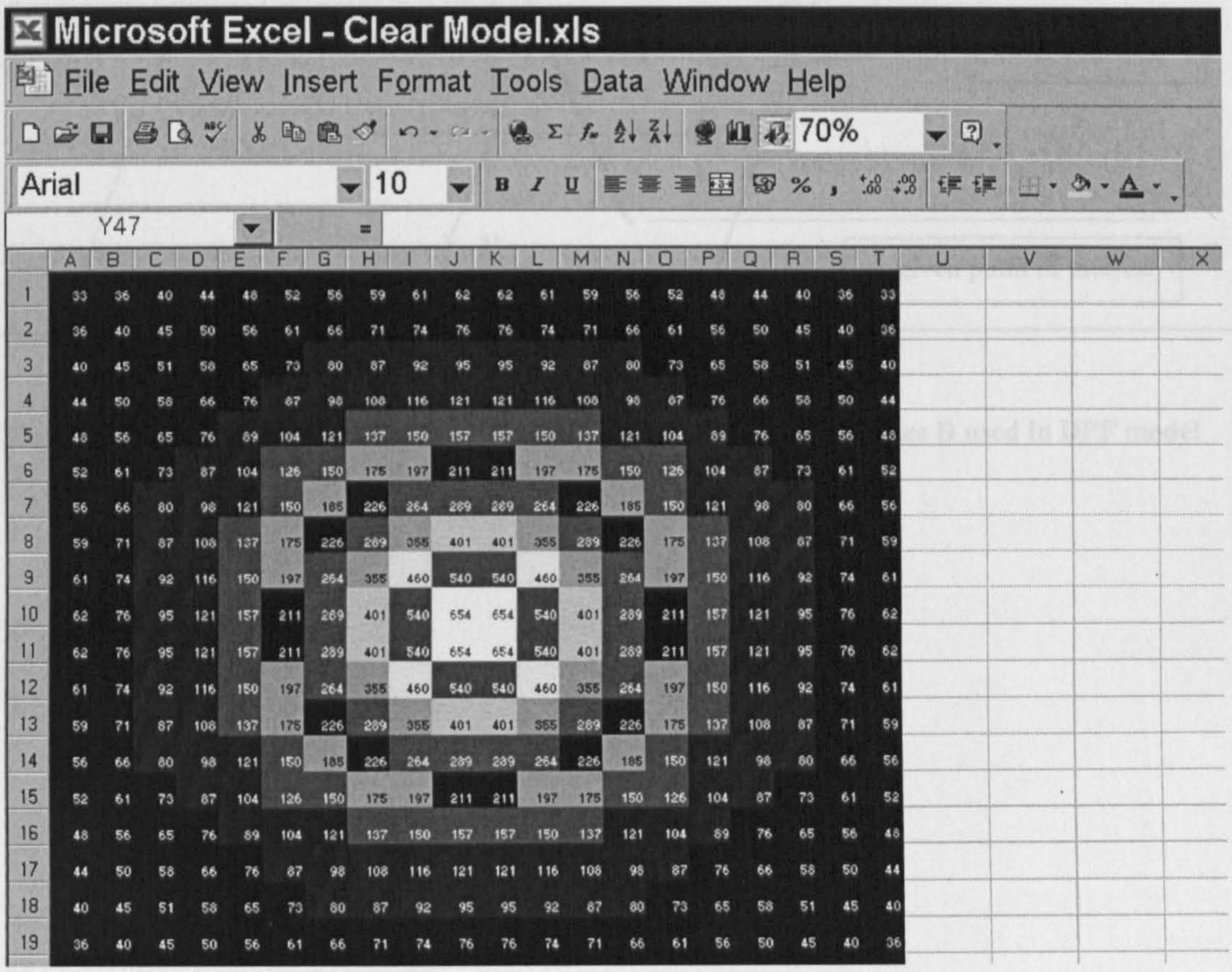

	A	B	C	D	E	F	G	H	I	J	K	L	M	N	O	P	Q	R	S	T
1	33	36	40	44	48	52	56	59	61	62	62	61	59	56	52	48	44	40	36	33
2	36	40	45	50	56	61	66	71	74	76	76	74	71	66	61	56	50	45	40	36
3	40	45	51	58	65	73	80	87	92	95	95	92	87	80	73	65	58	51	45	40
4	44	50	58	66	76	87	98	108	116	121	121	116	108	98	87	76	66	58	50	44
5	48	56	65	76	89	104	121	137	150	157	157	150	137	121	104	89	76	65	56	48
6	52	61	73	87	104	126	150	175	197	211	211	197	175	150	126	104	87	73	61	52
7	56	66	80	98	121	150	185	226	264	289	289	264	226	185	150	121	98	80	66	56
8	59	71	87	108	137	175	226	289	355	401	401	355	289	226	175	137	108	87	71	59
9	61	74	92	116	150	197	264	355	460	540	540	460	355	264	197	150	116	92	74	61
10	62	76	95	121	157	211	289	401	540	654	654	540	401	289	211	157	121	95	76	62
11	62	76	95	121	157	211	289	401	540	654	654	540	401	289	211	157	121	95	76	62
12	61	74	92	116	150	197	264	355	460	540	540	460	355	264	197	150	116	92	74	61
13	59	71	87	108	137	175	226	289	355	401	401	355	289	226	175	137	108	87	71	59
14	56	66	80	98	121	150	185	226	264	289	289	264	226	185	150	121	98	80	66	56
15	52	61	73	87	104	126	150	175	197	211	211	197	175	150	126	104	87	73	61	52
16	48	56	65	76	89	104	121	137	150	157	157	150	137	121	104	89	76	65	56	48
17	44	50	58	66	76	87	98	108	116	121	121	116	108	98	87	76	66	58	50	44
18	40	45	51	58	65	73	80	87	92	95	95	92	87	80	73	65	58	51	45	40
19	36	40	45	50	56	61	66	71	74	76	76	74	71	66	61	56	50	45	40	36

Figure 8.31 An example of lux plot [Courtesy: David Jenkins, Monodraught]

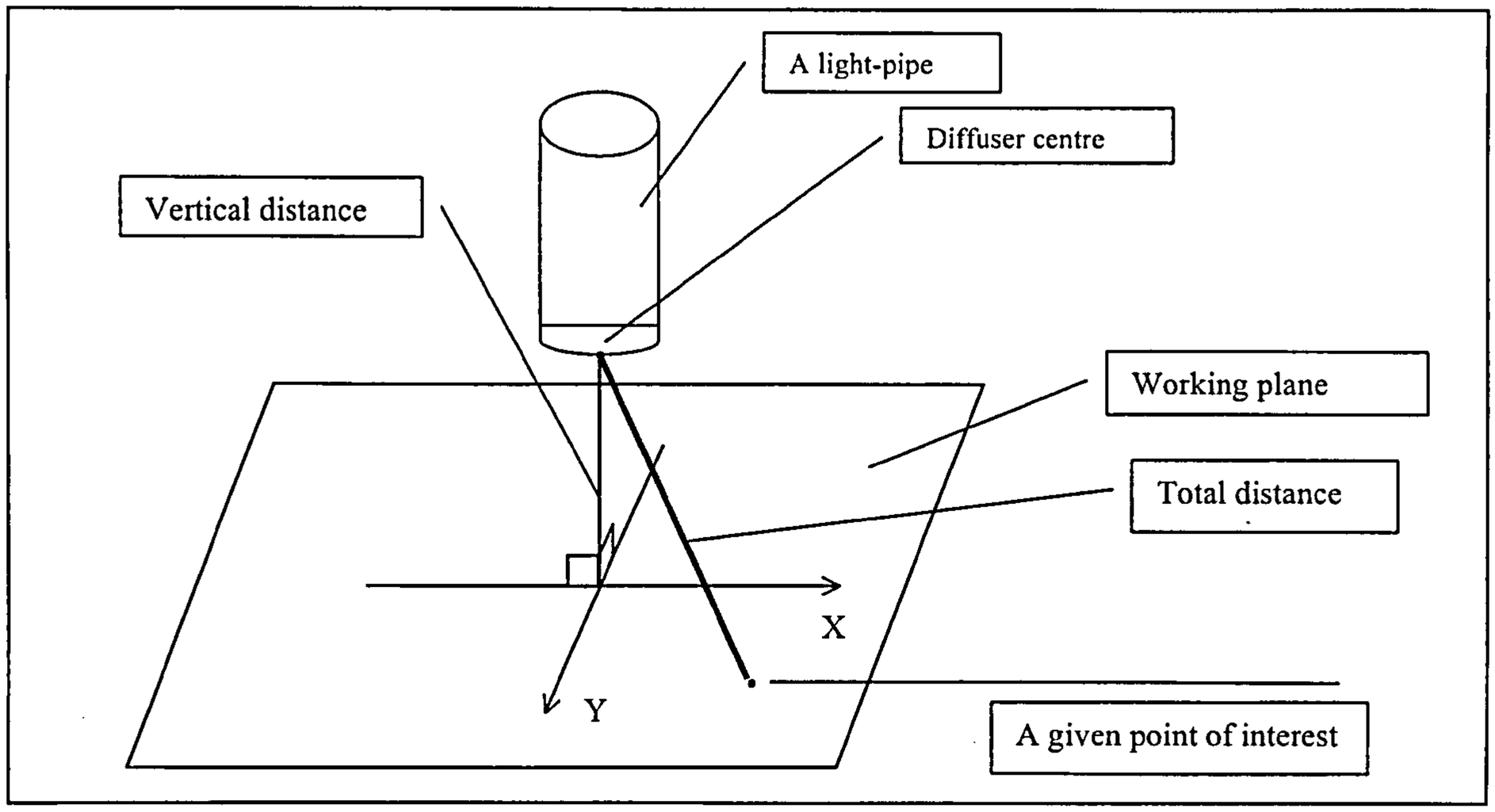

Figure 8.32 An illustration of "vertical" distance H, and "total" distances D used in DPF model

Table 8.1 Statistical results for the performance of S-DPF model under heavy-overcast sky conditions (kt≤0.2)

Light pipe	Slope	R-Square	RMSE, lux	MBE, lux	PAD (%)	Average internal illuminance, lux	Maximum internal illuminance, lux	Minimum internal illuminance, lux
Case 1	1.08	0.54	8	5	33	26	67	10
Case 2	0.94	0.72	9	0	29	37	83	11
Case 3	1.10	0.77	14	8	20	62	217	11
Case 4	0.96	0.86	17	0	19	57	313	11
Case 5	0.96	0.96	14	-2	15	93	297	11
Case 6	0.99	0.96	14	-2	9	113	365	16
Case 7	1.17	0.93	45	20	20	153	519	20

Case 1: light pipe 0.21m in diameter and 0.6m long,
Case 2: light pipe 0.21m in diameter and 1.2m long,
Case 3: light pipe in 0.33m diameter and 0.6m long,
Case 4: light pipe in 0.33m diameter and 1.2m long,
Case 5: light pipe in 0.45m diameter and 0.6m long,
Case 6: light pipe in 0.45m diameter and 1.2m long,
Case 7:light pipe in 0.53m diameter and 0.6m long

Table 8.2 Sample data of Internal illuminance distribution (0.33m-diameter light pipe, 18th Dec 2000)

Date	Time	S1 (LUX)	S2 (LUX)	S3 (LUX)	S4 (LUX)	S6 (LUX)	Average lux	SDV, lux
18-Dec-00	9:22:12	119	82	82	84	110	95	18
18-Dec-00	9:23:12	127	88	86	92	120	103	19
18-Dec-00	9:24:12	138	93	91	100	127	110	21
18-Dec-00	9:25:12	144	100	98	106	132	116	21
18-Dec-00	9:26:12	148	104	101	113	138	121	21
18-Dec-00	9:27:12	151	106	106	118	140	124	21
18-Dec-00	9:28:12	155	111	110	116	139	126	20
18-Dec-00	9:29:12	156	115	115	109	135	126	19
18-Dec-00	9:30:12	155	115	115	108	137	126	20
18-Dec-00	9:31:12	155	114	109	113	142	127	21
18-Dec-00	9:32:12	161	113	109	115	141	128	22
18-Dec-00	9:33:12	167	120	117	116	142	132	22
18-Dec-00	9:34:12	174	130	125	124	150	141	21
18-Dec-00	9:35:12	183	135	130	134	162	149	23
18-Dec-00	9:36:12	194	139	135	137	171	155	26
18-Dec-00	9:37:12	204	145	144	143	177	163	27
18-Dec-00	9:38:12	213	152	145	157	184	170	28
18-Dec-00	9:39:12	224	156	149	168	193	178	31
18-Dec-00	9:40:12	239	165	158	174	206	188	34
18-Dec-00	9:41:12	255	177	171	189	225	203	36
18-Dec-00	9:42:12	272	191	186	211	245	221	37
18-Dec-00	9:43:12	292	208	203	230	260	239	37
18-Dec-00	9:44:12	306	221	221	250	275	255	37
18-Dec-00	9:45:12	320	234	238	270	293	271	37
18-Dec-00	9:46:12	336	245	251	280	305	283	38
18-Dec-00	9:47:12	350	255	258	290	322	295	41
18-Dec-00	9:48:12	370	264	263	305	337	308	47
18-Dec-00	9:49:12	391	281	279	315	344	322	47
18-Dec-00	9:50:12	410	304	303	329	360	341	45
18-Dec-00	9:51:12	422	317	321	362	391	363	45
18-Dec-00	9:52:12	443	331	340	404	422	388	50
18-Dec-00	9:53:12	463	345	361	433	447	410	53
18-Dec-00	9:54:12	490	363	379	447	468	429	56
18-Dec-00	9:55:12	524	389	394	444	473	445	57
18-Dec-00	9:56:12	545	415	407	435	468	454	56
18-Dec-00	9:57:12	547	424	415	438	477	460	54
18-Dec-00	9:58:12	554	418	413	453	494	466	59
18-Dec-00	9:59:12	561	411	415	470	505	472	63
18-Dec-00	10:00:12	568	422	434	489	518	486	60
18-Dec-00	10:01:12	582	438	453	507	533	503	59
18-Dec-00	10:02:12	600	447	466	517	549	516	62
18-Dec-00	10:03:12	609	451	469	521	560	522	65
18-Dec-00	10:04:12	609	449	463	523	565	522	67
18-Dec-00	10:05:12	614	446	457	525	571	523	72
18-Dec-00	10:06:12	629	449	455	534	580	529	78
18-Dec-00	10:07:12	640	457	460	553	594	541	81
18-Dec-00	10:08:12	653	469	476	590	619	561	84

Table 8.3 Summary of the Internal illuminance distribution test results (Craighouse test room)

Diameter, m	Length, m	Averaged Standard Deviation, lux	Averaged Internal Illuminance, lux	Ratio between Standard Deviation and internal illuminance, %
0.33	0.6	80	603	13%
0.45	0.6	48	389	12%
0.45	1.2	63	495	13%

Table 8.4 Light pipe predicted light levels for mid-summer for Kew, UK. (Time = 10am 1st July, Height of diffuser to the working plane = 2m)

Length	Weather condition	Internal illuminance achieved at a horizontal distance of d # by a light pipe of diameter ϕ, lux											
		ϕ=210mm			ϕ=330mm			ϕ=420mm			ϕ=530mm		
		d=0m	d=1m	d=2m	d=0m	d=1m	d=2m	d=0m	d=1m	d=2m	d=0m	d=1m	d=2m
600mm	Clear *	140	100	50	425	295	140	740	515	245	1250	870	415
	Part-overcast ✦	80	60	30	245	170	85	430	300	145	725	505	240
	Overcast ♦	45	30	15	125	90	45	220	155	75	370	260	125
1200mm	Clear	80	55	30	295	205	100	555	385	185	995	695	330
	Part-overcast	45	35	15	170	120	60	320	225	110	575	400	190
	Overcast	25	20	10	90	60	30	165	115	55	295	205	100
1800mm	Clear	45	30	15	205	140	70	415	290	140	790	550	265
	Part-overcast	25	20	10	120	85	40	240	170	80	460	320	155
	Overcast	15	10	5	60	45	20	125	85	40	235	165	80
2400mm	Clear	25	20	10	140	100	50	310	220	105	630	440	210
	Part-overcast	15	10	5	80	60	30	180	125	60	365	255	120
	Overcast	10	5	5	45	30	15	95	65	30	185	130	65
3000mm	Clear	15	10	5	100	70	35	235	165	80	500	350	165
	Part-overcast	10	5	5	60	40	20	135	95	45	290	205	100
	Overcast	5	5	5	30	20	10	70	50	25	150	105	50
3600mm	Clear	10	5	5	70	50	25	175	125	60	400	280	135
	Part-overcast	5	5	5	40	30	15	100	70	35	230	160	80
	Overcast	5	5	5	20	15	10	55	40	20	120	85	40

Weather condition	Horizontal global illuminance	Sky clearness index, k_t
Clear *	88klux	0.7
Part-overcast ✦	50klux	0.4
Overcast ♦	25klux	0.2

d # = the distance between the projection of the diffuser centre on the working plane and the point of interest

Table 8.5 Light pipe predicted light levels for winter for Kew, UK. (Time = 10am 1st February, Height of diffuser to the working plane = 2m)

Length	Weather condition	Internal illuminance achieved at a horizontal distance of d # by a light pipe of diameter ϕ, lux											
		ϕ=210mm			ϕ=330mm			ϕ=420mm			ϕ=530mm		
		d=0m	d=1m	d=2m	d=0m	d=1m	d=2m	d=0m	d=1m	d=2m	d=0m	d=1m	d=2m
600mm	Clear *	20	15	10	65	45	20	110	80	40	190	135	65
	Part-overcast +	15	10	5	50	35	15	85	60	30	145	100	50
	Overcast †	10	10	5	35	25	15	60	45	20	105	75	35
1200mm	Clear	10	10	5	40	30	15	75	55	25	140	100	50
	Part-overcast	10	5	5	30	20	10	60	40	20	110	75	35
	Overcast	5	5	5	20	15	10	45	30	15	80	55	25
1800mm	Clear	5	5	5	25	20	10	55	40	20	105	75	35
	Part-overcast	5	5	5	20	15	10	40	30	15	80	55	30
	Overcast	5	5	5	15	10	5	30	20	10	60	40	20
2400mm	Clear	5	5	5	15	10	5	35	25	15	80	55	25
	Part-overcast	5	5	5	15	10	5	30	20	10	60	45	20
	Overcast	5	5	5	10	5	5	20	15	10	45	30	15
3000mm	Clear	5	5	5	10	10	5	25	20	10	60	40	20
	Part-overcast	5	5	5	10	5	5	20	15	10	45	30	15
	Overcast	5	5	5	5	5	5	15	10	5	35	25	10
3600mm	Clear	5	5	5	10	5	5	20	15	10	45	30	15
	Part-overcast	5	5	5	5	5	5	15	10	5	35	25	15
	Overcast	5	5	5	5	5	5	10	10	5	25	20	10

Weather condition	Horizontal global illuminance	Sky clearness index, k_t
Clear *	31klux	0.7
Part-overcast +	18klux	0.4
Overcast †	9klux	0.2

d # = the distance between the projection of the diffuser centre on the working plane and the point of interest

Table 8.6 Light pipe predicted light levels for spring and autumn for Kew, UK. (Time = 10am 1st April, Height of diffuser to the working plane = 2m)

Length	Weather condition	Internal illuminance achieved at a horizontal distance of d # by a light pipe of diameter ϕ, lux											
		ϕ=210mm			ϕ=330mm			ϕ=420mm			ϕ=530mm		
		d=0m	d=1m	d=2m	d=0m	d=1m	d=2m	d=0m	d=1m	d=2m	d=0m	d=1m	d=2m
600mm	Clear *	95	70	35	295	205	100	515	360	175	875	610	290
	Part-overcast +	55	40	20	160	110	55	280	195	95	470	330	160
	Overcast †	30	20	10	85	60	30	150	105	50	255	180	85
1200mm	Clear	55	40	20	200	140	70	380	265	130	690	480	230
	Part-overcast	30	20	10	110	75	40	205	145	70	370	260	125
	Overcast	15	15	5	60	45	20	115	80	40	205	140	70
1800mm	Clear	30	20	10	140	95	45	285	200	95	540	380	180
	Part-overcast	15	15	5	75	55	25	155	110	50	295	205	100
	Overcast	10	10	5	40	30	15	85	60	30	160	110	55
2400mm	Clear	20	15	5	95	65	35	210	145	70	425	300	145
	Part-overcast	10	10	5	50	35	20	115	80	40	230	160	80
	Overcast	5	5	5	30	20	10	65	45	20	125	90	45
3000mm	Clear	10	10	5	65	45	25	155	110	55	335	235	115
	Part-overcast	5	5	5	35	25	15	85	60	30	180	130	60
	Overcast	5	5	5	20	15	10	45	35	15	100	70	35
3600mm	Clear	5	5	5	45	30	15	115	80	40	265	185	90
	Part-overcast	5	5	5	25	20	10	65	45	20	145	100	50
	Overcast	5	5	5	15	10	5	35	25	15	80	55	30

Weather condition	Horizontal global illuminance	Sky clearness index, k_t
Clear *	68klux	0.7
Part-overcast +	39klux	0.4
Overcast †	19klux	0.2

d # = the distance between the projection of the diffuser centre on the working plane and the point of interest

Table 8.7 Light pipe predicted light levels for mid-summer season for Kew, UK. (Time = mid-noon 1st July, Height of diffuser to the working plane = 2m)

Length	Weather condition	Internal illuminance achieved at a horizontal distance of d# by a light pipe of diameter ϕ, lux											
		ϕ=210mm			ϕ=330mm			ϕ=420mm			ϕ=530mm		
		d=0m	d=1m	d=2m	d=0m	d=1m	d=2m	d=0m	d=1m	d=2m	d=0m	d=1m	d=2m
600mm	Clear *	160	110	55	475	330	160	830	580	275	1395	975	465
	Part-overcast ✦	110	75	40	330	230	110	570	400	190	965	675	320
	Overcast ✦	55	40	20	160	110	55	275	195	95	465	325	155
1200mm	Clear	90	65	30	335	235	110	625	440	210	1120	780	375
	Part-overcast	65	45	20	230	160	80	435	305	145	775	540	260
	Overcast	30	25	10	110	80	40	210	145	70	375	260	125
1800mm	Clear	55	40	20	235	165	80	475	330	160	895	625	300
	Part-overcast	35	25	15	160	115	55	330	230	110	620	435	205
	Overcast	20	15	10	80	55	30	160	110	55	300	210	100
2400mm	Clear	30	20	10	165	115	55	360	250	120	720	505	240
	Part-overcast	20	15	10	115	80	40	250	175	85	495	350	165
	Overcast	10	10	5	55	40	20	120	85	40	240	170	80
3000mm	Clear	20	15	10	115	80	40	270	190	90	575	405	195
	Part-overcast	15	10	5	80	55	30	190	130	65	400	280	135
	Overcast	10	5	5	40	30	15	90	65	30	195	135	65
3600mm	Clear	10	10	5	80	60	30	205	145	70	465	325	155
	Part-overcast	10	5	5	55	40	20	145	100	50	320	225	110
	Overcast	5	5	5	30	20	10	70	50	25	155	110	55

Weather condition	Horizontal global illuminance	Sky clearness index, k_t
Clear *	94klux	0.7
Part-overcast ✦	55klux	0.4
Overcast ✦	27klux	0.2

d# = the distance between the projection of the diffuser centre on the working plane and the point of interest

Table 8.8 Light pipe predicted light levels for winter for Kew, UK. (Time = mid-noon 1st February, Height of diffuser to the working plane = 2m)

Length	Weather condition	Internal illuminance achieved at a horizontal distance of d # by a light pipe of diameter ϕ, lux											
		ϕ=210mm			ϕ=330mm			ϕ=420mm			ϕ=530mm		
		d=0m	d=1m	d=2m	d=0m	d=1m	d=2m	d=0m	d=1m	d=2m	d=0m	d=1m	d=2m
600mm	Clear *	35	25	15	115	80	40	200	140	70	340	240	115
	Part-overcast ✦	25	15	10	70	50	25	125	85	45	210	150	70
	Overcast ♦	15	10	5	45	35	15	80	60	30	140	100	50
1200mm	Clear	20	15	10	75	50	25	140	100	50	260	180	90
	Part-overcast	15	10	5	45	35	15	90	60	30	160	115	55
	Overcast	10	5	5	30	20	10	60	40	20	105	75	35
1800mm	Clear	10	10	5	50	35	15	100	70	35	200	140	65
	Part-overcast	5	5	5	30	20	10	65	45	20	125	85	40
	Overcast	5	5	5	20	15	10	40	30	15	80	60	30
2400mm	Clear	5	5	5	30	25	10	70	50	25	150	105	50
	Part-overcast	5	5	5	20	15	10	45	30	15	95	65	35
	Overcast	5	5	5	15	10	5	30	20	10	65	45	20
3000mm	Clear	5	5	5	20	15	10	50	35	20	115	80	40
	Part-overcast	5	5	5	15	10	5	35	25	10	70	50	25
	Overcast	5	5	5	10	5	5	20	15	10	50	35	15
3600mm	Clear	5	5	5	15	10	5	35	25	15	90	60	30
	Part-overcast	5	5	5	10	5	5	25	15	10	55	40	20
	Overcast	5	5	5	5	5	5	15	10	5	35	25	15

Weather condition	Horizontal global illuminance	Sky clearness index, k_t
Clear *	41klux	0.7
Part-overcast ✦	24klux	0.4
Overcast ♦	12klux	0.2

d # = the distance between the projection of the diffuser centre on the working plane and the point of interest

Table 8.9 Light pipe predicted light levels for spring and autumn for Kew, UK. (Time = mid-noon 1st April, Height of diffuser to the working plane = 2m)

Length	Weather condition	Internal illuminance achieved at a horizontal distance of d # by a light pipe of diameter ϕ, lux											
		ϕ=210mm			ϕ=330mm			ϕ=420mm			ϕ=530mm		
		d=0m	d=1m	d=2m	d=0m	d=1m	d=2m	d=0m	d=1m	d=2m	d=0m	d=1m	d=2m
600mm	Clear *	115	80	40	355	245	120	620	430	205	1045	730	350
	Part-overcast +	65	45	25	200	140	65	345	240	115	585	410	195
	Overcast ♦	35	25	15	105	75	35	180	125	60	305	215	105
1200mm	Clear	65	45	25	245	170	80	460	325	155	830	580	275
	Part-overcast	40	25	15	135	95	45	260	180	85	465	325	155
	Overcast	20	15	10	70	50	25	135	95	45	240	170	80
1800mm	Clear	35	25	15	170	120	55	345	240	115	655	460	220
	Part-overcast	20	15	10	95	65	35	195	135	65	365	255	125
	Overcast	10	10	5	50	35	20	100	70	35	190	135	65
2400mm	Clear	20	15	10	115	80	40	255	180	85	520	365	175
	Part-overcast	15	10	5	65	45	25	145	100	50	290	205	100
	Overcast	10	5	5	35	25	15	75	55	25	150	105	50
3000mm	Clear	15	10	5	80	55	30	190	135	65	415	290	140
	Part-overcast	10	5	5	45	35	15	110	75	35	230	160	80
	Overcast	5	5	5	25	20	10	55	40	20	120	85	40
3600mm	Clear	10	5	5	55	40	20	145	100	50	325	230	110
	Part-overcast	5	5	5	30	25	10	80	55	30	185	130	60
	Overcast	5	5	5	20	15	5	45	30	15	95	70	35

Weather condition	Horizontal global illuminance	Sky clearness index, k_t
Clear *	76klux	0.7
Part-overcast +	44klux	0.4
Overcast ♦	22klux	0.2

d # = the distance between the projection of the diffuser centre on the working plane and the point of interest

Table 8.10 Measurement Settings

Diameter	Length	Bends no.	Vertical distance, cm	Total distance, cm Maximum value	Total distance, cm Minimum value
21	61	0	101	225	119
21	121	0	102	233	122
33	61	0	98	188	98
33	121	0	107	193	107
45	61	0	163	217	166
45	121	0	102	180	107
53	61	0	168	220	168
53	121	0	93	186	118
21	61	1	120	167	124
21	61	2	114	219	122
33	61	1	90	159	94
33	61	2	120	192	120
33	61	3	84	151	85
33	61	3	72	140	83
33	61	4	83	130	87
33	61	4	102	158	131
53	61	1	92	144	102

Table 8.11 Envelop for DPF models

Boundary	**Diameter**	**Length of tube**	**Vertical distance**	**Total distance**	**Bend no.**	α	k_t	E_{vg}
Unit	Cm	Cm	Cm	Cm	-	Degree	-	Lux
Minimum	21	61	70	80	0	15	0.01	1270
Maximum	53	120	170	230	4	57	0.86	97270

9. CONCLUSIONS AND FURTHER WORK

The present research set out to meet specific objective, itemised in Chapter 1. The overall aim of the research was to provide a general mathematical model for the prediction of light pipe daylighting performance. Based on two years' measurements on the daylighting performance of light pipes, large and reliable databases were obtained which enabled the mathematical modelling. These procedures had previously not been carried out.

The key points concluded throughout the research are now presented in turn.

i. Two years' data on light pipe daylighting performance under all weather conditions were measured. The data were measured on a minute-by-minute basis and provided detailed information on the performance and configurations of light pipes, weather conditions and the arrangement of sensors during the tests. The database enabled the opportunity to conduct the aimed mathematical modelling on light pipe. Moreover, this information has previously been unavailable and can be used by engineers, architects and researchers alike as a foundation for further study on light pipes.

ii. In an attempt to establish a mathematical model for light pipe daylighting performance assessment. An analysis of independent variables was conducted to identify the factor exerting the most significant influence on the performance of light pipes. It was found that the daylighting performance of light pipes is affected by light pipe configuration factors, external weather conditions and the position of the point of interest. Light pipe configuration factors include the aspect ratio and section area of light pipe tube, the reflectance of the internal surface of light pipe tube, number of bends, degree of bend and types of light pipe dome and diffuser. External weather condition includes global horizontal illuminance, solar attitude and sky clearness index. The performance of light pipe was also found affected by the vertical and horizontal distances between the point of interest and the centre of the light pipe diffuser. Therefore, proposed mathematical model were reported as a function of above-mentioned factors.

iii. Light pipes are daylighting devices that utilise both sunlight and skylight. This is in contrast to traditional daylighting devices such as windows, which owing to their design and orientation limitations utilise only sky-diffuse and reflected illuminance. Therefore, a new concept of Daylight Penetration Factor (DPF) has been introduced in present research to specify the performance of light pipes. DPF is the ratio of the internal illuminance to the corresponding total external illuminance at a given point. The introduction of DPF into daylighting research enables the performance comparison between innovative and traditional daylighting devices.

iv. Two mathematical models, S-DPF for straight light pipes and E-DPF for elbowed light pipes have been built to assess the performance of straight light pipes and elbowed light pipes. Compared to S-DPF model, E-DPF model uses an extra term to account for the effects of light pipe bend. The term is a function of bends number N, and when N is given the value of 0, E-DPF collapses to the exact form of S-DPF. S-DPF and E-DPF models predict the internal illuminances due to light pipes under all weather conditions. Since the DPF models use non site-specific information for light pipe performance assessment, it is considered to be world wide applicable. The DPF models were incorporated into Excel spreadsheets that facilitate the use of the DPF models. The DPF models are based on physical analysis of the working mechanism of light pipes and are adjustable by changing the value of coefficients employed in the model. The DPF model method therefore provides a flexible framework that enables a sustainable development of the mathematical modelling of light pipe daylighting performance. By carrying out more measurement, fitting and validation procedures that were developed in present research, the accuracy of the DPF models can be continuously improved.

v. In addition to traditional error evaluation techniques, i.e. MBE and RMSE, PAD, slope of best-fit trend line, coefficient of determination, a statistical residual analysis was also conducted to further investigate the robustness of the proposed models. The DPF models were further validated using independent data set, and compared to results given by independent researches in the field. Good agreements have been reached between present findings and results given by other research bodies. The validation of the DPF models using independent

data shows that the models can predict the performance of light pipes under all weather conditions with a good accuracy.

vi. It was found that the type of light pipe diffuser heavily affects the daylighting performance of light pipes. Comparison between light pipes with opal and clears diffuser showed that the amount of light delivered by the latter one was significantly more than that by the former one. This is due to the improved transparency of the diffuser, which allows a better daylight penetration into internal space. However, it is also found that although the penetration of daylight is improved by using clear diffusers, the internal distribution of the penetrated daylight is less uniform than that due to opal diffuse light pipes. This shortcoming becomes apparent when the external illuminance is high (higher than 30klux), that is certain pattern of "pools of light" can be observed within interior space due to the unsymmetrical distribution of daylight. DPF models given in present research were developed for opal diffuse light pipes. A Diffuser Factor (f_D) has been introduced to link the DPF models to the performance of clear diffuser light pipes.

vii. Practical engineering design tool have been produced based on DPF models. The guideline takes the form of six design tables that provide the internal illuminances that can be achieved by opal diffuser light pipes of varying geometrical configurations operating under typical London weather conditions. By applying an efficiency-loss factor of 0.2, the guideline can be adapted to aid the design of elbowed light pipe. Additionally, within the Excel Visual Basic Application environment, lux plot that can visually describe the internal illuminance distribution due to light pipes has been constructed based on DPF models. The lux plot [Courtesy: David Jenkins, Monodraught] can be used by building or lighting designers in both of their initial and final stages of design of light pipes. The application of the lux plot in the initial stage of design gives a general picture of how many and what kinds of light pipes are needed for a certain design purpose. While the application of the lux plot at the final stage of design helps to tune the design and provide a crosscheck.

viii. A new anisotropic model to correct diffuse irradiance measured by shadow band has been developed. This method is based on the use of a single diffuse radiance distribution index, b. Clearness index, k_t, is used as a parameter to determine the value of b, and b is then used to obtain the correction factor to account for the diffuse irradiance obscured by shadow band. The proposed method is validated using databases from sites with disparate sky conditions. The Drummond's isotropic method, which is based solely on geometric calculation, is compared against the proposed method that uses an anisotropic radiance distribution. Results show that for the case of Bracknell, England the RMSE, MBE and PAD of corrected diffuse irradiance obtained using the proposed method are 12W/m^2, -0.7 W/m^2 and 3% respectively. Corresponding RMSE, MBE and PAD due to Drummond's method are 16 W/m^2, -5.6 W/m^2 and 4% respectively. For the case of Beer Sheva, Israel, the proposed model produces an RMSE of 17 W/m^2, an MBE of 2W/m^2 and a PAD of 5%. The corresponding figures for Drummond's method are 23 W/m^2, -5W/m^2 and 7% respectively.

ix. The S-DPF model assumes that the internal illuminance distribution on a working plan below the light pipe diffuser is symmetrical to the diffuser centre and is a function of the vertical and total distances of one point to the diffuser centre. A purposed measurement was undertaken in Craighouse test room to test this assumption (Section 5.6). It was found that the asymmetrical distribution of internal illuminance although not very significant, has a substantial effect on the daylighting performance of light pipe. It is worthy however to point out that in real applications, especially for large rooms, usually a group of light pipes need to be installed to provide an even distribution of daylight within the space. For occasions where multi-light pipes were installed symmetrically to the room layout, the effect of asymmetrical distribution of internal illuminances can be reduced, and the predictions given by S-DPF model tends to be more accurate.

In order that future research follow in a logical manner from the present work, some suggestions for possible work are presented herein.

i. A 3-D light pipe DPF model

The DPF models predict the daylighting performance of light pipes based on a validated observation that the internal distribution of daylighting due to light pipes is approximately symmetrical to the axis of light pipe tube. This can however, be pointed out as a weak link in the chain of calculating the performance of light pipe system. DPF models predict not only the daylight transmittance of light pipe system, but also the internal illuminance level at given points. The linkage between above two functions of DPF models is the method of describing internal illuminance distribution. It has been found that the internal distribution of daylight due to light pipe is not always strictly symmetrical to the axis of light pipe tube. The deviation of the internal illuminances for points at different positions but having the same distances to the light pipe diffuser centre can be as high as 15%. This implies that the unsymmetrical internal illuminance distribution may be a major factor causing system bias of the DPF models. It is therefore suggested that more geometrical factors that describes the relative position of a given point to light pipe diffuser should be included into the DPF models, so as to take into account the effect of unsymmetrical internal illuminance distribution. One proposal that may be adopted would be to establish a 3-D coordinate system that can describe the geometrical relationship between the sun's position (solar altitude and azimuth), the light pipe tube's position and a given point's position. Once the 3-D DPF model that incorporates above-mentioned additional geometrical factors is constructed, further measurements on the internal illuminance distribution should be undertaken and the data obtained can then be used to determine the formal form of the 3-D DPF model. After that, considering practical issues such as capital and manpower limitations, experiments cannot be used to enumerate all possible cases of light pipe applications, computer aided design tool such as CAD or simulation package like Matlab may be used to build an computational model so as to extrapolate the 3-D DPF model.

ii. A general standard for evaluating traditional and innovative daylighting devices

Daylight factor has been accepted as an industry standard for window design. Windows are traditional daylighting device, but owing to their design and orientation limitations utilise only sky-diffuse and reflected illuminance. As a comparison, innovative daylighting devices such

as light pipe utilise both sunlight and skylight. However, for innovative daylighting devices, to date no general method is available to assess their daylighting performance. Based on the concept of light pipe daylight penetration factor, DPF, a reference method may be adopted for an agreed standard to assess all daylighting devices. In this respect the author would like to propose new tasks that may be included for further work. The first task is to design a method of a Light Pipe Figure of Merit (L-FoM) that would be the ratio of illuminance achieved by any given light pipe to illuminance due to a "reference" light pipe of prescribed dimensions. The second task is to design a Light Pipe to Window Figure of Merit (LW-FoM) that would be the ratio of illuminance achieved by any light pipe to illuminance due to a "reference" window of prescribed dimensions. The above L-FoM and LW-FoM would be evaluated under prescribed sky conditions and within the 3-D coordinate system proposed above (section i).

APPENDIX I: THE METHOD FOR CALCULATING THE VIEW FACTORS FROM DIFFERENTIAL AREAS TO SPHERICAL SEGMENTS BY NARAGHI

$I: D > \frac{1-LH}{\sqrt{1-L^2}}$ *and* $-1 < H < L$ (*where* $D = \frac{d}{r}, H = \frac{h}{r}, L = \frac{l}{r}$):

$$F_{dA_1-A_2} = \frac{1}{2\pi}\{\cos^{-1}(\frac{1-LH}{D\sqrt{1-L^2}}) + \frac{2(1-2L^2-D^2-H^2+2HL)}{\sqrt{(1+D^2+H^2-2HL)^2-4D^2(1-L^2)}} \times \tan^{-1}(\sqrt{\frac{(1+D^2+H^2-2HL+2D\sqrt{1-L^2})(D\sqrt{1-L^2}-1+LH)}{(1+D^2+H^2-2HL-2D\sqrt{1-L^2})(D\sqrt{1-L^2}+1-LH)}})$$

$$+2\frac{\sqrt{D^2-1+2HL-(D^2+H^2)L^2}-\sqrt{D^2-1+2H^2-(D^2+H^2)H^2}}{D^2+H^2}+2\frac{H}{(D^2+H^2)^{\frac{3}{2}}}[\sin^{-1}(\frac{H-(D^2+H^2)L}{\sqrt{H^2+(D^2-1)(D^2+H^2)}})$$

$$-\sin^{-1}(\frac{H(1-D^2-H^2)}{\sqrt{H^2+(D^2-1)(D^2+H^2)}})]+2\sin^{-1}(\frac{\sqrt{1-H^2}}{D})\} \qquad (4.18a)$$

$II: D < \frac{1-LH}{\sqrt{1-L^2}}$ *and* $-1 < H < L$:

$$F_{dA_1-A_2} = \frac{1}{\pi}\{\tan^{-1}\sqrt{\frac{1-H^2}{D^2+H^2-1}}-\frac{\sqrt{(D^2+H^2-1)(1-H^2)}}{D^2+H^2}-\frac{H}{(D^2+H^2)^{\frac{3}{2}}}\cos^{-1}(\frac{H\sqrt{D^2+H^2-1}}{D})\} \qquad (4.18b)$$

III: when $L>0$ $D>\frac{1-LH}{\sqrt{1-L^2}}$ and $H<-1$

when $L<0$ $D>\frac{1-LH}{\sqrt{1-L^2}}$ and $\frac{1}{L}<H<-1$

when $D>\frac{LH-1}{\sqrt{1-L^2}}$ and $H<\frac{1}{L}$:

$$F_{dA_1-A_2}=\frac{1}{2\pi}\{\cos^{-1}(\frac{1-LH}{D\sqrt{1-L^2}})+\frac{2(1-2L^2-D^2-H^2+2HL)}{\sqrt{(1+D^2+H^2-2HL)^2-4D^2(1-L^2)}}\tan^{-1}(\sqrt{\frac{(1+D^2+H^2-2HL+2D\sqrt{1-L^2})(D\sqrt{1-L^2}-1+LH)}{(1+D^2+H^2-2HL-2D\sqrt{1-L^2})(D\sqrt{1-L^2}+1-LH)}})$$

$$+2\frac{\sqrt{D^2-1+2HL-(D^2+H^2)L^2}}{D^2+H^2}+2\frac{H}{(D^2+H^2)^{\frac{3}{2}}}\cos^{-1}(\frac{H-(D^2+H^2)L}{\sqrt{H^2+(D^2-1)(D^2+H^2)}})\}$$

(4.18c)

IV: when $L>0$ $D<\frac{1-LH}{\sqrt{1-L^2}}$ and $H<-1$

when $L<0$ $D<\frac{1-LH}{\sqrt{1-L^2}}$ and $\frac{1}{L}<H<-1$

$$F_{dA_1-A_2}=-\frac{H}{(D^2+H^2)^{\frac{3}{2}}}$$

(4.18d)

V: when $D<\frac{LH-1}{\sqrt{1-L^2}}$ and $H<\frac{1}{L}$

$$F_{dA_1-A_2}=\frac{1}{2\pi}\{1+\frac{1-2L^2-D^2-H^2+2HL}{\sqrt{(1+D^2+H^2-2HL)^2-4D^2(1-L^2)}}\}$$

(4.18e)

APPENDIX II: LIST OF PUBLICATIONS

1. A Mathematical Model for the Performance of Light-pipes, X Zhang and T Muneer, *Lighting Research and Technology*, Vol.32(3), 2000

2. A Design Guide for Performance Assessment of Solar Light-pipes, X Zhang, T Muneer and J Kubie, *Lighting Research and Technology*, Vol.34(2), 2002

3. Light-pipes for Daylight Penetration Indoors, X Zhang, *Proceedings of Renewable Energy for Housing Conference*, The UK Solar Energy Society, 20 October 2000, Perth

4. A New Method for Correction Shadow Band Diffuse Irradiance Data, T Muneer and X Zhang, *Journal of Solar Energy Engineering*, American Society of Mechanical Engineering, Vol.124, 2002

5. Sky Luminance and Radiance Distributions - A Comparison Based on Data from Bahrain, Japan and Europe, T Muneer, F Fairooz and X Zhang, Light Research and Technology, *Lighting Research and Technology*, Special issue for CIBSE "An Expert's Conference: Tropical Daylight and Buildings", Singapore, 2002

6. Evaluation of An Innovative Sensor for Measuring Global and Diffuse Irradiance, and Sunshine duration, T Muneer, X Zhang and J Wood, submitted to International Journal of Solar Energy, in review.

7. Cost and Value Analysis of Piped Daylight, T Muneer and X Zhang, submitted to Commission International de l'Eclairage (CIE) TC3-38 Committee, 2002

8. Accuracy Analysis of Solar Position Algorithms Used within CIBSE Guides 'A' and 'J', CIBSE, August, 2000, in communication.